Centre Eau-Terre-Environnement

DÉVELOPPEMENT D'UN PROCÉDÉ D'OXYDATION ÉLECTRO-CATALYTIQUE POUR LE TRAITEMENT À LA SOURCE DES MICRO-ET NANO-PLASTIQUES PRÉSENTS DANS LES EAUX RÉSIDUAIRES DE BUANDERIES

Par

KIENDREBEOGO Marthe

Thèse présentée pour l'obtention du grade de
Philosophiae Doctor (Ph.D.)
en sciences de l'eau

Jury d'évaluation

Président du jury et Examinateur interne	KOKOU ADJALLÉ INRS-ETE
Examinateur externe	MANUEL J. RODRIGUEZ Université Laval
Examinateur externe	BENOÎT BARBEAU, École Polytechnique Montréal
Directeur de recherche	PATRICK DROGUI INRS-ETE

Mai 2023

REMERCIEMENTS

J'adresse ma profonde gratitude au Professeur Patrick DROGUI, pour m'avoir accueilli dans son équipe de recherche. Je le remercie sincèrement de l'intérêt particulier apporté à mon travail (technique de rédaction, présentation, etc). Ses orientations, critiques, commentaires et sa disponibilité à me booster régulièrement au travail m'ont permis de poursuivre ce projet, et de réaliser mes intérêts et objectifs.

J'exprime ma reconnaissance à mes collègues du laboratoire LEEPO-INRS, en particulier Karimiestahbanati M. Karimi, Yassine Ouarda, Alae Benguit et Sanae Benkeraach pour leurs précieux conseils, soutien moral et leur précieuse collaboration dans la rédaction des articles.

J'exprime ma gratitude au personnel de l'INRS-ETE pour toute l'aide technique et administrative que j'ai reçue tout au long de mes études.
Je remercie également le programme canadien de bourse pour la francophonie (PCBF) et le programme FONCER TEDGIEER pour le soutien financier.

Je remercie les membres du jury pour leur disponibilité à l'évaluation de cette thèse.

Enfin, les mots ne suffiront pas à remercier mon époux, Nathanaël qui malheureusement n'a pas attendu la fin de cette thèse avant de quitter ce monde, à mon fils Anaël et ma famille pour leur tolérance, soutien et leurs encouragements considérables tout au long de mon programme de doctorat.

RÉSUMÉ

Les micro- et nano-plastiques, qu'ils soient primaires ou secondaires sont aujourd'hui désignés comme polluants émergents. Leur présence dans les eaux usées, douces, marines, et même potables ainsi que leurs interactions entrainent des effets toxiques sur les organismes aquatiques. Ils sont retrouvés également dans les aliments tels que les fruits de mer (poisson, huitres, … etc.) et le sel marin. Généralement composés de polymères synthétiques et d'additifs, ce sont des particules du plastique utilisé couramment dans plusieurs domaines d'applications (l'industrie textile, cosmétique, ménager et électroménager, etc.), soit déjà avec la taille micro- et nano-particulaires ou macro-plastique qui par la suite de leur cycle de vie se fragmentent en de plus petites particules. Ils sont introduits dans les eaux douces et marines principalement par le biais des déchets plastiques non collectés, des rejets d'effluents des stations d'épuration dont les systèmes de traitement ne sont pas adaptés pour leur élimination. Des débordements des égouts lors de fortes pluies sont également à l'origine de la présence des micro- et nano-plastiques dans l'environnement. Leur capacité à s'accumuler, à adsorber et à transporter d'autres polluants organiques et métaux dans l'environnement font en sorte que leurs sources d'introduction sont à prendre en considération. Pour cela, plusieurs technologies de séparation des micro- et nano-plastiques dans les eaux ont été éprouvées. Celles-ci montrent des performances d'élimination efficaces avec une limite pour les MPs sub-micrométriques. Par ailleurs, elles constituent une solution partielle parce que les micro- et nano-plastiques séparées des eaux retournent dans l'environnement par le biais des boues de traitement. Dans ce travail, nous proposons d'étudier l'efficacité d'un procédé d'oxydation électro-catalytique pour la dégradation et traitement d'effluents réels de buanderie contaminés par des micro- et nano-plastiques.

La première partie de cette étude a consisté à tester les performances du procédé d'électro-oxydation dans les effluents synthétiques artificiellement contaminés par les micro-plastiques (MPs) de polystyrène en utilisant une électrode catalytique de diamant dopé au bore BDD (pour boron-doped diamond). L'effet du matériau (BDD, MMO (mixed metal oxide), IrO_2 (oxyde d'iridium)) et de la surface de l'anode de BDD (41.6 et 83 cm^2), de la densité du courant (36, 72, 108 mA/cm^2), du type (Na_2SO_4, NaCl, $NaNO_3$) et de la concentration d'électrolyte Na_2SO_4 (0.03, 0.04, 0.06 M) ont été testé pendant 6h d'électrolyse. Les résultats ont montré un taux d'élimination de 58 ± 21% et de 84 ± 8% de MPs (25 µm de taille nominal) après respectivement 1h et 3h

d'électrolyse en utilisant le BDD avec une densité de courant de108 $mA.cm^{-2}$ et 0.06 M de Na_2SO_4. Tous les paramètres de fonctionnement étudiés affectaient considérablement l'efficacité de dégradation des MPs, sauf la surface de l'anode qui a montré un effet négligeable. La combinaison des résultats d'analyse par la diffusion dynamique de la lumière, la microscopie à balayage électronique, du COT du filtrat des échantillons et de la spectroscopie infrarouge à transformée de Fourier suggèrent que les MPs se dégradent directement en produits gazeux. Par conséquent, l'EO est un procédé prometteur pour la dégradation des MPs dans l'eau.

Dans la deuxième partie de cette étude, l'électro-peroxydation a été appliquée et comparée à l'électro-oxydation de nano-plastiques (NPs) de polystyrène (100 nm de diamètre nominal) dans de l'eau synthétique en utilisant 3 différentes configurations de réacteurs électrolytiques. La production du peroxyde d'hydrogène à la cathode et l'utilisation de plusieurs électrodes ont été introduits dans l'objectif d'améliorer l'efficacité de dégradation et comprendre le rôle des oxydants in situ produits dans le mécanisme électrochimique de dégradation de NPs. L'efficacité du traitement a été suivie par la mesure du COT dans les échantillons, de l'absorbance UV_{vis} a 254 nm et analyses 3D de la fluorescence excitation émission. Les résultats obtenus indiquent que dans le processus d'EO, les NPs sont principalement oxydés à la surface de l'électrode de diamant dopé en bore (BDD) par : (i) $^{\bullet}OH$ issus de la décharge de la molécule d'eau et (ii) $SO_4^{\bullet-}$ via la réaction entre $S_2O_8^{2-}$ et $^{\bullet}OH$. Dans le procédé EO-H_2O_2, les NPs sont à la fois dégradés par les $^{\bullet}OH$ formés lors de la décomposition du H_2O_2 ainsi que par les $SO_4^{\bullet-}$ générés à partir de réactions directes ou indirectes avec H_2O_2. Par conséquent, pour le procédé EO-H_2O_2 l'efficacité de dégradation des NPs était environ de 2,6 fois plus élevé que le procédé EO lorsqu'une densité de courant de 36 $mA.cm^{-2}$, une concentration de 0.03 M de Na_2SO_4, avec un temps de réaction de 40 min ont été appliqués. Dans ces conditions le pourcentage de dégradation était de 86,8% avec une baisse du pH de la solution à 2 pour l'EO-H_2O_2. De plus, l'analyse de fluorescence 3D EEM a attesté la dégradation des NPs. Enfin, une évaluation économique incluant la consommation de l'énergie et de l'électrolyte (Na_2SO_4) a donné un cout d'exploitation de 2,3 $\$US.m^{-3}$ pour le traitement des NPs (10 mg/L) par le procédé EO-H_2O_2 soit environ 10 fois moins que le procédé EO. Par conséquent, la génération in situ des espèces oxygénées réactives peut considérablement améliorer la dégradation des NPs dans l'eau.

La troisième partie de cette thèse a traité de la dégradation de NPs dans des effluents réels d'une buanderie commerciale artificiellement dopés au NPs fluorescents de polystyrène (150 nm de

diamètre nominal). L'optimisation du procédé EO-H_2O_2 a été effectuée en utilisant une méthodologie de surface de réponse de plan central composite. Pour ce faire, la dégradation des NPs a été effectuée dans un réacteur comprenant deux électrodes de feutres de carbone (cathodes) et une électrode de BDD (anode). La dégradation des NPs a été suivie par la mesure de l'absorbance UV-vis à 225 nm et par l'analyse (avant et après traitement) par spectroscopie de fluorescence d'acquisition de matrices d'émission-excitation (3D-EEM) des eaux. La génération in situ d'espèces oxydantes lors de l'électrolyse contribue à majorer l'efficacité de dégradation des NPs avec des temps d'électrolyse dépendant de la charge initiale en COT des effluents. Malgré cette différence de COT initial, un taux de dégradation des NPs de plus 80% est enregistré au bout de 50 min d'électrolyse et ce, quelle que soit la charge organique présente dans les eaux. L'efficacité de traitement a également été évaluée par la mesure du COT. L'application des conditions optimales (densité de courant de 31,2 $mA.cm^{-2}$, 0.025 M Na_2SO_4 et un temps de traitement de 52 min) a permis d'enregistrer un taux de dégradation de 81,2 ± 4,5% NPS et un taux de minéralisation de 43.1 ± 3.3% (abattement du COT initial de 52 mg/L). Par ailleurs, des tests d'estimation de la toxicité de l'effluent (avant et après traitement) basés sur la létalité aiguë du crustacé *Daphnia magna* ont également été effectués. Une unité de toxicité de 5,1 UT a été mesurée dans l'effluent non traité, alors qu'une valeur inférieure 1 UT a été enregistré dans l'effluent reel traité après 52 min d'électrolyse.

ABSTRACT

Micro-plastics (MPs) and nano-plastics (NPs), regardless of being primary or secondary, are considered emerging pollutants. These pollutants that are present in wastewater, freshwater, marine ecosystems, and even drinking water are toxic because of their nature as well as their interactions with other contaminants. They are also found in foods such as seafood (fish, oysters, etc.) and sea salt. Generally composed of synthetic polymers and additives, they are plastic particles commonly used in several fields of application (textile, cosmetics, household and household appliances, etc.), either already with the micro- and nano-size particulates or macro-plastics which later in their life cycle fragment into smaller particles. They are introduced into fresh and marine waters mainly through plastic wastes, heavy rain overflows, and effluent discharges from treatment plants that are not capable of effectively removing MPs and NPs. Their ability to accumulate, adsorb and carry organic pollutants and metals imposes more negative effects on the environment. Several technologies for the separation of MPs and NPs in water have been tested. These technologies show effective removal performance with limited sub-micrometer MPs. They constitute a partial solution because the MPs and NPs separated from the water would return to the environment through the treatment sludge. In this work, we propose to study the effectiveness of an electro-catalytic oxidation process for the degradation of MPs and NPs in real laundry effluents.

The first part of this study consisted in testing the performance of the electro-oxidation process in synthetic effluents artificially contaminated with polystyrene MPs (25 µm nominal size) using a boron-doped diamond (BDD) electrode. The effects of anode material (BDD, MMO, IrO_2), area (41.6 and 83 cm^2), current density (36, 72, 108 mA/cm^2), electrolyte type (Na_2SO_4, NaCl, $NaNO_3$), and concentration (0.03, 0.04, 0.06 M) were tested for 6 hours of electrolysis. The results showed a removal rate of 58 ± 21% and 84 ± 8% of MPs after 1 h and 3 h, respectively using the BDD anode with a current density of 108 $mA.cm^{-2}$ and 0.06 M Na_2SO_4. The results illustrated all the studied operating parameters significantly affected the MP degradation efficiency, except the anode surface area which showed a negligible effect. The combination of dynamic light scattering, scanning electron microscopy, sample filtrate TOC and Fourier transform infrared spectroscopy results suggest that MPs degrade directly into gaseous products. Therefore, EO is a promising process for the degradation of MPs in water.

In the second part of this study, the electro-peroxidation (EO-H_2O_2) of polystyrene NPs (100 nm nominal diameter) in synthetic water was investigated using 3 different configurations of electrolytic reactors. The production of hydrogen peroxide at the cathode and the use of multiple electrodes have been introduced with the aim of improving the degradation efficiency and understanding the role of *in-situ* oxidants produced in the mechanism of electrochemical NP degradation. The efficacy of treatment was monitored by measuring the concentration of NPs using UV-Vis absorbance at 254 nm as well as the concentration of organic carbon using TOC analysis. In addition, 3D fluorescence excitation-emission was analyzed to confirm the removal of NPs. The obtained results indicated that in the EO process, the NPs are mainly oxidized at the surface of the BDD by (i) $^{\bullet}OH$ generated from the discharge of water molecules, and (ii) $SO_4^{\bullet-}$ via reactions between $S_2O_8^{2-}$ and $^{\bullet}OH$. However, in the EO-H_2O_2 process, NPs are degraded by $^{\bullet}OH$ formed from both the decomposition of H_2O_2 and $SO_4^{\bullet-}$ generated from direct or indirect reactions with H_2O_2. Therefore, for the EO-H_2O_2 process, NPs degradation efficiency could enhance about 2.6 times in comparison to the EO process and the percentage of degradation reached 86.8 %. In addition, 3D EEM fluorescence analysis confirmed the degradation of NPs. Finally, an economic evaluation including the consumption of energy and electrolyte gave an operating cost of 2.3 \$US.m^{-3} for the treatment of NPs by the EO-H_2O_2 process, i.e., approximately 10 times less than the EO process. Therefore, the *in-situ* generation of reactive oxygen species has a significant role in the degradation of NPs in water.

The third part of this thesis dealt with the degradation of NPs in real effluents from a commercial laundry that was artificially doped with polystyrene NPs (150 nm nominal diameter). The optimization of the EO-H_2O_2 process was carried out using a response surface methodology (RSM) by central composite design. To do this, the degradation of NPs was carried out in a reactor comprising two carbon-felt electrodes (cathodes) and one BDD electrode (anode). The degradation of NPs was monitored by measuring the UV-Vis absorbance at 225 nm as well as analyzing fluorescence spectroscopy of emission-excitation matrices (3D-EEM). Treatment efficacy to remove organic carbon was also assessed by TOC measurement. The in-situ generation of oxidizing species during electrolysis contributes to increasing the degradation efficiency of NPs, depending on the initial TOC load of the effluents. More than 80% degradation rate of NPs was recorded after 50 min of electrolysis, regardless of the organic load present in the water. At the obtained optimal condition using the developed RSM model (current density of

31.2 $mA.cm^{-2}$, 0.025 M Na_2SO_4, and 52 min treatment time) NPs degradation rate of 81.2 ± 4.5% and a mineralization rate of 43.1 ± 3.3% were recorded. In addition, the toxicity of the effluent (before and after treatment) was tested based on the acute lethality of the crustacean *Daphnia magna*. A toxicity unit of 5.1 TU was measured in the untreated effluent, while a lower value of 1 TU was recorded in the treated effluent after 52 min of electrolysis.

The objectives achieved through all parts of this study provide insight into the effectiveness of the degradation of MPs and NPs smaller than 25 µm by the electrochemical oxidation process. This process is a promising approach to mineralizing MPs and NPs in real wastewater, however, more research is required to improve the cost-effectiveness of the process.

TABLE DES MATIÈRES

LISTE DES TABLEAUX

LISTE DES FIGURES

LISTE DES ABRÉVIATIONS

BDD	Baron-doped diamant
DLS	Dynamic light scattering
DNA	N, N-Dimethyl-4-nitroso-aniline
EAOP	Electrochemical advanced oxidation process
FPA	Focal plane area
FTIR	Fourier transform infrared spectroscopy
GC	Gas chromatography
HDPE	High-density polyethylene
LC	Liquid chromatography
MBR	Membrane bioreactor
MPs	Microplastics
NPs	Nanoplastics
NTA	Nanoparticle tracking analysis
OCDE	Organisation de coopération et de développement économique
PA	Polyamine
PE	Polyethylene
PES	Polyester
PET	Polyethylene terephthalate
PP	Polypropylene
PS	Polystyrene
PVC	Polyvinyl chloride
SEM	Scanning electron microscopy
STEP	Station de traitement et d'épuration
3D EEM	Three dimensional excitation emission matrix
TED	Thermal extraction desorption
TOC	Total organic carbon
TSS	Total suspended solids
WEF	World economic forum

1. SYNTHESE

1.1. Introduction

L'accroissement démographique et la hausse des revenus ont entrainé une importante consommation des matières plastiques au cours de ces dernières décennies. Ainsi la production mondiale du plastique n'a cessé d'augmenter depuis 1950 de 1,5 à 367 millions de tonne (Mt) en 2020 (Europe, 2021). Selon l'organisation de coopération et de développement économique (OCDE), elle a plus que doublé entre 2000 et 2019 pour atteindre 460 Mt avec la stimulation de la production des objets jetables (OCDE, 2022). Par conséquent, la production mondiale annuelle des déchets plastiques est passée de 156 à 353 Mt pendant cette même période (OCDE, 2022). Deux tiers de ces déchets proviennent des emballages des produits de consommations et des textiles et près de 22 % de ces déchets sont abandonnés dans des décharges sauvages, brûlés à ciel ouvert ou rejetés dans l'environnement. En raison du faible coût, de la durabilité et de la malléabilité (Andrady & Neal, 2009), l'utilisation du plastique est illimitée dans chaque aspect de notre quotidien. Cependant, les inconvénients du plastique deviennent de plus en plus évidents. L'ensemble de la pollution de la surface des océans est estimée à près de 5 250 milliards de particules de plastique, soit 268 940 tonnes (Eriksen *et al.*, 2014).

Les déchets plastiques sont composés de débris de toute taille : des macro-plastiques facilement séparables aux particules invisibles à l'œil nu. Les gros débris une fois présents dans l'environnement, subissent des processus de vieillissement altéré et biotique qui entraînent leur dégradation et leur fragmentation en de particules de plus petites tailles appelées micro-plastiques (MPs) ou nano-plastiques (NPs) secondaires. A ces MPs/NPs secondaires s'ajoutent les MPs/NPs primaires dont les rejets mondiaux dans les océans ont été estimés à 1,5 Mtonnes/an, avec des estimations comprises entre 0,8 et 2,5 Mt/an selon que les simulations soient abusives ou non (Boucher & Friot, 2020). Cette dernière catégorie de micro/nano-plastiques sont volontairement ajoutés à des produits cosmétiques ou résultent de l'abrasion d'objets en plastique au cours de leur fabrication, de leur utilisation ou de leur entretien. La majeure partie de ces particules proviennent du lavage de textiles synthétiques et de l'abrasion des pneus sur les routes. 66% de ces micro-plastiques atteignent l'océan par le ruissellement de l'eau sur les routes, 25% par les systèmes de traitement des eaux usées et 7% par le vent (7 %)

(Boucher & Friot, 2020). Des études sur la surveillance environnementale à travers le monde mentionnent une quantité importante de MPs présents dans les eaux de surface, les sédiments côtiers, les sables de plage et les milieux marins profonds (Browne *et al.*, 2011a; Faure *et al.*, 2015a; Woodall *et al.*, 2014b).

Cette présence des micro/nano-plastiques dans l'environnement a éventuellement des impacts néfastes sur les organismes aquatiques et sur la santé publique comme le suggèrent plusieurs études à l'échelle du laboratoire (Avio *et al.*, 2015; Besseling *et al.*, 2014; Karami *et al.*, 2017). En plus de ces risques sanitaires, l'ensemble du cycle de vie des plastiques d'origine fossile contribue beaucoup aux émissions de gaz à effet de serre (OECD).

Évidemment, plusieurs solutions sont d'ores et déjà envisagées : sensibiliser et changer les comportements des industriels et des citoyens, adapter la formulation des produits, limiter les rejets industriels et domestiques, adapter les stations d'épuration... En parallèle, des projets se développent pour nettoyer la pollution déjà présente dans les océans. Le projet le plus médiatisé est Océan Clean up qui consiste à concentrer et à ramener les débris vers une plateforme capable de les traiter. Cependant cette solution s'attaquera aux macro-déchets flottant en surface des océans, mais n'interceptera que peu de micro-plastiques flottants et pas du tout les nano-plastiques. Une autre solution consisterait à utiliser une bactérie capable de dégrader le plastique et de briser ses liaisons moléculaires. Si la bactérie découverte ne s'attaque qu'au polyéthylène téréphtalate (PET) (Shosuke Yoshida *et al.*, 2016), les chercheurs ambitionnent de découvrir d'autres bactéries dégradant d'autres matières plastiques. Par ailleurs, plusieurs technologies avancées de traitement des eaux ont déjà été testées pour le traitement des micro- et nano-plastiques. On peut citer des exemples comme le filtre à sable rapide, le filtre à disque, la flottation par insufflation d'air (Talvitie *et al.*, 2017a), le bioréacteur à membrane (Lares *et al.*, 2018) et l'électrocoagulation (Perren *et al.*, 2018; Shen *et al.*, 2022). La technologie à membrane bien qu'elle montre les meilleures performances d'élimination, laisse passer une proportion importante des fibres (Talvitie *et al.*, 2017a), la plus petite fraction des micro-plastiques < 20 µm (Lares *et al.*, 2018; Michielssen *et al.*, 2016) et les nano-plastiques < 0,7 µm (Leslie *et al.*, 2017a) dans les effluents. Par conséquent les effluents en sortie de station de traitement déchargent entre 5.10^4-4.10^{10} particules par jour par station de traitement dans l'environnement (Sun *et al.*, 2019). Par ailleurs, les boues issues de ces procédés de séparation nécessiteraient un traitement additionnel pour prévenir le retour des MPs dans l'environnement.

Au regard de cette situation, nous proposons d'étudier la dégradation des micro/nano-polymères retrouvés dans les eaux résiduaires de buanderie commerciale, par les procédés électrochimiques. Ces procédés permettent la production des radicaux hydroxyles (^{o}OH) qui sont des oxydants puissants et non sélectifs (Guinea *et al.*, 2008). Il est également possible de générer simultanément d'autres espèces oxygénées réactives ($H_2S_2O_8$, H_2O_2, etc.) lors de l'électrolyse. L'utilisation de ces procédés regorge de nombreux autres atouts comme la réduction de formation des boues de traitement et le besoin de faibles quantités de réactifs. A ce sujet, le procédé d'électro-oxydation sera comparé à l'électro-peroxydation en utilisant une à deux pièces d'anodes et de cathodes pour l'oxydation des MPs et NPs de polystyrène dans l'eau. La combinaison de techniques analytiques telles que la spectroscopie infrarouge à transformée de fourier (IRTF), spectrophotométrie UV visible, spectroscopie de fluorescence, le carbone organique total (COT) d'échantillons filtrés et non, et la pesée de la masse ont permis d'évaluer l'efficacité des procédés. L'impact des paramètres opératoires (densité de courant, le type et la surface de l'anode et de la cathode, le type et la concentration de l'électrolyte) a été étudié dans l'eau synthétique dans l'optique de l'identification des meilleures conditions pour le traitement des eaux usées réels de buanderie. Toutefois, étudier davantage les procédés électrochimiques est crucial afin de baisser leurs consommations énergétiques et améliorer leurs performances d'élimination.

1.2. Plastiques, micro- et nano-plastiques dans l'environnement

1.2.1. Plastiques : Production, consommation et déchets

En 2021, la production mondiale des matières plastiques était estimée à 390.7 millions de tonnes contre 359 millions de tonne en 2018 (Figure1.1.) (Plastics, 2019; PlasticsEurope, 2022). Les plus gros producteurs que sont la Chine, l'Amérique du Nord, l'Asie et l'Europe enregistraient respectivement 32%, 19%, 17% et 15% de cette production mondiale. Il est important de noter que ces chiffres de production n'ont pas considérés la production des fibres. En 2018, la production mondiale des fibres synthétiques était de 73,4 millions de tonnes (IndustrievereinigungChemiefaser, 2018/2019). Par conséquent, ces données de la production mondiale du plastique selon (PlasticsEurope, 2022) sont sous-estimées. Par ailleurs, il est estimé que d'ici 2050, la demande dépassera trois fois la production de 2016 qui était de 335 millions de tonnes (WEF, 2016).

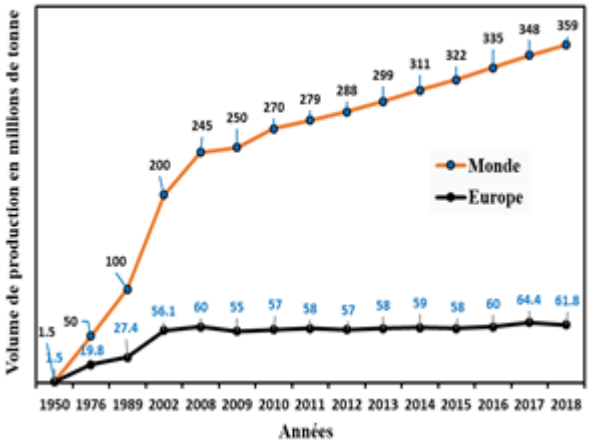

Figure 1. 1 : Évolution de la production de plastique dans le monde de 1950 à 2018, (PlasticsEurope Market research group, 2019).

Une étude comparative du marché de l'importation et de l'exportation des plastiques sur un échantillon de 7 pays (USA, Chine, Russie, Turquie, Corée du sud, Suisse, Arabie saoudite du sud) pour l'année 2018 est présentée dans la figure 1.2. (Plastics, 2019). On constate que l'importation de plastique est importante dans les pays comme les USA et la Corée du sud (Figure 1.2). Par contre, la Chine, l'Arabie saoudite et la Suisse présentent de faibles valeurs d'importation qui pourraient s'expliquer par la forte production au niveau local. La Chine, bien qu'elle soit le plus gros producteur exporte légèrement moins que les USA et la Turquie. Une grande partie des plastiques produits en Chine est éventuellement consommée dans son industrie. Ces produits industriels en plastiques, ou emballés dans le plastique, sont à leur tour distribués à travers le monde entier. 94% des exportations de la Chine sont constitués de produits manufacturés. Les USA sont présentés comme le premier partenaire commercial de l'industrie du plastique européen en 2018.

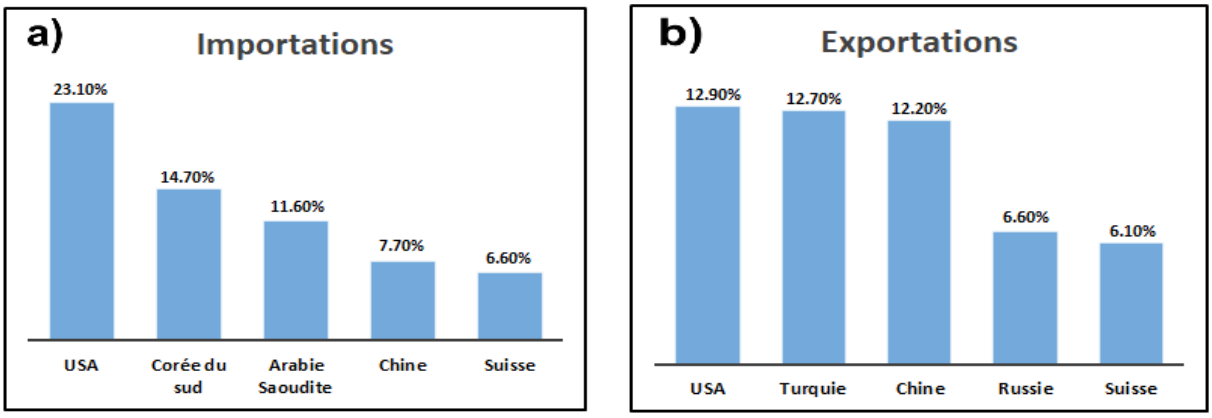

Figure 1. 2 : Marché du plastique dans les 7 pays partenaires commerciales du plastique hors Europe, (a) importations en 2018, (b) exportations en 2018 (PlasticsEurope 2019).

La production des polymères plastiques nécessite plusieurs étapes que sont : le craquage, l'oxydation ou la chloration, la polymérisation ou la polycondensation, l'ajout d'adjuvant (Fontanille & Yves Gnanou, 2013). La polymérisation consiste à lier à l'aide d'un catalyseur les monomères (comme le styrène, propylène, éthylène) entre eux de manière linéaire afin de créer la chaine polymérique. La polycondensation consiste à enlever les petites molécules, l'eau par exemple, pour former le polymère par condensation chimique (Fontanille & Yves Gnanou, 2013). Lors de la production des polymères plastiques, des additifs plastiques (bisphénol A, phtalates, etc) sont ajoutés afin de conférer aux matériaux plastiques des propriétés de plastifiants, retardateurs de flammes, stabilisants, ou antioxydants (OECD, 2009).

Les plastiques sont une grande famille de matériau constituée de plusieurs types de polymères classés en deux catégories de plastique : les thermoplastiques et les thermodurcissables (Plastics, 2019). Les thermoplastiques constituent la famille des plastiques qui peuvent être fondus lorsqu'ils sont chauffés et durcis une fois refroidis. Ces caractéristiques donnent au matériel son nom réversible. Autrement dit, ils peuvent être réchauffés, remodelés à plusieurs reprises. Les thermodurcissables sont de la famille des plastiques qui subissent un changement chimique lorsqu'ils sont chauffés. Par conséquent, après qu'ils soient chauffés et formés, ces plastiques ne peuvent pas être refondus et reformés.

Chaque plastique est conçu avec des caractéristiques spécifiques (Tableau 1.1) et est idéal pour l'application à laquelle il est destiné. Les produits en plastique ont des caractéristiques exceptionnelles telles qu' un poids léger, durable et polyvalent, et une production à faible coût

(Ivleva *et al.*, 2017). Ces performances le rendent indispensable dans plusieurs domaines. L'emballage est le plus grand secteur en termes de consommation des plastiques au monde. Cette consommation représente environ le quart de la production mondiale (Figure 1.3a). Il comprend les emballages de nourriture, des briques de lait, des sacs d'achats, et des bouteilles d'eau, qui sont des produits largement incorporés dans nos routines quotidiennes.

Six principaux types de plastiques produits de manière industrielle dominent le marché du plastique (Figure 1.3b). Il s'agit du polyéthylène (PE faible densité PEFD, PE haute densité, PEHD), du polypropylène (PP), du polychlorure de vinyle (PVC), du polystyrène (PS, et EPS expansé), du polyuréthane (PUR) et du polyéthylène téréphtalate (Andrady & Rajapakse, 2017). Ces polymères plastiques sont appelés les polymères de commodité ou de grande diffusion. Ils représentent à eux seuls plus de 80% de la demande de plastique en Europe (Plastics, 2019).

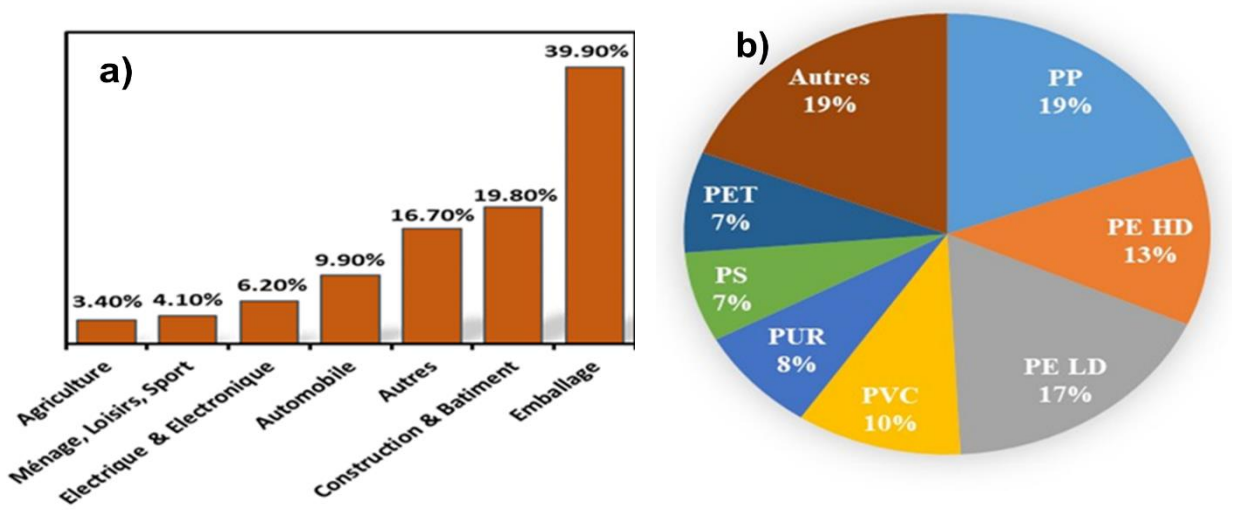

Figure 1. 3 : Demande européenne de plastique (a) par secteur d'activité en 2018 (b) par type de polymère (Plastics, 2019).

Tableau 1. 1 : Caractéristiques des différents polymères plastiques de grande diffusion.

Polymères	Monomères	Densité
Polyéthylène (PE)	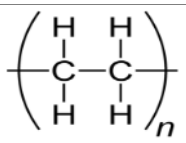	0,90 – 0,97
Polypropylène (PP)	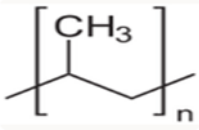	0,83 – 0,90
Polystyrène (PS)	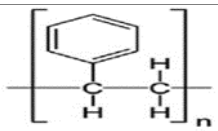	1,04 – 1,05
Polyuréthane (PUR)	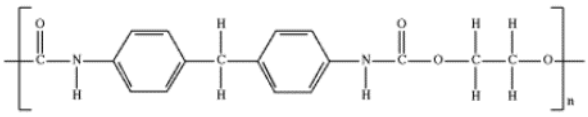	1,2
Polyéthylène téréphtalate (PET)	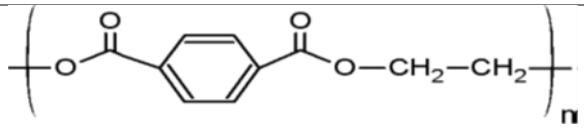	1,34 – 1,37
Polychlorure de vinyle (PVC)	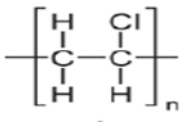	1,38 – 1,4

Après consommation, une partie des déchets plastiques sont collectés pour traitement. En ce qui concerne spécifiquement les matériaux d'emballage plastique, dont 78 millions de tonnes ont été produits en 2013, 14 % ont été recyclés, 14 % incinérés, 40 % mis en décharge et 32 % se sont retrouvés dans l'environnement à l'échelle mondiale (WEF, 2016). En 2018, sur près de 25 millions de tonnes de plastiques d'emballage produits en Europe 17,8 millions de tonnes de déchets plastiques ont pu être collectés (Plastics, 2019) soit 42% recyclés, et 39,5% utilisés dans la production d'énergie. Environ 18,5 % de ces déchets collectés sont encore envoyés à la décharge. Cependant, les restrictions relatives aux décharges ne sont pas toujours appliquées. Sur 30 pays en Europe, seulement 7 appliquent les règles relatives aux décharges

(PlasticsEurope, 2018). Par conséquent, ces déchets se retrouvent dans l'environnement par le biais du vent et se transforment en de plus petits débris de plastique qui aujourd'hui soulèvent des préoccupations mondiales au sujet de sa large distribution et de leurs conséquences environnementales. Bien que le Canada, par rapport aux autres pays comme les États-Unis, ou les pays de l'Union Européenne ou hors Union européenne, présente le moins de fuite de plastique dans l'environnement, il n'est pas prévu que ces chiffres connaissent une baisse dans 30 ans (Figure 1.4.). En effet, dans l'environnement, les plastiques subissent des processus de vieillissement qui entraînent leur dégradation et leur fragmentation en particules de plus en plus petites appelées micro-plastiques (MPs) (particules inférieurs à 5 mm) selon (Lambert & Wagner, 2016) puis en NPs (particules dont la limite de taille supérieure est fixée à 100 nm par certains auteurs (Lusher *et al.*, 2017) et 1000 nm pour d'autres (Cole & Galloway, 2015a; Cole *et al.*, 2014). Autrement, les NPs sont définies comme étant des particules comprises entre 1 et 1000 nm résultant de la dégradation d'objets industriels en plastique et pouvant présenter un comportement colloïdal (Gigault *et al.*, 2018b).

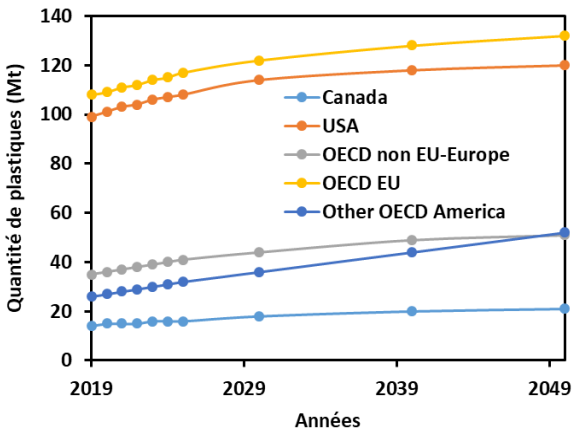

Figure 1. 4 : Estimations des fuites de plastique vers les milieux aquatiques à la fois en eau douce et dans l'océan par région. Source : OECD (2022), Global Plastics Outlook: Policy Scenarios to 2060.

1.2.2. Sources de provenance des micro- et nano-plastiques

En fonction de leurs sources de provenance, il est possible de distinguer des micro/nano-plastiques primaires et secondaires. L'utilisation des filets de pêche, des produits cosmétiques,

de nettoyage et les microfibres des vêtements issus des machines de lavage sont les principales sources de MPs dans les systèmes aquatiques par le biais des effluents des stations de traitement des eaux usées (Carr *et al.*, 2016; Duis & Coors, 2016; Murphy *et al.*, 2016a). Il a été montré qu'entre 4 594 et 94 500 particules de PE (164 – 327 µm) pouvaient être libérées lors d'une seule utilisation (≈ 5 mL) d'un produit cosmétique sous forme liquide (Napper *et al.*, 2015b). En outre, les granules utilisés pour l'industrie des plus grandes pièces plastiques et les microbilles utilisées comme abrasifs industriels (Figure 1. 5) (Lusher *et al.*, 2015) atteignent l'environnement suite à des problèmes lors du transport ou du stockage (Claessens *et al.*, 2013b; Gregory, 2010). Par ailleurs, un tissu en acrylique peut produire jusqu'à 729 000 fibres contre 138 000 et 496 000 fibres par lavage pour des tissus en polyester-coton et en polyester seul (Napper & Thompson, 2016a). Dépendamment du système de traitement utilisé et de la taille des MPs considérée, les stations de traitement vont éliminer plus ou moins efficacement les MPs dans des effluents. (Carr *et al.*, 2016). Malgré cette efficacité relative, les stations de traitement conventionnels demeurent des sources et des voies potentielles de rejets de micro/nano-plastiques dans l'environnement vu les grandes quantités d'effluents rejetés par jour (Dris *et al.*, 2015a; Gundogdu *et al.*, 2018b). D'après les statistiques, environ 8 milliards de microbilles sont libérées quotidiennement dans les milieux aquatiques par l'intermédiaire des STEPs (Rochman *et al.*, 2015). Il a été estimé qu'entre 63 000 et 430 000 tonnes de MPs sont déversés sur les sols européens via les boues d'épuration (Nizzetto *et al.*, 2016). Ces auteurs estiment que ces MPs finissent par retourner et s'accumuler dans les systèmes aquatiques (Leslie *et al.*, 2017a; Michielssen *et al.*, 2016). Cette catégorie de micro- et nano-plastiques qui arrivent dans les eaux déjà avec leur taille micro ou nanométrique sont désignés comme les MPs/NPs primaires. Les MPs secondaires proviennent de la dégradation des gros matériaux plastiques conduisant également à la libération de micro puis en nano-plastiques dans l'environnement (da Costa *et al.*, 2016). (Lambert & Wagner, 2016) par exemple ont caractérisé la formation des NPs lors de la dégradation d'un couvercle de tasse à café jetable en PS sous rayonnements UV. Leurs résultats ont clairement montré une augmentation de la formation de NPs au fil du temps d'exposition. Après 56 jours d'exposition, la concentration de nano-plastiques dans l'échantillon en fin d'exposition était de 1,26 x 10^8 particules/mL (taille moyenne des particules 224 nm), contre 0,41 x 10^8 particules/mL dans le témoin. En plus de la photo-oxydation sous rayonnements UV (Cai *et al.*, 2018b), l'hydrolyse, la bio-assimilation, les fractures mécaniques dues à l'abrasion du sable et des turbulences de l'eau, sont des mécanismes par lesquels les méso-plastiques et micro-plastiques sont fragmentés

(Cooper & Corcoran, 2010a; Gewert *et al.*, 2015a). Les polymères contenant des hétéroatomes tels que le poly(uréthane) (PU) et le PET se dégradent principalement par hydrolyse (Gewert *et al.*, 2015a).

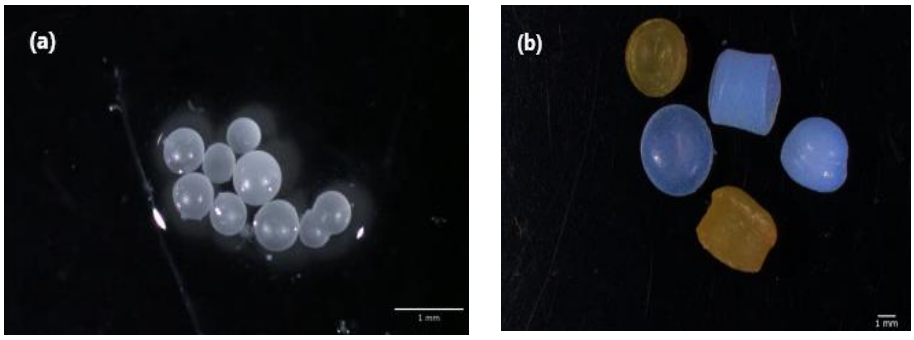

Figure 1. 5 : (a) Microbilles de Polyéthylène retrouvées dans un produit cosmétique et (b) granulés pour l'industrie récoltés sur la plage d'Equihen (Hermabessiere, 2018).

1.2.3. Apparition de micro- et nano-plastiques dans le milieu aquatique

De nombreuses études ont examiné la présence des MPs dans les milieux marins, les eaux douces, les eaux des stations d'épuration, et ce à travers de nombreux pays (Tableau 1. 2). Il ressort que la pollution de ces milieux par les MPs est globale. En plus, les premiers rapports des médias sur la présence des micro-plastiques dans l'eau potable sont apparus en 2017, suivis des publications scientifiques en 2018 (Eerkes-Medrano *et al.*, 2018). Cependant, il est possible que cette omniprésence des micro-plastiques dans les eaux soit sous ou surestimée, car de nombreuses études mentionnent les limites de leurs dispositifs d'échantillonnage et indiquent qu'entre 22% et 90% de particules suspectées être des micro plastiques ne le sont pas après analyses par spectroscopie FT-IR (Lares *et al.*, 2018; Magnusson & Norén, 2014; Ziajahromi *et al.*, 2017b). Afin d'augmenter la précision sur la quantification des MPs, plusieurs analyses de détection ont été effectués pour accompagner l'identification des MPs par la caractérisation chimique par spectroscopie FTIR. Cependant certaines études se sont limitées au comptage visuel par microscopie (Eriksen *et al.*, 2013b; Free *et al.*, 2014; McCormick *et al.*, 2014b; Vermaire *et al.*, 2017). Hidalgo-Ruz et al. (2012) estime l'erreur qui accompagne les résultats de quantification des MPs de moins de 100 µm à plus de 70%. Malgré que les protocoles analytiques aient été optimisés pour analyser avec précision les MPs dans les eaux réelles (Hurley *et al.*,

2018; Löder *et al.*, 2015; Tagg *et al.*, 2016; Tagg *et al.*, 2015), la détection des nano-plastiques est toujours difficile. En effet, à ce jour, aucun rapport n'a signalé l'occurrence des NPs dans les eaux réelles. Le tableau 1.2 permet d'illustrer, pour différents pays, les valeurs minimales-maximales, les moyennes et les décharges théoriques relatives de MPs détectées dans les influents et effluents des stations d'épuration et dans les eaux de surface.

Tableau 1. 2 : Concentrations en nombre de particules (+ MPs/L), (* MPs/m^3), (MPs/km^2) dans les différentes eaux et les décharges de stations de traitement en (***MPs/jour/station).**

Matrices	Continent/Pays	Taille MPs (µm)	Concentration (Nombre de particules)	Références
Eau marine	Amérique	-	1534 **	(Law *et al.*, 2010)
	Amérique	-	26898 **	(Eriksen *et al.*, 2013c)
	Asie	-	87000 **	(Yamashita & Tanimura, 2007)
	Australie	-	4256-8966 **	(Reisser *et al.*, 2013)
	Europe	-	243853 **	(Cozar *et al.*, 2015)
Eau de surface	USA	> 333	0,81-17,93 *	(McCormick *et al.*, 2014b)
	Canada	> 100	0,05-240 *	(Vermaire *et al.*, 2017)
	Chine	> 50 > 48	1660-8925 * $1{,}26.10^4$ *	(Di & Wang, 2018a) (Free *et al.*, 2014)
	Pays bas	> 30	27000 *	(Karlsson *et al.*, 2017a)

	Royaume uni	> 270	0,028 *		(Sadri & Thompson, 2014)
Influents avant traitement	USA	> 20	133 *		(Michielssen *et al.*, 2016)
	Danemark	> 10	2223 - 10044. 10^3 *		(Simon *et al.*, 2018)
	Finland	> 20	610. 10^3 *		(Talvitie *et al.*, 2015)
		> 250	57,6. 10^3 *		(Lares *et al.*, 2018)
	Pays-bas	> 0,7	68-910 *		(Leslie *et al.*, 2017a)
	France	> 100	293. 10^3 *		(Dris *et al.*, 2015b)
Effluents apres traitement	Allemagne	> 10	0,08-7,52.10^3 *	2,79.10^8 - 2,62.10^9 ***	(Dubaish & Liebezeit, 2013)
	Australie	> 25	1,5. 10^3 *	4,60 .10^{11} ***	(Ziajahromi *et al.*, 2017b)
	USA	> 125	4 *	5,28.10^7 ***	(Mason *et al.*, 2016a)
		> 40	0,0 *	0,0 ***	(Carr *et al.*, 2016)
	Finlande	> 20	20-300 *	1,26.10^9-6,59.10^{10} ***	(Talvitie *et al.*, 2017a)
	Scoland	> 65	0,25. 10^3 *	6,52 .10^{10} ***	(Murphy *et al.*, 2016a)
Eaux potables	République tchèque.	< 10	EB: 1473 – 3,605 $^+$ ET : 33 – 628 $^+$		(Pivokonsky *et al.*, 2018)

	14 pays	> 2,5	ER : 0 – 61 ⁺	(Kosuth *et al.*, 2018)
	Allemagne	> 20	ESB, EST: 0 – 7 *	(Mintenig *et al.*, 2019)
	Allemagne	> 5	BR: 0,118 ± 88 ⁺ BC: 11 ± 8 ⁺ BV: 50 ± 52 ⁺	(Schymanski *et al.*, 2018)
	-	> 1	BR: 4,889 ± 5,432 ⁺ BV : 6,292 ± 10,521 ⁺	(Ossmann *et al.*, 2018)

EB : Eau brute, ESB : Eau souterraine, BR : Bouteille réutilisable, ER : Eau de robinet, ET : Eau traitée, EST : Eau souterraine traitée, BV : Bouteille en verre, BC : Bouteille en carton.

Grâce à ces valeurs (tableau 1.2), il est possible d'observer une large variation des concentrations de micro-plastiques de 0 à plus de 10^3 MPs/m^3 ou MPs/km^2 dans toutes les matrices aquatiques. Une comparaison entre ces différents résultats serait biaisée du fait de la différence des méthodes d'échantillonnages et d'analyse utilisées par ces études. Par conséquent, l'importance de la contamination des eaux entre pays, ne pourrait être classée. Néanmoins, on constate que les eaux de surface sont largement plus concentrées que les effluents qui sortent des stations de traitement malgré l'effet de dilution des grandes quantités des eaux de surface. Ces fortes concentrations dans les eaux de surface sont dues d'une part à l'accumulation des faibles concentrations relatives en MPs des effluents des différentes stations d'épuration et d'autre part à de nombreuses autres sources terrestres. En plus, les MPs retrouvées dans les eaux sont de différents types de polymères et présentent des formes très diversifiés (Figure 1. 6).

Pour les eaux de surface, les plus grandes concentrations sont détectées en Chine et au Pays-Bas ou celles-ci atteignent respectivement $2{,}7.10^4$ MPs/m^3 et $1{,}26.10^4$ MPs/m^3 pour des particules de tailles > 270 µm et > 48 µm. Par contre pour les effluents, les USA enregistrent les plus faibles valeurs variant de 0-4 MPs/m^3. Ce qui expliquerait les plus faibles valeurs de MPs dans les eaux de surface qui s'y trouvent.

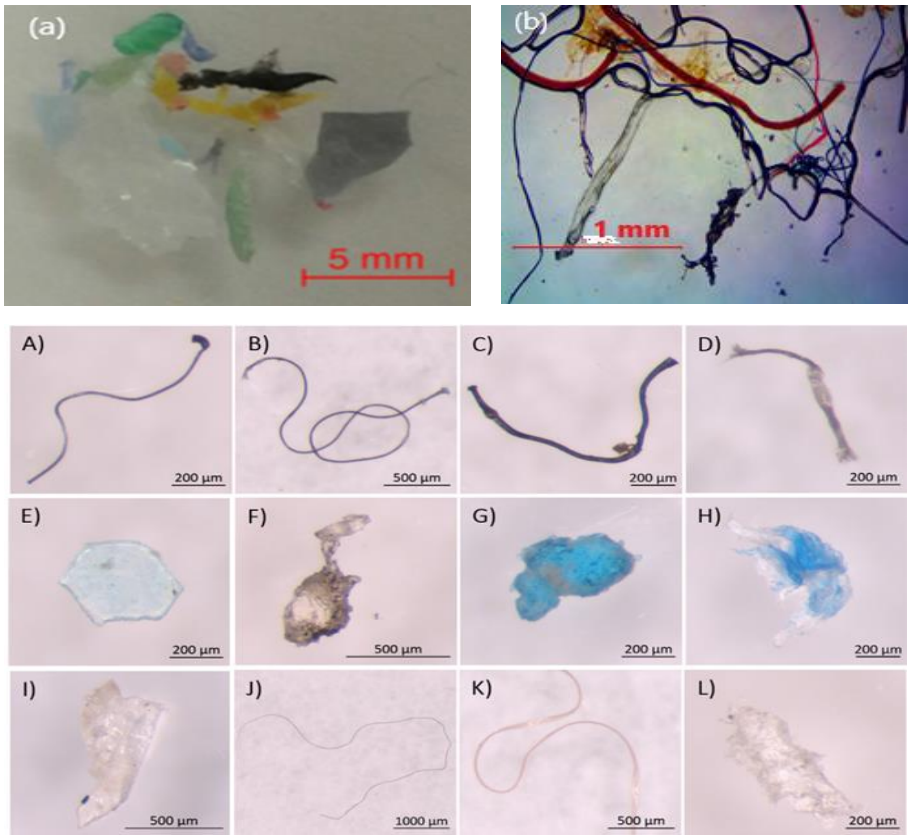

Figure 1. 6 : Formes de MPs dans les eaux de surface et sédiments (rivière d'Ottawa et affluents) (Vermaire *et al.*, 2017), aspects de polymères détectés des effluents a différentes étapes de traitement (Lares *et al.*, 2018).

1.2.4. Impacts et toxicité des micro- et nano-plastiques

À travers des simulations moléculaires, (Rossi *et al.*, 2014a) a démontré que les particules de PS nanométriques peuvent facilement pénétrer dans les membranes lipidiques des organismes et lorsque dissoutes dans la membrane, elles entraînent des changements dans la structure membranaire. Ce qui affecte la fonction cellulaire par l'effet de réduction de la diffusion moléculaire. (Tian Xia *et al.*, 2008) a par ailleurs montré que les NPs de PS à 60 nm étaient hautement toxiques pour les cellules macrophages (RAW 264.7) et épithéliales (BEAS2B) (Tian Xia *et al.*, 2008). Certaines particules de PS de 44 nm affectent la viabilité cellulaire, l'expression génique inflammatoire et la morphologie cellulaire, avec une forte régulation induite de gènes IL-6 et IL-8, cytokines impliquées dans les pathologies gastriques (Forte *et al.*, 2016). L'étude de

(Kashiwada, 2006) a montré une accumulation de nanoparticules de latex dans les branchies, les intestins, les testicules, le foie et le sang du poisson *Oryzias latipes*. Les NPs ont également été identifiés dans le cerveau des organismes. Ils sont donc capables de traverser la barrière hémato-encéphalique essentielle à la protection du cerveau contre les toxines systémiques et au maintien de l'homéostasie requis pour la fonction neuronale (Almutairi *et al.*, 2016). Une étude réalisée par (Wegner *et al.*, 2012) a évalué les effets des NPs de PS (30 nm) sur la production de pseudofèces et le poids de matières fécales des moules bleues (*Mytilus edulis* L.). Il a remarqué que l'activité filtrante de cette espèce de moule en présence de nano-plastique de PS avait été réduite. (Bergami *et al.*, 2016) a également utilisé des NPs à base de polyesters carboxylés et aminés (40–50 nm) pour étudier la mortalité et les effets sublétaux sur les larves d'*Artemia franciscana*. Les NPs ont nui à l'alimentation, à la motilité et à la mue multiple des larves. Plusieurs autres effets toxiques ont également été constatés auprès des organismes (Tableau 1.3). Les particules de NPs étant plus petites que les particules de MPs, elles sont susceptibles de présenter des effets toxiques légèrement différentes que les MPs (Chae & An, 2017a). (Ward & Kach, 2009) a analysé dans un écosystème marin, la toxicité des NPs de PS (100 nm) sur deux espèces de bivalves (*Mytilus edulis* et *Crassostrea virginica)* après 45 minutes d'exposition en enregistrant à la fois l'ingestion des deux espèces. Les résultats ont conclu que les NPs restent plus longtemps dans le corps que les MPs et peuvent être transportés vers la glande digestive (Ward & Kach, 2009). Par ailleurs, un test de toxicité utilisant des MPs et NPs simples et fluorescentes (50 nm, 500 nm et 6 µm) a montré que les NPs de PS à 50 nm n'affectaient pas la fécondité des copépodes marins (*Tigriopus japonicus*), mais toutes les autres tailles de plastiques (500 nm et 6 µm) inhibaient physiquement leur fécondation (Lee *et al.*, 2013). La dépendance de la toxicité des micro-plastiques en fonction de la taille des particules (50 et 500 nm et 6 µm) a aussi été analysées par (Jeong *et al.*, 2016b). L'exposition aux billes de plastique avait démontré une augmentation du stress oxydatif et des enzymes anti-oxydantes, et une diminution du taux de croissance, de la fécondité, de la durée de vie, du temps de reproduction et de la taille du corps de la rotifère *Brachionus koreanus*. Ces résultats ont conclu que la toxicité des MPs et NPs dépend de la taille et que les plus petites particules de plastiques sont plus toxiques que les plus grosses (Chae & An, 2017a; Jeong *et al.*, 2016b).

Tableau 1. 3 : Impacts des MPs et NPs de PS et PE sur les organismes aquatiques.

Plastique	organisme(s) aquatiques	Taille MPs	Concentrations MPs	Observations	Références
PS	*Chlorella* sp. et *Scenedesmus* sp.	20 nm	> 0,55 $g.L^{-1}$	Interference avec la photosynthèse	P. Bhattacharya et al., 2010
	Scenedesmus obliquus	70 nm	> 30 - 103 $mg.L^{-1}$	Inhibition de la croissance et réduction de la concentration chlorophyllienne des cellules	(Besseling *et al.*, 2014)
	Daphnia magna	70 nm	> 30 - 103 $mg.L^{-1}$	Réduction du taux de reproduction et de la taille corporelle	
	Phaeodactylum tricornutum	23 nm	10-100 $g.L^{-1}$	Formation accélérée de polymères extracellulaires bactériennes	(Chen *et al.*, 2011)
	Tigriopus japonicus	500 nm	1,25 et 25 $mg.L^{-1}$	Baisse de la fécondité	(Lee *et al.*, 2013)
	Mytilus edulis et crassostrea virginica	100 nm	$1.3.10^{7}$ $NPs.L^{-1}$	Accumulation des particules dans le tube digestif	(Ward & Kach, 2009)
	Mytilus.edulis	30 nm	0,1; 0.2 et 0.3 $g.L^{-1}$	Réduction de la capacité de filtration, production de pseudo -fèces	(Wegner *et al.*, 2012)
	*Larves de Artemia franciscana*l	40 nm	0,5; 25 et 50 mg/Ml	Entrave à la motilité des larves	(Bergami *et al.*, 2016)
	Carassius carassius	28 nm	10 $g.L^{-1}$	Changement dans le métabolisme des graisses	(Cedervall *et al.*, 2012)
	Carassius carassius	24 et 27	9.3×10^{15} $particles.L^{-1}$	Altération des comportements physiologiques et métaboliques	(Mattsson *et al.*, 2015)

	Paracentrotus lividus embryos	90 nm	> 3.85 $mg.L^{-1}$	Sévères défauts de développement	(Della Torre *et al.*, 2014)
PE et PS	*Mytilus galloprovincialis*	< 100 µm +pyrene	20 $g.L^{-1}$ PE/PS + 50 $mg.L^{-1}$ pyrene	Altération des réponses immulogiques, effets neurotoxiques, début de géno-toxicité et changements dans l'expression génétique	(Avio *et al.*, 2015)
PE	*Tripneustes gratilla*	10−45 µm	1, 10, 100, et 300 $spheres.mL^{-1}$	Pas d'effets significatifs	(Kaposi *et al.*, 2014)
	Eisenia andrei	>250 et < 1000 µm	62, 5; 125 et 500 $mg.kg^{-1}$	Effets histopatlogiques	(Rodriguez-Seijo *et al.*, 2017)
	Lumbricus terrestris	< 150 µm	1,2% (w/w) dans du sol	Croissance réduite et augmentation du taux de mortalité	(Huerta Lwanga *et al.*, 2016)
	Pomatoschistus microps	1–5 µm + Cr(VI)	0,184 $mg.\ L^{-1}$ + 18,9 $mg.L^{-1}$ Cr(VI)	Diminution de la performance des prédateurs (≤67%) Et une important inhibition de l'activité enzymatique (≤31%)	C.-S. Chen et al., 2011

1.3. Procédés électrochimiques d'oxydation avancée

Par l'application du courant électrique, les procédés électrochimiques d'oxydation avancée dégradent les polluants simultanément à la surface des électrodes par le transfert d'électron et par la production des espèces oxygénées réactives ($^{\bullet}OH$, $O_2^{\bullet-}$, $HO_2^{\bullet-}$, H_2O_2, etc.) dans la solution. Par comparaison avec les autres oxydants chimiques, le radical ^{o}OH a le potentiel redox le plus élevé (2.80 SHE) quel que soit le pH du milieu. Parmi les procédés électrochimiques d'oxydation avancée, on retrouve des procédés comme l'électro photo-catalyse, l'électro-oxydation, l'électro-Fenton, l'électro-photo-Fenton.

1.3.1. Électro-photo-catalyse

L'électro-photocatalyse est un procédé de dégradation qui consomme moins de produits chimiques mais aboutit à un certain niveau de dégradation ou à une minéralisation totale des polluants récalcitrants (Daghrir *et al.*, 2013a; Guitaya *et al.*, 2015; Hassen Trabelsi *et al.*, 2016). Il combine un photocatalyseur (semi-conducteur) et des radiations lumineuses, assisté par l'électrochimie. L'application d'une énergie supérieure ou égale à la différence d'énergie entre les bandes du photocatalyseur conduit à un transfert des électrons de la bande de valence à la bande de conduction, formant ainsi des trous positifs dans la bande de valence. En présence d'accepteurs d'électrons tels que O_2, H_2O et OH^-, ces charges photocatalysées entraînent la génération d'espèces oxygénées réactives ($HOO^{\bullet}$, H_2O_2, $O_2^{\bullet-}$, $OH^{\bullet}$). Le polluant va donc être oxydé soit directement par les trous « h^+ » à la surface du photo-catalyseur ou par ces espèces ainsi générées qui migrent dans l'eau. L'application du potentiel permet d'éviter la recombinaison des électrons/trous. Par conséquent, il se produit une augmentation de l'oxydation directe des polluants à la surface du photocatalyseur et la production de $OH^{\bullet}$ par l'oxydation des OH^- et de la molécule d'eau. Par ailleurs, l'utilisation de cathode comme le graphite ou le carbone vitreux afin de générer du peroxyde d'hydrogène dans la solution par réduction cathodique de l'oxygène, pourrait améliorer la production des $OH^{\bullet}$ disponibles pour la dégradation des polluants. Bien que tous ces éléments permettent d'améliorer l'efficacité du procédé, ce procédé comporte des limites telles que l'encombrement des sites actifs des photo-catalyseurs due à une grande concentration des polluants et la durée de vie des photo-catalyseurs et des lampes.

1.3.2. Électro-oxydation

L'électro-oxydation (EO) est un procédé prometteur pour le traitement de diverses eaux usées polluées par des composés organiques non oxydables chimiquement ou difficilement oxydables tels que les produits pharmaceutiques, les pesticides et les hydrocarbures aromatiques polycycliques (HAPs), retrouvés dans les effluents industriels et les eaux usées municipales (Garcia-Segura *et al.*, 2015a; M. Panizza *et al.*, 2001; Yassine *et al.*, 2018). En effet, les stations de traitement municipales ne sont pas en mesure d'éliminer complètement ces composants. La présence de ces polluants dans les effluents déversés permanemment dans l'environnement présente une importance particulière car elles peuvent causer de la toxicité chronique avec des effets subtils sur les animaux et les plantes aquatiques.

Par l'application de l'électro-oxydation, des taux d'élimination de COT allant jusqu'à 100% ont été reportés pour le bisphénol A et l'acide clofibrique respectivement après 14h et 7h d'électrolyse lorsque l'anode DDB (diamant dopé au bore) est utilisée (Murugananthan *et al.*, 2008; Sirés *et al.*, 2006).

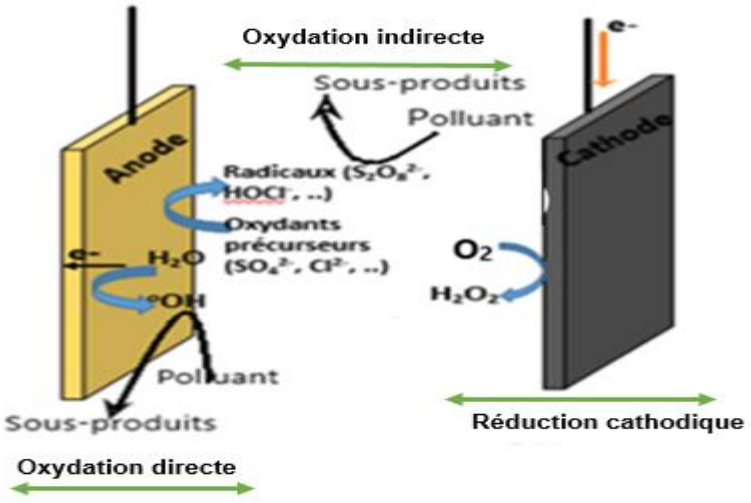

Figure 1. 7 : Principe de l'électro-oxydation.

L'EO est un procédé basé sur la génération *in situ* des radicaux hydroxyles et des oxydants à longue durée de vie (par exemple les ions hypochlorites, ions persulfates) (Figure 1.7) par les processus électrochimiques direct (Comninellis & Chen, 2010; Martínez-Huitle & Brillas, 2009) et indirect (Michaud *et al.*, 2000; Rajkumar *et al.*, 2007) suivant les réactions (Eq.1.1-1.5).

Équation 1.1 : $2\,Cl^- \rightarrow Cl_2 + 2e^-$

Équation 1.2 : $Cl_2 + H_2O \rightarrow HOCl + H^+ + Cl^-$

Équation 1.3 : $HOCl \rightarrow H^+ + OCl^-$

Équation 1.4 : $2HSO_4^- \rightarrow S_2O_8^{2-} + 2H^+ + 2^{e-}$

Équation 1.5 : $S_2O_8^{2-} + H_2O \rightarrow 2HSO_4^- + {}^1/_2\,O_2$

L'action directe d'oxydation anodique des composés organiques s'effectue en deux étapes (Comninellis, 1994; Drogui *et al.*, 2007). Premièrement, une décharge anodique de la molécule d'eau est obtenue avec formation du radical hydroxyle (^{o}OH) adsorbé sur des sites actifs de l'électrode (M) (Eq.1.6-1.8). Par la suite, le polluant organique (R) est oxydé par les radicaux libres adsorbés sur l'électrode formant ainsi un produit organique partiellement oxydé (RO). Ce produit oxydé (R) peut être davantage oxydé en CO_2 et H_2O (Eq.1.7-1.8) par les radicaux hydroxyles qui sont continuellement formés par la décharge anodique de l'eau.

Équation 1.6 : $M + H_2O \rightarrow M(OH^{\circ}) + H^+ + e^-$

Équation 1.7 : $R + M(OH^{\circ}) \rightarrow M + RO + H^+ + e^-$

Équation 1.8 : $R + M(OH^{\circ}) \rightarrow M + mCO_2 + nH_2O + H^+ + e^-$

Toutefois, l'efficacité de ce procédé dépend principalement de plusieurs conditions : la passivation des électrodes, le matériau d'anode, la densité du courant, la nature et concentration du polluant organique, et l'électrolyte de support. De nombreux auteurs soutiennent que l'électrode de DDB (diamant dopé au bore) est l'anode la plus efficace pour la dégradation des polluants organiques réfractaires sans que la nature du polluant n'affecte significativement l'efficacité du procédé (Rodrigo *et al.*, 2010). Après 4 h de traitement de l'acide 2,4 dichlorophenoxy-propionique, des taux d'abattement de 63, 82, et 97 % de COT pour des densités de courant respectives de 100, 300, and 450 mA.cm^{-2} ont été rapportés (Brillas *et al.*, 2007). Ce qui confirme l'efficacité du DDB et montre l'importance de la densité du courant appliquée dans l'efficacité de l'électro-oxydation (Anglada *et al.*, 2009; Khandegar & Saroha, 2013). L'augmentation de la densité de courant, a donc eu un effet positif sur la production de radicaux hydroxyles à la surface du BDD suivant la réaction (Eq.1.9) pendant l'électrolyse.

Équation 1.9 : $H_2O + BDD \rightarrow BDD(OH^{\circ})$

Pour ce qui est de la nature de l'électrolyte de support, les effets isolés et combinés des électrolytes tels que le NaCl, Na_2CO_3 et Na_2SO_4 sur la dégradation du buprofézine (250 mg. L^{-1}) avec l'anode BDD en appliquant une densité de courant de 60 mA.cm^{-2} ont été expérimentés (Errami *et al.*, 2012). Il ressort qu'une minéralisation de 80% a été obtenue avec l'électrolyte NaCl (1g. L^{-1}) contre 92% de minéralisation avec un mélange équimolaire (NaCl + Na_2CO_3) après 2h de traitement. (Durán *et al.*, 2018) a démontré une grande réduction de COD par l'application de l'électro-oxydation sur des effluents d'eau de lavage des machines. L'électro-oxydation de ces eaux sans ajout d'électrolyte et à l'aide du Ti/Pt a permis un abattement de COD de 35% après 6h d'électrolyse. Avec l'ajout de 7g/L de Na_2SO_4 à ces eaux de buanderies l'abattement de COD a atteint 71% pour ce même temps de traitement. Ce qui pourrait s'expliquer par une oxydation additive due aux radicaux sulfates ($SO_4^{2\bullet-}$) et persulfates ($S_2O_8^{2-}$) ayant une durée de vie plus longue que les radicaux hydroxyles. Lorsque le BDD est appliqué avec des densité de courant de 33,3 et 66,6 mA.cm^{-2}, l'élimination du COD atteint respectivement 80 et 88,9% après 6h. Cependant, lorsque le Ti/Pt est appliqué, l'élimination a tendance à diminuer (71- 68%) avec l'augmentation de la densité de courant (de 33,3 à 66,6 mA.cm^{-2}). Il faut noter qu'une consommation d'énergie de près de 400 kWh.dm^{-3} a été nécessaire pour atteindre cette efficacité optimale.

Bien que l'électro-oxydation soit un procédé efficace pour la dégradation des polluants réfractaires, l'application de fortes densités de courant limitent majoritairement ce procédé à cause des réactions parasites telles que la formation d'oxygène (Eq. 1.10) au détriment des radicaux hydroxyles.

Équation 1.10 : $H_2O + M(OH^{\circ}) \rightarrow M + O_2 + 3H^+ + 3e^-$

1.3.3. Électro-fenton et Électro-photo-fenton

L'électro-Fenton est connu comme un traitement d'électro-oxydation indirecte basé sur l'utilisation combinée du peroxyde d'hydrogène (H_2O_2) et du fer (Fe^{2+})(Brillas *et al.*, 2009; Sirés *et al.*, 2007) a un pH acide. L'H_2O_2 est constamment fourni dans les eaux par réduction cathodique de l'oxygène (O_2) (Murugananthan *et al.*, 2011) suivant l'équation1.11. L'H_2O_2 réagit avec le Fe^{2+} ajouté pour produire des radicaux hydroxyles par la réaction de Fenton (Eq. 1.12). Le Fe^{2+} nécessaire à cette réaction de Fenton est régénéré dans la solution par la réduction cathodique du fer ferrique Fe^{3+} (Eq.1.13) (Borràs *et al.*, 2013).

Équation 1.11 : $O_2 + 2H^+ + 2e^- \rightarrow H_2O_2$

Équation 1.12 : $H_2O_2 + Fe^{2+} + H^+ \rightarrow Fe^{3+} + OH^{\circ} + H_2O$

Équation 1.13 : $Fe^{3+} + e^- \rightarrow Fe^{2+}$

Équation 1.14 : $Fe(OH)^{2+} + hv \rightarrow Fe^{2+} + OH^{\circ}$

Équation 1.15 : $2Fe(C_2O_4)_n^{3-2n} + hv \rightarrow 2Fe^{2+} + (2n-1)C_2O_4^{2+} + 2CO_2$

Le couplage de ce procédé avec les rayonnements UV ou solaires améliore la régénération du Fe^{2+} par photo-réduction du $Fe(OH)^{2+}$ qui est la forme prédominante du fer ferrique Fe(III) à un pH 2.5–4.0 suivant l'équation (1.14) (Sun & Plgnatello, 1993; Zepp, 1992) et par la photolyse des complexes Fe(III)–carboxylate (Eq.1.15) (Sirés *et al.*, 2006). L'EF et le EPF combinent deux sources de production de radicaux hydroxyles. C'est à dire que les polluants organiques peuvent être détruit simultanément par les radicaux hydroxyles homogènes formés à partir de la réaction de Fenton et par les radicaux hydroxyles BDD(˙OH) hétérogènes produits à la surface de l'anode à partir de la décharge de la molécule d'eau (Panizza & Cerisola, 2005). Sous des conditions similaires l'acide 4-Chlorophenoxyacetique et l'acide 2,4,5-trichlorophenoxyacetique, tous deux à concentration initiale de 100 mg/L de COT, ont pu être totalement éliminées respectivement après 540 et 360 min d'EO à l'aide de l'anode Si/BDD et une cathode en graphite (Brillas *et al.*, 2004). Cependant, l'EF réduit ces durées respectives de complète minéralisation à 15 et 10 min pour une densité de courant 33.3 mA/cm^2. L'EO a nécessité plus de temps pour une élimination complète de la matière organique, car comme le montre la Figure 1. 8 (Yu *et al.*, 2014) sur le mécanisme général de dégradation des polluants aromatiques par procédé EO, EF ou EPF (Brillas *et al.*, 2004; Murugananthan *et al.*, 2008), l'acide oxalique et l'acide formique formés après oxydation des composés par les radicaux hydroxyles à la surface de l'anode sont difficilement éliminées par la suite.

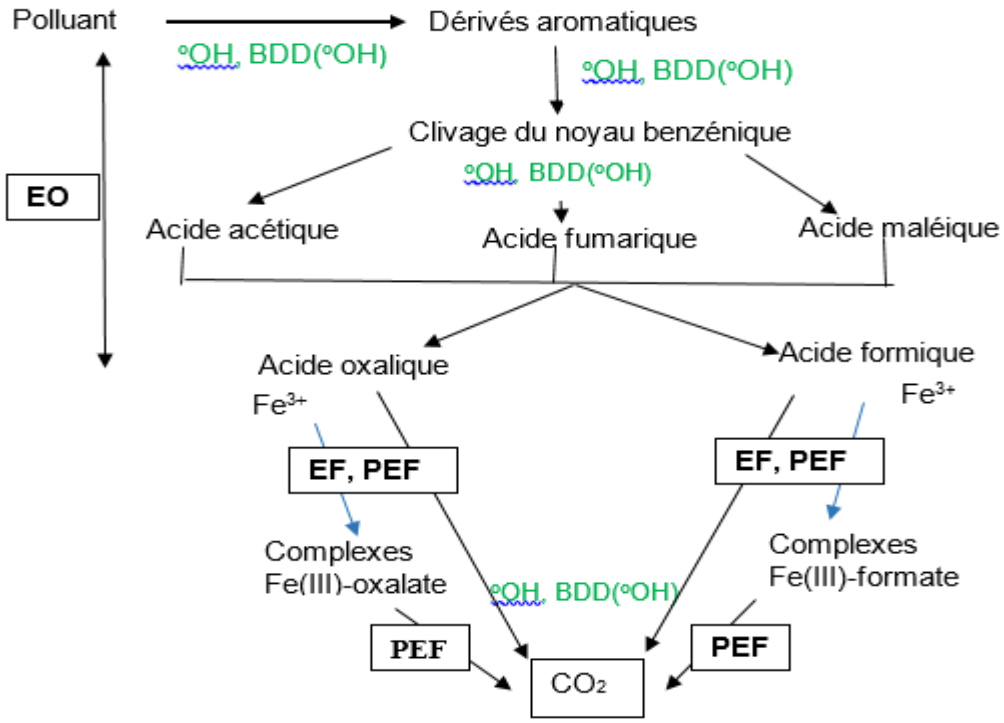

Figure 1. 8 : Mécanisme général de dégradation des polluants aromatiques par EO, EF, EPF modifié de Xinmin Yu et al, 2014.

L'efficacité de l'EF et EPF dépend essentiellement des paramètres tels que le pH, l'intensité du courant, la nature des électrodes, la nature de l'électrolyte, le rapport Fe^{2+}/H_2O_2.

Le pH est le facteur clé du procédé électro-Fenton et EPF car la réduction de l'oxygène en peroxyde d'hydrogène se fait en milieu acide. De plus, en milieu acide, l'espèce Fe^{2+} est la plus dominante par rapport à Fe^{3+}, ce qui favorise la réaction de Fenton. En effet, pour la dégradation de 41 mg. L^{-1} d'ibuprofène avec une concentration en Fe^{2+} de 0,5 mM et une densité de courant de 33,3 $mA.cm^{-2}$ pour 6h, (Ciríaco *et al.*, 2009) a obtenu des taux d'abattements en COD croissants dans l'ordre suivant : pH = 2 < pH = 6 < pH = 3. A des valeurs de pH élevées, trois éléments majeurs réduisent l'efficacité du procédé électro-Fenton : 1) une dissociation rapide du H_2O_2 en oxygène et molécules d'eau, 2) une réduction de l'oxygène en ions hydroxydes et non en peroxyde d'hydrogène, 3) une diminution de la quantité de Fe^{2+} dans le milieu par précipitation du Fe^{3+} en $Fe(OH)^{3+}$. En revanche, en milieu très acide, l'efficacité de l'EF est limitée par la formation de complexe stable entre le Fe^{2+} et H_2O_2 au détriment de la formation des radicaux

hydroxyles. Par ailleurs (Tang & Huang, 1996) montrent qu'en milieux très acides (pH ≤ 2), le piégeage des radicaux hydroxyles (^{o}OH) par les protons H^+ est accéléré (Eq. 1.16).

Équation 1.16 : $O_2 + 2H^+ + 2e^- \rightarrow OH^- + HO_2^-$

Tous ces éléments peuvent jouer sur le rapport molaire (Fe^{2+}/H_2O_2) optimal qui est également un facteur déterminant dans l'efficacité du procédé électro-Fenton. Ce rapport optimal est spécifique à chaque polluant. Des faibles ou des fortes concentrations en peroxyde d'hydrogène et en Fe^{2+} peuvent limiter la production des radicaux hydroxyles (Pozza *et al.*, 2005), à cause de la prédominance des réactions parasites (Eq.1.17,1.18). Généralement des rapports de 0,1; 0,2 et 0,5 sont testés (Ciríaco *et al.*, 2009; Guinea *et al.*, 2010).

Équation 1.17 : $Fe^{2+} + OH^{\circ} \rightarrow Fe^{3+} + OH^-$

Équation 1.18 : $H_2O_2 + OH^{\circ} \rightarrow H_2O + HO_2^{\circ}$

L'efficacité de L'EF est dépendante de l'intensité du courant. En effet, il contrôle la vitesse de production du peroxyde d'hydrogène et le taux de régénération du Fe^{2+} (Sires *et al.*, 2014). Par conséquent, augmenter l'intensité du courant accroit la production du peroxyde d'hydrogène et l'électro-régénération du fer ferrique (Fe^{3+}) en fer ferreux (Fe^{2+}), ce qui améliore la production des radicaux hydroxyles. (Brillas *et al.*, 2007), pour la minéralisation du 2-4DP (217 mg. L^{-1}) à pH = 3, avec [Fe^{2+} / Fe^{3+}] = 1 mM et en présence d'une anode Si/BDD et cathode ADE, a obtenu un taux de minéralisation décroissant dans l'ordre suivant de densités du courant 450 (97%) > 300 (88%) > 100 (82%) mA.cm^{-2}. Cependant, lorsque l'intensité de courant appliquée est au-dessus de la valeur optimale, la réduction de l'oxygène peut conduire à la formation d'eau et ces réactions (Eq.1.19-1.20) augmentent progressivement avec les fortes intensités, ce qui limite l'électro-régénération du fer ferrique (Fe^{3+}) en fer ferreux (Fe^{2+}). Par conséquent, les fortes intensités de courant causent la chute de l'efficacité du procédé électro-Fenton (Zhang *et al.*, 2007).

Équation 1.19 : $O_2 + 4H^+ + 4e^- \rightarrow H_2O$

Équation 1.20 : $2H^+ + 2e^- \rightarrow H_2$

Bien que les procédés EF et EPF présentent des limites dues aux réactions parasites discutées ci-dessus, les procédés électrochimiques pourraient être efficaces pour la dégradation des micro/nano-plastiques.

Généralement, dans les systèmes de traitement des eaux usées, il est judicieux d'appliquer ces procédés comme traitement tertiaire pour permettre une production optimale des radicaux hydroxyles à des valeurs de pH acide (H_2O_2 /Fe^{2+}) et une action efficace de ces radicaux hydroxyles sur les polluants organiques. Ce placement permet aussi d'éviter une diminution de l'efficacité du traitement biologique par une carence en nutriments pour les bactéries.
Par ailleurs, ces procédés ne nécessitent pas un grand investissement financier (faible emprise au sol et de consommation de réactifs) et ne comporte apparemment pas de pollution secondaire parce que la minéralisation des composés réfractaires produit du CO_2 et de l'eau.

1.3.4. Importance de la configuration de la cellule électrolytique

Afin d'obtenir un traitement efficace des eaux usées par procédé électrolytique, en termes de performance et d'économie, l'un des facteurs les plus importants à prendre en compte est la conception de la cellule électrochimique. Généralement, les facteurs tels que le transport de masse, la cinétique des réactions et la densité de courant électrique (intensité du courant rapportée à la surface des électrodes) sont les facteurs pris en compte pour la conception des configurations électrolytiques (Bebelis *et al.*, 2013; Chen, 2004). Plusieurs types de cellules électrochimiques telles que les réacteurs divisés, cellules non divisées avec des électrodes à plaques parallèles, réacteurs bipolaires avec écoulement, cellules non divisées à deux électrodes avec agitation et une enveloppe thermo stabilisateur externe sont répertoriées dans la littérature pour le traitement des eaux usées (Martinez-Huitle *et al.*, 2015). À l'échelle du laboratoire, ces configurations ont été utilisées avec succès pour la détermination de l'influence des paramètres opératoires ou des conditions de fonctionnement sur la dégradation des polluants. Ce qui permet de comprendre les mécanismes des processus électrochimiques pour les polluants réfractaires qui sont pour la plupart dissous dans l'eau. Plusieurs études (Zanin *et al.*, 2012; Zhang *et al.*, 2013) portant sur le traitement des polluants par l'électrolyse ont déterminé si l'oxydation directe et indirecte sont favorables pour une électrode donnée (type de matériau) et détaillent les produits intermédiaires et finaux obtenus dans des conditions de fonctionnement optimisées. Les principaux points à prendre en compte dans la conception de la cellule électrolytique sont : i) la forme des électrodes ; ii) le type d'électrolyte ; iii) les modèles d'écoulement ; iv) le transfert de chaleur et; v) l'identification des paramètres de mise à l'échelle. Pour ce qui est de l'écoulement, les cellules à réservoir mixte sont le plus utilisées à l'échelle laboratoire à cause de leur simplicité

en termes d'évaluation de traitement et d'interprétation mathématique des résultats. Les cellules à recirculation sont l'alternative la plus courante trouvée dans la littérature aux cellules à réservoirs mixtes. Ce type de cellule est généralement associé à des études en laboratoire dans lesquelles non seulement la cinétique mais aussi quelques informations supplémentaires sur les performances sont nécessaires à la discussion sur l'applicabilité de la technologie à plus grande échelle. Étant donné que la plupart des réactions pertinentes se produisent à la surface des électrodes, le transport de masse d'espèces à partir et vers la surface des électrodes est généralement le point crucial. Ainsi, cette limitation devrait être résolue dans le choix de la configuration pour une conception appropriée du modèle. Par conséquent, l'utilisation d'une cellule indivisée représente un dispositif approprié pour l'étude d'oxydation électrochimique des MPs/NPs dans les eaux résiduaires de buanderie. Notre objectif étant donc de comprendre d'abord la dégradation des MPs/NPs par oxydation électrochimique et de valider le concept au laboratoire. La conception de la cellule électrolytique inclue la forme, le nombre d'électrodes, le type et la concentration en électrolyte.

1.4. Problématique, hypothèses, objectifs et originalité

1.4.1. Contexte et problématique

Les travaux de (Thompson *et al.*, 2004) mettant en évidence la présence de micro-plastiques (MPs) dans les matrices environnementales (notamment dans les eaux et sédiments) a été l'élément déclencheur de l'intensification de la recherche sur les MPs. Par conséquent, de 2004 à 2019 on a assisté à une importante augmentation des articles publiés à ce sujet. Le nombre grimpant de ces publications ont permis de mieux éclairer les sources de provenance, la définition, le devenir, la dynamique, et l'occurrence des micro-plastiques dans les milieux aquatiques et les aliments (Carr *et al.*, 2016; Karbalaei *et al.*, 2018; Luo *et al.*, 2021). En outre, leur interaction avec les autres polluants tels que les hydrocarbures aromatiques polycycliques (HAPs), polychlorobiphényles (PCBs), les métaux lourds (Liu *et al.*, 2016; Williams *et al.*, 2020) et leur toxicité sur les organismes aquatiques ont été mis en évidence (Sangkham *et al.*, 2022; Yin *et al.*, 2021). Plusieurs technologies de traitement de cette pollution dans les eaux ont été étudiées pour pallier à ce problème. Malgré cet état de fait, un certain nombre de difficultés se posent encore. Récemment, il a été retrouvé des MPs dans le placenta et des échantillons de sang humain (Leslie *et al.*, 2022; Ragusa *et al.*, 2021). En plus il a été démontré que les MPs

affectent principalement le micro-biome intestinal humain et provoquent une cytotoxicité pulmonaire in vitro (Dong *et al.*, 2020; Smith *et al.*, 2018). En raison de cette toxicité potentielle pour l'homme et pour les organismes aquatiques, leur présence dans les eaux est à prendre en compte.

Une méthode analytique standard est la condition préalable à une comparaison fiable de l'efficacité des procédés de traitement des eaux quant à l'élimination des MPs/NPs. Actuellement, différentes méthodes d'échantillonnage, de traitement et d'identification sont utilisées pour la quantification des MPs/NPs dans les eaux. En effet, pour les eaux de surface, les concentrations de MPs sont estimées généralement en nombre de particules/km^2 ou en nombre de particules/m^3. Pour les influents/effluents des stations de traitement, elles sont quasiment exprimées en nombre de particules/L ou par m^3. Cependant, la surveillance environnementale nécessite des mesures en masse/volume. Pour ce qui est de l'évaluation des performances des procédés d'oxydation avancée, ce sont traditionnellement les mesures par spectrophotométrie UV-vis, de COT, COD, chromatographiques qui sont directement utilisées. Présentement, la méthode TED-GC-MS semble la mieux adaptée pour la quantification d'un polymère ayant une faible concentration massique. Cependant, elle reste encore inaccessible. Par conséquent, la quantification des performances de dégradation des MPs/NPs dans les effluents synthétiques ou réels reste une contrainte.

Afin d'améliorer l'élimination des MPs sub-micrométriques (< 300 µm dans les effluents des systèmes conventionnels de traitement) et (< 20 µm et microfibres pour les technologies membranaires de traitement) il est nécessaire qu'une meilleure approche de traitement des eaux contenant des MPs/NPs soit trouvée en vue de leur dégradation. Celle-ci permettra, d'une part, de réduire l'effet d'accumulation des faibles concentrations de micro- et nano-plastiques par le rejet des grandes quantités d'effluents dans l'environnement. D'autre part, dégrader les MPs dans les eaux résiduaires préviendrait aussi leur retour dans l'environnement. En effet, une quantité importante de MPs se retrouve dans les boues de traitement issues des technologies de séparation. Ces boues sont utilisées pour l'amendement des sols. Le traitement des micro-plastiques des eaux résiduaires fait majoritairement appel à des procédés physico-chimiques (incluant coagulation/floculation, décantation et filtration). En revanche, ce type de traitement (basé sur la séparation des micro-plastiques) se traduit par un transfert de pollution (de la phase liquide vers la phase solide) plutôt que par une véritable dépollution. Il en résulte une étape

supplémentaire de gestion de ces déchets plastiques. Les techniques de micro- et nano-filtrations sont également efficaces pour l'enlèvement des micro- et nano-plastiques mais elles sont très coûteuses et ne font que déplacer le problème. Pour y remédier, il est donc indispensable de trouver un moyen de dégrader complètement ces polluants en développant des traitements plus poussés par oxydation avancée. Ainsi, le choix d'une dégradation des particules par oxydation avancée adaptée au traitement des micro- et nano-plastiques a été privilégié. Le traitement par oxydation avancée est important pour minéraliser les polymères de MPs de petites tailles identifiés comme sources potentielles de la présence des MPs dans l'environnement.

Les procédés d'oxydation avancée sont l'une des technologies efficaces à la dégradation des polluants récalcitrants dans les eaux usées. Ils constituent donc une approche alternative pour l'élimination des MPs/NPs dans les effluents. Il existe très peu d'études dans la littérature portant sur la dégradation électrochimique ou photo-catalytique des MPs. Une étude récente a montré qu'une technologie de type électro-Fenton basée sur une cathode TiO_2/graphite, était capable de dégrader des micro-plastiques (100-200 µm) de chlorure de polyvinyle (PVC) avec une élimination de 75% après 6h d'électrolyse. Pour le procédé de photo-catalyse, une exposition de plus de 10 h n'a pas été suffisante à obtenir une efficacité de dégradation acceptable pour des micro-plastiques d'une taille de 25-500 µm (Ariza-Tarazona *et al.*, 2019). En outre pour parvenir à une élimination de 65% de micro-plastique de 154.8 ± 1.4 µm, il a fallu deux semaines sous irradiation de lumière visible (Uheida *et al.*, 2021). Par contre pour les nano-plastiques de 140 nm, 96 h ont été relativement suffisantes pour obtenir une minéralisation de 80% de nano-plastiques (Robert *et al.*, 2022). Ce qui montre que la taille des particules est un paramètre qui influence l'efficacité de dégradation des micro- et nanoparticules par les procédés d'oxydation avancée. Cependant, dans les eaux résiduaires les MPs/NPs retrouvés sont de taille, type (polymère) très diversifiés. Il est nécessaire que plusieurs études soient effectuées dans ce sens afin de déterminer et la comparaison de l'efficacité réelle des procédés quant à la diversité de la taille des MPs/NPs.

Les procédés électrochimiques d'oxydation avancée sont des techniques respectueuses de l'environnement qui ont attiré de plus en plus l'attention pour le traitement des eaux usées contenant des composés réfractaires. La force majeure de ces procédés est l'électro-génération des radicaux hydroxyles (puissants oxydants) sans ajout permanent de produits chimiques. L'une des limites majeures de ces procédés est la forte consommation énergétique lorsque de densités

de courant élevées sont appliquées. Cependant la production des radicaux hydroxyles en dépend. Aussi, comparativement aux polluants réfractaires dont l'efficacité des procédés électrochimiques ont été antérieurement démontrées, les MPs/NPs sont des grosses molécules (> 1000 $g.mol^{-1}$) synthétiques, sous forme de particules souvent non visibles à l'œil nu et non dissoutes dans l'eau. Ils sont persistants et formés de plusieurs monomères.

Le défi de cette étude serait donc d'élaborer un procédé d'oxydation électrochimique capable de dégrader/minéraliser les MPs/NPs dans les effluents réels avec une faible consommation énergétique. Pour ce faire, des méthodes analytiques devraient être adaptées pour l'évaluation de performance de traitement.

1.4.2. Hypothèses

Le procédé d'oxydation électro-catalytique (OEC) consiste à traiter les micro- et nano-plastiques dans un réacteur composé d'une anode à forte surtension en oxygène capable de générer des radicaux hydroxyles ($^{\bullet}OH$) et ce, par oxydation anodique de la molécule d'eau. Il est à rappeler que les radicaux $^{\bullet}OH$ sont les oxydants les plus forts que l'on puisse utiliser pour le traitement des eaux. Ainsi, grâce à des anodes électro-catalytiques, les radicaux $^{\bullet}OH$ seront générés et s'attaqueront aux micro- et nano-plastiques à la surface des électrodes. D'autres espèces oxygénées réactives (tels que H_2O_2, $H_2S_2O_8$, etc) seront simultanément générées en solution et contribueront à la dégradation des micro- et nano-plastiques. Le peroxyde d'hydrogène (H_2O_2) peut être généré *in-situ* par réduction cathodique de l'oxygène dissous sur une électrode appropriée de feutre de carbone, alors que les persulfates ($H_2S_2O_8$) peuvent être générés par oxydation des ions sulfates sur une anode de diamant dopé au bore (DDB).

Hypothèse 1.

La génération in situ d'espèces oxygénées réactives ($^{\bullet}OH$, $H_2S_2O_8$, etc) et l'utilisation d'électrodes volumiques ou sous forme de métal déployé constituent les deux éléments clés pour décontaminer les eaux des MPs/NPs, soit directement à la surface des électrodes ou indirectement par les espèces oxygénées réactives par le procédé d'électro-oxydation.

Hypothèse 2.

L'analyse de la granulométrie reliée à la mesure de masse des particules dans un même échantillon et les mesures d'absorbance à la spectrophotométrie UV-vis permettraient une quantification respective des micro-plastiques et des nano-plastiques dans l'eau. Par ailleurs, la combinaison de ces mesures avec les méthodes qualitatives de caractérisation de la matière organique totale dissoute et colloïdale dans les effluents (3D-EEM), de la taille-forme des micro/nano-plastiques (MEB) et d'identification de groupes fonctionnels (spectroscopique IRTF) permettraient d'obtenir une compréhension plus complète des mécanismes de dégradation électro-catalytique des micro- et nano-plastiques dans l'eau. Celles-ci pourraient confirmer l'effectivité de la dégradation des micro- et nano-plastiques par les espèces oxygénées réactives produits in situ.

Hypothèse 3.

Le fait de générer simultanément les persulfates et le peroxyde d'hydrogène dans une même cellule électrolytique permettrait d'initier l'activation des persulfates en oxydants radicalaires ($SO_4^{2\cdot-}$, $^{\bullet}OH$) plus puissants qui pourraient avoir un impact positif sur l'oxydation des micro- et nano-plastiques. Par conséquent, l'EO-H_2O_2 pourrait davantage dégrader/minéraliser les micro- et nano-plastiques.

Hypothèse 4.

L'apport de radiations UV (l ≈ 220 - 460 nm) permettrait d'activer les persulfates et accroitre la concentration des radicaux sulfates et hydroxyles nécessaires pour l'oxydation de la matière organique. Il serait également possible d'initier directement la réaction de décomposition de H_2O_2 sous irradiation lumineuse (λ=254 nm). Ce qui permettrait une dégradation totale des nano-plastiques par le procédé (EO-H_2O_2) /UV.

Hypothèse 5.

Le traitement des effluents de buanderie par l'EO-H_2O_2 sans aucune filtration préalable pourrait avoir un effet négatif sur l'efficacité de dégradation des nano-plastiques et les autres polluants de base dissouts. En effet, les eaux usées de buanderie contiennent des polluants non solubles qui pourraient interférer et inhiber l'action des oxydants produits in situ sur les nano-plastiques et la fraction dissoute des polluants de base. Le traitement des effluents avec préfiltration permettrait

alors aux oxydants de dégrader et de minéraliser efficacement les nano-plastiques y comprise la fraction dissoute de polluants de base des eaux.

1.4.3. Objectifs

Objectif global : Ce travail a pour but de concevoir, de tester et d'optimiser à l'échelle de banc d'essai en laboratoire, l'efficacité d'un procédé d'oxydation électro catalytique (OEC) pour la dégradation des micro-plastiques (MPs) et nano-plastiques (NPs) dans les eaux et effluents résiduaires de buanderie.

Objectif 1 : Mettre premièrement au point une méthode d'analyse quantitative alliant à la fois le profil de taille (diffusion dynamique de la lumière laser) /concentration massique des particules de micro-plastique et qualitative basée sur les propriétés morphologiques (analyse MEB) et physico-chimiques de surface (spectroscopie IRTF) des particules. Cette mise au point permettra d'évaluer la performance du procédé de dégradation et d'apprécier le comportement des micro-plastiques au cours du traitement.

Objectif 2 : Concevoir et construire un réacteur OEC avec une configuration qui offre la possibilité d'utiliser deux montages électrolytiques (2 et 3 électrodes), avec et sans irradiation UV, en intégrant des électrodes appropriées et une injection d'air, et ce, pour la dégradation des MPs/NPs.

Objectifs 3 : Tester l'efficacité du procédé d'électro-oxydation (EO) et déterminer les meilleures conditions opératoires pour le traitement des eaux synthétiques contaminées par les micro-plastiques (25 µm de diamètre nominal). Pour ce faire, il est prévu d'étudier plusieurs paramètres : le type d'anode (MMO, IrO_2 et BDD), la surface anodique active (41cm^2 versus 83 cm^2), le type (Na_2SO_4, $NaNO_3$, NaCl) et concentration (0.03 - 0.06 M) de l'électrolyte, le temps de traitement (60 - 360 min).

Objectif 4 : Évaluer la capacité des réacteurs électrolytiques à générer *in situ* des espèces oxygénées réactives ($^{\bullet}OH$, H_2O_2, $H_2S_2O_8$) en utilisant des méthodes directe et indirecte de quantification (dosage colorimétrique à la solution de sulfate de cérium acidifiée, mesure des absorbances au spectrophotomètre UV-vis du N, N-Dimethyl-4-nitroso-aniline et de l'ion tri-

iodure I_3^-). Il s'agit de mettre en évidence la contribution des oxydants dans le processus d'oxydation électro-catalytique des nano-plastics (100 nm de diamètre nominal de NPs de polystyrènes) et de comparer l'efficacité du procédé EO, EO-H_2O_2 et (EO-H_2O_2) /UV.

Objectif 5 : Appliquer le procédé OEC pour le traitement des effluents réels de buanderies (identifiés comme étant un vecteur potentiel de contamination des eaux municipales par les MPs/NPs) dopés de NPs avec les meilleures conditions préalablement obtenus pour le traitement des eaux synthétiques. L'optimisation du procédé OEC pour le traitement des effluents réels sera effectuée par la méthodologie de surface de réponse. Trois facteurs numériques et un facteur catégorique sont étudiés : densité de courant (12 à 36 mA/cm^2), le temps de réaction (20 - 60 min), concentration du Na_2SO_4 (0.004-0.03 M), et la charge initiale de l'effluent en carbone organique total.

1.4.4. Originalité

Le traitement des micro-plastiques des eaux résiduaires fait majoritairement appel à des procédés physico-chimiques (incluant coagulation/floculation, décantation et filtration). En revanche, ce type de traitement (basé sur la séparation des micro-plastiques) se traduit par un transfert de pollution (de la phase liquide vers la phase solide) plutôt que par une véritable dépollution. Il en résulte une étape supplémentaire de gestion de ces déchets plastiques. Les techniques de micro- et nano-filtrations sont également efficaces pour l'enlèvement des micro- et nano-plastiques mais elles sont très coûteuses et ne font que déplacer le problème. Pour y remédier, il est donc indispensable de trouver un moyen de dégrader complètement ces polluants en développant des traitements plus poussés par oxydation avancée. Ainsi, le choix d'une dégradation des particules par oxydation électrolytique adaptée au traitement des micro- et nano-plastiques a été privilégié. Ce processus est respectueux de l'environnement, car il les dégrade sous forme de molécules de CO_2 et d'eau, non toxiques pour l'écosystème aquatique. Il ne requiert pas forcement d'ajout de produits chimiques. Le procédé OEC proposé comprend une préfiltration grossière réalisée à l'aide d'un filtre à poche (20 à 50 μm de diamètre de pores) permettant de retenir les grosses particules de plastiques pour ainsi focaliser les forces d'oxydation sur les polluants plastiques sous forme colloïdale (0.001 μm à 1μm) et dissoute (< 0.001μm). La plupart des technologies électrochimiques ont été utilisées pour l'enlèvement des

polluants de base (ex. demande chimique et biologique en oxygène, etc.) présents dans les rejets de buanderies commerciales, alors que la technologie OEC proposée permet à la fois d'éliminer ces polluants de base et les micro-plastiques et nano-plastiques. Au meilleur de nos connaissances, il s'agit de la première fois qu'une telle approche technologique OEC est proposée pour la dégradation à la source des émissions des MPs/NPs présents dans les eaux de buanderies commerciales.

1.5. Méthodologie générale

1.5.1. Choix du polluant plastique modèle : le Polystyrène (PS)

La plus grande utilisation du plastique est faite dans le domaine de l'emballage. Le PS sous toutes ses formes, soit crystal, choc ou expansé est largement utilisé dans la fabrication des boites, boitiers, d'emballages des produits alimentaires, et des appareils électroménagers. Par conséquent, dans les eaux de surface, le polystyrène est le polymère plastique synthétique le plus courant (PS : 38,5 %), suivi du polypropylène (PP : 29,4 %) et le polyéthylène (PE : 21%) (Di & Wang, 2018a). En revanche, dans les stations d'épuration de traitement des eaux usées, le PS vient après le PE, PES, PET (Mintenig *et al.*, 2017; Ziajahromi *et al.*, 2017b). Le PS est représentatif des matériaux de micro-plastiques parce qu'il est aussi très résistant, il possède des doubles liaisons carbone-carbone, et sa toxicité sur le fonctionnement des cellules sanguines et la photosynthèse des organismes aquatiques a été largement démontrée. Les tailles nominales de 20 µm et 25 µm sont les tailles limites de mailles/pores les plus utilisées pour la caractérisation des micro-plastiques contenus dans les effluents de stations d'épuration de traitement d'eaux usées (Sun *et al.*, 2019). Les propriétés physico-chimiques du PS (tableau 5) montrent qu'il s'agit d'un polymère hydrophobe ayant plusieurs noyaux aromatiques et qui reste quasiment à la surface de l'eau (densité = 1,05 g/cm^3 ≈ 1). Pour les maintenir en suspension dans l'eau synthétique, des traces de surfactants y sont donc ajoutés dans les suspensions commerciales de microbilles de PS fournies par les compagnies de fabrication de ces produits.

Tableau 1. 4 : Caractéristiques physico-chimique du PS

	Styrène	Polystyrène
Structure moléculaire	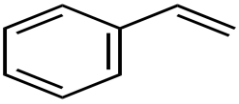	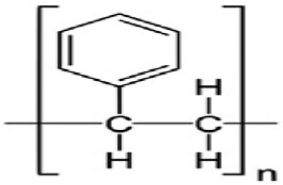
Formule	C_8H_8	$(C_8H_8)_n$
Poids moléculaire (g/mol)	104,1491	
Lambda max (nm)	-	589
Diamètre moléculaire nm	0,593	-
Solubilité dans l'eau à 25 º C (g/L)	0,3	-
Densité (g/m^3)	0,9060	1,05

1.5.2. Solutions synthétiques de micro- et nano-plastiques de PS

Les solutions synthétiques de micro- et nano-plastiques de PS ont été respectivement préparées à partir de dilutions de concentrés de micro et nano-plastiques dans de l'eau distillée. Des suspensions mono-dispersées de micro et de nano-billes de polystyrène sont utilisées comme source de micro- et nano-plastiques. Elles sont fournies par la compagnie Thermo-Scientific. Ce sont des concentrées de 10% (100 g/L) de MPs et de 1% (10 g/L) de NPs avec respectivement un diamètre nominal de 25 µm et de 100 nm et une uniformité de taille ≤ 15%. Ces micro/nano-billes ont été utilisées pour préparer une suspension de 100 mg/L de MPs et 10, 20 mg/L de NPs dans l'eau désionisée. Ces concentrations ont été préalablement validées par les techniques analytiques utilisées. Les suspensions ont été préparées avant chaque expérimentation. La quantité d'électrolyte ajoutée pour l'amélioration de la conductivité électrique est de 4,25 g/L pour Na_2SO_4 et $NaNO_3$, et de 3,50 g/L pour NaCl. Ces quantités correspondent respectivement à 0,03,

0,05 et 0,06 M. Le pH de toutes les solutions préparées est d'environ 6,0. Enfin, 50 mL d'échantillons sont prélevés pour caractériser la suspension avant le traitement.

1.5.3. Échantillonnage et dopage des effluents réels à l'aide de nano-plastiques fluorescents

Des nano-plastiques fluorescents (150 nm de diamètre nominal) ont été choisis afin de faciliter leur identification dans les effluents réels contenant de la matière organique. Pour simuler les conditions réelles de traitement, les effluents d'une buanderie hospitalière et hôtelière ont été prélevés à plusieurs reprises dans la période de Février à Mai 2022. Le choix pour ces eaux se justifie par la forte probabilité de retrouver des microfibres textiles après le lavage des vêtements. Ces eaux sont des vecteurs potentiels de contamination des eaux usées municipales par les MPs/NPs. Avant le dopage au NPs, un prétraitement de microfiltration (1.6 μm) a été appliqué afin d'éliminer la matière en suspension pour ainsi focaliser les forces d'oxydation sur les polluants plastiques dissoute, notamment les nano-plastiques (< 0.001 μm).. Les ions inorganiques, le pH, la conductivité, et la matière organique et les métaux lourds de ces effluents ont été préalablement mesurés. Pour chaque expérimentation, 1L de l'effluent est utilisé.

1.5.4. Unités expérimentales

Le réacteur est en plexiglas avec des dimensions de 14,5 cm (longueur) × 6,4 cm (largeur) × 17,7 cm (hauteur). Le fond de ce réacteur comporte 3 délimitations au niveau de sa largeur offrant ainsi la possibilité de positionner trois électrodes avec un espacement de 1 cm entre les électrodes. Cette flexibilité permet d'augmenter la surface des électrodes par ajout d'une troisième anode ou cathode. Il comporte aussi un espace permettant l'immersion verticale d'une lampe UV. Une injection d'air (900 $mL.min^{-1}$) peut être effectuée dans le fond du réacteur grâce à une ouverture (orifice de 1 cm de diamètre) située à 2.0 cm du fond du réacteur. Un agitateur (barreau aimanté) est placé au fond du réacteur pour assurer le mélange de l'effluent à traiter.

Le premier montage expérimental (Unité U-1) comprenait deux électrodes (une anode et une cathode). Le niobium recouvert de diamant dopé au bore (Nb/BDD), l'oxyde de métal mixte (MMO) et l'oxyde d'iridium (IrO2) ont respectivement été utilisés comme électrode anodique. Le titane (Ti) de cathode a été utilisé comme électrode cathodique. Il s'agit d'électrodes circulaires (12 cm de diamètre et 0,1 cm d'épaisseur) utilisées sous forme de grille métallique. La distance

inter-électrodes est de 1 cm. L'anode et la cathode sont verticalement fixées dans le réacteur et entièrement immergées dans l'effluent à traiter. Elles sont respectivement reliées à la borne positive et négative d'un générateur de courant continu modèle DCS40-75E (série Sorensen DCS, San Diego, États-Unis) ayant un courant nominal maximal de 75 A et une tension maximale de 40 V. Le volume utile du réacteur électrolytique était de 900 mL. Le réacteur a été gradué pour le contrôle du volume réactionnel à cause des grands volumes de prélèvement d'échantillons et de l'évaporation constatée pour quelques tests. Le réacteur a été placé dans un bac contenant des glaçons de manière à mettre toute la surface externe du réacteur en contact direct avec les glaçons afin d'atténuer l'évaporation de la solution due à la hausse de température causée par l'électrolyse à des intensités de courant élevées.

Le deuxième montage expérimental (Unité U-2) est composé de trois électrodes. Une électrode de BDD (12 cm de diamètre et 0.1 cm d'épaisseur) utilisée sous forme de métal déployé (grille) et deux électrodes pleines de feutre de carbone (FC) (longueur 11 cm, largeur 10 cm et épaisseur 1 cm). Les deux électrodes de FC sont placées de part et d'autre de l'anode de BDD (configuration : FC-BDD-FC) (figure 1.9). La distance inter-électrodes est de 1 cm. (FC-BDD-FC). Ce feutre de carbone est composé de 99 à 99,7 % de carbone et 0,02 à 0,25 % de cendres. La résistance électrique est égale à 0.5Ω. Une autre configuration de l'unité U-2 consistait à utiliser deux anodes de BDD et une cathode de titane (Ti). Les électrodes de BDD sont placées de part et d'autre de l'électrode de Ti (configuration BDD-Ti-BDD) (Figure 1.9). Le réacteur était aménagé de manière à pouvoir immerger verticalement une lampe UVc à basse pression de mercure ayant une puissance de 18 W. Le volume utile était de 800 mL lorsque les cathodes de feutre de carbone étaient utilisées.

Un bac de recirculation de 500 mL a été connecté au réacteur afin d'éviter le déversement d'une légère mousse formée au-dessus du réacteur dans les premiers moments de traitement des eaux usées réelles et pour favoriser davantage le transport de masse. La recirculation de l'eau au moyen d'une pompe péristaltique a fonctionné à une vitesse constante de 400 $mL.min^{-1}$.

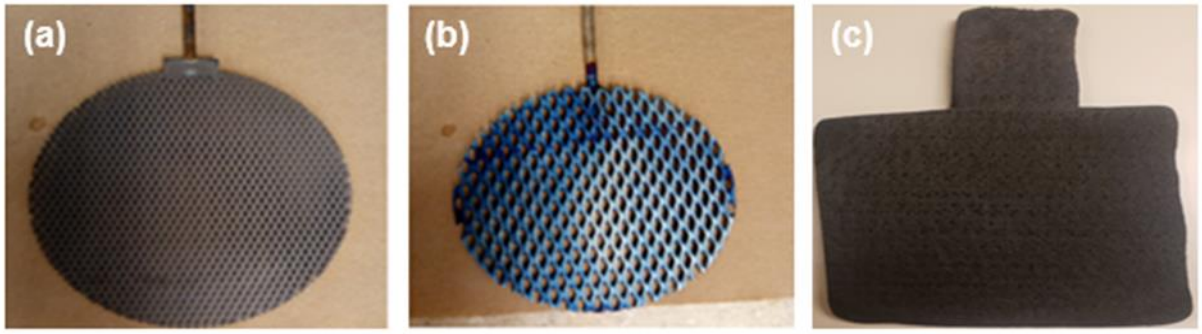

Figure 1. 9 : Photographies des électrodes (a) BDD , (b) Titane, (c) feutre de carbone.

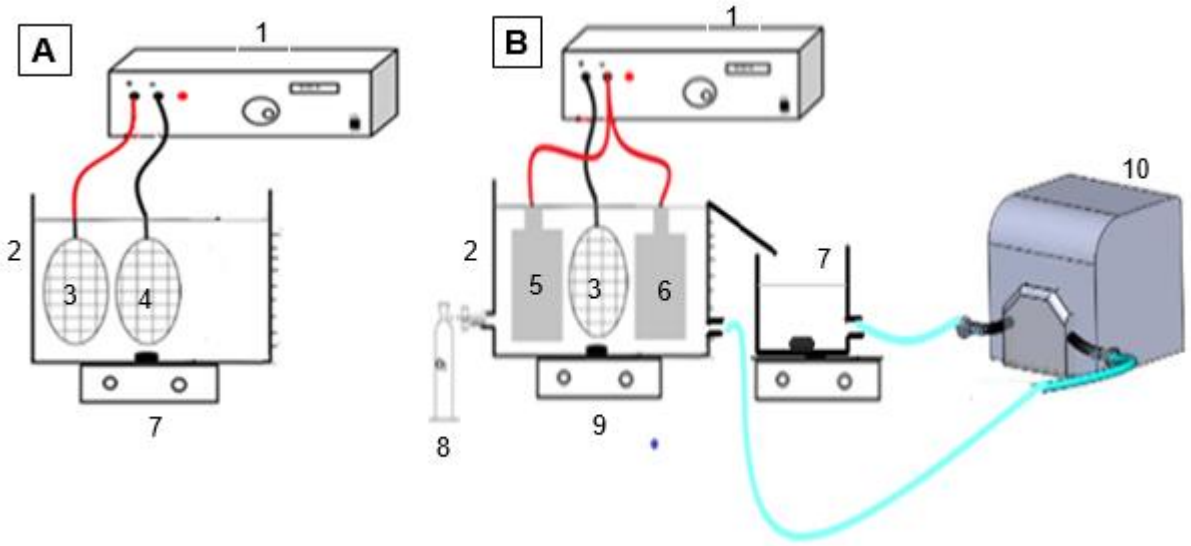

Figure 1. 10: Structure schématique des unités expérimentales A) U-1, B) U-2.

(1) Générateur à courant continu

(2) Cellule électrolytique

(3) Anode : BDD, MMO ou IrO_2

(4) Cathode de titane

(5) et (6) Cathodes de feutre de carbone

(7) Bac de recirculation

(8) Injecteur d'air comprimé

(9) Agitateur

(10) Pompe péristaltique

1.5.5. Procédure expérimentale et mise en œuvre du procédé OEC

La première phase a consisté à l'évaluation de l'electroooxydation des micro-plastiques dans l'eau synthétique. Pour ce faire des anodes actives tels que l'IrO_2, MMO et non active comme le BDD ont été utilisées afin de choisir l'anode la plus performante pour la suite des expérimentations. Il a donc été expérimentalement déterminé pour une même intensité de courant (9 A) appliquée, l'efficacité de dégradation de micro-plastiques en fonction du type d'anode (108,4 et 216,3 mA/cm^2 pour BDD, 108,4 mA/cm^2 pour MMO, 432,7 mA/cm^2 pour IrO2) et du temps d'électrolyse (60 à 360 min). L'effet de la densité de courant en utilisant le BDD (108, 72, 36 mA.cm^{-2}) et de la surface (83 et 41, 6 cm^2) de l'anode la plus performante ont été aussi testés. La contribution de l'action indirecte de l'électro-oxydation pour la dégradation des micro-plastiques a aussi été évaluée par l'effet du type d'électrolyte (Na_2SO_4, $NaNO_3$, NaCl) et de la concentration du Na_2SO_4 (0,03 ; 0,04 ; 0,06 M). Les températures initiales des solutions étaient toutes fixées à 20º C. Les essais sont effectués à température ambiante au cours desquels la température de la solution est suivie à l'aide d'un thermocouple scientifique J-KEM. La solution est mélangée par agitation avec un barreau aimanté. Le temps d'échantillonnage était de 1, 2, 3 et 6 h. Lors de l'utilisation des fortes densités de courant (108, 72 mA.cm^{-2}) il a été constaté une élévation de la température (≥ 45 ºC) de l'eau pendant après 3 h l'électrolyse. Afin de vérifier l'effet que pourrait apporter l'élévation de la température de l'eau pendant l'électrolyse sur la dégradation des micro-plastiques, une solution de micro-plastiques a été portée à ébullition sous agitation pendant 6h dans un bécher. Il était ajouté à chaque 15 min une eau déjà bouillante dans le bécher de sorte à respecter le volume d'eau initiale dans le bécher. Un échantillon avant et après traitement a été analysé.

La consommation énergétique a été calculé en considérant les meilleures conditions opératoires obtenues de l'électro-oxydation suivant l'équation (1.21).

Équation 1.21 : $Consommation\ energétique\ \left({KWh}/{m^3}\right) = \frac{I \times T \times t}{V} \times 10^{-3}$

Où I, T, t et V représentent respectivement l'intensité du courant (A), le potentiel électrique (v), le temps (h) et le volume (m^3).

La deuxième étape a été consacrée à évaluer la production d'espèces oxydantes (•OH, $H_2S_2O_8$, H_2O_2, etc.) lors de l'électrolyse en utilisant respectivement les unités expérimentales U-1 et U-2. La production des radicaux hydroxyles et des persulfates ont été évaluée suivant les densités de

courant (36, 72 et 108 mA.cm^{-2}) et les concentrations de Na_2SO_4 (0.03 et 0.06 M). Celle du H_2O_2 a été réalisée avec des densités de courant inférieures (6, 12, 36 mA.cm^{-2}), avec et sans injection d'air et en présence d'une et 2 pièces de CF afin de réduire la consommation énergétique et obtenir à la fois une dégradation efficace des NPs. L'utilisation des différents montages de réacteur a permis de comparer l'efficacité de dégradation du procédé d'électro-oxydation et de l'électro-peroxydation sur les NPs. Par ailleurs, la dégradation des NPs a été suivie dans une solution de H_2O_2 seul a une concentration de 0.14 M sous agitation pendant 2h. Cette concentration est approximative de la concentration maximale du peroxyde mesurée dans les prélèvements pendant l'électrolyse. L'effet des persulfates seuls sur la dégradation des NPs a été évalué en soumettant une solution de Na_2SO_4 sous électrolyse pendant 2h. Par la suite l'électrolyse a été mise en stand-by avec un ajout de NPs sous agitation pendant 2h. La production des persulfates a été évaluée avant l'ajout des NPs. Ces tests ont permis de comprendre et d'apprécier la contribution de chaque espèce oxygénée réactive électro-générée dans le mécanisme de dégradation des NPs.

La troisième étape a permis d'appliquer les meilleures conditions précédemment déterminées, afin d'évaluer l'efficacité du procédé d'électro-peroxydation pour dégrader et minéraliser les NPs dans des effluents réels de buanderie prétraités par microfiltration. Par la suite, une méthodologie de plan de surface de réponse comprenant un plan factoriel (PF) et un plan central composite (PCC) a été appliquée pour optimiser le traitement des effluents de blanchisserie dopés en nano-plastiques fluorescents. Trois paramètres numériques que sont : la densité du courant (12-36 mA.cm^{-2}), la concentration du Na_2SO_4 (0.004-0.03 M), le temps d'électrolyse (20-60 min) et un paramètre catégorique relatif à la charge initiale de COT des eaux (faible, élevé) ont été étudiés. Au cours de ces tests, la spectrophotométrie UV-vis à 225 nm a été mesurée pour évaluer indirectement dans les effluents réels la concentration de nano-plastiques fluorescents résiduels. L'analyse du COT et les scans EEM 3D ont été effectués pour estimer les performances du procédé sur le traitement global des eaux.

1.5.6. Méthodes analytiques des MPs/NPs

Dans les effluents synthétiques, l'analyse de l'efficacité de l'oxydation électro-catalytique des micro-plastiques (MPs) a été réalisée de manière directe et indirecte en fonction du temps de traitement. L'analyse directe des MPs a été réalisée en combinant les analyses massique et

granulométrique (diffusion dynamique de la lumière Laser) pour un même échantillon prélevé au cours du temps d'électrolyse. Les mesures indirectes des MPs ont consisté à évaluer le carbone organique total dans les filtrats des échantillons (mesure du degré de minéralisation), à analyser la morphologie des MPs (au microscope électronique à balayage (MEB)) et à identifier les groupements fonctionnels de la suspension des MPs grâce à l'analyse spectroscopique à infrarouge à transformée de Fourier (IRTF).

Dans un premier temps l'exactitude des mesures granulométriques et massiques a été évaluée. Pour ce faire trois différentes concentrations (100, 50, 10 mg/L) de MPs ont été fixées et leurs mesures granulométrique et massiques ont été effectués. Les coefficients de variation et les diamètres moyens obtenus par la mesure granulométrique pour ces trois concentrations ont été comparés au coefficient de variation de la taille des microbilles et au diamètre nominal donné par le fournisseur. Les masses de MPs obtenues par pesée ont aussi été comparées aux masses théoriques selon les concentrations préparées (5 ; 2,5 et 0,5 mg/L). Il faut noter que pour qu'une distribution par de taille par diffraction laser soit fiable, la transmittance de la lumière donnée par la mesure doit diminuer de 100% a une valeur comprise entre 75-90%. Pour le polystyrène un indice de réfraction de 1,59 a été utilisé pour le calcul de la distribution.

Ensuite le mode de la distribution de taille a été considéré pour le suivi du comportement des MPs et la performance de la dégradation des MPs a été évaluée en utilisant le rendement sur la perte de masse des MPs lors du traitement. Ce rendement a été calculé en utilisant l'équation (1.22) :

Équation 1.22 : $Perte\ de\ masse\ (\%) = \frac{M_0 - M_t}{M_0} \times 100$

Où M_0 et M_t représentent la masse initiale et finale des MPs, respectivement.

Pour l'analyse massique, les suspensions ont été filtrées avec des filtres en nitrocellulose 0,22 µm pour séparer les MPs. Les filtres ont ensuite été séchés dans une étuve à 40 °C pendant 24 heures pour évaporer l'eau. La différence de masse de filtre avant et après filtration/séchage représente la masse de MPs. Par ailleurs, la quantité de sel restée dans le filtre après séchage a été mesurée à l'aide de solutions d'électrolyte sans MPs. Ces données ont été utilisées pour corriger les erreurs dues au sel restant dans les filtres lors de l'analyse de la dégradation MPs.

Pour ce qui est de l'eau synthétique de NPs, la dégradation/minéralisation des nano-plastiques a été évalué par mesures de l'absorbance spécifique au spectrophotomètre UV vis à 254 nm et du

carbone organique total résiduel dans les échantillons non filtrés. Afin de confirmer les résultats, l'analyse des scans de spectres 3D a la spectroscopie de fluorescence pour suivre l'évolution de la matière organique dissoute de NPs dans l'eau synthétique a été utilisé. L'Absorbance spécifique UV-vis 254 nm est un indice utilisé pour estimer la teneur des substances aromatiques. Elle est un indice caractéristique des substances possédant une ou plusieurs doubles liaisons (Chen *et al.*, 2020a; Yakimenko *et al.*, 2016; Zheng *et al.*, 2016). Une courbe d'étalonnage des NPs en fonction de l'absorbance relative a été utilisée pour calculer la concentration résiduelle en NPs et définir l'efficacité de la dégradation. Les concentrations de la courbe d'étalonnage sont comprises entre 0 et 8 mg. L^{-1} afin de prendre en compte les plus petites concentrations après le processus de traitement. Le COT a été mesuré par combustion totale à 680 ºC sous un flux d'oxygène et sur un catalyseur en platine avec un dosage par spectroscopie IR à la sortie de la chambre de combustion grâce à l'analyseur Shimadzu TOC 5000A. Afin de s'assurer que cette méthode permet la combustion complète des NPs de 100 nm, le COT de différentes concentrations de solution de NPs a été analysé afin de vérifier la proportionnalité des concentrations entre elles. Dans l'eau synthétique, les spectres obtenus par spectroscopie de fluorescence d'acquisition de matrices d'émission-excitation (3D-EEM) fournissent directement les matrices tridimensionnelles émission/excitation/intensité de la matière organique liée uniquement aux NPs. Cela a permis l'identification de pic fluorescent correspondant à la matière organique lié au NPs et de suivre l'évolution de son intensité avec le temps de traitement. Les intervalles de l'excitation se situent entre 220 nm et 650 nm et de 230 à 600 nm respectivement avec des incréments de 5 nm.

Dans les effluents, le suivi de la dégradation des NPs a été réalisé par méthode indirecte de mesure de l'élément fluorescent incorporé dans les NPs. Il faut signaler que cette incorporation n'est pas en surface des microsphères. Elle sert à leur traçabilité dans les mélanges. Des analyses de l'absorbance au spectrophotométrie UV-vis à 225 nm ont également été effectuées. Un pic a été détecté à cette longueur d'onde lorsqu'une matrice synthétique de NPs a été scannée entre 200-800 nm au spectrophotomètre UV-vis. La courbe d'étalonnage est réalisée par addition de standard des NPs dans une matrice synthétique a des concentrations comprises entre 0 et 10 mg/L de NPs. Les mesures d'absorbance à 225 nm ne permettent pas d'obtenir des valeurs justes de concentrations NPs dans les effluents réels mais permet d'avoir une idée sur l'évolution global de la dégradation des NPs pendant l'électrolyse. Les mesures de COT ont permis d'évaluer l'efficacité du procédé sur le traitement global des effluents. À mesures indirectes, s'ajoute

l'analyse (avant et après traitement) par spectroscopie de fluorescence d'acquisition de matrices d'émission-excitation 3D-EEM des eaux réelles de buanderie contaminées par des NPs de polystyrène.

1.5.7. Mésure des persulfates

Pour réaliser la mesure des persulfates électro-générés *in situ* dans la solution au cours de l'électrolyse, la méthode de Wessler basée sur l'oxydation des ions iodure (I^-) en iode (I_2) a été utilisée. Lorsqu'un agent oxydant comme $S_2O_8^{2-}$ est présent dans une solution, les ions I^- sont oxydés pour donner I_2. Par la suite, I_2 réagit avec I^- présent en excès dans la solution pour former l'ion tri-iodure (I_3^-) (Entezari & Kruus, 1994). La méthode est basée sur le titrage direct de I_2 produit à partir de l'oxydation de I^-. I_3^- est analysé par des mesures d'absorbance à 353 nm (ε = 26303) (Koda *et al.*, 2003) à l'aide d'un spectrophotomètre UV-vis (Carry UV 50, Varian Canada) et en utilisant une cellule de 1 cm (trajet optique).

1.5.8. Mésure de la concentration en péroxyde d'hydrogène

La concentration de H_2O_2 est déterminée par dosage volumétrique basé sur la réaction entre le H_2O_2 par une solution acide (H_2SO_4) de sulfate de cérium ($Ce(SO_4)_2$, $2(NH4)_2SO4$, $2H_2O$) en présence d'un indicateur coloré : le 1,10-Phenanthroline ferreux sulfate à 0.025 M. Une solution de 20 mL prélevée du réacteur est versée dans un bécher avec addition de deux à trois gouttes de l'indicateur coloré. Se servant de la solution titrante (solution de sulfate de cérium) contenu dans la burette, cette solution est dosée en contrôlant le changement de coloration de la solution jusqu'à disparition du rouge et apparition du bleu pâle. Grace à l'équation (Y= aX +b) issue de la courbe de calibration déterminée, la concentration en peroxyde d'hydrogène a été déterminée durant les essais.

Où Y est la concentration du peroxyde d'hydrogène à déterminer et X est le volume « tombé » de la solution de sulfate de cérium.

1.5.9. Mesure des radicaux hydroxyles dans la solution

Les radicaux hydroxyles ont été estimés selon la méthode rapportée par (Daghrir *et al.*, 2013b; García-Gómez *et al.*, 2014). Il a été démontré que le DNA est blanchi sélectivement par oxydation chimique avec des radicaux hydroxyles et ne réagit pas avec l'oxygène ($^1O_2$), les anions

superoxydes (O_2^-) ou d'autres peroxydes (Simonsen *et al.*, 2010). Par conséquent, la concentration du DNA est suivie pendant l'électrolyse et un échantillon est prélevé à chaque 5 min. Le blanchiment du DNA a été contrôlé par des mesures d'absorbance à 440 nm. La courbe d'étalonnage du DNA a été obtenue en traçant l'absorbance à 440 nm en fonction de la concentration DNA (de 0 à 9 mg. L^{-1}). Avant l'électrolyse, le DNA (*p*-nitrosodimethylaniline) est préparé à une concentration de 8 mg/L. Un échantillon est prélevé a l'instant t = 0 min. Le taux de production de •OH est égal au taux de disparition de DNA par l'hypothèse de la réaction de premier ordre, selon l'équation (1.23) :

Équation1.213: $V = \frac{dC}{dt} = -kC$

Où V, C, k et t correspondent respectivement au taux de production de •OH, à la concentration de DNA, à la constante de vitesse de réaction du premier ordre et au temps de réaction. L'intégration de l'équation (1.24) donne :

Équation 1.24 : $Ln(\frac{Co}{C}) = kt$

Où C_0 et C sont la concentration initiale de DNA et la concentration de DNA au temps t. La valeur de k pourrait être calculée à partir de la pente d'un tracé de $Ln(C_0/C)$ en fonction de t.

1.5.10. Evaluation de la toxicité

Des tests de toxicité ont été effectués suivant la méthode de référence du Centre d'Expertise en Analyse Environnementale du Québec (CEAEQ) avec des nouveau-nés de Daphnia magna (< 24 h) provenant de la culture du laboratoire Bureau Veritas à Saint-Laurent, Québec. Leur milieu de culture était de l'eau reconstituée respectant les caractéristiques suivantes (dureté 180 mg $CaCO_3$/L, oxygène dissous > 100 %, pH 7- 8, à 20,0 ± 2,0 ºC et 16 h de lumière – 8 h de photopériode d'obscurité). Les organismes ont été nourris une fois par jour. Conformément à la méthode analytique MA 500-D.mag 1.1R3m, *Daphnia magna* (<24 h) ont été exposées 48 h, à des effluents réels de buanderie non dopés, des effluents dopés aux NPs avant et après traitement. Le facteur de dilution recommandé pour la toxicité de l'effluent est compris entre 0,5 et 0,7 (USEPA, 2002). Par conséquent des concentrations de %, 6,25 %, 12,5 %, 25 %, 50 %, 100% (v/v) ont été évaluées. Chaque concentration nécessitait 4 répétitions, avec cinq nouveau-nés par test, placés dans un réservoir-test contenant 10 ml d'eau reconstituée et d'effluent. Des tests de contrôle ont été effectués simultanément. Un débit d'air de 37,5 ± 12,5 mL/min/L a été

appliqué pour augmenter le taux d'oxygène dissous à 100 % après 30 min d'aération. Les effets additifs des paramètres chimiques, biologiques et physiques des effluents ont été évalués par des mesures de pH, de dureté, d'oxygène dissous, de température et de conductivité avant et après une exposition de 48 h. La méthode visuelle a été utilisée pour évaluer les critères de toxicité consistant en l'immobilité (antennes ne bougent pas) et la mortalité (incapable de nager).

1.6. ORGANISATION DE LA THESE

Cette thèse comprend trois parties principales (Partie-I, Partie-II et Partie-III). La Partie-I comprend l'introduction générale (Chapitre 1) et une synthèse bibliographique présentée sous forme d'article de revue de littérature (Chapitre 2). La Partie-II est composée de trois articles de recherche (Chapitres 3, 4 et 5). La Partie–III comprend la conclusion générale et les perspectives des travaux (chapitre 6).

La Partie-I est premièrement constituée d'une revue de littérature (Chapitre 1) portant sur la problématique des plastiques, micro-et nano-plastiques (MPs et NPs) dans l'environnement ainsi que sur les procédés de traitement (dont les procédés électrochimiques d'oxydation avancée) pouvant être potentiellement utilisés pour la décontamination de ces polluants plastiques. Un état actuel des connaissances des procédés de traitement ainsi que les forces/limites des différentes techniques analytiques des MPs et NPs dans les eaux sont également discutés sous forme d'article synthèse (Chapitre 2) publié dans *Marine Pollution Bulletin*, *168 :112374 :* K*arimi Estahbanati, Kiendrebeogo et al. (2021) Treatment processes for microplastics and nanoplastics in water: State-of-the art review*. Les objectifs et la démarche méthodologique de cette thèse sont également résumés dans la Partie-I.

La Partie-II (comprenant les chapitres 3, 4 et 5) présente sous forme d'articles scientifiques, les résultats et discussions des travaux de recherche. Le chapitre 3 traite de la dégradation de micro-plastiques (MPs) par oxydation anodique d'une suspension synthétique mono-dispersée de polystyrène (diamètre nominal 25 μm). Les résultats issus de ces travaux ont été valorisés sous forme d'article publié dans *Environmental Pollution 269 : 116168 : Kiendrebeogo et al. (2021) Treatment of microplastics in water by anodic oxidation: A case study for polystyrene.* Le chapitre 4 porte sur le rôle des espèces oxygénées réactives générées lors de la dégradation électrochimique des nano-plastiques (NPs) de polystyrène en solution aqueuse. Le procédé d'électro-peroxydation (EO-H_2O_2) constitué d'une anode de diamant dopé au bore (DDB) et d'une

cathode de feutre de carbone (pour la génération de H_2O_2) a été comparé au procédé d'électro-oxydation (EO) comprenant une anode de DDB et une cathode de titane (Ti). Cette partie des travaux a été publié dans *Sciences of Total Environment, 808 : 151897* : *Kiendrebeogo et al. (2021) Electrochemical degradation of nanoplastics in water: Analysis of the role of reactive oxygen species*. Le chapitre 5 porte pour sa part, sur le traitement par électro-peroxydation des eaux réelles de buanderie artificiellement contaminées par des nano-plastiques de polystyrène. Ces résultats ont fait l'objet d'un article soumis à la revue Separation and Purification Technology (soumis le 04 Avril 2023) *: Kiendrebeogo et al.* (2023) Nanoplastics removal from spiked laundry wastewater using electro-peroxidation process.

La troisième partie (Partie-III) de l'étude constituée uniquement du chapitre 6 présente un bilan général des résultats et discussions des travaux portant sur la dégradation des MPs/NPs et traitement des effluents de buanderie identifiés comme étant une source potentielle de la présence de microfibres dans les eaux usées municipales. Les perspectives pour les travaux futurs sont également présentées dans ce chapitre.

2. TREATMENT PROCESSES FOR MICROPLASTICS AND NANOPLASTICS IN WATERS: STATE-OF-THE-ART REVIEW

PROCÉDÉS DE TRAITEMENT DES MICROPLASTIQUES ET DES NANOPLASTIQUES DANS LES EAUX : REVUE SUR L'ÉTAT DE L'ART

Karimi Estahbanati M. R[1*], Marthe K.[1], Ali Khosravanipour M.[1,2], Patrick D.[1*], Tyagi RD[3,4]

[1] Institut national de la recherche scientifique (INRS) - Centre Eau Terre Environnement (ETE), 490 rue de la Couronne, Québec (QC), CANADA, G1K 9A9

[2] Institut de recherche et de développement en agroenvironnement, 2700 Rue Einstein, Québec, CANADA, QC G1P 3W8

[3] Distinguished Prof, School of Technology, Huzhou University, China

[4] Chief Scientific Officer, BOSK Bioproducts, 100-399 rue Jacquard, Québec, CANADA, G1N 4J6

Marine Pollution Bulletin 168 (2021) 112374.

https://doi.org/10.1016/j.marpolbul.2021.112374

Abstract

In this work, established treatment processes for microplastics (MPs) and nanoplastics (NPs) in water as well as developed analytical techniques for evaluation of the operation of these processes were reviewed. In this regard, the strengths and limitations of different qualitative and quantitative techniques for the analysis of MPs and NPs in water treatment processes were first discussed. Afterward, the MPs and NPs treatment processes were categorized into the separation and degradation processes and the challenges and opportunities in their performance were analyzed. The evaluation of these processes revealed that the MPs or NPs removal efficiency of the separation and degradation processes could reach up to 99% and 90%, respectively. It can be concluded from this work that the combination of separation and degradation processes could be a promising approach to mineralize MPs and NPs in water with high efficiency.

Keywords: Microplastics; nanoplastics; analysis; process; wastewater; effluent.

2.1. Introduction

The widespread use of plastic-based products and their resistance to degradation led to plastics accumulation in the environment. The accumulated plastics are fragmented and degraded by biotic agents, generating smaller particles called microplastics (MPs, less than 5 mm) (Lambert & Wagner, 2016) and then nanoplastics (NPs, less than 1000 nm) (Cole & Galloway, 2015b; Gigault *et al.*, 2018a). Studies on environmental monitoring reported the presence of MPs in surface waters, coastal sediments, beach sands, and deep marine environments (Browne *et al.*, 2011b; Faure *et al.*, 2015b; Woodall *et al.*, 2014a). Therefore, the release of MPs and NPs to the environment is recognized as a significant problem related to water pollution (Lambert & Wagner, 2016).

Some pieces of compelling evidence show the toxicity of MPs and NPs for aquatic life. Molecular simulation has demonstrated that NPs can easily penetrate the lipid membranes of organisms and cause change to the membrane structure, reduction of molecular diffusion, and seriously affecting cell function (Rossi *et al.*, 2014b). NPs have also been identified in the brain of organisms, so they can cross the blood-brain barrier. In general, the toxicity of MPs and NPs could depend on their size during which the smaller plastics are more toxic than the larger ones (Chae & An, 2017b; Jeong *et al.*, 2016a). Besides, MPs and NPs can adsorb and transfer persistent organic pollutants due to their hydrophobicity and large surface-to-volume ratio. Most commonly adsorbed pollutants include polychlorinated biphenyls, organochlorine pesticides, polycyclic aromatic hydrocarbon, dichlorodiphenyltrichloroethane, and metals (e.g., Al, Zn, Pb, Cu, Ag, and Pb) (Campanale *et al.*, 2020). Changes in environmental conditions such as pH, temperature, and ionic strength as well as type, density, and crystallinity of polymer can affect the kinetics of pollutant adsorption on the MPs and NPs surface. The adsorbed pollutants can then desorb and affect metabolic and physiological processes as well as human and ecosystem health (Zhang *et al.*, 2019).

The MPs and NPs can be categorized into primary and secondary MPs and NPs. The primary ones are released into the environment at the MPs and NPs size, while the secondary MPs and NPs were generated from the decomposition of large plastic materials. The MPs and NPs pollution in water could originate from domestic (cosmetic products and washing machines (Carr *et al.*, 2016; Duis & Coors, 2016)) and industrial (plastic manufacturing (Lechner *et al.*, 2014) and

textile industries (Deng *et al.*, 2020)) activities. For example, it has been shown that between 4,594 and 94,500 polyethylene (PE) particles (with a size of 164-327 µm) can be released from 5 mL of cosmetic product (Claessens *et al.*, 2013a; Napper *et al.*, 2015a). Besides, an acrylic fabric can release up to 729,000 fibers per wash compared to 138,000 and 496,000 fibers for polyester (PES)-cotton and PES fabrics (Napper & Thompson, 2016b). From another perspective, the breakage of MPs can lead to the release of NPs in the environment (da Costa *et al.*, 2016). The photo-oxidation under UV radiation (Cai *et al.*, 2018c), hydrolysis, bio-assimilation, mechanical fractures due to sand abrasion, and water turbulence are the phenomena by which the mesoplastics and MPs are fragmented (Cooper & Corcoran, 2010b; Gewert *et al.*, 2015b). For example, a study (Lambert & Wagner, 2016) demonstrated that the concentration of NPs in water reached 1.26×10^{8} particles/mL (with average particle size at 224 nm) after the degradation of an unused disposable polystyrene (PS) coffee cup lid for 56 days.

Various research has been performed on the fate and occurrence of MPs and NPs in the environment as well as WWTPs (Hou *et al.*, 2021). PE, PS, and polypropylene (PP) are the most found MPs and NPs in the natural waters (Di & Wang, 2018b; Karlsson *et al.*, 2017b; Silva *et al.*, 2018). While in the influent and effluent of wastewater treatment plants (WWTPs), PES, PE, polyethylene terephthalate (Ziajahromi *et al.*), and polyamide (PA) are the most common polymers (Sun *et al.*, 2019). (Mason *et al.*, 2016b) stated that the type and concentration of MPs present in the effluents of different WWTPs are a function of the size of the population served, the rainwater flow that enters WWTP, and the filtration characteristics used in the WWTPs. The surface water can be more concentrated in MPs and NPs than effluent (Mason *et al.*, 2016b; McCormick *et al.*, 2014a), despite the dilution effect from the large quantities of surface water. This observation may be due to the accumulation of MPs in the environment over time. For surface water, a concentration as high as 213×10^{3} MPs/m^3 was reported for Netherlands (Mughini-Gras *et al.*, 2021). On the other hand, the USA recorded the lowest values for the effluents which varies in the range of 0-4 MPs/m^3 (Mason *et al.*, 2016b). A part of these differences could be due to the water treatment efficiency as well as the fate and occurrence of MPs and NPs in treatment plants. More than half of the MPs and NPs could be separated in the primary treatment, and most of the remained particles could be removed through the secondary treatment in WWTPs (Hou *et al.*, 2021). Nevertheless, a significant number of MPs could appear in effluents and then accumulate in the environment through time because of the high volume of effluents.

Due to the abundance of MPs and NPs in waters as well as their toxicity for human health, the investigation of developed technologies for their removal is essential. Although some review works have been performed to evaluate the effects of MPs on the performance of WWTPs (Enfrin *et al.*, 2019; Shen *et al.*, 2020; Zhang & Chen, 2020), this field of research lacks a comprehensive review to compare the challenges and opportunities of different processes developed exclusively for the MPs and NPs removal. Besides, the previous works focused on the removal of MPs and it is also essential to evaluate thoroughly the NPs removal from water. This review aims to evaluate the current developments and future trends of the processes to remove MPs and NPs pollutions from water.

2.2. MPs and NPs analysis techniques

The selection of suitable analysis techniques is a critical task in the evaluation and comparison of the processes for the treatment of MPs and NPs in water. The analysis techniques can qualitatively or quantitatively assess the characteristics of MPs and NPs. Although qualitative analysis could provide some insights about the performance of treatment processes, quantitative analysis is usually essential for a precise evaluation of the removal efficiency as well as the comparison of processes. In this section, the strengths and limitations of different techniques that were developed for the analysis of MPs and NPs in water treatment processes are discussed.

In general, MPs and NPs analysis consist of identifying their size, concentration, number, and chemical composition. The MPs analysis techniques are more advanced developed than the NPs due to the limitations of analytical devices in the nanometer range. Most of the studies dealing with MPs pollution in water have only considered particles larger than 10 µm (Lares *et al.*, 2018; Mason *et al.*, 2016b; Mintenig *et al.*, 2017; Talvitie *et al.*, 2017a). On the other hand, the adaptation of the MPs characterization techniques for the analysis of NPs in real samples is challenging due to technical limitations (Rios Mendoza *et al.*, 2018; Schwaferts *et al.*, 2019; Strungaru *et al.*, 2019). The analysis of MPs and NPs may be underestimated or overestimated, as many studies mentioned the limits of their sampling and measurement devices. Although some analysis techniques are limited due to being based on microscopy, they could be coupled with Fourier-transform infrared spectroscopy (FTIR) to be able to confirm the plastic nature of the found particles (Eriksen *et al.*, 2013a; Free *et al.*, 2014; McCormick *et al.*, 2014a; Vermaire *et al.*, 2017). Interestingly, up to 90% of the suspected microparticles in the previous works were identified

using FTIR analysis to have non-plastic nature (Lares *et al.*, 2018; Magnusson & Norén, 2014; Ziajahromi *et al.*, 2017b). Besides, more than 70% of error is estimated to be accompanied by the results of quantification of MPs smaller than 100 µm (Dris *et al.*, 2015b; Hidalgo-Ruz *et al.*, 2012b; Leslie *et al.*, 2017b; Michielssen *et al.*, 2016; Murphy *et al.*, 2016b; Talvitie *et al.*, 2015). Therefore, it is essential to develop tailored analysis techniques to accurately analyze the MPs and NPs.

The most common techniques for the analysis of MPs and NPs in water treatment processes are depicted in Fig. 2.1. As seen, various techniques were employed for the qualitative analysis of MPs and NPs including stereo microscopy, scanning electron microscopy, FTIR, dynamic light scattering (DLS), and nanoparticle tracking analysis (NTA). On the other hand, for the quantitative analysis, weight measurement by scale, pyrolysis/gas chromatography (GC), total organic carbon (TOC) analyses, and UV-vis spectrophotometry were used. The analysis of MPs and NPs by these techniques would be sensitive to impurities found in real waters. For example, the presence of impurities could lead to an overestimation of the number of MPs and NPs by the DLS and NTA methods or affect the wavelength and intensity of bands appearing in the FTIR spectra. Thus, it may be essential to pretreat samples before any analysis by removing organic and inorganic matter. Catalytic oxidation in a humid environment is a pretreatment method for MPs and NPs (Erni-Cassola *et al.*, 2017; Julie Masura *et al.*, 2015; Karami *et al.*, 2016). Although this method allows efficient removal of organic matter from samples, it would change the particle size of MPs and NPs. To avoid that, the enzymatic maceration of organic matter is an alternative (Mintenig *et al.*, 2017). The pretreatment using H_2O_2 is one of the most popular methods of digestion which can also be used in combination with other oxidation methods (Elkhatib & Oyanedel-Craver, 2020).

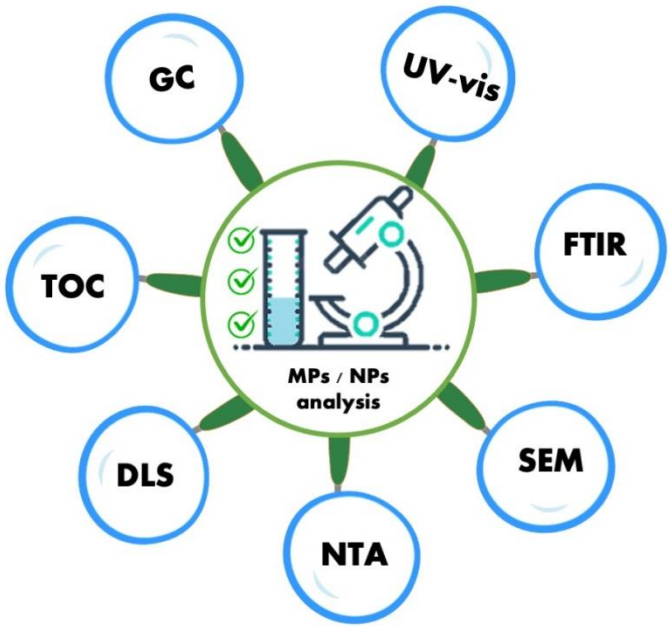

Figure 2. 1 : Most common MPs and NPs analysis techniques for water treatment processes

In general, a very critical point in the study of MPs and NPs removal technologies is the lack of standard procedures for sampling real water, pre-processing of samples, and analyzing MPs and NPs. This lack of knowledge complicates the comparisons between the existing works. For example, the majority of studies on the occurrence of MPs and NPs in water are reported as the number of particles per volume or surface area of water, while the mass concentrations are generally necessary for environmental monitoring. Besides, no reliable method has been developed so far to simultaneously analyze the MPs and NPs physically and chemically. Therefore, one technique is required to analyze the size and the concentration of MPs and NPs, and another to investigate their chemical structure to determine the type of polymer. The challenges and opportunities of different qualitative and quantitative analysis methods for MPs and NPs are discussed in the following subsections.

2.2.1. Qualitative analysis

Stereo microscopy is one of the earliest techniques for measurement of the size, characterization of the morphology, and counting of the number of MPs. This technique could be appropriate in the analysis of MPs due to its low cost. The main challenge of employing this method is the

confident identification of sub-hundred-micron (<100 µm) particles with no color or normal shape as plastics (Shim *et al.*, 2017). This limitation also made it inappropriate for NPs identification. Besides, the analysis results of this technique are operator-dependent (Hidalgo-Ruz *et al.*, 2012b). SEM analysis provides the tool for the observation of MPs and even NPs (Enfrin *et al.*, 2020a). SEM is the most employed microscopic technique for the analysis of MPs and NPs since is almost not limited by their size.

To assure the plastic nature of MPs and NPs as well as determine the type of plastics, spectroscopic techniques can be used. FTIR is the most common spectroscopy technique for the analysis of MPs and NPs. This technique is mainly applied for the analysis of MPs when they can be sorted individually by hand, i.e., their size should be usually higher than 500 µm. This limitation could be enhanced to 10 µm thanks to the combination of Focal Plane Array with micro-FTIR imaging for mapping the surface of the filters used for the recovery of MPs (Browne *et al.*, 2011b; Löder *et al.*, 2015; Mintenig *et al.*, 2017). Indeed, the FPA/micro-FTIR can analyze each particle in a mixture of microparticles (Araujo *et al.*, 2018; Erni-Cassola *et al.*, 2017; Lares *et al.*, 2018). It is difficult to analyze the particles with 10-20 µm size by FTIR because of the lateral resolution limitations (Li *et al.*, 2018a). Besides, this technique is very sensitive to the adsorbed impurities on the surface of MPs in real waters. Carbonyl index analysis to quantify the degree of chemical oxidation of polyolefins is a common approach in the analysis of the photocatalytic degradation of MPs and NPs (Jiang *et al.*, 2020). The carbonyl index is defined as the ratio of absorbance of the carbonyl group (around 1710 cm^{-1}) to a reference band (like 1380 cm^{-1}) (Llorente-García *et al.*, 2020). To overcome the size limitation of the FTIR technique, Raman spectroscopy can be employed that can analyze the particles as small as 1 µm (Araujo *et al.*, 2018; Erni-Cassola *et al.*, 2017; Lares *et al.*, 2018). Other advantages of the Raman spectroscopy in comparison to FTIR are (i) having a higher sensitivity to non-polar functional groups, (ii) having no sensitivity towards disturbing signals of water and atmospheric CO_2, and (iii) the possibility of analysis of dark and non-transparent particles (Sun *et al.*, 2019). However, on the other hand, the Raman technique (i) is sensitive to the interference of pigments and contaminants, (ii) requires expensive instruments, and (iii) needs careful purification (Elkhatib & Oyanedel-Craver, 2020). Therefore, the combination of FTIR and Raman would be optimal for reliable and complete detection of microplastics.

DLS and NTA methods use laser light to provide information about the physical properties, size, and number of MPs and NPs. The DLS technique can measure the particles as small as 10 nm (Filipe *et al.*, 2010; Pecora, 2000; Silva *et al.*, 2018). Although these methods use sphere-based models for calibration, they are generally suitable for analyzing MPs and NPs with different shapes. NTA is less limited to particle size than DLS and provides information on the number and concentration of particles (Schwaferts *et al.*, 2019).

2.2.2. Quantitative analysis

A major challenge in the analyses of MPs and NPs in removal processes from water is their quantitative analyses. The analysis of the weight of MPs and NPs in real water using a balance is problematic due to their very low concentration as well as their separation from other types of pollution and minerals. To perform a quantitative analysis of MPs and NPs, TOC analysis is a simple and reliable method (Durán *et al.*, 2018). Although the presence of non-organic pollution does not disturb the TOC analysis, the organic carbon sources could interfere with the analysis of MPs and NPs. Besides, the digestion time should be adjusted to assure the complete dissolution of MPs during the sample preparation.

Another approach for the quantitative analysis of MPs and NPs is coupling the pyrolysis to gas chromatography-mass spectroscopy (GC-MS) (Dekiff *et al.*, 2014; Dumichen *et al.*, 2017; Fries *et al.*, 2013; Nuelle *et al.*, 2014) or liquid chromatography (LC) (Elert *et al.*, 2017; Hintersteiner *et al.*, 2015). This technique not only can provide quantitative data to determine the amounts of MPs and NPs but also would determine the type of polymer by analysis of the (i) decomposition temperature as well as (ii) the evolved byproducts (Rajala *et al.*, 2020b). However, it does not provide direct information on the particle size and number and usually allows the quantification of only one type of polymer. The coupled LC can be in the form of size exclusion chromatography which separates dissolved analytes based on their hydrodynamic volume which depends on the effective size of the molecules. The pyrolysis coupling with GC-MS has been validated for the identification of NPs of PS (50-1000 nm) (Mintenig *et al.*, 2018). This technique provided the tool to analyze MPs < 1.2 µm in real water for the first time (Ter Halle *et al.*, 2017), however, it suffers from the detection of MPs in very low concentrations. It is worth mentioning this limitation to detect MPs differs depending on the type of material. For example, (Mintenig *et al.*, 2018) reported the limitation of 100 ng to detect NPs of PS, *i.e.* 4 mg/L concentration in a 25 µL sample. This limitation

could decrease up to 20 µg/L with ultra-filtration pre-concentration. It is challenging to define the pre-concentration factor in real water, but generally, a factor of 100 would be sufficient (Mintenig *et al.*, 2018). In another work, (Fries *et al.*, 2013) reported the detection limit as low as 10 µg to ensure GC-MS sensors could detect the degradation products.

UV-vis spectrophotometry is a promising technique for the quantitative analysis of NPs (Batool & Valiyaveettil, 2020), which was effective to analyze NPs of PS (0.05 – 0.1 µm) with a concentration as low as 2 mg/L (Chen *et al.*, 2020c). This analysis technique is fast and cost-effective and could be a reliable method for the analysis of NPs. For example, the concentration NPs could be analyzed using the UV-vis spectrophotometry at 201 nm (Chen *et al.*, 2020c) or 260 nm (Wang *et al.*, 2020a) for PS and 454 nm (Batool & Valiyaveettil, 2020) for perylene-3,4,9,10-tetracarboxylic tetrabutylester encapsulated poly(vinyl acetate). Moreover, the estimative quantification of MPs using turbidity is possible for high concentrations of MPs. It has been shown that the turbidity increases almost linearly with the concentration of MP at turbidities higher than 1.5 for the pristine 15 µm PE. For the 140 µm PE, however, the critical turbidity increased up to 3, since the bigger MPs tend to sediment faster. Therefore, turbidity would be a reliable quantitative method for the approximation of weathered MPs (Lapointe *et al.*, 2020b).

2.3. MPs and NPs removal technologies

Different technologies were developed for the removal of MPs and NPs from water. Figure 2 shows the number of published works in recent years on the processes for the treatment of water to remove MPs and NPs. In Figure 2.2a, the studies are categorized based on the works performed on the MPs and NPs removal. As seen, the published works on the removal of MPs have substantially increased in recent years, for example, it almost doubled in 2020 in comparison to 2019. Besides, the first observed work on the removal of NPs published in 2016 and the research in this field attracted significantly higher attention in 2020. In Figure 2.2b, the previous works are categorized based on the type of removal process (separation and degradation). This figure shows an increasing trend in the number of published works on both separation and degradation processes, for example, they increased more than two times in 2020 comparison to 2019.

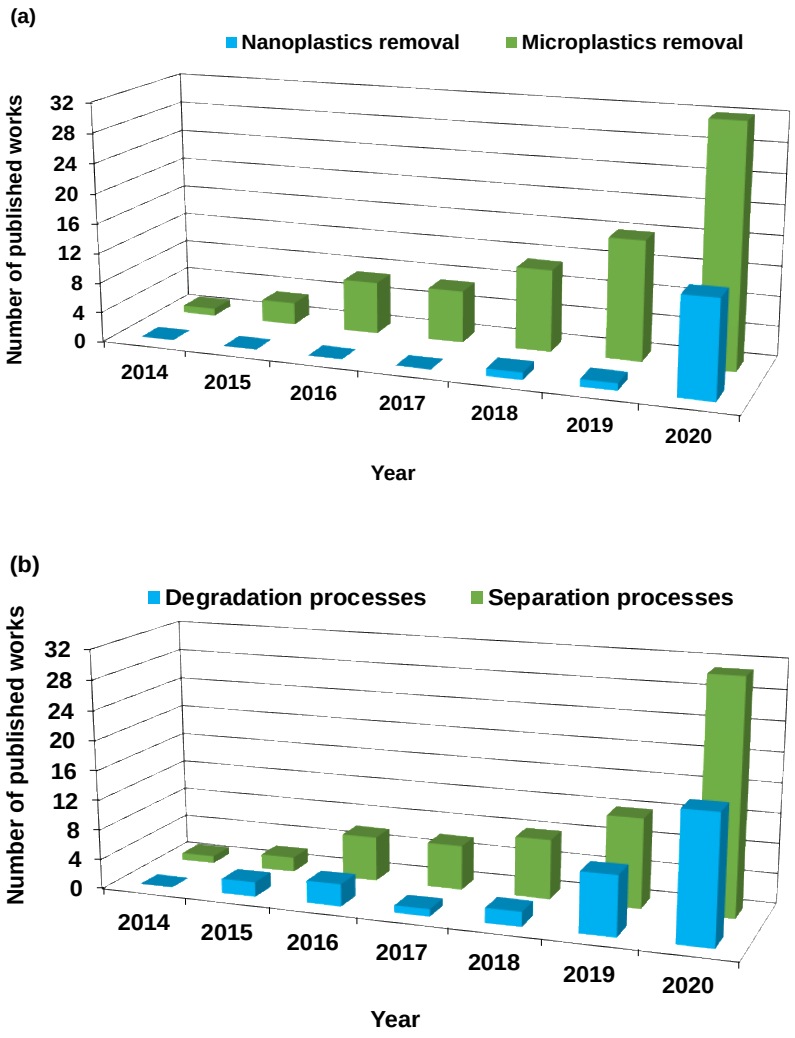

Figure 2. 2 : Rising interest in the processes for removal of MPs and NPs from water (a) removal of NPs vs. MPs, and (b) degradation processes vs. separation processes.

The number of MPs in the influent of WWTPs, the outlet of the primary settling tank, and the outlet of the secondary settling tank could be as high as 31,400, 12,580, and 7863 MPs/L, respectively (Hidayaturrahman & Lee, 2019). Therefore, most of the MPs can be eliminated from water during the primary and secondary treatment in the WWTPs. Nevertheless, to achieve quality standards, different technologies were developed to reduce the amount of this type of pollution through tertiary treatment. The large MPs (0.5–5 mm) can be easily separated by primary settling in WWTPs (Liu *et al.*, 2021). At the pretreatment stage of treatment in WWTP 35%-59% of MPs

could be removed through grease skimming and grit removal (Sun *et al.*, 2019). Besides, 50%-98% of MPs could be removed from the influents through the primary treatment (Gies *et al.*, 2018; Gundogdu *et al.*, 2018a). The abundance of different shapes of MPs in the effluent of WWTPs depends on the characteristics of the influent and treatment process. Most of the previous works reported microfibers as the most abundant MP at the effluent of WWTPs (Bayo *et al.*, 2020; Liu *et al.*, 2020), while microbeads were also found as the most abundant MPs in other works (Hidayaturrahman & Lee, 2019). A comparative study showed the microfibers are more efficiently removed from water in the primary treatment of WWTPs in comparison to the secondary and tertiary stages (Liu *et al.*, 2021). Besides, it was reported that the primary and secondary treatments are the least and most effective steps for the removal of granular MPs. Interestingly, 60% of the suspected MPs in the effluent of RO were identified as plastic, while this value was 10% for the effluent of primary treatment. Therefore, it would be concluded that the secondary treatment is less effective in the removal of MPs in comparison to non-plastic microparticles, which could be attributed to the lower density of MPs. Besides, although reverse osmosis was found to be effective in the removal of irregular and granular MPs, interestingly, it was not capable of substantially reducing the number of microfibers. Observation of MPs at the effluent of RO seems to be surprising due to the small size cut-off of RO membranes. However, other works also reported the possibility of observing small contaminant in the effluent of RO (Cook *et al.*, 2009). This would be attributed to the presence of large pores, membrane imperfections, or simply the gaps between pipelines (Ziajahromi *et al.*, 2017b).

The secondary treatment usually involves biological digestion followed by the separation of flocs by sedimentation. The MPs can be therefore trapped in the flocs of the sludge or extracellular bacterial polymers in the aeration tank. Some of the previous works comprehensively reviewed the biodegradation of MPs and NPs which occurs in the secondary treatment (Sharma *et al.*, 2020; Zhang *et al.*, 2020a; Zhang & Chen, 2020). It is reported that this treatment can eliminate 1.8%-36% of the MPs from the primary treatment effluent (Sun *et al.*, 2019). Some research articles also reported that the secondary effluent can be free of MPs (Michielssen *et al.*, 2016; Sutton *et al.*, 2016), which could be attributed to either low number of MPs in the influent or low sample volume for their analytical method. The previous research findings also reported the secondary treatment can remove mainly the MPs larger than 20 µm (Carr *et al.*, 2016; Dubaish & Liebezeit, 2013; Dyachenko *et al.*, 2017; Mason *et al.*, 2016b; Talvitie *et al.*, 2017a; Talvitie *et al.*,

2017b; Zhang *et al.*, 2020c; Ziajahromi *et al.*, 2017b). Therefore, the tertiary treatments could be necessary since not only small MPs and NPs can be present in the influents but also the treatment processes cause the braking of MPs and NPs into smaller particles. For example, it has been shown that the NPs with a 398 nm size could break into smaller fragments of 74, 54, and 51 nm by sonicator, impeller, and pump, respectively (Enfrin *et al.*, 2020a). Therefore, the developed tertiary treatment processes should be capable of effectively removing MPs smaller than 20 µm and NPs. Thus, the development and analysis of different tertiary treatment processes are necessary to cover various types and concentrations of MPs and NPs.

Table 2.1 presents different treatment processes for the removal of MPs and NPs in waters. This table summarizes the recent studies based on the type of treatment process, MPs/NPs type and size, matrix, operating conditions of the process, and used analytical methods. It provides the tool to compare different processes for the removal of MPs and NPs. The analysis of the efficiency of different processes is an appropriate approach for their comparison. For instance, several studies reported the elimination of more than 88% of the MPs in secondary effluents, while 99.9%, 98.5%, 97%, and 95% of the rest could be eliminated using membrane bioreactor (Misra *et al.*, 2020), disc filtration, rapid granular filtration, and dissolved air flotation, respectively (Talvitie *et al.*, 2017a). The presented works in Table 2.1 are discussed in the related section along with their comparison with other works.

1 **Tableau 2. 1 : Recent works on the treatment processes for the removal of MPs and NPs in waters.**

Treatment process	MPs/NPs type and size	Matrix	Operating conditions	Analytical methods	Results and comments	Reference
Filtration, centrifugation, coagulation	PET (< 400 nm)	Deionized water	- Filter pore size: 0.22, 0.7, 1, 1.6, and 3 µm - Centrifugation speed: 5,000-10,000 rpm - Centrifugation time: 1-10 min - Coagulant: $Al_2(SO_4)_3$ + polymer - Coagulation mixing speed: 150 rpm - Coagulation mixing time: 13 min	- Turbidity - Size distribution analysis	- Filtration with 0.22 µm filter: 92 ± 3% removal - Centrifugation with 10,000 rpm for 10 min: 99±1% removal - Flocculation for 10 min: 77±15% removal	(Murray & Örmeci, 2020)
Dynamic membrane	1.65-516 µm	Synthetic wastewater made from tap water	- Filter size: 90 µm - Filter thickness: 550 mm - Effective diameter: 100 mm - Flow rate: 10 L/ h	- Laser diffraction particle size analysis - Turbidity	- Turbidity reduced from 195 NTU to ≤ 1 NTU after 20 min	(Li *et al.*, 2018b)

MBR	PES, PE, PS, PP, PA, polyurethane, polyvinyl chloride (PVC), polyacrylamide, polyacrylate, alkyd resin, polyphenylene oxides, and ethylene-vinyl acetates (> 300 µm, 100-300 µm, and 20-100 µm)	Primary effluent	- Effective surface: 8 m^2 - Nominal pore size: 0.4 µm - Hydraulic retention time: 20-100 h - Flowrate: 40-90 L/h	- Stereo microscopy with an integrated HD camera	- Elimination of 99.9% of MPs	(Talvitie *et al.*, 2017a)
Disc filtration		Secondary effluent	- Number of discs: 2 (24 filters each) - Filtering surface: 5.76 m^2 - Filter pore size: 10 and 20 µm - Coagulant: Iron salt (2 mg/L) - Polymer: cationic (1 mg/L) - Hydraulic retention time: 4 min - Flowrate: 20 m^3/h		- Elimination of 40-98.5% of MPs (from 0.5-2.0 MPs/L to 0.03-0.3 MPs/L)	
Rapid granular filtration		Secondary effluent	- Gravel bed depth: 1 m - Grain size: 3-5 mm and 0.1-0.5 mm (quartz)		- Elimination of 97% of MPs (from 0.7 to 0.02 MP/L)	
Dissolved air flotation		Secondary effluent	Coagulant: Polyaluminium Chloride (40 mg/L)		- Elimination of 95% of MPs (from 2.0 to 0.1 MPs/ L) - The smallest size fraction (20-100 µm) was the most	

					common before and after treatment	
Disc filtration	PE, PS, and PVC	Synthetic wastewater	- Number of discs: 13 - Filter pore size: 18 µm	- FPA-µFTIR	- Elimination of 89.7% (based on numbers) or 75.6% (based on weight) of MPs	(Simon *et al.*, 2019)
Membrane bioreactor	PES, PE, polyamide, PP (0.25 and 5.0 mm)	Municipal wastewater	- Membrane pore size: 0.4 µm	- Optical microscopy - FTIR - Raman	Influents: 57.6 MPs/L	(Lares *et al.*, 2018)
Secondary treatment			- Volume index of activated sludge: 62 mL/g - TSS: 10.3 mg/L		- Elimination of 98.3% of MPs - Final effluent with 1.0 MPs/L	
Photocatalysis	PE film (50 µm thickness)	Synthetic wastewater made from deionized water	- Photocatalyst: zinc oxide - Reactor: petri dish - Illumination source: 50 w dichromatic halogen lamp - Temperature: ambient	- Digital microscopy - Dynamic mechanical analysis -FTIR	- 30% increase of viscoelastic properties - Formation of hydroperoxides, peroxides, and unsaturated compounds	(Tofa *et al.*, 2019a)

Photocatalysis	PE (500 µm)	Synthetic wastewater made from distilled water	- Photocatalyst: N-TiO_2 - Photocatalyst loading: 10 mg - Reactor type: batch reactor - Temperature: 20 °C - Illumination source: 27 w fluorescent lamp with visible radiation (400-800 nm) - Illumination time: 20 h	- SEM - Optical microscopy - ATR-FTIR - Mass loss analysis	- Mass reduction: 3% after 10 h	(Ariza-Tarazona *et al.*, 2019)
Electrooxidation	-	Washing machine effluent	- Anode material: BDD - Anode surface: 63.5 cm^2 - Current density:16.6, 36.6, and 66.6 $mA.cm^{-2}$ - Electrolysis time: 6 h	- COD analysis - TOC analysis - Spectrophotometry	- 88.9% COD reduction in 6 h	(Durán *et al.*, 2018)
Electrooxidation	PS (25 µm)	Synthetic wastewater	- Anode material: BDD, MMO, and IrO_2 - Anode surface: 83 and 41.6 cm^2 - Current intensity: 3, 6, 9 M - Electrolysis time: 1-6 h	- Weight analysis - granulometric analysis - COD analysis	- Elimination of 89 ± 8% of MPs - Optimum condition of 0.03 M electrolyte concentration, Na_2SO_4 as	(Kiendrebeogo *et al.*, 2021b)

				- TOC analysis - SEM	electrolyte material, 9 A current intensity, and 6 h electrolysis time.	
Coagulation	PE and PES (< 500 µm)	Artificial wastewater	- MP concentration: 100, 300, 500, 700, and 1000 mg/L - Coagulant: PAC and $FeCl_3$ - Coagulant dose: 30, 60, 90, 120, and 180 mg/L	- SEM - FTIR	- Elimination of 75.61% of MPs - Elimination higher in alkaline condition than acidic	(Zhou *et al.*, 2021)
Coagulation	PE (15 µm), rayon (8.7 or 20.6 µm), and PES (17.5- 50.6 µm)	Simulated drinking water	- Coagulant: Alum - Coagulant dose: 5 and 10 mg/L	- Zeta potential - Turbidity	- Finial turbidity < 1.0 NTU	(Skaf *et al.*, 2020)
Flocculation	PS (0.05-0.1 µm)	Artificial wastewater	- Flocculant: Mg/Al-layered double hydroxides - Mg/Al ratios: 0:1, 1:1, 2:1, 3:1, 4:1, or 1:0	- UV-vis spectrophotometer - Zeta potential - SEM	- Elimination ≥ 90%	(Chen *et al.*, 2020c)

Coagulation and flocculation	PE (15 and 140 µm), PS (140 µm), PES	Municipal wastewater	- UV intensity: 10 mW/cm^2 - Coagulation time: 2 min - Flocculation time: 4 min	- Quartz crystal microbalance with dissipation monitoring (QCM-D)	- PES removal: 97% - PE removal: 99% - PS removal: 84%	(Lapointe *et al.*, 2020b)
Electrocoagulation	PE (300-355 µm)	Artificial wastewater	- Current density: 15 mA/cm^2 - Electrolyte: NaCl (10 g/L) - Initial MP concentration: 0.1 g/L - Electrode: Al	- TSS analysis - Counting fluorescent particles	- Elimination ≥ 90% - Optimal elimination of 99.24%	(Perren *et al.*, 2018)
Primary treatment	25-500 µm	Influent and effluent from WWTP	- Screening (mesh size: 5 mm), - Grit removal - Sedimentation	- FTIR analysis - Spectroscopy - IR microscopy	- MPs removal from 3.0 to 1.5 MPs/L	(Ziajahromi *et al.*, 2017b)
Primary and secondary treatment			- Primary screening (mesh size: 3 mm) - Grit removal and sedimentation - Aeration - UV disinfection		- Removal of 66% of MPs - MPs removal from 1.44 to 0.48 MPs/L	

Primary, secondary, and tertiary (reverse osmosis) treatment			- Screening (mesh size: 3 mm) - Sedimentation - Biological treatment - Flocculation - Disinfection - Ultrafiltration - Reverse osmosis - De-carbonation		- Removal of > 90% of MPs - MPs removal from 2.2 to 0.21 MPs/L	
Primary and secondary treatment	PES, PE, PP (> 55 µm)	Influents and effluents from WWTP	- Rough filter - Ventilated sand and oil retainer - Primary settling - Aeration - Final settling	- Microscopy - µRaman analysis	- Elimination of 73-79% of MPs	(Gundogdu *et al.*, 2018a)
Primary and secondary treatment	> 1 µm	Influent and effluent from WWTP	- Vertical screening - Primary clarification - Trickling filters - Secondary clarifiers	- Microscopy - FTIR analysis	- Removal > 99% of MPs	(Gies *et al.*, 2018)
Primary, secondary, and tertiary treatment	20-200 µm	Influent and effluent	- Screening - Grit removal - Pre-aeration - Primary sedimentation	- Stereo microscopy	- Removal of 98% of MPs	(Talvitie *et al.*, 2015)

		from WWTP	- Activated sludge treatment - Secondary sedimentation - Tertiary biological filtration			
Primary, secondary, and tertiary treatment	≥ 500 µm and ≤ 500 µm	Influent and effluent from WWTP	- Primary skimming - Biological treatment - Filtration	- ATR-FTIR - FPA-µFTIR	- Removal of 93% of MPs with < 500 µm size - Removal of 98% of synthetic fibers by filtration	(Mintenig *et al.*, 2017)
Activated sludge filter and secondary clarification	20 µm - 4.75 mm	Secondary effluent	- Screening - Skimming - Anaerobic digester	- Stereo microscopy	- Removal of 95.6% of MPs	(Michielssen *et al.*, 2016)
Tertiary treatment		Tertiary effluent	- Granular sand filtration - Chlorination-dechlorination		- Removal of 97.2% of MPs	
MBR		Primary and tertiary effluents	- Microfilter pore size: 0.2 µm		- Removal of 99.4% of MPs	

2

The developed processes for the removal of MPs and NPs from waters could be categorized as separation and degradation processes. As seen in Figure 3, the separation treatment processes include rapid granular filtration, disc filtration, membrane filtration, MBR, dynamic membrane filtration, coagulation and electrocoagulation, and air flotation. On the other hand, the degradation processes comprise catalytic degradation, photocatalytic degradation, and electrochemical degradation. According to Figure 2.3, the separation processes could remove at least 90% of MPs or NPs. The degradation processes have a lower efficiency than the separation processes and it could be as low as 50% (for catalytic degradation). In this section, the challenges and opportunities in the application of these methods for MPs and NPs treatment are discussed in detail.

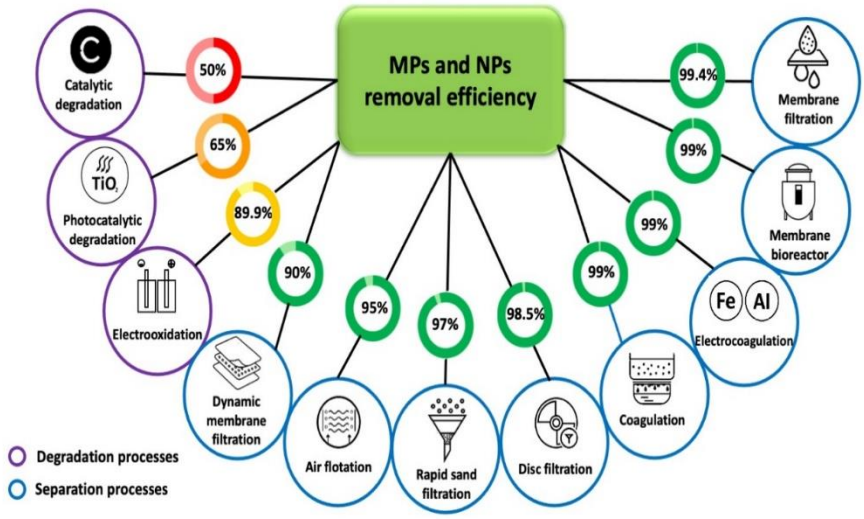

Figure 2. 3 : Developed treatment processes for the removal of MPs and NPs from water along with their maximum reported removal efficiency.

2.3.1. Separation processes

2.3.1.1. Rapid granular filtration

The main role of the rapid granular filter is to separate the suspended solids from the water through the entire depth of the filtration. In this process, the MPs would be removed from water by (i) trapping between the pores formed by the gravel or anthracite grains, or (ii) adsorption on the silica grains (Rajala *et al.*, 2020b). Although a regular backwash can be carried out on the rapid granular filter for its regeneration, the presence of hydroxyl groups on the MPs surface could hinder their easy detachment from the filter (Enfrin *et al.*, 2019). (Hidayaturrahman & Lee, 2019) examined three WWTPs in South Korea and concluded that 73.8% of MPs could be removed from sewage using the rapid granular filtration in full-scale. Similarly, (Bayo *et al.*, 2020) showed that a full-scale rapid granular filtration process can remove 75.49% of MPs from wastewater. (Talvitie *et al.*, 2017a) considered a filter with 1 m depth of sand and 3-5 mm grain size as well as 0.5 m depth of quartz with a grain size of 0.1-0.5 mm for full-scale removal of MPs. They reported an MPs removal efficiency of 97% as well as a drop in the MPs frequency from 0.7 to 0.02 MPs/L. In a lab-scale study, granular filtration removed 60%~80% of 10 µm MPs, though it increased up to 95%~100% using a combination of sand filtration with biochar (Wang *et al.*, 2020e). The mechanism of MPs removal was found to be stuck for sand filter whilst it was stuck, trapped, and entangled for the combined granular and biochar filtration. The different MPs removal efficiencies obtained in the previous works using granular filtration could be ascribed to the dependency of this process on the size of MPs. It has been shown that the removal efficiency of rapid granular filtration depends on the size of MPs and the lowest removal efficiency (86.9% ± 4.9%) was obtained for the MPs with a 10-20 µm size (Zhang *et al.*, 2020c). Interestingly, the reduction in the size of MPs and NPs did not reduce the removal efficiency, and 1 µm MPs and 180 nm NPs had a higher removal efficiency than the ones with a size of 10-20 µm.

2.3.1.2. Disc filtration

Disc filtration could be employed for the removal of MPs either with the aerobic digestion process with activated sludge or as tertiary treatment. In this process, the removal of MPs is based on physical retention in the filters and the formation of mud cake on the filter panels. This removal can be improved by the use of coagulants for faster cake formation. Controlling the water level inside the filter is important since the formation of the cake decreases the filtration rate, causing

a rise in the water level. Consequently, the filter usually includes a level sensor that starts the backwashing when required. A pilot-scale study has demonstrated the elimination of 40% - 98.5% of MPs larger than 20 µm with disc filters after 4 min of water retention time (Talvitie *et al.*, 2017a). They suggested the control or regular monitoring of the quality of water before the coagulation, as excessive addition of coagulant could lead to rapid fouling of the filter. In this case, the accelerated frequency of backwashing under high pressure could reduce the efficiency of removing MPs in the effluents. Simon et al. (Simon *et al.*, 2019) evaluated the application of a disc filter containing 13 discs with a polyester mesh size of 18 µm as a tertiary treatment for the removal of MPs in full-scale. They showed that the disc filter can remove 89.7% of MPs larger than 10 µm from wastewater. In a case study, they estimated the annual MPs discharge from a disc filter-assisted (as tertiary treatment) WWTP that receives around 10,000 $m^3.day^{-1}$ of wastewater to be as low as 1.1 kg.

2.3.1.3. Membrane filtration

The membrane pore size could be designed to be smaller than the MPs and NPs to remove them effectively. In a lab-scale study, Murray and Örmeci (Murray & Örmeci, 2020) used membranes having 0.22 µm (nylon syringe filter, Derian) and 0.7 µm (GF/F glass microfiber filters, Whatman) rated pore diameters to separate MPs. They reported that these membranes could be used in the microfiltration process to separate respectively 92 ± 3% and 84 ± 3% of NPs with a size of 333 ± 76 nm (based on SEM images) or 217 ± 4 nm (based on Zetasizer measurements). Taking advantage of the negative charge of the aged MPs and NPs, the membrane charge could be modified to enhance the removal efficiency by electrostatic attractions. In another research work, home-made ultrafiltration membranes with positive, neutral, and negative surface charges were synthesized from Polyacrylonitrile and employed for NPs removal on lab scale. It was found that the positively charged membrane increased the selectivity to 50 nm NPs of PS (which were even smaller than the membrane pores) (Wang *et al.*, 2020a). It is reported that membrane filtration using neutral membrane illustrated 92.4% removal efficiency for the 500 nm NPs, while it was 12.3% and 2.3% for 100 and 50 nm NPs, respectively. The removal efficiencies of positively surface charged membranes for these NPs, however, improved to 99.4%, 99.3, and 89.9% respectively. Interestingly, the membrane efficiency could enhance around 39 times after the surface charge modification. Analysis of the flux of the positively surface charged membrane in

the second cycle was almost similar to the first cycle, while it reduced significantly in the non-modified membrane. Metal-organic framework-based foams showed a great capacity for the lab-scale microfiltration process to remove NPs (273 nm) with a removal efficiency of 95.5% and excellent recyclability (10 cycles) (Chen *et al.*, 2020b). In another work, 99.3% of the MPs (mainly 10-1000 µm) found in synthetic seawater (made from edible salts) were successfully separated by nylon and polycarbonate filter papers (0.2 µm pore size and 25 mm diameter) through lab-scale ultrafiltration and microfiltration (Yaranal *et al.*, 2020). To conclude, membrane filtration is a promising approach for the removal of MPs, however, the economic feasibility of nanofiltration is challenging because of the required high pressures and its low rate of treatment.

A challenge in the application of membrane filtration is the fouling of the membrane which reduces the throughput. The small MPs and NPs could impose a more intense fouling effect than the big ones because they cause complete to intermediate pore blocking (Enfrin *et al.*, 2020b). At the beginning of treatment, the membrane fouling by MPs is intermediate and it can cause complete blocking over time. The cake formation could then occur and the dominant membrane clogging mechanism at a prolonged time is internal pore blocking (Hou *et al.*, 2021). It is worth mentioning that this mechanism was obtained using fresh MPs/NPs and it could be changed to cake layer formation and internal pore-blocking after environmental aging. Dynamic membrane filtration and sequential membrane filtration are developed to decrease the membrane fouling and therefore reduce the maintenance cost and energy input.

2.3.1.4. Membrane bioreactor

MBR is the most investigated membrane filtration technology for the removal of MPs and one of the promising ones. MBR processes can be developed by the combination of membrane filtration with aerobic bioreactors (AeMBR) or anaerobic bioreactors (AnMBR). AeMBR generally is characterized by a higher operating cost than AnMBR because of the need for aeration to activate microorganisms (Zaouri *et al.*, 2021). The MPs and NPs removal efficiency of AnMBR is generally higher than AeMBR. For instance, the MPs removal of 94% was reported for AnMBR after 6 h (Pittura *et al.*, 2021), while for AeMBR it took 3 months to reach 98.3% (Maliwan *et al.*, 2020). The main common drawback of these two processes is membrane fouling. Various factors such as operating conditions, membrane specifications, and wastewater characteristics affect the membrane fouling during the separation of MPs and NPs (Maliwan *et al.*, 2020). In general, the

fouling and permeability properties of AeMBR and AeMBR processes are different. Based on the filter resistance analysis, Maliwan et al. (Maliwan *et al.*, 2020) showed that the scouring property of MPs reduced the fouling during the operation.

MBR generally has one of the highest MPs removal efficiency compared to other wastewater treatment processes (Shen *et al.*, 2020). Leslie et al. reported that only 25% of MPs were removed using an MBR with a pore size of 0.08 µm (Leslie *et al.*, 2017b). This could be due to the presence of long fibers that potentially cross the membranes longitudinally and especially because of the high applied pressure in the MBRs. Besides, abrasion can increase the size of the membrane pores and reduce its performance during time. Contradictory, most of the works suggested the MBR as an effective process for the removal of MPs. The removal of MPs using a pilot-scale MBR has been reported to be more than 99% (Hou *et al.*, 2021; Lares *et al.*, 2018; Lv *et al.*, 2019; Michielssen *et al.*, 2016; Ngo *et al.*, 2019; Padervand *et al.*, 2020; Talvitie *et al.*, 2017a). This could be because of the high hydraulic retention time of MBRs (24-100 hours) which would favor the formation of biofilms and trap of MPs (Talvitie *et al.*, 2017a).

2.3.1.5. Dynamic membrane filtration

Dynamic membrane technology has been studied for the treatment of municipal wastewater (Ersahin *et al.*, 2014; Lu *et al.*, 2016; Padervand *et al.*, 2020; Poerio *et al.*, 2019; Salerno *et al.*, 2017). This technology has a unique character since using the existing contaminants in the water to form a filtration layer, without introducing additional chemicals or other contaminants. Various factors, such as the membrane material, membrane pore size, size of MPs, and concentration of MPs affect the performance of dynamic membrane filtration (Sol *et al.*, 2020). Li et al. (Li *et al.*, 2018b) demonstrated the formation of a dynamic membrane on the sieve after 20 min of filtration of synthetic wastewater with 1 g/L of diatomite in the lab scale. They showed that the mesh combined with the newly formed layer led to a removal of nearly 90% of the particles larger than 90 µm. Although this work was carried out with MPs larger than 5 µm, this technique would also be applied to NPs. The required time for the formation of the dynamic membrane could be one of its limits for the removal of MPs and NPs.

2.3.1.6. Coagulation, electrocoagulation, and flocculation

The main difference between electrocoagulation and coagulation is the in-situ generation of metal ions and hydroxyl ions by electrodes in electrocoagulation. Otherwise, they have the same principle according to which the cationic (like Fe and Al) and anionic (like hydroxyl) ions in the solution neutralize the charges of MPs and NPs and make them unstable. These pollutants can then form larger and more stable aggregates to promote their gravity separation from water. Since the weathering oxidation of MPs would cause the formation of hydroxyl ions on their surface (Enfrin *et al.*, 2019), in the secondary effluents, the free MPs and NPs are either neutral or negatively charged. In this case, favorable conditions can be provided for the effective removal of MPs and NPs using coagulation or electrocoagulation. It is worth mentioning that even neutral MPs and NPs can be adsorbed on metallic hydroxides ($Fe(OH)_3$ or $Al(OH)_3$) formed during the coagulation/ electrocoagulation. During these processes, the removal of MPs and NPs can be attributed to co-precipitation or electrostatic attraction on the surface of metallic hydroxides. MPs and NPs can act as a ligand to bind the formed metallic hydroxides. In general, both coagulation and electrocoagulation are effective for the removal of MPs (Hidayaturrahman & Lee, 2019; Hou *et al.*, 2021; Ma *et al.*, 2019a; Perren *et al.*, 2018; Rajala *et al.*, 2020a; Shahi *et al.*, 2020). A recent study demonstrated that a full-scale coagulation process removed 40.5–54.5% of MPs, most of them were in the form of fibers (Wang *et al.*, 2020d). Lab-scale research showed that the coagulation process is 25% more effective with Al^{3+} ions than Fe^{2+} ones to eliminate MPs of 0.1-5 mm size (Ma *et al.*, 2019b). It is also reported that by the addition of anionic surfactant as a coagulant aid, the MPs removal enhanced to more than 60%. Analysis of the effect of MPs size on a lab-scale coagulation process showed the removal was almost complete for the 30-100 nm MPs, while it almost halved for the 10-30 nm ones (Shahi *et al.*, 2020). In contrast, the lab-scale removal efficiency of 15 µm PE MPs (77%) using 0.45 mg Al/L was higher than the 140 µm ones (64%) (Lapointe *et al.*, 2020b). While the weathering of the 140 µm MPs increased its removal efficiency up to 89% because of enhancing the physical and chemical heterogeneity of the MPs surface. Moreover, a lab-scale study showed the addition of sand to the coagulation process can enhance the MPs removal by around 27% (Shahi *et al.*, 2020). Coprecipitation by calcium carbonate could remove more than 99% of poly(methyl methacrylate) and poly(vinyl acetate) NPs from the water in the lab-scale after 30 min (Batool & Valiyaveettil, 2020). This method was effective since the removal was more than 96% after just 3 min. According to a study (Perren *et*

al., 2018), a lab-scale electrocoagulation process could eliminate more than 99% of the MPs with 300 µm size. The combination of coagulation and electrocoagulation with membrane filtration is suitable for the removal of MPs and NPs from secondary effluents (Enfrin *et al.*, 2019).

The flocculation is another approach to separate MPs and NPs from waters that can be employed individually or in combination with the coagulation/electrocoagulation (to neutralize the charge of MPs and NPs) (Magalhães *et al.*, 2020). Analysis of the MPs sedimentation rate at lab scale showed the relatively low affinity between MPs and Al-based coagulants compared to cationic polyacrylamide (as a flocculant), confirming the importance of the flocculation process (Lapointe *et al.*, 2020b). Interestingly, in other lab-scale studies, more than 90% and 80% of NPs removed from water using Mg/Al (Chen *et al.*, 2020c) and Ca/AL (Chen *et al.*, 2020d) layered double hydroxides as a flocculant, respectively. Electrostatic adsorption and intermolecular force were suggested as the main mechanisms for NPs capture by this method. PE and PP MPs (250–350 µm) were separated in pilot-scale using the pH-induced sol-gel formation of silanes to make large agglomerates (2–3 cm) that could be easily separated and then recycled (Herbort *et al.*, 2018b). The same authors analyzed different linear and branched alkyltrichlorosilanes for the agglomeration of MPs and reported the intermediate chain length ones with carbon atoms between 3 and 5 are the best suited (Sturm *et al.*, 2020). The shorter alkyl groups or the longer ones with the number of carbon atoms more than 8 were not suitable because the MPs could not be localized sufficiently. The combination of coagulation and flocculation in lab-scale could remove up to 99% of weathered PE MPs and, interestingly, 97% of the highly stable pristine PE MPs (Lapointe *et al.*, 2020b).

2.3.1.7. Air flotation

Air flotation is one of the methods used to remove flocs and suspended compounds such as MPs and NPs during primary and secondary water treatment. It consists of an injection of pressurized air into the water to produce air bubbles of size between 20-70 µm which attach to the MPs and NPs and carry them to the water surface (Talvitie *et al.*, 2017a). The application of this process in tertiary treatment would allow better control of the bubble size because of the lower organic matter concentrations. The dominant mechanism of MPs removal by the conventional air flotation process is the hydrophilic/hydrophobic interaction. In a lab-scale study, it was shown that the adhesion of MPs of PE and PET to microbubbles was stronger than that of PA which has

hydrophilic groups on its surface (Wang *et al.*, 2020c). However, in the presence of cetyltrimethylammonium bromide (CTAB) as a surfactant, the charge attraction is dominant. The removal efficiency of the air flotation process considerably depends on the size of MPs. For example, the air flotation process could reach the complete removal efficiency of the MPs with 20~25 μm size by increasing the saturation pressure up to 0.50 MPa (Wang *et al.*, 2020c). Nevertheless, for the MPs in the range of 15~20, 10~15, 5~10, and 2~5 μm, it could not pass 79%, 76%, 49%, and 46% at this pressure, respectively. The integration of 40 mg/L of polyaluminium chloride as flocculant with air flotation at a pressure of 1 atm allowed the elimination of 95% of MPs (20-300 μm) in a full-scale study (Talvitie *et al.*, 2017a). Regarding the MPs in the range of 20-100 μm, contradictory results are reported in the literature. For example, Talvitie et al. (Talvitie *et al.*, 2017a) reported that the full-scale air flotation process can remove MPs as small as 20-100 μm. While, Enfrin et al. (Enfrin *et al.*, 2019) showed that in this process MPs with a 20-100 μm size may largely escape the removal process. They attributed this result to the fact that the smallest particles have a higher surface charge density and are therefore more difficult to destabilize. Thus, the air flotation process would be necessary to be coupled with other processes for effective removal of small MPs and NPs. The surface-functionalized microbubbles could remove over 94% of 5 μm PS from artificial water on lab-scale (Zhang *et al.*, 2021a). For poly-(methyl methacrylate), however, the removal was not as high as PS because of the presence of humic acid. This technique could completely remove both MPs from river water with MPs concentrations lower than 18.6×10^5 particles/mL.

2.3.2. Degradation processes

The degradation processes could be promising alternatives to remove small MPs and NPs from waters. Besides, these processes can be environmentally friendly solutions for the elimination of MPs in the concentrate stream of the separation processes. The degradation of NPs seems more promising than MPs since the reactivity with hydroxyl radicals substantially increases at higher surface areas of plastic (Bianco *et al.*, 2020). Catalytic, photocatalytic, and electrochemical degradation are three processes tested for the degradation of MPs and NPs. All the works on the degradation of MPs and NPs were performed on the lab scale, therefore, further research is necessary to evaluate the challenges in their scale-up.

2.3.2.1. Catalytic degradation

Catalytic degradation is a process that can result in the mineralization of MPs and NPs. Since some catalysts are active at the ambient or moderate temperature and pressure, they can be employed for the degradation of MPs and NPs in water. For example, in a lab-scale study, the encapsulated manganese carbide nanoparticles in helically N-doped carbon nanotubes (Mn@NCNTs) can decompose MPs (Kang *et al.*, 2019). Although the synthesized catalyst was stable, its recyclability was a challenging task. The MPs degradation efficiency at ambient conditions was around 5% and 7% after 8 h in the presence of catalyst only and both catalyst (Mn@NCNTs) and peroxymonosulfate, respectively. Under hydrothermal conditions at 120 ° C, however, the removal efficiency reached around 17% in the presence of the catalyst. It was claimed that at a high concentration of 5 g/L, around 50% of MPs were degraded through the catalytic process under optimized conditions. A vast range of intermediates was found by HPLC analysis after the catalytic decomposition of MPs, including tetracosane, heneicosane, nonadecanol, pentadecanedioic acid, nonadecane, benzyl butyl phthalate, 14-Methoxy-14-oxotetradecanoic acid, dimethyl suberate, methyl 10-undecenoate, decanoic acid, methyl 8-oxooctanoate, pimelic acid, 6-Decennial, 2-Ethylcaproic acid, succinic acid, 1-Hexanoic acid, levulinic acid, 3-Butenoic acid, propionic acid, acetic acid, and formic acid. The generated intermediates were reported to be environmentally friendly, without any negative effect on the aquatic microorganisms (Kang *et al.*, 2019).

2.3.2.2. Photocatalytic degradation

Photocatalytic degradation is the most studied degradation process for the removal of MPs and NPs from water. The use of solar energy for this degradation is an environmental solution in solving this problem. The photocatalyst is activated by a photon of light whose energy is greater than or equal to the bandgap of the photocatalyst (Karimi Estahbanati *et al.*, 2019a; Karimi Estahbanati *et al.*, 2019b). The activation leads to the transfer of electrons from the valence band to the conduction band, forming positive holes in the valence band (Estahbanati *et al.*, 2019; Karimi Estahbanati *et al.*, 2017). In the presence of electron acceptors such as O_2, H_2O, and OH^-, these charges generate reactive oxygen species ($HOO^\bullet$, H_2O_2, $O_2^{\bullet-}$, $OH^\bullet$) (Feilizadeh *et al.*, 2019; Karimi Estahbanati *et al.*, 2020). Therefore, the MPs and NPs are oxidized either directly by the holes on the surface of the photocatalyst or by the generated reactive oxygen species which can

migrate into the water. A possible mechanism of photocatalytic degradation of MPs is presented by Jing *et al.* (Jiang *et al.*, 2020). In this mechanism, the formed hydroxyl radicals by the photogenerated holes attack the C–H bond of the PE molecule and separate a proton. The generated radical reacts with dissolved oxygen to generate an alcoholic group which can be more easily break and form an oxygen-centered radical. Afterward, the C–C bond of the C atom where the oxygen-centered radical is locating breaks, forming an aldehyde molecule and a carbon chain free radical. The breakage of C–C bonds could continue till the complete degradation of by-products into CO_2 and H_2O.

A 5.38% mass reduction was observed after photocatalytic degradation of high-density polyethylene (HDPE) MPs (200–250 µm) using enhanced hydroxy-rich ultrathin BiOCl with mannitol (Jiang *et al.*, 2020). This mass reduction was 24 times higher than that of BiOCl nanosheets (0.22%) and without photocatalyst (0.04%). The degradation of low-density polyethylene film with 50 µm thickness using zinc oxide photocatalyst activated by visible light showed (i) changes in the viscoelastic properties of the plastic, (ii) a 30% increase in the carbonyl index, and (iii) the formation of unsaturated groups such as hydroperoxides, peroxides, and carbonyl on the surface of the microfilm (Tofa *et al.*, 2019a). In another work, the same authors showed the plasmonic ZnO-Pt demonstrated 15% higher photocatalytic activity than ZnO alone (Tofa *et al.*, 2019b). The analysis of the degradation efficiency of 500 µm PE MPs (extracted from toothpaste) using an N-TiO_2 photocatalyst showed around 2.86% mass reduction after 8 h (Ariza-Tarazona *et al.*, 2019). The rate of photocatalytic PS NPs degradation enhanced by decreasing the NP size (for 140 nm was higher than 508 nm) (Allé *et al.*, 2020). The same conclusion was reported for HDPE MPs (200–250 µm) (Jiang *et al.*, 2020). Similarly, the mass loss of 814 and 382 µm HDPE spherical MPs using the photocatalytic process were 0.22% and 4.65%, respectively (Llorente-García *et al.*, 2020). Besides, the mass loss of 5 × 5 mm and 3 × 3 mm low-density polyethylene films with 146 nm thickness was 0.97% and 1.38%, respectively. These could be attributed to the higher surface area of the smaller NP that leads to faster degradation by hydroxyl radicals (Bianco *et al.*, 2020). The rate of HDPE MPs (200–250 µm) degradation was dependent on the surface hydroxyl groups on the surface of BiOCl (Jiang *et al.*, 2020). Analysis of the pH of water showed the rate of photocatalytic degradation of NPs was higher at acidic (pH=4) and near neutral (pH=6.3) than basic (pH=9) conditions (Allé *et al.*, 2020). Similarly, HDPE MPs (200–250 µm) were degraded faster in acidic condition than the basic one, which was

reported to be attributed to the Coulomb repulsion in the alkaline condition (Jiang *et al.*, 2020). Using a design of experiment approach to optimize the photocatalytic degradation of MPs demonstrated the maximum mass loss was 7.8% after 6 h (Razali *et al.*, 2020). However, the degradation increased up to 38% after five cycles. Besides, increasing the reaction temperature using solar thermal collector (from 35 to 50°C) and size of PP sheet (from 25 to 100 mm^2) had a more significant effect on the MP weight loss than the photocatalyst loading (1-3 g/l) (Razali *et al.*, 2020). The photocatalytic degradation of MPs under visible light using a continuous flow reactor demonstrated more than 65% reduction in the volume of MPs after two weeks (Uheida *et al.*, 2020). Fifteen by-products formed through photocatalytic degradation of PP in this flow reactor, which was found to have a low toxicity effect on the human and aquatic environment. The photocatalytic degradation efficiency of PS MPs in water was around half of that in water (Nabi *et al.*, 2020). This would be attributed to the lack of intimate contact between the photocatalyst film and MPs which were suspended in water, while in the solid phase the MPs were placed on the top of the photocatalyst film with direct contact. Besides, the hydrophilicity of the PS MPs hinders the facile attack of the generated hydroxyl radicals from the photogenerated holes.

2.3.2.3. Electrochemical degradation

The electrochemical degradation process is usually used for the removal of organic pollutants that are chemically non-oxidizing or difficult to oxidize (Debik *et al.*, 2020; Garcia-Segura *et al.*, 2015b; Panizza *et al.*, 2001; Yassine Ouarda *et al.*, 2018). It is a process based on the in-situ generation of hydroxyl radicals by direct and indirect electrochemical processes. The direct action of anodic oxidation of MPs and NPs takes place in two stages. First, an anodic discharge of water molecules is obtained with the formation of a hydroxyl radical ($OH^{\bullet}$) adsorbed on active sites of the electrode. Subsequently, the MPs and NPs are oxidized by the adsorbed radical and form partially oxidized products. These products can be further oxidized by the hydroxyl radicals which are continuously formed by the anodic discharge of water until complete oxidation of MPs and NPs to CO_2 and H_2O (Comninellis, 1994; Drogui *et al.*, 2007). Therefore, the electro-oxidation mechanism of MPs and NPs would follow that of photocatalytic degradation.

The electrochemical process is well-suited for tertiary treatment. Durán et al. (Durán *et al.*, 2018) demonstrated relatively high MPs (from washing machine effluent) removal capability by electro-oxidation. With an improved conductivity by the addition of 7 g/L of Na_2SO_4 and the application of

a current density of 16.6 mA.cm^{-2} on BDD (boron-doped diamond), the COD reduced up to 79.7% after 6 h. This was possible owing to the assistance of sulfate ($SO_4^{2-\bullet}$) and persulfate ($S_2O_8^{2-\bullet}$) radicals which are weaker oxidants than hydroxyl radicals but have a longer lifespan. It is worth mentioning that $H_2S_2O_8$ (a powerful oxidant) can be generated in the solution during the electrolysis using BDD in the presence of sulfate. On the other hand, when a current density of 66.6 mA.cm^{-2} was applied, the elimination of the COD reached 88.9%. This shows that the applied current density is a major factor in the electrooxidation of MPs, similar to the degradation of other pollutions (Melián *et al.*, 2016). In another work, (Miao *et al.*, 2020a), removed 56 wt% of PVC MPs using electro-Fenton technology. Similarly, 58 ± 21% of MPs were degraded by the electrooxidation process just in 1 h (Kiendrebeogo *et al.*, 2021b). It was also revealed that up to 89 ± 8% of MPs could be degraded after 6 h using BDD as the anode, current intensity of 9 A (108.4 mA.cm^{-2}), and 0.03 M Na_2SO_4 as the supporting electrolyte. The SEM analysis of the remained MPs in water after the electrooxidation demonstrated all of them were unchanged, suggesting the complete mineralization of MPs at the anode surface. DLS also confirmed this suggestion by observation of the formation of no MPs with lower size than the initial MPs. It was also verified by detecting no C=O bond by FTIR analysis on the MPs after electrooxidation (Kiendrebeogo *et al.*, 2021b).

It can be concluded that the electrochemical processes could be a promising approach for the degradation of MPs in industrial and municipal effluents, however, the effects of anode fouling and mutual contaminations should be further studied. Besides, more efforts are required to reduce the high energy consumption of the electrochemical process as the key parameter that increases its operating costs. The electrochemical processes can be applied for the elimination of MPs and NPs in the concentrate of the separation processes. From this point of view, the electrochemical processes are promising alternatives for the management of the waste of separation processes.

2.3.3. Innovative processes

Different innovative methods have been suggested for the removal of MPs and NPs from waters in recent years. Considering the significance of modern technologies to solve contemporary issues, these methods must be considered for future research and development. Table 2.2 presents these methods along with their removal efficiencies. These innovative methods include light-driven micromotors (Wang *et al.*, 2019), magnetic extraction (Grbic *et al.*, 2019; Misra *et al.*,

2020; Rius-Ayra *et al.*, 2020; Sun *et al.*, 2020; Tang *et al.*, 2021), extraction with ionic liquids (Elfgen *et al.*, 2020; Misra *et al.*, 2020), adsorption (Herbort & Schuhen, 2017; Herbort *et al.*, 2018a; Tiwari *et al.*, 2020), and electrosorption (Xiong *et al.*, 2020). As seen in Table 2.2, even if these methods are at the beginning of their development for MPs and NPs removal, their removal efficiencies are relatively great. Therefore, further research should be performed to elucidate the potential of these approaches.

Tableau 2. 2 : Innovative approaches for the removal of MPs and NPs in waters.

Method	MP/NP	Type of plastic	Removal efficiency (%)	Reference
Photocatalytic removal by Au@Ni@TiO_2 micromotors	MP	PS	71%	(Wang *et al.*, 2019)
Magnetic extraction by hydrophobic Fe nanoparticles	MP	PE, PS, PET, PVC, PP, and polyurethane	92% (10-20 µm) 93% (1 mm)	(Grbic *et al.*, 2019)
Magnetic extraction by polyoxometalate -supported ionic liquid	MP	PS	> 90%	(Misra *et al.*, 2020)
Magnetic extraction by powdered iron	MP	HDPE	~ 100%	(Rius-Ayra *et al.*, 2020)
Magnetic extraction by sunflower pollen grains	MP	PS	75%	(Sun *et al.*, 2020)
Magnetic extraction by	MP	PE, PET, and polyamide	~ 100% (first cycle) ~ 80% (forth cycles)	(Tang *et al.*, 2021)

magnetic carbon nanotubes				
Removal by inorganic-organic hybrid silica gels	MP	-	-	(Herbort & Schuhen, 2017)
Agglomeration by organic-chemical stressors	MP	PE	-	(Herbort *et al.*, 2018a)
Adsorption by Zn/Al layered double hydroxides	NP	PS	100% (pH = 4) 37% (pH = 9)	(Tiwari *et al.*, 2020)
Electrosorption	NP	PS and PVC	0.707 mg NPs/(g AC)	(Xiong *et al.*, 2020)

2.4. Conclusion and perspectives

In this review, the potentials of different qualitative and quantitative techniques for MPs and NPs analysis which could be employed to study water treatment processes were first discussed. Afterward, the main water treatment processes based on separation and degradation for the removal of MPs and NPs from waters were reviewed. It was observed that in general, the separation processes illustrate a higher removal performance than the degradation processes. In this regard, MPs or NPs removal efficiencies up to 97% for rapid granular filtration, 98.5% for disc filtration, 99.4% for membrane filtration, 99% for MBR, 90% for dynamic membrane filtration, 99% for coagulation, 99% for electrocoagulation, and 95% for air flotation were reported. On the other hand, for the degradation processes, the MPs or NPs removal efficiencies up to 50%, 65%, and 89.9% were reported for catalytic, photocatalytic, and electrochemical degradation, respectively. In the light of this literature review, it was observed that the separation processes face the issue of MPs and NPs management after their separation and on the other hand, the degradation

processes would not be economically viable. Therefore, we suggest the employment of the degradation processes to treat the concentrate stream of the separation processes. This approach could increase the elimination performance of both MPs and NPs while reducing the costs of their degradation.

The removal of MPs and NPs from water is an emerging field of research that is rapidly evolving. Most of the previous works focused on the elimination of MPs from water rather than the NPs. A few works were performed on the elimination of NPs from water using filtration and flocculation processes. However, no work was observed on the performance of MBR, dynamic membrane filtration, electrocoagulation, air flotation, and electrooxidation processes for the removal of NPs. Therefore, more study is essential to elucidate the potential of these processes in the removal of NPs in water.

Acknowledgments

The authors would like to acknowledge the financial support from the Fonds de recherche du Québec–Nature et technologies (FRQNT), the CREATE-TEDGIEER program, the National Sciences and Engineering Research Council of Canada (NSERC), and the Canadian Francophonie Scholarship Program.

Au vu de la littérature dans la partie synthèse, la plupart des procédés de dégradation électrochimique se sont concentrés sur la dégradation des molécules organiques dissous (pesticides, colorants, médicaments, etc.) et leurs sous-produits. Traditionnellement les performances de ces procédés sont évaluées par les méthodes directes d'analytiques du COT, de la DCO, et indirecte (absorbances spécifiques au spectrophotomètre UV-vis). Ce qui ne s'applique pas forcement aux MPs/NPs.

Par ailleurs, en considérant les challenges évoqués dans le chapitre 2 sur les techniques analytiques des MPs/NPs dans l'eau et dans la perspective de démontrer la faisabilité de la dégradation par OEC des MPs/NPs (25 µm et 100 nm de diamètre nominal), il est nécessaire de commencer cette étude par ajuster certaines techniques analytiques déjà utilisées dans la littérature à la spécificité de la taille des particules et du type de polymère utilisés au cours de nos travaux. Cela permet la détermination de la plage de concentration des particules dans l'eau synthétique pour laquelle les résultats sont fiables face aux limites de la méthode ou de la combinaison de 2 techniques analytiques considérées. Ces concentrations pourront être liées directement ou indirectement au MPs/NPs pour l'évaluation de la performance du procédé OEC.

Par conséquent, plusieurs électrodes d'anode pour l'OEC des MPs ont été testés et l'électrode de BDD a été choisie pour étudier l'influence de différents paramètres opératoires tels que la densité de courant, la surface de l'anode, le type de l'électrolyte (effet de l'oxydation directe et indirecte) et la concentration du Na_2SO_4. Ce qui a permis de déterminer si l'oxydation directe et indirecte sont bénéfiques à la dégradation des particules de micro-plastiques dans le chapitre 3.

3. TREATMENT OF MICROPLASTICS IN WATER BY ANODIC OXIDATION: A CASE STUDY FOR POLYSTYRENE

TRAITEMENT DES MICROPLASTICS DANS L'EAU PAR OXYDATION ANODIQUE : UNE ÉTUDE DE CAS POUR LE POLYSTYRÈNE

Marthe K[1], M.R. Karimi Estahbanati[1], Ali Khosravanipour M.[1], Patrick D.[1*], RD. Tyagi

[1] Institut national de la recherche scientifique (INRS) - Centre Eau Terre Environnement (ETE), 490 rue de la Couronne, Québec (QC), CANADA, G1K 9A9

Environmental Pollution 269 (2021) 116168

https://doi.org/10.1016/j.envpol.2020.116168

Abstract

Water pollution by microplastics (MPs) is a contemporary issue which has recently gained lots of attentions. Despite this, very limited studies were conducted on the degradation of MPs. In this paper, we reported the treatment of synthetic mono-dispersed suspension of MPs by using electrooxidation (EO) process. MPs synthetic solution was prepared with distilled water and a commercial polystyrene solution containing a surfactant. In addition to anode material, different operating parameters were investigated such as current intensity, anode surface, electrolyte type, electrolyte concentration, and reaction time. The obtained results revealed that the EO process can degrade 58 ± 21% of MPs in 1 h. Analysis of the operating parameters showed that the current intensity, anode material, electrolyte type, and electrolyte concentration substantially affected the MPs removal efficiency, whereas anode surface area had a negligible effect. In addition, dynamic light scattering analysis was performed to evaluate the size distribution of MPs during the degradation. The combination of dynamic light scattering, scanning electron microscopy, total organic carbon, and Fourier-transform infrared spectroscopy results suggested that the MPs did not break into smaller particles and they degrade directly into gaseous products. This work demonstrated that EO is a promising process for degradation of MPs in water without production of any wastes or by-products.

Keywords:

Microplastic; polystyrene; electrooxidation; degradation; polymer.

3.1. Introduction

Plastics are used in all consumer sectors, so that global production is growing every year. It rose from 322 million tons in 2015 to 360 million tons almost in 2018 (Plastics, 2019). It is estimated up to 10% of the produced plastics fragments would be found in the marine environment (Cole *et al.*, 2011). Once present in the marine environment, the plastics undergo aging processes that cause their degradation and fragmentation into small particles called microplastics (MPs, particles less than 5 mm) (Lambert & Wagner, 2016) and then into nanoparticles (particles less than 100-1000 nm)(Gigault *et al.*, 2018b). Polystyrene is one of the most widely used commercial plastic in the world (Wegner *et al.*, 2012; Zarfl & Matthies, 2010), therefore, it is one of the most commonly found polymers in marine environments (Hidalgo-Ruz *et al.*, 2012a; Moore, 2008).
The release of MP into the marine environment is recognized as an important problem related to water pollution (Lambert & Wagner, 2016). It has been shown that in aquatic environments, these MPs adsorb toxic substances and can be ingested by aquatic organisms. Afterwards, they accumulate in the food chain and subsequently reach humans (Chae & An, 2017a; Hans Bouwmeester *et al.*, 2015). Among different toxic effects on aquatic organisms which have been proved by previous studies, there is a decrease in growth rate, fertility, lifespan, and reproductive time (Besseling *et al.*, 2014; Jeong *et al.*, 2016b; Wegner *et al.*, 2012). Polystyrene is a plastic material whose toxicity has been widely demonstrated (Besseling *et al.*, 2014; Lee *et al.*, 2013; Rossi *et al.*, 2014a).

Although MPs are detected at low concentrations in wastewater treatment plants' effluents, these effluents are still a potential way to release MPs because of the large volume of effluents discharged into the aquatic environment (Ziajahromi *et al.*, 2017b). It has been shown that the wastewater treatment plants fragment 80% of MPs into nanoplastics which can increase the number of plastic particles around 10 times (Enfrin *et al.*, 2019). The concentration of MPs with size of 10-300 µm in wastewater treatment plants' influents and effluents has been reported in a range of 1-10044 and 0-447 particles/L, respectively (Sun *et al.*, 2019). Accordingly, the conventional treatment is unable to completely remove the MPs and it is essential to develop other technologies to remove MPs in the effluent of wastewater treatment plants.

The previous efforts to develop such technology focused on the separation processes such as rapid sand filtration, disc filtration, dissolved air flotation, MBR/ultrafiltration, dynamic membrane

filtration, and electrocoagulation (Lares *et al.*, 2018; Li *et al.*, 2018c; Perren *et al.*, 2018; Talvitie *et al.*, 2017a). Since all of these technologies just separate MPs and does not degrade them, additional efforts are required to manage the separated MPs. A limited research concerned the degradation of MPs and most of these works performed on photocatalytic degradation of MPs which showed generally a couple of weeks is required to obtain an acceptable degradation efficiency (Horikoshi *et al.*, 1998; Phonsy *et al.*, 2015b). This long processing time does not present a bright perspective because of the current photocatalysis technology. Therefore, development of efficient technologies to degrade MPs in a reasonable time scale is essential. In addition, the degradation processes should be studied to evaluate the possibility of developing a hybrid zero-discharge process by coupling (i) the separation of MPs into a concentrated stream with (ii) the degradation of MPs in the concentrated stream. This configuration hinders the discharge of small MPs into the aquatic environments.

In recent years, electrooxidation (EO) process has been developed for the degradation of persistent pollutants, such as pesticides, dyes, pharmaceuticals, and petrochemicals found in effluents (Amer, 2019; Francisca *et al.*, 2013; Garcia-Segura *et al.*, 2015a; Tran, 2009; Yassine *et al.*, 2018). This process is environmentally friendly as it could degrade MPs into nontoxic molecules like water and carbon dioxide without addition of chemicals. EO is based on *in-situ* generation of oxidizing radicals like hydroxyls ($^{\bullet}OH$) by direct and indirect electrochemical process. The standard reduction potential of hydroxyl radicals (E ($^{\bullet}OH$ /H_2O): 2.80 V/SHE) allows it to break the polymeric bonds of MP and degrade them. Therefore, EO is a promising zero sludge technology to degrade MPs at atmospheric condition. To the best of our knowledge, there is no work on electrooxidation of MPs found in the literature.

The aim of this study was to explore the degradation of MPs from water using anodic oxidation. As polystyrene MPs exhibit the highest toxicity among common MPs, polystyrene microbeads with 26 µm size were used as a representative MP. An experimental approach was followed to determine the best operating parameters of the EO process (current intensity, anode surface area, anode material, electrolyte type, electrolyte concentration, and time) to effectively oxidize MPs in water. For each parameter, the MPs degradation performance was evaluated using removal efficiency and mode size of MPs, which were obtained by weight loss and dynamic light scattering (DLS) analyses, respectively. The samples were examined by microscopic, spectroscopic, and total organic carbon (TOC) analyses to evaluate the shape and size, surface functional groups, and formed by-products, respectively, and then evaluate the obtained results

through parametric study. In addition, total current efficiency of the EO process was evaluated and an economic analysis was conducted for different conditions. Finally, a mechanism of polystyrene degradation was proposed based on the obtained results.

3.2. Materials and methods

3.2.1. Preparation of water sample

The mono-dispersed suspension of polystyrene microbeads with 10% MP concentration (100 g/L) supplied by thermo scientific USA and used as the MP source. The nominal diameter and uniformity of size of MPs were 25 µm and 15%, respectively. These microbeads were used to make 100 mg/L MP suspension in deionized water. The suspensions were prepared spontaneously before starting the experiments. The amount of added electrolyte for the improvement of electrical conductivity was 4.25, for both Na_2SO_4 and $NaNO_3$, and 3.50 g/L for NaCl. These amounts correspond to 0.03, 0.05, and 0.06 M, respectively. The pH of all prepared solutions was approximately 6.0. Finally, 50 mL samples were taken to characterize the sample before treatment.

3.2.2. Experimental unit

The EO reactor was made of plexiglass with dimensions of 14.5 × 6.4 × 17.7 cm and an operating volume of 900 mL. All experiments were made in batch mode. Boron-doped diamond (BDD), mixed metal oxide (MMO), and iridium oxide (IrO_2) electrodes were employed as anodes and titanium electrode was used as cathode. The electrodes were gridded and had a circular shape with a diameter of 12 cm, a thickness of 0.1 cm, and a surface area of 113.1 cm^2. In the reactor, the anode and cathode were fixed vertically with 1 cm space and were connected to the positive and negative outputs of a DC power supply, respectively. The reactor was placed in a box containing ice cubes to put the entire external surface of the reactor in direct contact with the ice cubes.

3.2.3. Experimental procedure

The tests were carried out at room temperature. The temperature of solutions was followed by a scientific J-KEM thermocouple. To mitigate the evaporation of solution due to the temperature rise caused by electrooxidation at high current intensities, a cooling system was employed. The solution was mixed by agitation with a magnetized bar. In a typical experiment, the current densities set at 108 and 216 $mA.cm^{-2}$ for BDD, 108 $mA.cm^{-2}$ for MMO, and 433 $mA.cm^{-2}$ for IrO_2. In addition, the initial concentration of microbeads and the electrolyte concentration (Na_2SO_4) were set at 100 mg/L, and 0.03 M, respectively. The sampling time was 1, 2, 3, and 6 h. To assure that high water temperature (which was observed in a few experiments at high current) has no effect on the results, a control test carried out without electrooxidation at 100°C for 6 h. EO tests consisted of analyzing different operating parameters, such as current density (3, 6, and 9 A), types of oxygen-intensive anodes (BDD, MMO, and IrO_2), anode surface area (41.5 and 83 cm^2), and type (Na_2SO_4, $NaNO_3$, NaCl) as well as concentration (0.03, 0.04, 0.06 M) of electrolyte.

3.2.4. Analytical procedure

The electrooxidation of MPs performance was assessed by combining the evolution of the particle size profile of MPs with the mass loss of MPs over time. In addition, scanning electron microscopy (SEM), Fourier-transform infrared spectroscopy (FTIR), and TOC analyses were performed to evaluate the obtained results.

3.2.4.1. Particle size analysis

The particle size distribution of MP in water was measured by dynamic diffusion of light using a particle size analyzer (Laser Scattering Particle Size Distribution Analyzer LA-950, HORIBA, 0.01-3000 µm). A refraction index of 1.59 was used for the analyses. In addition to particle size distribution, the mode size distribution was considered for assessment of the particle size during treatment. For each analysis, 50 ml of sample was injected into the particle size analyzer.

3.2.4.2. Removal efficiency analysis

The elimination of MPs was followed by measuring the weight of MPs in 50 ml samples taken during the EO treatment. The samples were filtered with 0.22 µm pore size nitrocellulose filters to separate the MPs. The filters were then dried in an oven at 40 °C for 24 hours to evaporate water.

The amount of remained electrolyte salt in the filter after drying was measured using electrolyte solutions without MP. These data were used to correct the errors due to the remaining salt in the filters during the analysis of MP degradation. The mass loss of MP was calculated using Eq. (3.1):

Équation 3.1: $Weight\ loss\ (\%) = \frac{W_0 - W_t}{W_0} \times 100$

where W_0 and W_t are the initial and final mass of MPs, respectively.

In order to calculate the total current efficiency (TCE) for anodic oxidation of MP, the COD values of the water before and after treatment were determined by MA. 315–DCO 1.1 method. The samples were first digested in a CR 3200 thermo reactor at 150°C for 2 h. The COD values were then obtained by analysis of the samples using Spectrophotometer-Vis UV0811M136. The TCE values were then calculated using the following equation (Ciríaco *et al.*, 2009; Durán *et al.*, 2018):

Equation 3.2 : $TCE\ (\%) = FV_s \cdot \frac{(COD_0 - COD_t)}{8I\Delta t} \times 100$

where COD_0 and COD_t are initial and final chemical oxygen demands, respectively, in g O_2. L^{-1}, I represents the current intensity (A), F is the Faraday constant (96487 C mol^{-1}), V_s is the water volume (L), 8 is the oxygen equivalent mass (g $eq.^{-1}$), and Δt is the electrooxidation time interval (s).

3.2.4.3. SEM analysis

The size and shape of MPs before and after EO were analyzed by SEM analysis. After mixing, 1 mL of sample was placed on specimen stub and dried at room temperature for 24 hours. The samples were then covered with a layer of gold by SPI coasting device to make them electrically conductive. The shape and size of MPs were analyzed using ZEISS EVO 50 smart device. The INCA software was used to capture the images.

3.2.4.4. FTIR analysis

For FTIR analysis, 700 mL of sample was filtered to separate the MPs. The MPs were then analyzed by FTIR Spectrometer (Nicolet 50, Thermo Fisher, USA) equipped with an attenuated total reflectance (ATR) diamond crystal module. The range of scanning set from 500 to 4000 cm^{-1} and the collection time was 16 s. The obtained spectrums were compared with the reference spectrum recorded with particles before EO.

3.2.4.5. TOC analysis

The presence of dissolved organic carbon in the samples during the EO was analyzed after filtration of remained MPs through a filter with pore size of 0.22 µm to evaluate the generation of by-products. Nitrocellulose filter was used for separation of the remained MPs. The TOC analysis was then conducted using Shimadzu VCPH device.

3.2.4.6. Analysis of energy and electrolyte cost

To conduct the economic analysis, the energy consumption was first calculated using Eq. (3.3):

Equation 3.3 : $Energie\ consumption\ \left(KW-h/_{m^3}\right)=\frac{I\times T\times t}{V}\times 10^3$

where I, T, t, and V represent current intensity (A), electrical potential (v), time (h), and volume (m^3), respectively. Energy consumption and electrolyte costs were two factors considered for estimating the operating cost of EO. A unit cost of 0.06 \$KW-h.m^{-3} was used to calculate energy cost. The cost of chemicals was estimated based on a unit cost of 0.3, 0.06, 0.4 \$US/kg for Na_2SO_4, NaCl, and $NaNO_3$, respectively.

3.3. Results and discussion

3.3.1. Characterization of MPs

Figure 3.1a depicts the size distribution of MPs before EO which obtained by DLS analysis. It was observed that the size range is 17-45 µm and the distribution is unimodal with 26 µm mode size with a standard deviation of 4 µm. The mode size is close to the nominal diameter size of 25 µm which indicated by the supplier. The respective D10, D50, and D90 were obtained at 21.20, 26.15, and 32.60 µm, respectively. Figure 3.1b shows the morphology of particles which obtained by an optical microscope. It can be seen that all the particles are in spherical shape that confirms the obtained values from DLS analysis were the diameter of spheres.

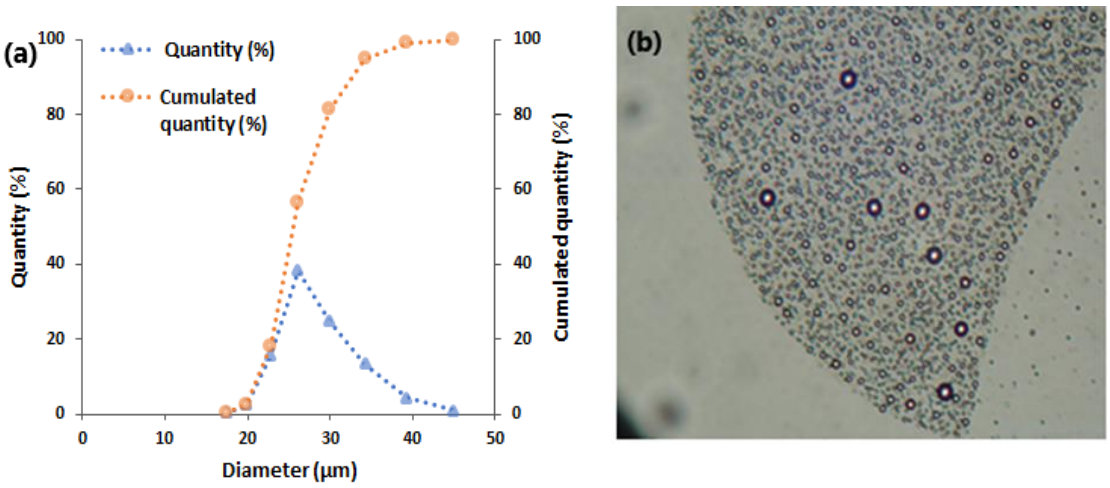

Figure 3. 1 : (a) Size distribution of the used MP, (b) a view of MPs under an optical microscope.

3.3.2. Parametric study of MPs EO

3.3.2.1. Effect of the applied current intensity

In order to investigate the effect of current intensity, a series of experiments were conducted at 3, 6, and 9 A using BDD and 0.03 M Na_2SO_4 solution. Figure 3.2 depicts mass removal percentage and MPs mode size over EO time. It shows a significant effect of current intensity on the MPs weight loss and a reduction in the MPs size. It can be seen that the weight loss starts from the beginning of treatment and increases depending on the current intensity. To achieve an elimination efficiency of 89 ± 8%, an EO operating time of 6 hours was required with a current intensity of 9 A (which is equal to the current density of 108.4 $mA.cm^{-2}$). A degradation efficiency of 56 ± 10% was recorded at 6 A (72.28 $mA.cm^{-2}$) and a very low degradation of MP was observed at 3 A (36.14 $mA.cm^{-2}$). A very good degradation efficiency at 9 A could be explained by the high sensitivity of BDD to the current intensity. The higher applied current density allowed the anode to oxidize more water molecules into hydroxyl radicals that helps in the enhancement of MPs oxidation. To compare with previous studies, for washing machine effluent treatment which contained microfibers, a COD removal of 85% was achieved at 180 min, current density of 66.6 $mA.cm^{-2}$, and Na_2SO_4 concentration of 7 g/L (Durán *et al.*, 2018).

In order to analyze the size of MPs during the EO process, the DLS analysis was conducted. According to Figure 3.2b, at 3 and 6 A, even after 6 h the degradation was not complete and the MPs with the size of around 26 µm were observed. It can also be observed that no MPs with lower size was detected, which suggests the complete degradation of MPs at anode. At 9 A, however, after 2 h all the MPs are broken apparently into small particles. This result can be attributed to the degradation of MPs or decrease in their amount/size below the detectable values of the DLS analysis. Observation of a determinative effect of current intensity and time in EO process is in line with other studies (Dia *et al.*, 2016; Drogui *et al.*, 2007). To assess that, a DLS analysis was carried out with a concentration of 40 mg/L of MPs without treatment. That is almost the same amount of MP after its degradation at 9 A after 2 h. The results showed that the most frequent remained particle size was about 26 µm which confirms the remained MPs were not actually degraded into smaller particles.

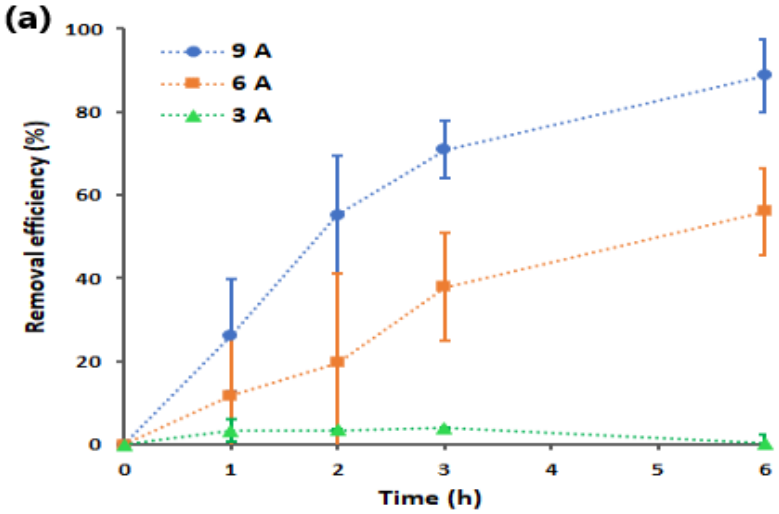

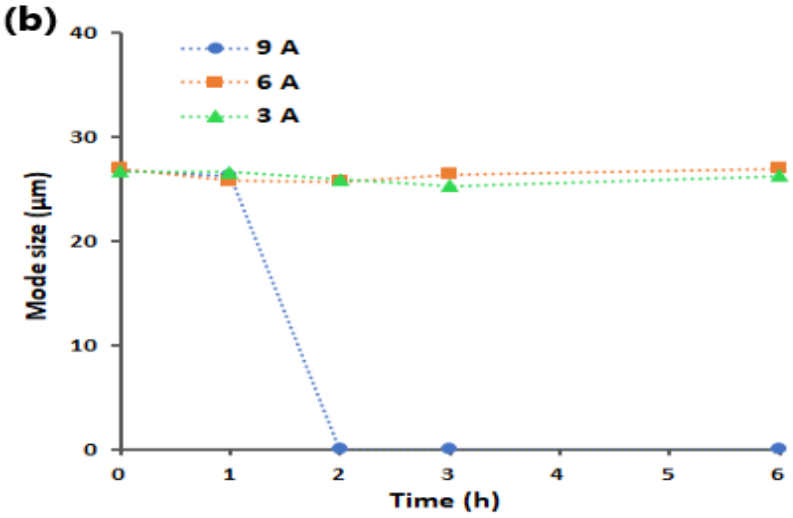

Figure 3. 2 : The effect of current density on the EO of MPs. (a) Removal efficiency (%), (b) Mode size (µm).

3.3.2.2. Effect of the anode surface area

The effect of anode surface area was evaluated by comparing the EO processes with 41.6 and 83 cm^2 surface areas at a constant of 9 A and 0.03 M Na_2SO_4 solution. As it can be seen from Figure 3.3a, in these conditions the anode surface area had almost no effect on the removal efficiency as after 6 h of operation the efficiency for both mentioned anodes reached around 90%. Despite this, at 41.6 and 83 cm^2 the potential was respectively 15 and 11 V, leading the reduction of energy consumption by increasing the anode surface area from 1080 to 792 kWh/m^3. The electrical resistivity decreased while increasing the electrode surface area. Figure 3.3b shows the effect of anode surface area on the reduction of the size of MPs. It shows that at higher anode surface area, no MPs with 26 µm size was detected by DLS analysis after 2 h. However, at smaller anode surface area, 6 h of electrooxidation time was required for MPs (with 26 µm size) disappearance in the solution. This discrepancy can be mainly attributed to the fact that when the anode area increases, the exchange surface area of electrode/electrolyte augments, so that shorter time was recorded for MPs degradation.

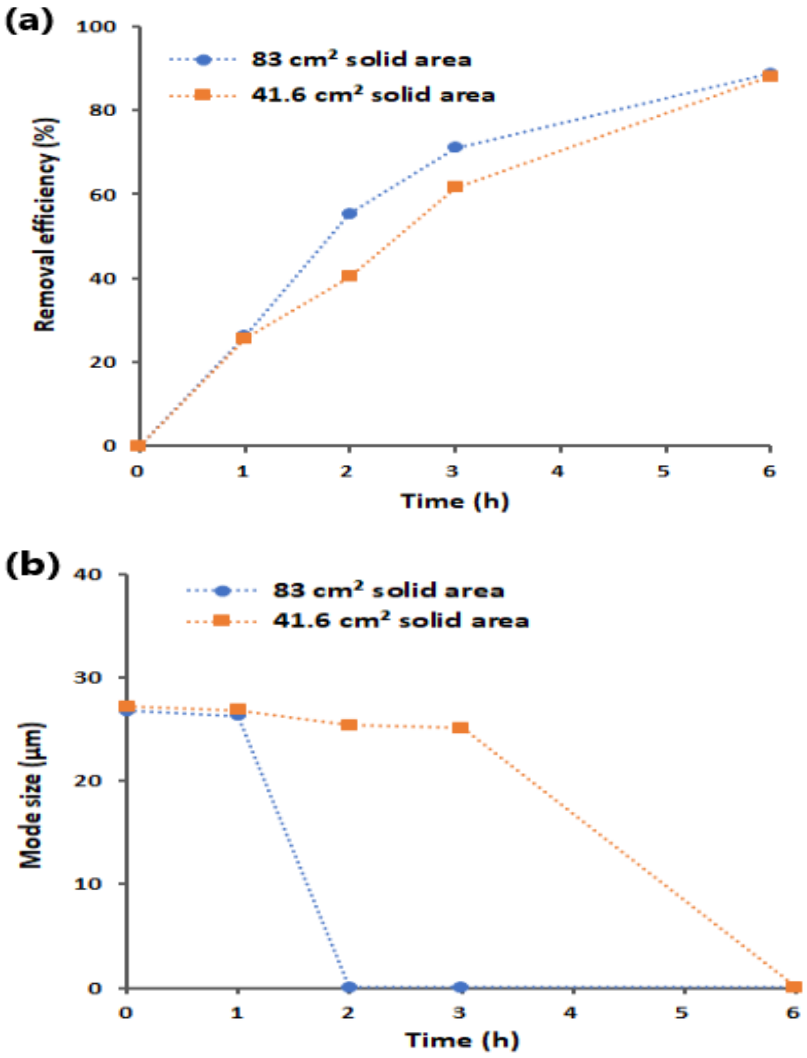

Figure 3. 3 : The effect of anode surface area on the EO of MPs. (a) Removal efficiency (%), (b) Mode size (µm).

3.3.2.3. Effect of the anode material

The electrode material defines the capacity for the generation of oxidants. As a result, the selection of electrode material is critical for an efficient EO process (Bhuta, 2014). The effect of anode material was analyzed by conducting experiments using BDD, MMO, and IrO_2 as anode material. For these experiments, the same intensity of 9 A and a Na_2SO_4 concentration of 0.03 M were applied during 6 h. Figure 3.4 shows the performance of EO process at different types of anode materials. A removal efficiency of 89%, 22%, and 12% was observed using BDD, IrO_2, and

MMO, respectively (Figure 3.4a). It shows that BDD is substantially more powerful than IrO_2 and MMO for the degradation of MPs, as its reaction rate was around 4 and 7.4 times more than those two materials, respectively. Observation of a higher removal efficiency by BDD can be attributed to its higher rate of hydroxyl radical generation, as the previous research showed that BBD can produce around 4 times more hydroxyl radical than MMO (Yassine *et al.*, 2018). According to Figure 4b, after 2 h of EO using BDD, no MPs was detected by DLS analysis. However, even after 6 h of EO using MMO and IrO_2, the MPs with initial size of 26 µm were detected. These results are in line with other researches that demonstrated that BDD has much higher oxidation potential than other common anodes such IrO_2 and MMO (Ciríaco *et al.*, 2009; Flox *et al.*, 2006; Martínez-Huitle *et al.*, 2004; Zhao *et al.*, 2009). BDD shows a great potential to react with pollutants due to the generation of a large amount of hydroxyl radicals (Frontistis *et al.*, 2017; Yassine *et al.*, 2018). However, for the case of MMO, it is shown that it has a strong reactivity with produced hydroxyls radicals which reduces the amount of available hydroxyls radicals (Durán *et al.*, 2018; M. Panizza *et al.*, 2001; Ozcan *et al.*, 2008; Wang & Li, 2011).

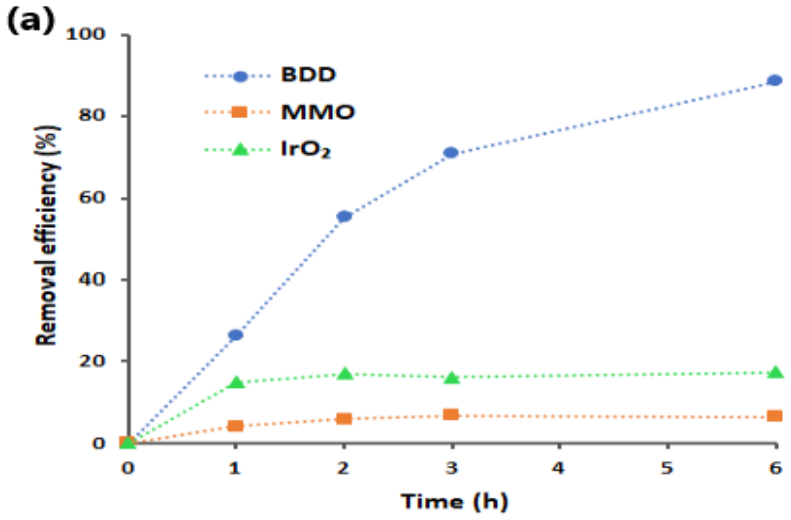

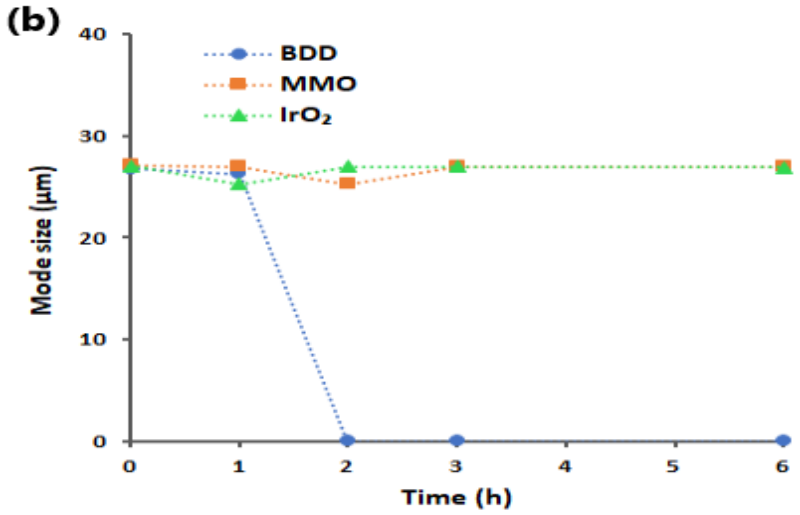

Figure 3 4 : The effect of anode material on the EO of MPs. (a) Removal efficiency (%), (b) Mode size (µm).

3.3.2.4. Effect of the supporting electrolyte type

Some experiments were conducted using Na_2SO_4, $NaNO_3$, and NaCl as supporting electrolyte to determine the effect of electrolyte type as well as the contribution of direct and indirect oxidation of MPs. The electrolytes were used at different concentrations to be able to impose the same current intensity of 9.0 A and electrical potential of around 14.9 V. The pH of solutions was fixed close to 6.0. Figure 3.5 presents the effect of electrolyte type on the removal efficiency and mode size of MPs. As Figure 3.5a shows, the removal efficiency was almost the same for NaCl and Na_2SO_4 till 2 h, but it increased faster afterwards using Na_2SO_4. For the case of $NaNO_3$, the removal efficiency was almost constant till 3 h and a significant increase was obtained between 3 and 6 h. As can be seen from Figure 3.5a, 89% removal efficiency was achieved after 6 h of EO using Na_2SO_4. However, 58% and 52% removal efficiencies were obtained with NaCl and $NaNO_3$, respectively. It shows that the rate of EO using Na_2SO_4 was 1.53 and 1.71 times higher than NaCl and $NaNO_3$, respectively. Other works also reported a higher EO rate using Na_2SO_4 which confirm the obtained result in this work (Durán *et al.*, 2018; Panizza & Cerisola, 2005). According to Figure 5b, no MP with the initial size of around 26 µm was detected after 2 and 3 h using Na_2SO_4 and NaCl, respectively. However, even after 6 h, these MPs were detected using $NaNO_3$.

The different behavior of the electrolytes can be attributed to the action of different produced oxidizing species. In the case of NaCl, chloride ions are oxidized into chlorine gas (Cl_2) at anode (Eq. 3.4)), which reacts with water in the next step to form hypochlorous acid (Eq. (3.5)) and then dissociates into hypochlorite ions (Eq. (3.6)) (Durán *et al.*, 2018; Ozcan *et al.*, 2008). When Na_2SO_4 is used as supporting electrolyte, it dissociates into hydrogen sulfate and then persulfate ions ($S_2O_8^{2-}$), sulfate radicals ($S_2O_4^{-\bullet}$) are formed through Eqs. (3.7, 3.8) (M. Panizza *et al.*, 2001; Wang & Li, 2011). These highly reactive species could indirectly oxidize MPs and increase the removal efficiency. However, in the case of using $NaNO_3$ as supporting electrolyte, no oxidizing agent could be produced in the solution and only. It is worth noting that nitrate can be electrochemically reduced to ammonia (see Eqs. (3.9) and (3.10)) ((Dia *et al.*, 2017; Li *et al.*, 2009; Renata & Luís, 2013).

Équation 3.4 : $2Cl^- \rightarrow Cl_2 + 2e^-$

Équation 3.5 : $Cl_2 + H_2O \rightarrow HClO + Cl^- + H^+$

Équation 3.6 : $HClO \rightarrow ClO^- + H^+$

Équation 3.7 : $2HSO_4^- \rightarrow S_2O_8^{2-} + 2H^+ + 2e^-$

Equation 3.8: $SO_4^{2-} + OH^\bullet \rightarrow SO_4^{\bullet-} + OH^-$

Équation 3.9 : $NO_3^- + H_2O + 2e^- \rightarrow NO_2^- + 2OH^-$

Équation 3.10 : $NO_2^- + 5H_2O + 6e^- \rightarrow NH_3 + 7OH^-$

Accordingly, the relatively low percentage of MP removal recorded using $NaNO_3$ can be attributed to nitrate reduction into nitrite (NO_2^-) and ammonia (NH_3) (Dia *et al.*, 2017). In fact, using $NaNO_3$ as supporting electrolyte, the electrochemical decomposition of MPs was only due to direct anodic oxidation (by means of $^\bullet$OH radicals generated on the BDD). When Na_2SO_4 and NaCl were used as supporting electrolyte, the electrochemical decomposition of MPs could be carried out by using two paths: direct anodic oxidation and indirect electrochemical oxidation via mediators such as active chlorine species (ex HClO, ClO^-, etc), persulfate ions ($S_2O_8^{2-}$) and sulfate radicals ($S_2O_4^{-\bullet}$). The direct anodic oxidation takes place on the surface of anode material, whereas indirect electrochemical oxidation takes place in aqueous solution. The two effects can lead to the formation of powerful oxidizing agents capable of effectively removing MPs.

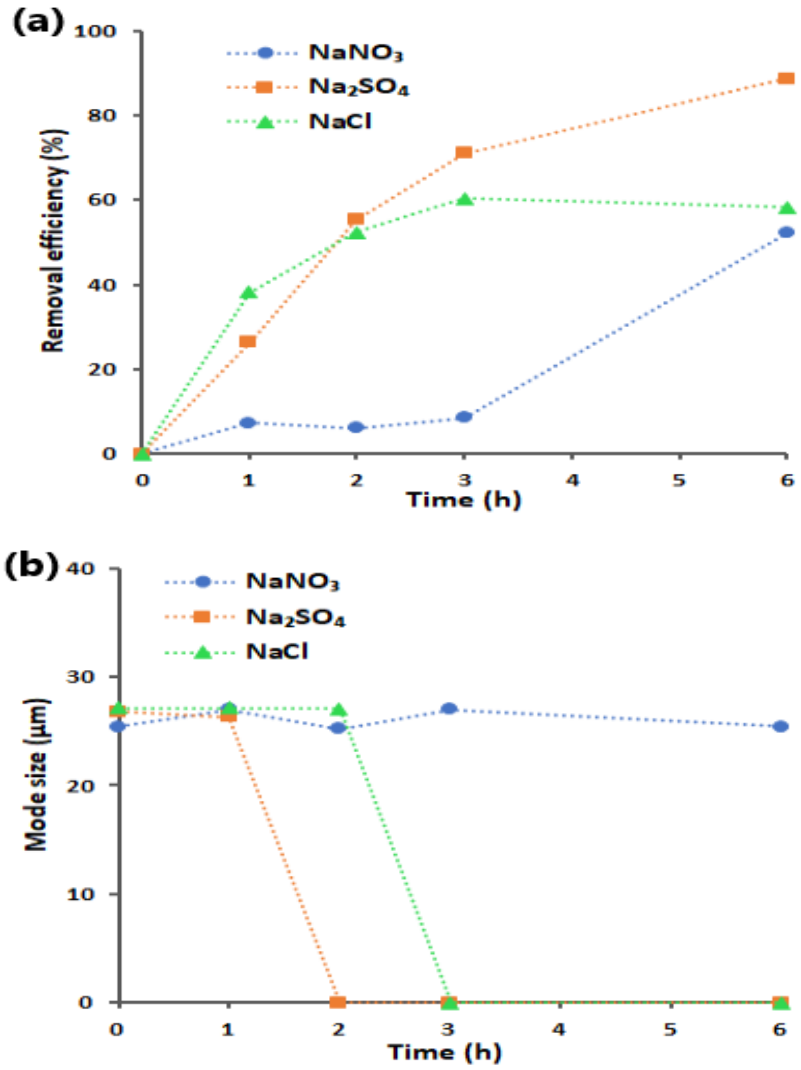

Figure 3 5 : The effect of electrolyte type on the EO of MPs. (a) Removal efficiency (%), (b) Mode size (µm).

3.3.2.5. Effect of the applied electrolyte concentration

The electrolyte concentration is a determining parameter in the EO process as it affects the operating costs in terms of electrolyte consumption and electrical energy consumption. The influence of the electrolyte concentration on the removal efficiency and mode size of MPs was investigated by conducting experiments at 0.03, 0.04, and 0.06 M Na_2SO_4. These experiments were conducted using one BDD anode at 9 A. As it can be seen in Figure 3.6, the removal efficiency enhanced by increasing the electrolyte concentration. MPs degradation of 25 ± 13%, 45 ± 17%, and 58 ± 21% were obtained with electrolyte concentrations of 0.03, 0.04, and 0.06 M,

respectively after 1 h of electrooxidation. However, at prolonged time of 6 h, these removal efficiencies increased to 89 ± 8%, 83 ± 8% and 84 ± 8% after 6 h of treatment which are almost the same. As it can be seen from Figure 6b, no MPs with initial size of 26 µm was detected after 1 h at 0.06 M of electrolyte, however, this operating time increased to 2 h at 0.03 and 0.04 M. Therefore, the DLS analysis confirmed that the rate of EO was higher at 0.06 M.

A cost analysis was performed to analyze the effect of electrolyte concentration on the operating cost of the EO process. The experimental results showed that, for electrolyte concentrations of 0.03, 0.04, and 0.06 M, the average electrical potential was around 15, 13, and 11 V, respectively. The electrical energy consumption analysis showed at 0.06 M, after 1 h (58 ± 21% removal efficiency) and 6 h (84 ± 8% removal efficiency) energy consumption were 132 and 1080 Kwh.m^{-3}, respectively.

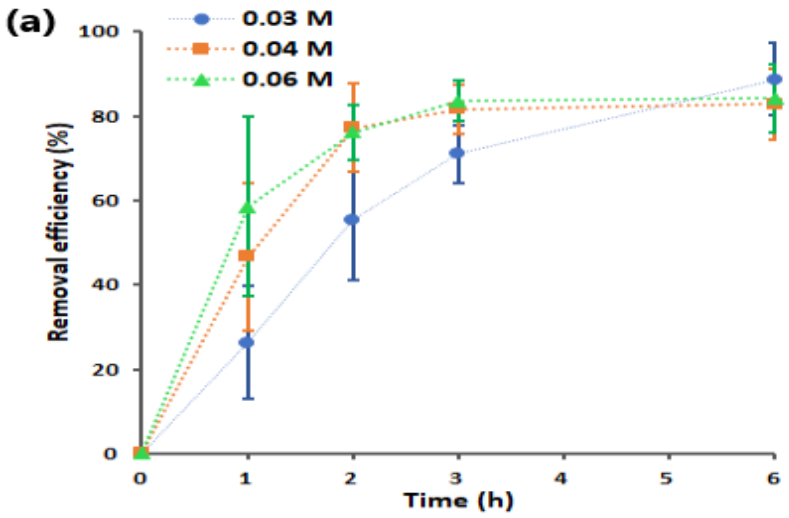

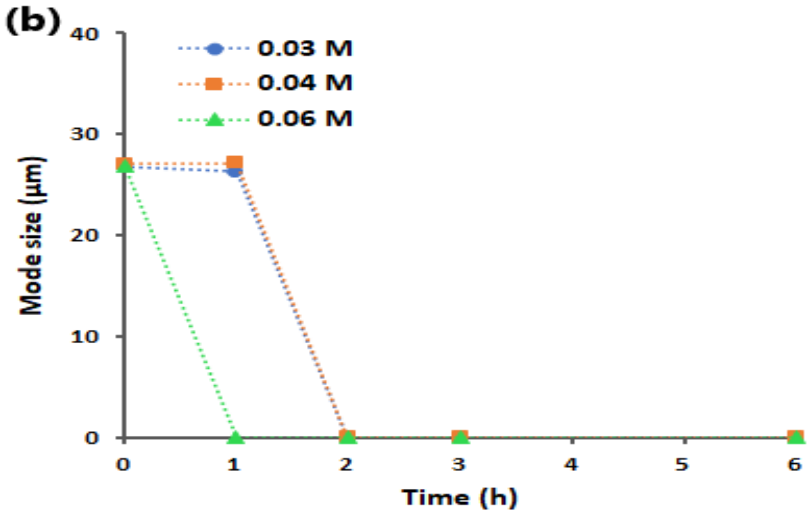

Figure 3. 6 : The effect of electrolyte concentration on the EO of MPs. (a) Removal efficiency (%), (b) Mode size (µm).

3.3.3. Total current efficiency analysis

The total current efficiency was calculated using Eq. (3.2) at 1, 2, 3, and 6 h for the experiments that were conducted using BDD anode material at 9 A with 0.06 M Na_2SO_4. The TCE values of 6%, 3%, 2%, and 1% were obtained after 1, 2, 3, and 6 h of EO, respectively. As expected, gradual decrease in TCE can be observed which demonstrates the loss of EO capacity by passing time (D. Gandini *et al.*, 2000; Ignasi *et al.*, 2008). This trend can be attributed to the decrease of the organic pollutants amount in the solution (Ciríaco *et al.*, 2009; Sirés *et al.*, 2006). On the other hand, as the rate of transfer of the MPs towards the electrode depends on its concentration, the mass transfer limitation increased by COD reduction through time. The low energy efficiency values obtained in this study could therefore be explained mainly by the nature of the aromatic polymer which resist against degradation and the mass transfer limits. Lower energy efficiency value than 10% with a TOC removal of nearly 90% was also reported for the EO of clofibric acid as an aromatic compound, using Ti/BDD with a current density of 150 $mA.cm^{-2}$ (Sirés *et al.*, 2006).

3.3.4. Microscopic analysis of MPs before and after electrooxidation

SEM analysis was performed to find the change in the MPs size and shape during the EO process and evaluate the obtained results from weight loss and DLS analyses. The SEM image of MP particles before and after 1 h of EO are presented in Figure 3.7a and b, respectively. These figures clearly show the size of MPs is around 26 µm before and after electrooxidation, which confirm the obtained values in the mode size analysis. It is worth noting that no MPs were observed in the SEM analysis of the samples that were treated for more than 2 h of electrooxidation, confirming that MPs were completely degraded in these experimental conditions (according to results obtained from DLS analysis). The SEM images also showed the EO had no obvious effect on the spherical shape of the MPs. In Figure 3.7b, the formation of a layer of salt around the MP particles can be observed which is attributed to the deposition of electrolyte as layer of salt after drying the sample for the SEM analysis.

A statistical analysis was performed by ImageJ software on the obtained size of MPs using the SEM images. In these calculations, at least 20 data were collected to find an average value for the MPs diameter. This analysis showed the average size of MPs before and after 1 h electrooxidation time was 22.66 and 25.24 µm, respectively. This statistical analysis also confirmed the obtained average of MPs by DLS analysis.

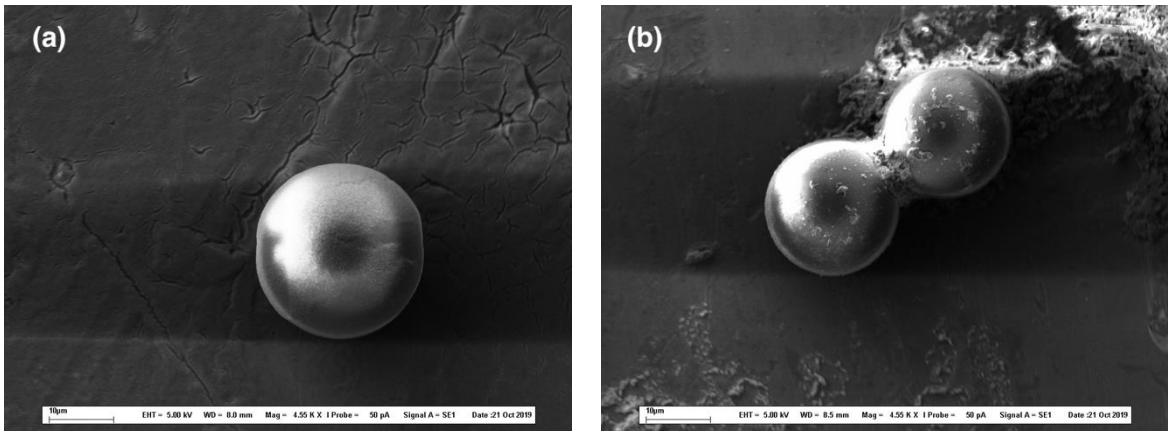

Figure 3. 7 : SEM images of MPs (a) before and (b) after 1 h of electrooxidation using BDD anode at 9 A with 0.06 M Na_2SO_4.

3.3.5. Spectroscopic analysis of MPs before and after electrooxidation

The MP samples were analyzed by FTIR spectroscopy to evaluate the formed functional groups on the surface of MPs. The FTIR spectra before and after electrooxidation are compared in Figure 3.8a. As it can be seen, in contrast to previous research on photo-oxidation (Cai *et al.*, 2018b; Jean-Luc Gardette *et al.*, 2008), no peak at 1712 cm^{-1} was recorded. This peak corresponds to C=O bonds. Accordingly, it may be concluded that the MPs were directly oxidized on the anode and no partially oxidized MPs were released into the water. This result may suggest that the direct oxidation of MPs on the surface of anode is the dominant mechanism in the degradation of MPs.

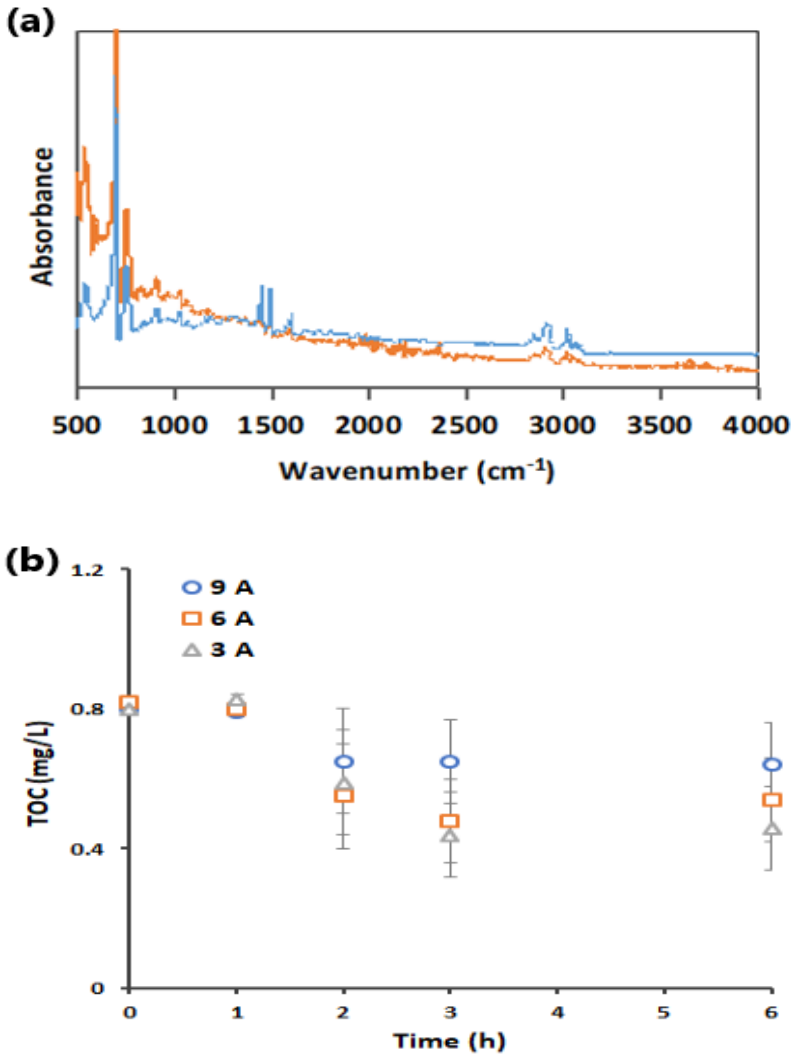

Figure 3. 8: (a) FTIR spectra of MPs before (▬) and after (▬) 1 h of EO, (b) TOC analysis of filtered treated water at different current intensities.

3.3.6. TOC analysis of treated water

The treated water was filtered (0.22 µm filter pore size) and analyzed by TOC analyzer to evaluate the amount of generated liquid by-products through electrooxidation of MPs. To do so, the MPs were first filtered to separate the unreacted MPs from water and the filtrate was analyzed. The TOC analysis results for current intensities imposed of 3, 6, and 9 A are depicted in Figure 3.8b. Around 0.8 ± 0.02 mg/L of TOC was initially recorded before electrooxidation owing to the presence of surfactant in the filtered samples. As it can be seen, the TOC decreased through time for all current intensities that can be attributed to the degradation of surfactants in the purchased MP sample. According to Figure 3.8b, the TOC analysis showed no increase in the amount of organic carbon after electrooxidation time of 1, 2, 3, and 6 h. This result shows that no liquid by-products formed through electrooxidation of MP. This observation also shows no nanoplastics with a size lower than the filter pore size (0.22 µm) was available in the filtrate. Accordingly, all the MP particles were successfully filtered and calculated in the analysis of MP removal efficiency. The slight contradiction between the MPs mass removal percentage results, and the mode size results in some samples can be related to insufficient accuracy of DLS analysis at low MPs concentrations. It is worth underlining that validity of the DLS analysis could be assured only when the transmission of light was lower than 75-90 %, but the transmission passed this limit at removal percentages higher than 40%.

3.3.7. The proposed degradation mechanism

The mechanism of polystyrene MPs degradation by anodic oxidation in water using BDD electrode was proposed based on the obtained results in this study. At the first step, hydroxyl radicals are generated from water on the surface of the anode as is shown in Eq. (3.11). These radicals have a great affinity to make a reaction (Alves *et al.*, 2013; Feng *et al.*, 2013; Urtiaga *et al.*, 2014) and degrade polystyrene. As it can be seen from Eq. (3.12), the generated hydroxyl radicals initiate the degradation of polystyrene with breaking carbon-hydrogen bond which leads the formation of carbon-oxygen bond. In the next step, the polymeric bond can be broken through breakage of C-C or C-Ph bonds (where Ph denotes phenolic group, see Eq. (3.13)). The short lifetime and the high reactivity of the hydroxyl radicals makes the carbonyl bond detection very

difficult (García-Gómez *et al.*, 2014). Further oxidation of the degraded polymeric chain can lead to additional decomposition of the formed compounds and finally complete oxidation to produce carbon dioxide and water, based on Eq. (3.14), as is reported by previous researchers (E. Weiss *et al.*, 2006; Panizza & Cerisola, 2009; Sirés *et al.*, 2006). A more detailed mechanism of EO of MP is currently under investigation in our research group.

Equation 3.11 : $BDD + H_2O \rightarrow BDD(OH^{\circ}) + H^+ + e^-$

Équation 3.12 : $-(CH_2 - CHPh - CH_2 -) + BDD(OH^{\circ}) \rightarrow -\left(CH_2 - CO^{\circ}Ph - CH_2 -\right) + H^+ + e^- + BDD$

Équation 3.13 : $-\left(CH_2 - CO^{\circ}Ph - CH_2 -\right) \rightarrow CH_2 - CO - Ph + -CH_2^{\circ}$

Or $-\left(CH_2 - CO^{\circ}Ph - CH_2 -\right) \rightarrow CH_2 - CO - CH_2 + Ph^{\circ}$

Équation 3.14 : $CH_2 - CO - Ph; -CH_2^{\circ};\ CH_2 - CO - CH_2;\ Ph^{\circ}; + BDD(OH^{\circ}) \rightarrow CO_2 + H_2$

3.3.8. Analysis of energy and electrolyte cost

A cost analysis was performed at optimum condition to analyze the effect of electrolyte type on the operating cost of the current EO process. The cost analysis data are presented in Table 3.1. As it can be seen, the energy consumption (calculated using Eq. (3.3)) of Na_2SO_4 electrolyte was higher than $NaNO_3$ and NaCl, which was attributed to higher applied electrical potential at constant electrical current intensity during this process. In addition, it can be seen that energy cost was dominant in the value of total operating cost. After 6 h EO, the total operating cost was 68.5, 59.9, and 57.6 \$/m^3 for Na_2SO_4, NaCl, and $NaNO_3$, respectively, during which 89%, 58%, and 52% removal efficiencies were obtained. After 1 h EO, which 23%, 38%, and 7% removal efficiencies were obtained, these values were 11.4, 8.9, and 10.4 \$/m^3, respectively. These results are comparable with the literature results of energy consumption analysis for recalcitrant pollutants by EO (Canizares *et al.*, 2006; Durán *et al.*, 2018). It can be concluded from this comparison that the treatment of MPs using Na_2SO_4 for 6 h is the best condition because a significantly higher removal efficiency was obtained without any substantial increase in the total operating cost. Moreover, in contrast to NaCl, the EO process using Na_2SO_4 does not produce toxic chlorine gas. (Perren *et al.*, 2018) reported the cost of MPs separation with electrocoagulation process to be around £0.05 (Can\$ 0.086). The lower cost than the current

work is attributed to the big size of MPs (around 0.3 mm) as well as the separative nature of process that does not degrade the MPs. It is worth mentioning that research is being conducted on hybrid advanced oxidation processes to economically treat complex water matrix containing MPs like laundry wastewater.

Tableau 3. 1 : Cost analysis of MP EO using Na_2SO_4, $NaNO_3$, and NaCl as electrolyte after 1 and 6 h.

	Unit	Electrolyte type		
		Na_2SO_4	**NaCl**	**$NaNO_3$**
Removal efficiency (%)	(%/6 h)	89	58	52
	(%/h)	23	38	7
Energy consumption	(kWh/m^3/6 h)	1120	995	932
	(kWh/m^3/h)	169	145	146
Energy cost	($/6 h)	67.2	59.7	55.9
	($/h)	10.1	8.7	8.7
Electrolyte cost	($)	1.3	0.2	1.7
Total operating cost	($/6 h/$m^3$)	68.5	59.9	57.6
	($/h/$m^3$)	11.4	8.9	10.4

3.4. Conclusion

The EO process using BDD anode electrode is an effective technology for the treatment of water contaminated by MPs. Using Na_2SO_4 (0.03 M) as a supporting electrolyte and a current intensity of 9 A during 6 h of electrolysis time ensures a high degradation efficiently of MPs (89 ± 8 %). The DLS results suggested that the MPs did not break into the smaller particles and they transformed directly into the gaseous products (such as CO_2). The SEM, TOC, and FTIR analyses also confirmed the mineralization of MPs during the application of EO process, by indicating no broken MPs, detecting no organic carbon, and observing no oxidized functional group after MPs oxidation. The EO process could be the basis of a process for MPs degradation from real wastewaters, but the consequences of anode fouling and mutual contaminants interactions must be further investigated.

Acknowledgements

The authors would like to acknowledge the financial support from the Fonds de recherche du Québec – Nature et technologies (FRQNT), the CREATE-TEDGIEER program, National Sciences and Engineering Research Council of Canada (NSERC), and Canadian Francophonie Scholarship Program.

Au regard des performances du procédé EO (89% de dégradation de particules de MPs de 25 µm de diamètre) enregistrées après 6h d'électrolyse et dans l'optique de réduire la consommation énergétique, il est nécessaire de mettre à profit la capacité de l'électrode de cathode à produire d'autres espèces oxygénées réactives comme le H_2O_2. Ce qui permettrait de générer in situ plus d'espèces radicalaires additionnelles plus forts. Ce, par la dissociation du H_2O_2 en présence de rayonnements UV et l'activation des persulfates par le H_2O_2. Ce qui permettrait de dégrader plus de MPs/NPs avec une réduction du temps de traitement (ces hypothèses seront vérifiées dans le chapitre 4).

Au vu de la différence de taille des particules de plastiques dans les eaux (c'est-à-dire micro-plastique et nano-plastique) et dans l'optique de mieux comprendre le mécanisme de la dégradation OEC (oxydation directe et indirecte) sur les plus petites particules aussi, il a été nécessaire d'étudier la dégradation des NPs (100 nm) dans les mêmes conditions que les MPs (25 µm). Ce qui permet de comparer les meilleures conditions du procédé EO en fonction de la taille des particules (Chapitre 4)

De ce fait, les conditions de dégradation des particules de micro-plastiques ont été appliquées pour le traitement des NPs et pour l'évaluation de la production in situ des oxydants de la cellule électrolytique en utilisant le montage à 2 électrodes pour le procédé EO et à 2 ou 3 électrodes avec ou sans injection d'air pour les procédé EO-H_2O_2 et EO-H_2O_2/UV.

4. ELECTROCHEMICAL DEGRADATION OF NANOPLASTICS IN WATER: ANALYSIS OF THE ROLE OF REACTIVE OXYGEN SPECIES

DÉGRADATION ÉLECTROCHIMIQUE DES NANOPLASTIQUES DANS L'EAU : ANALYSE DU RÔLE DES ESPÈCES OXYGÉNÉES RÉACTIVES

Marthe K[a], Karimi Estahbanati M.R[a*], Yassine O[a], Patrick D[a*], Tyagi RD[b]

[a]Institut national de la recherche scientifique (INRS) - Centre Eau Terre Environnement (ETE), 490 rue de la Couronne, Québec (QC), CANADA, G1K 9A9

[b] Distinguished Prof Huzhou University, China, Chief Scientific Officer, BOSK Bioproducts, Québec, CANADA

Science of the Total Environment 808 (2022) 151897

https://doi.org/10.1016/j.scitotenv.2021.151897

Abstract

Micro-plastics and nano-plastics (NPs) are emerging water contaminants which have recently gained lots of attention because of their effects on the aquatic systems and human life. Most of the previous works on the treatment of plastic pollution in water have been focused on micro-plastics and a very limited study has been performed on the NPs treatment. In this work, the role of main reactive oxygen species (ROSs) in the electro-oxidation (EO) and electro-peroxidation (EO-H_2O_2) of NPs in water is investigated. In-situ generation of hydroxyl radicals ($^{\bullet}OH$), persulfates ($S_2O_8^{2-}$), and hydrogen peroxide (H_2O_2) were performed using boron-doped diamond (BDD) as the anode, whereas titanium (in EO process) and carbon felt (CF, in EO-H_2O_2 process) were used as cathode. In the EO process, NPs were mainly oxidized by two types of ROSs on the BDD surface: (i) $^{\bullet}OH$ from water discharge and (ii) $SO_4^{\bullet-}$ via $S_2O_8^{2-}$ reaction with $^{\bullet}OH$. In EO-H_2O_2 process, NPs were additionally degraded by $^{\bullet}OH$ formed from H_2O_2 decomposition as well as $SO_4^{\bullet-}$ generated from direct or indirect reactions with H_2O_2. Analysis of the degradation of NPs showed that EO-H_2O_2 process was around 2.6 times more effective than EO process. The optimum amount of NPs degradation efficiency of 86.8% was obtained using EO-H_2O_2 process at the current density of 36 $mA.cm^{-2}$, 0.03 M Na_2SO_4, pH of 2, and 40 min reaction time. In addition, 3D EEM fluorescence analysis confirmed the degradation of NPs. Finally, the economic analysis showed the treatment of NPs using EO-H_2O_2 process had an operating cost of 2.3 $\$US.m^{-3}$, which was around 10 times less than the EO process. This study demonstrated the in-situ generation of ROSs can significantly enhance the degradation of NPs in water.

Keywords: Nanoplastic; polystyrene; water treatment; electrooxidation; H_2O_2 electrogeneration; degradation.

4.1. Introduction

Nanoplastics (NPs) have become a new emerging contaminant owing to their undeniable evidence occurrence due to bulk plastic degradation to form smaller particles down to the nanoscale (Cai *et al.*, 2021; Ekvall *et al.*, 2019), their difficulty in recycling (i.e. in biosolids) or elimination by conventional waste-water treatment technologies (Enfrin *et al.*, 2019). NPs can be defined as a subgroup of plastics with an effective diameter less than 1,000 nm (da Costa *et al.*, 2016; Gigault *et al.*, 2018b). Polymer nanoparticles that are produced intentionally for specific purposes such as cosmetic products (Hernandez *et al.*, 2017) and synthetic microfibers (MFs) from the laundry of synthetic textile are important sources of microplastics (MPs) and NPs can enter the environment through wastewater treatment plants (De Villiers, 2019; Kelly *et al.*, 2019). The concentration of NPs was estimated to be beyond 10^{14} times that of MPs in marine environments (Wang *et al.*, 2020b). Despite the vast presence of NPs in the environment, we are lacking harmonized and reliable methodologies for analyzing NPs in waters (Cai *et al.*, 2021). Polystyrene (PS) is one of the most widely used plastics in real daily life (over 23 million tons per year), making it one of the most significant constituents of NPs (Lithner *et al.*, 2011). On the other hand, the literature review demonstrated that PS is one of the most toxic polymers in the form of MPs and NPs (Karimi Estahbanati *et al.*, 2021a).

The size of plastic particles is an important key in the connection with their toxicity in the waters because the smaller the plastic the bigger its capacity to absorb higher concentrations of contaminants (Liu *et al.*, 2016). For example, NPs with a size of 50 nm can adsorb more toxic compounds than MPs around 10 µm in size (Ma *et al.*, 2016). This may indirectly increase the exposure of Polycyclic Aromatic Hydrocarbons (PAHs) to organisms and thus increase their potential carcinogenic and mutagenic potency (White, 1986) as that is known for the properties of the styrene monomer (Lithner *et al.*, 2011). In addition, NPs can enter into cells by **endocytic** pathways and accordingly cross the blood-brain barrier (Koziara *et al.*, 2003), or penetrate the chorion of fish eggs (Kashiwada, 2006). Incineration of MPs and NPs aggregated in wastewater plant biosolids causes serious environmental problems due to the release of NPs. That increases direct exposure of PAHs to aquatic organisms (Liu *et al.*, 2016) such as incineration by-products whose toxicity is still unrecognized (Miyake *et al.*, 2017).

Current conventional sewage sludge treatment as lime stabilization and biological degradation causes the formation of smaller plastic particles (González-Pleiter *et al.*, 2019; Mahon *et al.*,

2017). That means the majority of biosolids used as agricultural fertilizer could threaten human health because of the high NPs content (Karimi Estahbanati *et al.*, 2021c). Several methods have been tested for the upcycling of plastic waste that contributes to the reduction of environmental pollution by plastic particles (Karimi Estahbanati *et al.*, 2021b). For example, microbial degradation of polymers got increasing attention from researchers (Ali *et al.*, 2014; Paco *et al.*, 2017), however, this method usually takes several weeks or even months to convert the plastics. The pyrolysis of plastics is another approach for upcycling plastics particles to value-added products (i.e. fuel or chemical feedstock). However, the produced waste oil from this process may pollute the environment by the generation of contaminants like plastic particles (Miao *et al.*, 2020b).

The previous studies on the treatment of NPs in waters focused on their separation (Chen *et al.*, 2021; Murray & Örmeci, 2020). Interestingly, only one article addressed the degradation of NPs using the photocatalytic process (Dominguez-Jaimes *et al.*, 2021). Once again, this showed that it takes several days to achieve an NPs removal efficiency as previously demonstrated for MPs degradation (Ariza-Tarazona *et al.*, 2019; Phonsy *et al.*, 2015a). On the other hand, aging of MPs proceeds at a very slow rate, causing a very long time for the degradation of the current environmental NPs pollution (Luo *et al.*, 2021). However, studies have shown effective removal of MPs using electrochemical processes for hours' treatment time (Kiendrebeogo *et al.*, 2021a; Miao *et al.*, 2020b). Thus, it is very important to investigate electrochemical treatments for the degradation of NPs in waters in the order to prevent their accumulation in the sewage sludge and biosolids. Electrochemical advanced oxidation processes (EAOPs) generate diverse reactive oxygen species (ROSs) such as hydroxyl radical ($^{\bullet}OH$, E_0 = 2.8 V vs. NHE) and hydrogen peroxide (H_2O_2, E_0 = 1.8 V vs. NHE) at high concentrations. These processes have proven to be ecofriendly and effective ways for eliminating persistent contaminants in water (Miao *et al.*, 2020b). Sulfate radical ($SO_4^{\bullet-}$, E_0 = 2.6 V vs. NHE) is considered an important constituent of AOPs (Deng & Zhao, 2015; Wacławek *et al.*, 2017) which exhibits a great capability for degradation of plastic particles (Kang *et al.*, 2019). This radical can be formed from $S_2O_8^{2-}$ activation via H_2O_2 (Hilles *et al.*, 2015). During an electro-oxidation (EO) process, the $^{\bullet}OH$ can be formed at the anode from the oxidation of water. These radicals can also be formed in the bulk of solution using the continuous electro-generation of H_2O_2 from O_2 reduction (Zhou *et al.*, 2018; Zhou *et al.*, 2019).

Several studies reported that CF cathode is efficient in the generation of H_2O_2 in O_2-saturated solutions compared to other carbonaceous materials (Bañuelos *et al.*, 2016; Cotillas *et al.*, 2015;

Garcia-Segura *et al.*, 2012). H_2O_2 is electrogenerated from the two-electron reduction of O_2 on carbonaceous cathodes, such as carbon felt, vitreous carbon, O_2-diffusion electrodes, or graphite (Komtchou *et al.*, 2015). Besides, (Guitaya *et al.*, 2015) identified the best cathode material (carbon felt versus graphite felt) for H_2O_2 production. Carbon felt was more appropriate for H_2O_2 formation than graphite felt. After 60 min of electrolysis time, a concentration of 19.6×10^{-5} M was recorded with carbon felt, whereas 5.59×10^{-5} M was measured for graphite felt (a concentration three times lower). The amorphous structure of carbon felt facilitates the trapping of dissolved oxygen so that it can be reduced into H_2O_2, compared with the hexagonal structure of graphite felt which is less appropriate for oxygen trapping (Yue *et al.*, 1990).

This paper studies the role of ROSs in the electrochemical degradation of NPs in water. In this regard, the effects of current density and Na_2SO_4 concentration on the concentration of in-situ electro-generated $^{\bullet}OH$ and $S_2O_8^{2-}$ using boron-doped diamond (BDD) were first investigated, respectively. In addition, the role of the carbon-felt (CF) cathode in the in-situ electro-generation of H_2O_2, as well as the effects of current density, air injection, and using one and two pieces of cathodes on the concentration of generated H_2O_2 were studied. Afterward, the effects of the concentration of Na_2SO_4, and the concentration of NPs on the rate of NPs degradation were evaluated. Total organic carbon (TOC) and three-dimensional excitation and emission matrix fluorescence (3D EEM) analyses were used to assess the mineralization and degradation of NPs. Finally, an economical study was performed on the electrochemical degradation of NPs in water.

4.2. Materials and methods

4.2.1. Chemicals and preparation of synthetic NPs effluents

The aqueous suspension of PS nanospheres (1% solids) with a diameter of 100 ± 4 nm and a coefficient of variation of 7.7% was provided by Thermo Scientific USA. The NPs synthetic solution was prepared by adding PS nanospheres at a concentration of 10 and 20 mg/L and sodium sulfate (Na_2SO_4) was used as a supporting electrolyte. Na_2SO_4 was an analytical grade reagent supplied by the Mat laboratory (Quebec, QC, Canada). Different concentrations of Na_2SO_4 (0.007, 0.030, and 0.060 M) were tested to assess its effect on treatment performances. All the NPs degradation experiments were performed by preparing spontaneously a new synthetic solution with a final volume of 1 L from which 800 or 900 mL was used. RNO (N, N-Dimethyl-4-nitroso-aniline, $C_2H_6N_2O$, 97%) supplied by Sigma Aldrich was used as a probe molecule to assess the production of $^{\bullet}OH$ during electrolysis. The RNO stock solution was prepared by dissolving 49.4 mg/L of RNO in 1 L of a buffer solution consisting of anhydrous dibasic sodium phosphate (99%) crystalline monobasic potassium phosphate (99%). The buffer solution was adjusted to pH 7. H_2O_2 (30%) used for the calibration curve was analytical grade from Sigma Aldrich.

4.2.2. Electrolytic setups

The electrochemical treatment of NPs was carried out in the batch mode with niobium-covered boron-doped-diamond (Nb/BDD) as anode and titanium (Ti) or CF as the cathode. The reactor was made of Plexiglas with a dimension of 14.5 cm (length) × 6.4 cm (width) × 17.7 cm (height). Accordingly, three types of electrode combination (anode-cathode) were employed to conduct the experiments: (i) Ti-BDD, (ii) CF-BDD, and (iii) CF-BDD-CF. The distance between electrodes was 1.0 cm. Ti and BDD electrodes were grid and circular shape with a diameter of 12 cm, a thickness of 0.1 cm, and a surface area of 113 cm^2. The CF electrode was made of 10-20 µm interwoven fibers and had an 11 cm (length) × 9 cm (width) main side rectangular shape and a thickness of 1 cm. CF consisted of 99.00 to 99.70% of carbon and 0.02 to 0.25% of ashes. The Anodes and cathodes were connected respectively to the positive and negative outlets of a digital DC generator model 382275 (EXTECH Instruments, Montréal, Canada) with a maximum current supply of 20 A at an open circuit potential of 30 V. In some experiments the system was fed with

900 mL.min^{-1} of compressed atmospheric air injection into the reactor to saturate continuously the solution subjected to the treatment with oxygen. During electrolysis, the solution was mixed using a magnetic stirrer and air bubbling. The air flowmeter was fixed to 900 mL.min^{-1}. Ultraviolet Germicidal Bulb UV-C 254 nm lamp (PL-L18W/TUV/2G11) purchased by LSE light was immersed in the solution as a catalyst to perform EO-H_2O_2/UV.

4.2.3. Experimental procedure

The degradation of NPs was conducted using two different oxidation processes: (i) EO using an electrochemical reactor comprising of Ti (cathode) and BDD (anode) on which •OH was formed (Configuration Ti-BDD); (ii) EO with in-situ H_2O_2 generation (EO-H_2O_2 process) consisted in treating NPs using an electrochemical reactor comprising of BDD (anode) and CF (cathode) on which H_2O_2 was formed (configuration CF-BDD). The first sets of electrochemical oxidation experiments were focused on evaluating the potential of ROS production. During these tests, the concentration of ROS (including •OH, H_2O_2, and $S_2O_8^{2-}$) was measured to investigate their contribution to the NPs oxidation. The production of •OH by BDD anode was measured at the current densities of 36, 72, and 108 mA.cm^{-2}, and the generation of H_2O_2 by CF cathode was evaluated at current densities of 6, 12, and 36 mA.cm^{-2} (i.e., 0.5 to 3.0 A). In addition, the effect of $S_2O_8^{2-}$/H_2O_2 activation during the EO-H_2O_2 process was analyzed. During these tests, the degradation of NPs was analyzed by TOC, UV-vis spectrophotometry, and 3D EEM techniques to evaluate the performance of different electrochemical oxidation processes.

4.2.4. Analysis techniques

4.2.4.1. Hydroxyl radical concentration measurements

The production of •OH was estimated by its reaction with RNO according to the method reported by (García-Gómez *et al.*, 2014). RNO is an organic dye that is bleached selectively by oxidation with •OH and does not react with single oxygen, superoxide anions (O_2^{-}), or other peroxy compounds (Muff *et al.*, 2011; Simonsen *et al.*, 2010). To measure the amount of generated •OH during the EO experiments, the amount of removed RNO was monitored by the measurement of absorbance band at 440 nm using a UV-visible spectrophotometer (UV 0811 M136, Varian, Australia. The RNO calibration curve was obtained by plotting the RNO absorbance as a function

of RNO concentration (from 0 to 5.81× 10^{-5} M). The rate of •OH production is equal to the rate of RNO disappearance by the assumption of the first-order reaction, according to Eq. (4.1):

Equation 4.1 : $V = \frac{dC}{dt} = -kC$

where *V*, *C*, *k*, and *t* correspond to the production rate of •OH, the RNO concentration, the first-order reaction rate constant, and the reaction time, respectively. The integration of Eq. (4.1) gives:

Equation 4.2 : $Ln(\frac{Co}{C}) = kt$

where C_0 and C_t are the initial concentration of RNO and the concentration of RNO at time t. The value of *k* could be calculated from the slope of a plot of *t* versus $Ln(C_0/C)$ in Eq. (4.2).

4.2.4.2. Peroxydisulfate concentration measurements

The Wessler method was used to measure the concentration of peroxydisulfate ($S_2O_8^{2-}$) through the oxidation of iodide ions (I^-) into iodine (I_2) (Ishibashi *et al.*, 2000; Xiang *et al.*, 2011). When an oxidizing agent like $S_2O_8^{2-}$ is present in the solution, I^- ions are oxidized to give I_2 (see Eq. (4.3)). Subsequently, I_2 reacts with I^- present in excess in the solution to form tri-iodide (I_3^-) ion according to Eq. (4.4) (Entezari & Kruus, 1994). The Wessler method is based on the direct titration of I_2 produced from the oxidation of I^-:

Equation 4.3 : $S_2O_8^{2-} + 2I^- \rightarrow 2SO_4^{2-} + I_2$

Equation 4.4 : $I_2 + I^- \leftrightarrow I_3^-$

I_3^- is analyzed by absorbance measurements at 353 nm (Koda *et al.*, 2003). To do so, samples were taken and diluted 4 times at different reaction times (0 to 180 min). From the diluted solution, 10 ml was mixed with an excess of potassium iodide (500 mg). The mixture was allowed to react for 15 min while stirring. Then, the obtained solution was analyzed at 353 nm using a UV-vis spectrophotometer (Carry UV 50, Varian Canada).

4.2.4.3. H_2O_2 concentration measurement

The volumetric dosage method (Sigler & MAster, 1957) was used to measure H_2O_2 concentration. Under acidic conditions (H_2SO_4, 9 N), a 5.88 × 10^{-3} M cerium solution ($Ce(SO_4)_2$, $2(NH_4)_2SO_4$,$2H_2O$) was used for the titration of the sample that was mixed with three drops of Fe(O-

phen)$_3^{2+}$ as an indicator. The gradual change of the solution color from red to blue indicated the total oxidation of H_2O_2 using the cerium solution. To quantitatively determine the concentration of H_2O_2, a calibration curve was obtained by plotting the cerium volume as a function of H_2O_2 concentration (from 0 to 2.06 M corresponding 0 to 70 mg/L).

4.2.4.4. NPs concentration measurement

The concentration of NPs in the solution was determined by the spectrophotometric spectral absorption measurements of C=C bonds of PS at 254 nm. A calibration curve of NPs versus relative absorbance was used to calculate the residual NPs concentration and define the degradation efficiency. The removal efficiency was accordingly calculated according to Eq. (4.5):

Equation 4. 5 : $Degradation\ efficiency\ (\%) = \frac{C_0 - C_t}{C_0} \times 100$

where C_o and C_t are the initial and final concentrations of NPs in the sample, respectively.
To evaluate the obtained results from the spectrophotometric analysis, the NPs degradation was also measured based on TOC analysis. To do so, the samples were analyzed using a Shimadzu TOC 5000A analyzer (Shimadzu Scientific Instruments, Kyoto, Japan).

4.2.4.5. 3D EEM analysis

To decompose the fluorescence components in the NPs samples and track dissolved organic matter evolution during treatment, 3D EEM analysis was performed using Varian Cary Eclipse Fluorescence Spectrophotometer (USA). Emission scans were performed from 230 to 600 nm at 5 nm increments, with excitation wavelengths from 220 to 650 nm at 5 nm intervals. The scanning rate was maintained at 1,200 nm/min. The slit widths for excitation and emission were 10 nm. A 290 nm emission cut-off filter was used in scanning to eliminate second-order Raleigh light scattering.

4.2.5. Energy consumption analysis

Energy consumption is an important factor concerning EAOPs. Eq. (6) was employed to express that in kWh.m^{-3}:

Equation 4.6 : $EC\ (kWh \cdot m^{-3}) = \frac{T \times I \times t}{V} \times 10^3$

where *T*, *I*, *t*, and *V* represent the average cell voltage (V), the applied current (A), the duration of electrolysis (h), and the volume of treated water (m^3).

The operating cost was estimated considering energy consumption and electrolyte costs. The cost of electricity and electrolyte was estimated based on a unit cost of 0.06 $US/kWh and 0.3 $US/kg for Na_2SO_4 (industrial grade).

4.3. Results and discussion

4.3.1. In-situ ROS production

The performance of electrochemical processes in the degradation and mineralization of organic pollutants are related to the amount of in-situ electro-generated ROSs (Daghrir *et al.*, 2013c; Komtchou *et al.*, 2015; Sanni *et al.*, 2021). Accordingly, some tests were conducted to evaluate the efficacy of the electrolytic cell to produce $^{\bullet}OH$, H_2O_2, and $S_2O_8^{2-}$. According to previous studies, BDD anode is the only non-active electrode capable of oxidizing the sulfate (SO_4^{2-}) to persulfate ($S_2O_8^{2-}$) which can contribute to oxidizing organic compounds when Na_2SO_4 is used as a supporting electrolyte (Canizares *et al.*, 2005; Serrano *et al.*, 2002). In addition, using CF as the cathode is more appropriate than carbon-graphite for H_2O_2 formation (Guitaya *et al.*, 2015; Khataee *et al.*, 2011; Komtchou *et al.*, 2015). Consequently, the combination of BDD anode and CF cathode was used for the analysis of ROSs electro-generation and their potential in the degradation of NPs. In the following sub-sections, the potential of BDD anode in the generation of $^{\bullet}OH$ and $S_2O_8^{2-}$ as well as CF cathode in the production of H_2O_2 are analyzed.

4.3.1.1. Electrochemical generation of hydroxyl radicals and persulfates

In this study, the evaluation of $^{\bullet}OH$ production was carried out by following the bleaching of RNO by $^{\bullet}OH$ during the EO process with the selected electrode set (Nb/BDD). Fig. 4.1 depicts the concentration of generated $^{\bullet}OH$ and $S_2O_8^{2-}$ through time. Fig. 4.1a illustrates the $^{\bullet}OH$ generated in the absence of NPs at different current densities of 36, 72, and 108 $mA.cm^{-2}$. The inset panel of Fig. 4.1a shows the RNO disappearance rate following a first-order kinetic model. As observed from these results, the amount of $^{\bullet}OH$ increases with electrolysis time and current density. In addition, the $^{\bullet}OH$ formation obeys the first-order kinetic with the rate constant (k) of 0.0861, 0.1472, and 0.2150 min^{-1} for 36, 72, and 108 $mA.cm^{-2}$, respectively. Total removal of RNO (8 mg/L) was obtained after 20 and 30 min for 72 and 108 $mA.cm^{-2}$, respectively, while it took over

30 min for 36 mA.cm^{-2}. In addition, it can be seen from Fig. 1a that the •OH production rate reached 0.39, 0.75, and 1.11 × 10^{-5} M.min^{-1} after 20 min electrolysis time for 36, 72, and 108 mA.cm^{-2}, respectively. A relatively high rate of •OH production (1.11 × 10^{-5} M.min^{-1}) was recorded in our study using BDD/Nb electrodes and 108 mA.cm^{-2} current density compared to the study where the production rate was 0.4 × 10^{-5} M.min^{-1} after 20 min of electrolysis time under different operating conditions (Ti/PbO_2 anode, current density of 67 mA.cm^{-2} and recirculation flow rate 232 ml.min^{-1}) (García-Gómez *et al.*, 2014). Several authors consider BDD as the electrode of choice for efficient and complete degradation of refractory pollutants (Martínez-Huitle & Panizza, 2018). Indeed, many studies mentioned that the interaction between •OH and the surface of BDD anodes is considered to be very weak resulting in a much greater O_2 overvoltage than the other anodes such as platinum and lead dioxide (PbO_2), iridium (IV) oxide (IrO_2) (Ciríaco *et al.*, 2009; Ignasi *et al.*, 2008; Martínez-Huitle *et al.*, 2004; Yassine *et al.*, 2018).

$S_2O_8^{2-}$ generation was analyzed in the absence of NPs at two different initial Na_2SO_4 concentrations (i.e. 0.03 and 0.06 M) and at a pH of 5 using the current density of 108 mA.cm^{-2} for 180 min electrolysis time. As shown in Fig. 1c, $S_2O_8^{2-}$ production after 180 min enhanced from 0.48 to 0.72 mM by increasing the Na_2SO_4 concentration from 0.03 to 0.06 M. However, by applying a lower current intensity the $S_2O_8^{2-}$ generation decreased. For example, at 36 mA.cm^{-2} (67% reduction at current density) and 0.06 M Na_2SO_4, the $S_2O_8^{2-}$ concentration reduced to 0.19 mM (73% reduction), which shows a significant effect of the current density on the $S_2O_8^{2-}$ generation (the data are not shown in Fig. 4.1b). Previous studies also reported the generation of $S_2O_8^{2-}$ by BDD anode via various ways: (i) direct oxidation of SO_4^{2-} by electron transfer according to Eq. (4.7) (Davis *et al.*, 2014; Serrano *et al.*, 2002; Smit & Hoogland, 1971a; Smit & Hoogland, 1971b), (ii) indirect oxidation of SO_4^{2-} by BDD(•OH) (Eq. (4.8)) (Barreto *et al.*, 2015; Ganiyu & Martínez-Huitle, 2019; Serrano *et al.*, 2002), and (iii) recombination of principal intermediate ($SO_4^{\bullet-}$ species) on the anode surface during indirect oxidation (Eq. (4.9)) (Barreto *et al.*, 2015; Ganiyu & Martínez-Huitle, 2019).

Équation 4.7 : $2SO_4^{2-} \rightarrow S_2O_8^{2-} + 2e^-$

Equation 4.8 : $2HSO_4^- + 2BDD(OH^\bullet) \rightarrow S_2O_8^{2-} + 2H_2O$

Equation 4.9 : $SO_4^{\bullet-} + SO_4^{\bullet-} \rightarrow S_2O_8^{2-}$

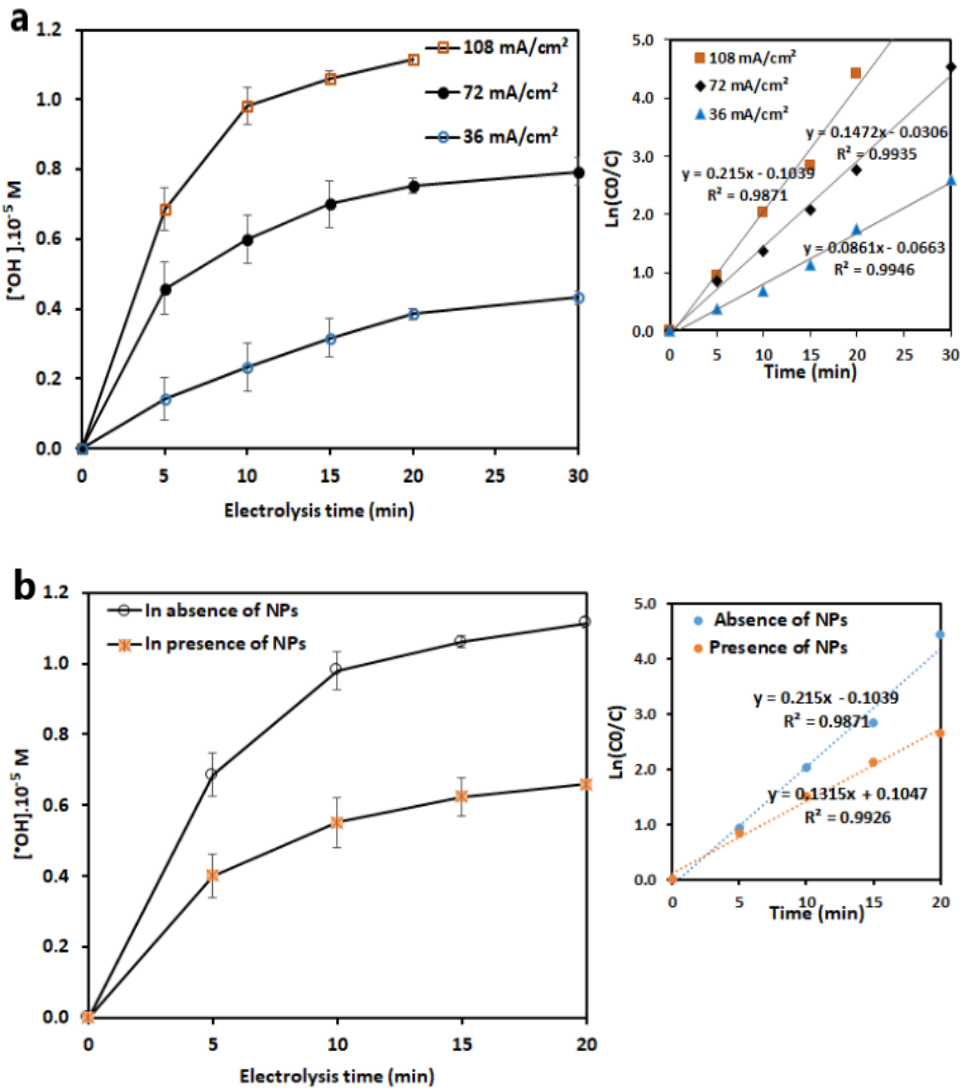
a
[•OH].10-5 M
Electrolysis time (min)
108 mA/cm²
72 mA/cm²
36 mA/cm²
Ln(C0/C)
Time (min)
y = 0.215x - 0.1039
R² = 0.9871
y = 0.1472x - 0.0306
R² = 0.9935
y = 0.0861x - 0.0663
R² = 0.9946
b
[•OH].10-5 M
Electrolysis time (min)
In absence of NPs
In presence of NPs
Ln(C0/C)
Time (min)
Absence of NPs
Presence of NPs
y = 0.215x - 0.1039
R² = 0.9871
y = 0.1315x + 0.1047
R² = 0.9926

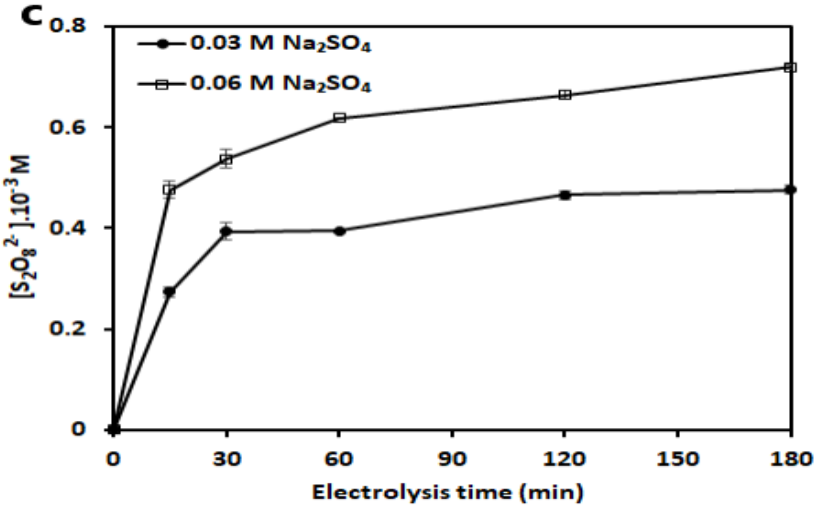

Figure 4. 1: Analysis of simultaneous production of ROSs in the absence and presence of NPs a) $^{\bullet}OH$ at different current densities in the absence of NPs, b) Effect of the presence of NPs on the concentration of $^{\bullet}OH$ during the electrolysis, the inset figures represent the first-order reaction kinetics analysis of RNO. [Na_2SO_4] = 0.03 M. c) $S_2O_8^{2-}$ at the current density of 108 mA.cm^{-2}.

4.3.1.2. Electrochemical generation of H_2O_2

To investigate the performance of CF cathode to produce H_2O_2, several experiments were performed in the absence of NPs with 1.0 g/L Na_2SO_4 (as supporting electrolyte) at an initial pH of 5. These experiments were conducted at the current densities of 6, 12, and 36 mA.cm^{-2} using two CF cathodes and in the continuous injection of air to assure oxygen saturation. The H_2O_2 concentration in the solution at different reaction times and current densities are illustrated in Fig. 4.2a. As it can be seen, the H_2O_2 concentration increased significantly up to 30 min and reached around 0.14 ± 0.013, 0.13 ± 0.01, 0.14 ± 0.04 M for 6, 12, and 36 mA.cm^{-2}, respectively then decreased slightly until 1 hour. This behavior has been also reported by previous studies (Li *et al.*, 2020; Salmerón *et al.*, 2019). It can also be seen from Fig. 4.2a that the current density has no significant effect on the H_2O_2 concentration produced during electrolysis. In addition, the concentration of H_2O_2 has fluctuated a lot after 30 min of electrolysis. This is due to parasitic reactions that can take place in the cell (Salmerón *et al.*, 2019). There may be an electrochemical reduction of H_2O_2 continuously accumulated in the solution at the cathode following the Eq. (4.10). This explains the spontaneous variation of its concentration over time.

Equation 4.10 : $H_2O_2 + 2H^+ + 2^+ \rightarrow 2H_2O$

In addition, the presence of BDD in the undivided cell could promote the oxidation of H_2O_2 at the surface of the anode (Eqs.(4.11)-(4.12)) and its decomposition in the electrolysis medium according to Eq. (4.13) (Özcan *et al.*, 2008).

Équation 4. 11 : $H_2O_2 \rightarrow HO_2^{\bullet} + H^+ + e^-$

Équation 4. 12 : $HO_2^{\bullet} \rightarrow O_2 + H^+ + e^-$

Équation 4. 13 : $H_2O_2 \rightarrow H_2O + 1/2O_2$

Furthermore, the temperature measured during electrolysis time increased from 20 ± 1.2 to 40 ± 3.4 ºC. That did not favor the stabilization of H_2O_2. It has been shown by (Badellino *et al.*, 2006) that by reducing the temperature from 18 to 10 ºC, the final concentration of H_2O_2 can be increased three times. This can be explained by the decrease in the solubility of oxygen and the increase in H_2O_2 dissociation under high temperatures (Badellino *et al.*, 2006; Özcan *et al.*, 2008). Fig. 4.2b shows the effects of the number of cathodes and air injection on H_2O_2 production. As expected, the concentration of generated H_2O_2 is significantly higher when using two cathodes in comparison to one cathode, especially in the presence of air injection. In addition, it is inferred from this figure that the air injection can enhance H_2O_2 generation in both cases of using one or two cathodes. Comparing these results with the maximum H_2O_2 concentration of 1.44 mg/L that was obtained at a previous study by (Komtchou *et al.*, 2015) using 17.7 mA.cm^{-2} current density and with 113 cm^2 CF surface area, confirms that the surface area of CF and O_2 saturation promotes the production of H_2O_2.

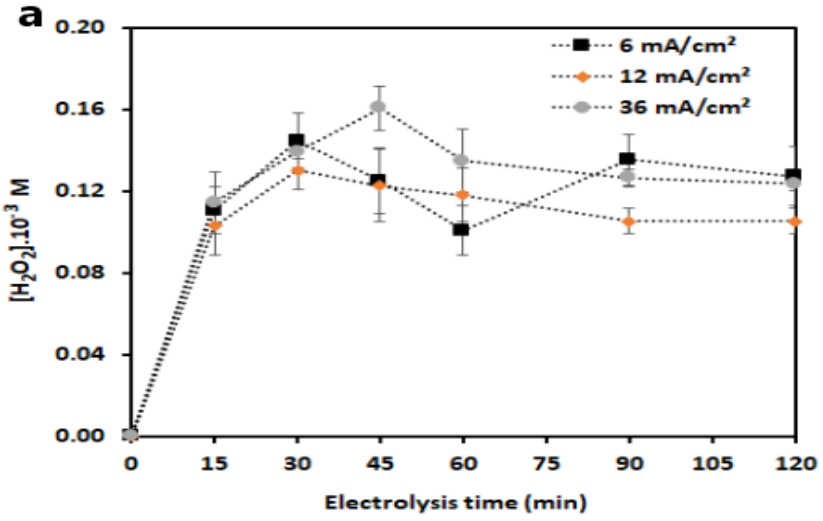

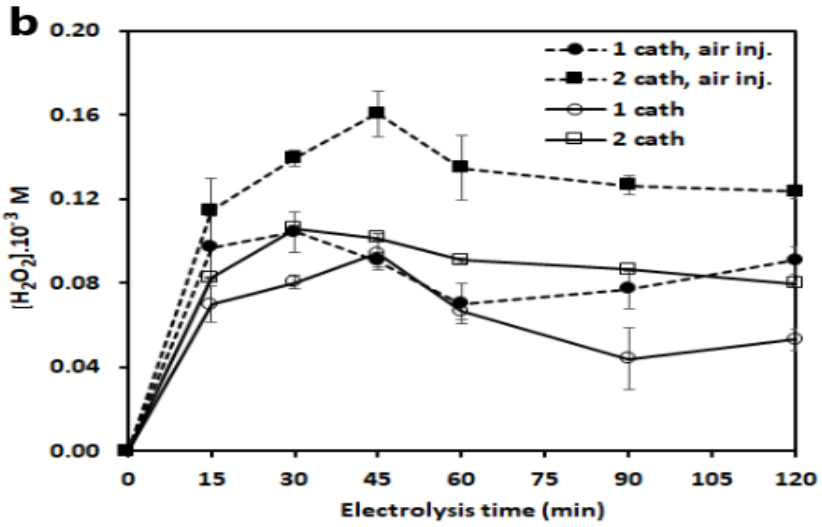

Figure 4. 2 : H_2O_2 production at different reaction time a) at different current densities using 2 cathodes with air injection, and b) with/without air injection and at a different number of cathodes.

4.3.2. Hydroxyl radical's contribution and NPs degradation kinetics

4.3.2.1. Hydroxyl radical contribution

After evaluating the production of •OH radicals in the absence of NPs, the amount of •OH was also tracked in the presence of NPs using a synthetically contaminated solution with 10 mg/L NPs. By comparing the amount of •OH electrogenerated in the presence and absence of 10 mg/L of NPs for a current density of 108 $mA.cm^{-2}$, it can be seen clearly that the •OH concentration decreased by almost 50% (Fig. 4.1b). •OH production decreased from 0.7×10^{-5} to 0.4×10^{-5} M and 1.1×10^{-5} to 0.6×10^{-5} M after 5 and 20 min of electrolysis, respectively. This would mean that a fraction of the electrogenerated •OH is used for NPs degradation. It's known that ROSs react favorably with electron-rich compounds (Stichnothe *et al.*, 2002). For the case of PS NPs, •OH reacted with the carbon double bonds (–C=C–) and attacked the aromatic nucleus, which is the major component of PS molecular.

4.3.2.2. Kinetic study of NPs degradation by EO process

It is known that the concentration of ROSs influences the performance of EAOPs in the degradation of pollutants (Komtchou *et al.*, 2015; Özcan *et al.*, 2008). To analyze that for NPs,

the concentration of NPs during the EO process was measured at different current densities (36, 72, and 108 mA.cm^{-2}). These experiments were conducted using BDD anode and Ti cathode and in the presence of 0.03 M Na_2SO_4 and initial NPs concentration of 10 mg/L for 360 min. The initial and final pH values were 5.3 ± 0.3 and 9.5 ± 0.6, respectively. Fig. 4.3 shows the percentage of NPs removal changes depending on the current density imposed. The increase of current density from 36 to 72 mA.cm^{-2} improved the degradation efficiency by around 20%, whereas an increase of current density up to 108 mA.cm^{-2} had no positive effect. The major electrogenerated ROSs involved in NPs degradation during the EO process include BDD($^{\bullet}$OH) produced directly at BDD surface from water discharge (Eq. (4.14)) (Panizza & Cerisola, 2005) and indirectly through the reaction between $S_2O_8^{2-}$ and BDD($^{\bullet}$OH) according to Eq. (4.15) (Dos Santos *et al.*, 2020). Previous studies reported $S_2O_8^{2-}$ (E^0 = 2.08 V) capacity to oxidize and modify the organic molecules (Canizares *et al.*, 2005; Marselli *et al.*, 2003). To observe the sole effect of $S_2O_8^{2-}$ on NPs degradation, NPs were added into the final solution of a test that was performed at 0.19 mM $S_2O_8^{2-}$ using BDD at 36 mA.cm^{-2} to obtain a final NPs concentration of 10 mg/L. The solution was stirred for 120 min and NPs concentration was monitored. The results showed that the NPs concentration was constant after 120 min. Consequently, the sole presence of $S_2O_8^{2-}$ in our conditions does not degrade NPs, which is similar to the results obtained by (García-Gómez *et al.*, 2014).

Équation 4. 14 : $BDD + H_2O \rightarrow BDD(OH^{\bullet}) + H^+ + e^-$

Équation 4. 15 : $S_2O_8^{2-} + BDD(OH^{\bullet}) \rightarrow BDD + HSO_4^- + SO_4^{\bullet -} + 1/2O_2$

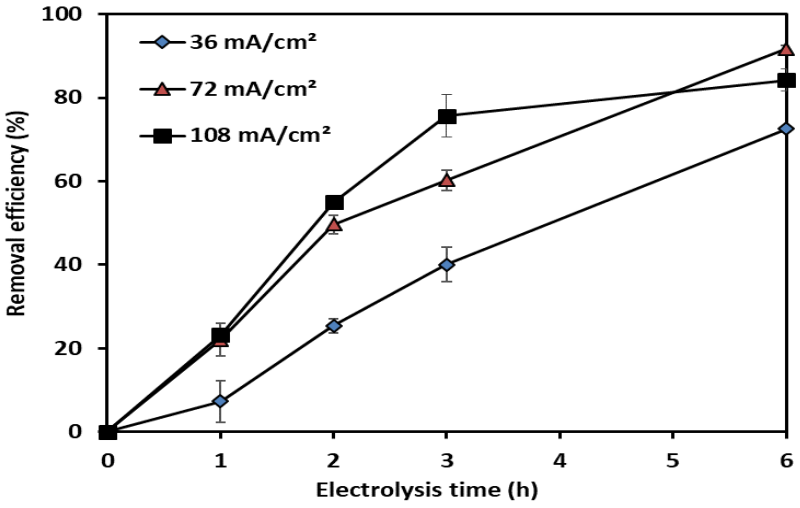

Figure 4. 3 : Influence of applied current density on the degradation rate of NPs during EO treatment. Cathode = Ti, anode = BDD anode, $[NPs]_0$ = 10 mg/L, $[Na_2SO_4]$ = 0.03 M, volume = 900 mL.

The obtained results were used to develop pseudo-first-order and pseudo-second-order kinetic models. The pseudo-first-order kinetic model is described by Eq. (4.16):

Equation 4.16 : $Ln(\frac{Co}{C}) = k_1 t$

where C_0, C, and k_1 represent the initial concentration of NPs, the concentration of NPs at time t, the first-order reaction rate constant (min^{-1}).

For the pseudo-second-order kinetic model, the equation described below was applied:

Equation 4. 17 : $\frac{1}{C} - \frac{1}{C0} = k_2 t$

where k_2 and t are the second-order reaction rate constant ($L.mg^{-1}\ min^{-1}$) and the reaction time, respectively.

The regression coefficient (R^2) was used for the selection of the most suitable model.

The calculated values of k_1, k_2, and R^2 obtained at different applied current densities are summarized in Table 4.1.

Tableau 4. 1 : Apparent rate constants as well as their R^2 for the oxidation of NPs by EO process at different applied current intensities under conditions described in Fig. 4.3b.

Cell	**[NPs] mg/L**	**Current density ($mA.cm^{-2}$)**	**Pseudo-first-order**		**Pseudo-second order**	
Ti cathode/BDD anode			k_1	R^2	k_2	R^2
	10	36	0.2235	0.9802	0.0456	0.8608
	10	72	0.4202	0.9809	0.0905	0.9668
	10	108	0.3211	0.9198	0.189	0.9243

In general, the R^2 of the pseudo-first-order kinetic model is relatively higher than that of the pseudo-second-order kinetic model, which shows that the first-order kinetic model describes very well the degradation of NPs by the EO process. In addition, it can be seen that k_1 values were decreased from 0.4202 to 0.3211 min^{-1} although increasing current density from 72 and 108 $mA.cm^{-2}$. Indeed, while imposing a current density of 108 $mA.cm^{-2}$, secondary reactions (such as the oxygen evolution) occurred significantly (Martinez-Huitle *et al.*, 2015) or a fraction of $^{\bullet}OH$ produced was possibly wasted in the reaction of recombination (Martinez-Huitle *et al.*, 2015). Therefore, it can be considered that 108 $mA.cm^{-2}$ was higher than the current density that was corresponding to the diffusion limitation.

4.3.3. Contribution of hydrogen peroxide in NPs degradation

The contribution of H_2O_2 in the degradation of NPs was analyzed during the EO process. To do so, CF was employed for the in-situ generation of H_2O_2. The experiments were conducted with 0.9 L/min air injection, 36 $mA.cm^{-2}$ anode current density, 1 g/L Na_2SO_4, 6 h electrolysis time, and 10 mg/L initial concentration of NPs. The use of one piece of CF cathode was compared to the use of two pieces of CF cathodes. The initial and final pH values were 5.1 ± 0.1 and 2.5 ± 0.0, respectively. As it can be seen in Fig. 4.4, using CF cathode the removal efficiency of NPs was 42 ± 0.2% after 60 min of electrolysis, while it was only 16.2 ± 1.9% using Ti as the cathode. It should be mentioned that the improvement in removal efficiency using CF cathode compared to Ti could be expected if the concentration of H_2O_2 was higher (Badellino *et al.*, 2006). To evaluate the sole effect of H_2O_2 in the degradation of NPs, 0.14×10^{-3} M stabilized H_2O_2 solution (high amount based on Fig. 4.2) was prepared and NPs added to obtain a final concentration of 10 mg/L NPs at pH of 2. The analysis of the concentration of NPs showed that H_2O_2 injection could not induce NPs degradation (data not shown). Consequently, the high rate of NPs removal recorded in the experiments could be attributed to the regeneration of $SO_4^{\bullet-}$ in the solution by the activation of electrogenerated $S_2O_8^{2-}$ (Eqs. (4.7)-(4.9)) via EO-H_2O_2 through (i) direct reaction between $S_2O_8^{2-}$ and electrogenerated H_2O_2 at air diffusion cathode according to Eq. (4.18), (ii) indirect reaction between $S_2O_8^{2-}$ and $^{\bullet}OH$ from H_2O_2 dissociation due to the increase in the temperature of medium from 25 ºC to 45 ºC (Eq.(4.19)), and (iii) cathodic reduction based on Eq. (4.20) (Divyapriya & Nidheesh, 2021; Dos Santos *et al.*, 2020; Hilles *et al.*, 2016b; Lin *et al.*, 2016; Niu *et al.*, 2020). Moreover, according to Eq. (4.18), during the regeneration of $SO_4^{\bullet-}$, $^{\bullet}OH$ was

also produced simultaneously in the solution and contributed to the enhancement of the performance of the treatment system. It was shown in the literature that the reduction potential of $SO_4^{\bullet-}$ (E^0 = 2.6 V) is slightly lower than $^{\bullet}OH$ (E^0 = 2.8 V) (Fan *et al.*, 2014); therefore $SO_4^{\bullet-}$ can attack a vast range of aromatic and cyclic organic molecules (Deng & Ezyske, 2011; Matta *et al.*, 2010; Wojnarovits & Takacs, 2019). Consequently, NPs were oxidized simultaneously through $^{\bullet}OH$ addition to unsaturated bonds and H-abstraction as well as $SO_4^{\bullet-}$ electron transfer (Cai *et al.*, 2018a; Lan *et al.*, 2017). It is reported in the literature that both the radicals represent comparable oxidation rates, however, the $SO_4^{\bullet-}$-mediated oxidation is more effective than the $^{\bullet}OH$-mediated one because of its electrophilic character and longer half-life (Divyapriya & Nidheesh, 2021; Lan *et al.*, 2017; Nidheesh & Rajan, 2016). In another work, it was shown that $SO_4^{\bullet-}$ can effectively degrade cosmetic polyethylene MPs (Kang *et al.*, 2019).

Another contribution of H_2O_2 in EO-H_2O_2 process efficiency consisted in the regeneration of SO_4^{2-} ions by reaction between H_2O_2 and $SO_4^{\bullet-}$ as per Eqs. (4.21)-(4.22) (Lin *et al.*, 2016). This can explain why the pH of the solution during EO-H_2O_2 experiments decreased from 5 to 2 (Eqs. (4.22) and (4.23)). Thus, $SO_4^{\bullet-}$ and $^{\bullet}OH$ could be regenerated continuously by the conversion of $SO_4^{\bullet-}$ and $S_2O_8^{2-}$ in the solution. However, during the EO process, the regeneration of SO_4^{2-} ions is not possible. During EO experiments (Fig. 3) the pH increased from 5 to 9. That can be explained by the reaction of added SO_4^{2-} with $^{\bullet}OH$ (Eq. (4.23)) (Durán *et al.*, 2018; Tsitonaki *et al.*, 2010).

Équation 4. (18 – 23) :

$$S_2O_8^{2-} + H_2O_2 \rightarrow 2SO_4^{\bullet-} + 2OH^{\bullet} \quad (18)$$

$$S_2O_8^{2-} + OH^{\bullet} \rightarrow HSO_4^{-} + SO_4^{\bullet-} + 1/2\, O_2 \quad (19)$$

$$S_2O_8^{2-} + e^{-} \rightarrow SO_4^{\bullet-} + SO_4^{2-} \quad (20)$$

$$H_2O_2 + SO_4^{\bullet-} \rightarrow SO_4^{2-} + HO_2^{\bullet} + H^{+} \quad (21)$$

$$SO_4^{\bullet-} + HO_2^{\bullet} \rightarrow SO_4^{2-} + H^{+} + O_2 \quad (22)$$

$$SO_4^{2-} + OH^{\bullet} \rightarrow SO_4^{\bullet-} + OH^{-} \quad (23)$$

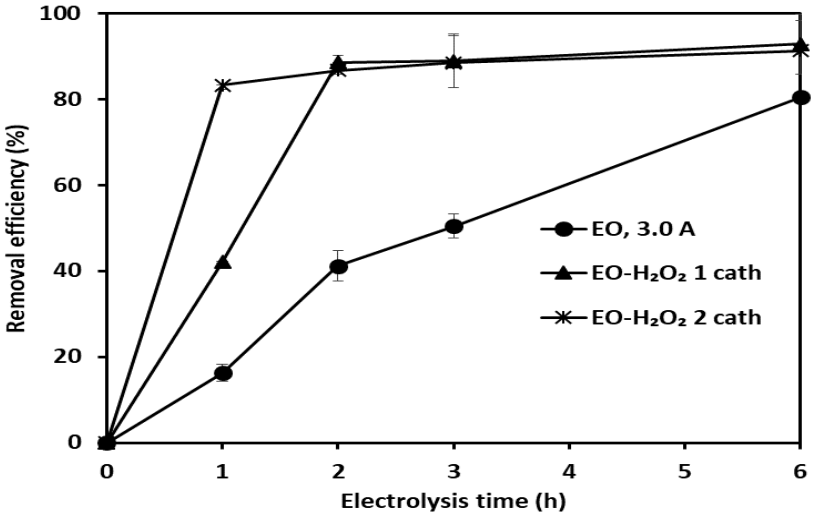

Figure 4. 4 : Degradation of NPs during the electrolysis by EO and EO-H_2O_2 processes using Ti-BDD configuration for EO, CF-BDD and CF-BDD-CF configuration for EO-H_2O_2. $[NPs]_0$ = 10 mg/L, $[Na_2SO_4]$ = 0.007 M, current density = 36 mA.cm^{-2}, volume = 800 mL, initial pH = 5.1 ± 0.1, final pH = 2.5 ± 0.0.

4.3.4. Effect of UV application to electro-peroxidation NPs removal

To evaluate the effect of UV coupled to electro-peroxidation on NPs degradation, additional experiments were carried out using the previous electro-peroxidation conditions: 3.0 A of current intensity under UV irradiations (254 nm) and in the presence of 10 mg/L of initial NPs concentration. pH 2 and 7 were tested. H_2O_2 concentration electrogenerated in the medium is illustrated in Fig. 4.2. The results are shown in fig.4. 5. At pH 2 and 7, EO-H_2O_2/UV NPs removal efficiency recorded was respectively 88.8 ± 0.13% and 79.6 ± 3.5%) after 1h electrolysis. Compared to 83.2±4.9 % removal obtained in EO-H_2O_2 treatment, slightly up and down removal efficiency was registered respectively at pH 2 and 7. That was a surprise since several studies (Beltran *et al.*, 1993; Chu *et al.*, 2011; Tan *et al.*, 2013; Xu *et al.*, 2009) have allowed or enhanced pollutant degradation by OH radicals production via H_2O_2/UV process in presence of H_2O_2 low doses. In additional it's known that H_2O_2 photolysis was is favorable with the pH increasing (Guittonneau *et al.*, 2005; Liao & Gurol, 1995) . The negative results observed in this study can be explained probably by the negative impact of H_2O_2 which can have a scavenging effect on the hydroxyl radicals produced, according (see Eq.4.24) (Yang *et al.*, 2010).

Équation 4.24 : $H_2O_2 + OH^{\bullet} \rightarrow OH_2^{\bullet} + H_2O$

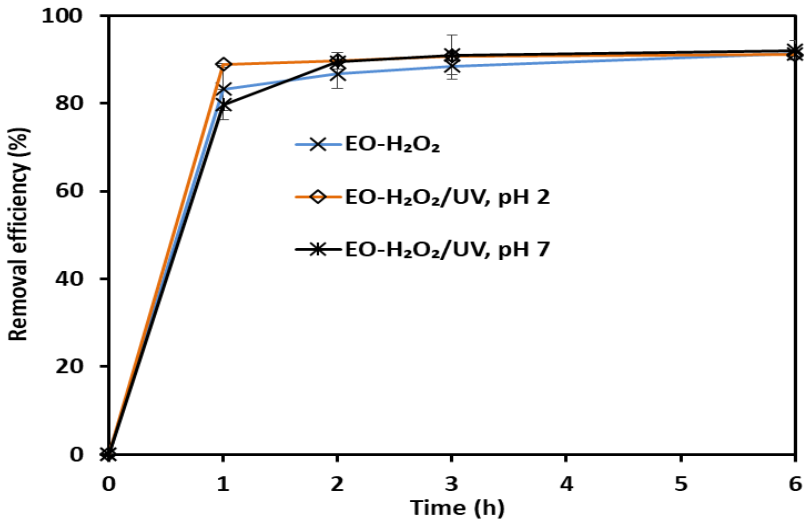

Figure 4. 5 : Degradation of NPs solution by EO-H_2O_2/UV process at 3.0 A, $[NPs]_0$= 10 mg/L, $[Na_2SO_4]$ = 0.007 M

4.3.5. Mineralization of NPs

Through the degradation of bio-refractory compounds by EAOPs, numerous by-products would be formed (Sires *et al.*, 2014). To verify the performance for processes to further oxidize NPs until complete mineralization to water and carbon dioxide, the residual TOC of the samples was measured. The TOC of the samples treated by EO and EO-H_2O_2 are compared in Fig. 4.5. The initial TOC was 8.79 ± 0.44 mg/L, while at the end of treatment is reduced to 3.85 ± 0.41, 3.18 ± 0.24, and 2.08 ± 0.76 mg/L in EO, EO-H_2O_2 using one piece of the cathode, and EO-H_2O_2 using 2 pieces of cathodes processes, respectively. It can be concluded from these results that 23.5% of NPs transformed into by-products which were difficult to mineralize. Based on Fig. 4.5, the TOC removal efficiency after 6 h of electrolysis was 56.2 ± 4.6%, 63.8 ± 2.7%, and 76.3 ± 8.6% for EO, EO-H_2O_2 using one piece of the cathode, EO-H_2O_2 using 2 pieces of cathodes processes, respectively. Nevertheless, the corresponding NPs removal efficiencies were 80.4 ± 2.23%, 92.8 ± 6.3%, and 91.26 ± 3.04%, respectively (see Fig. 4.4).

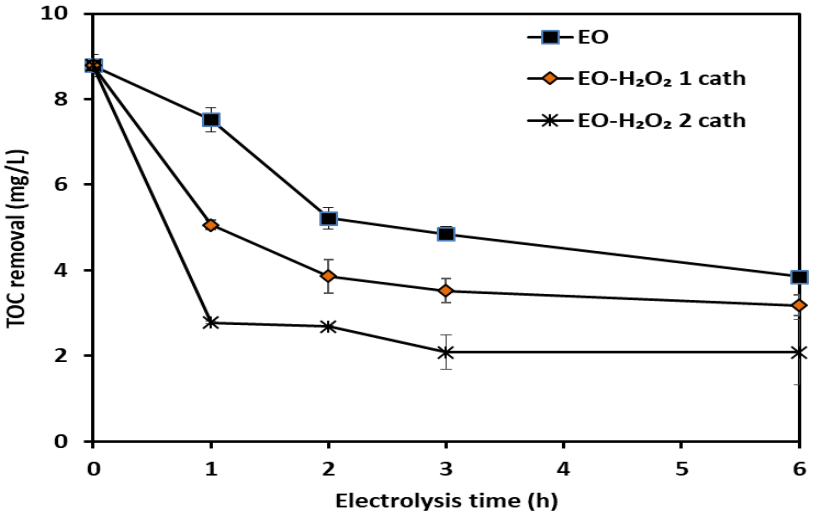

Figure 4. 6 : TOC removal during the electrolysis time for the mineralization of NPs using EO and EO-H_2O_2 processes. The experimental conditions are similar to Figure 4. 4.

4.3.6. Effect of electrogenerated persulfates concentration

Additional experiments were conducted to determine the best operating conditions during the treatment of NP-containing effluent using the EO-H_2O_2 process. Since the $S_2O_8^{2-}/H_2O_2$ ratio is an important key to achieve a higher removal efficiency (Hilles *et al.*, 2016b), 0.007, 0.03, and 0.06 M Na_2SO_4 concentrations were tested to identify the best concentration for which the highest NPs degradation could be reached. These tests were conducted for 90 min using the following conditions: 36 $mA.cm^{-2}$ current density, initial NPs concentration of 10 mg/L, BDD as the anode, two pieces of CF cathodes, and air injection. The obtained NP removal efficiencies at different Na_2SO_4 concentrations are illustrated in Fig. 4.6a. After 40 min, the degradation efficiency of NPs with 0.03 M Na_2SO_4 was around 86%, while it was only 27% at 0.007 M Na_2SO_4. That can be ascribed to the greater production of $SO_4^{\bullet-}$ and $^{\bullet}OH$ in the solution due to the greater rate of $S_2O_8^{2-}$ electrogeneration at higher Na_2SO_4 concentration (Fig. 4.1c). As result, more $S_2O_8^{2-}$ is involved in Eq. (4.16). On the other hand, increasing the Na_2SO_4 concentration to 0.06 M had almost no effect in comparison to 0.03 M. That indicates the accumulated H_2O_2 under our electrolysis conditions was not sufficient to react with $S_2O_8^{2-}$. After 60 min the removal efficiencies reached 83.2 ± 4.9%, 88.9 ± 1.5%, and 89.0 ± 1.9% while imposing 0.007, 0.03, and 0.06 M Na_2SO_4, respectively.

Finally, to evaluate the robustness of our process, the initial concentration of NPs was increased to 20 mg/L. The results are shown in Fig. 4.6b. After 60 min of treatment, a high elimination rate was obtained reaching 93% of the NPs. These results indicate that increasing the concentration from 10 to 20 mg/L does not affect the performance of the process. The reduction rate obtained for a concentration of 10 mg/L was quite similar to that obtained with 20 mg/L after 60 min of treatment (88.9 ± 1.5% vs 93 ± 2.2%). Generally, the increase in the concentrations of pollutants has a negative effect on their elimination. In our case, the increase in the concentration of NPs increases its availability and the possibility of being oxidized by $^{\bullet}OH$ and $SO_4^{\bullet-}$. This indicates that the limit of pollutant concentration is not yet attained in our study (M. Murugananthan et al, 2008).

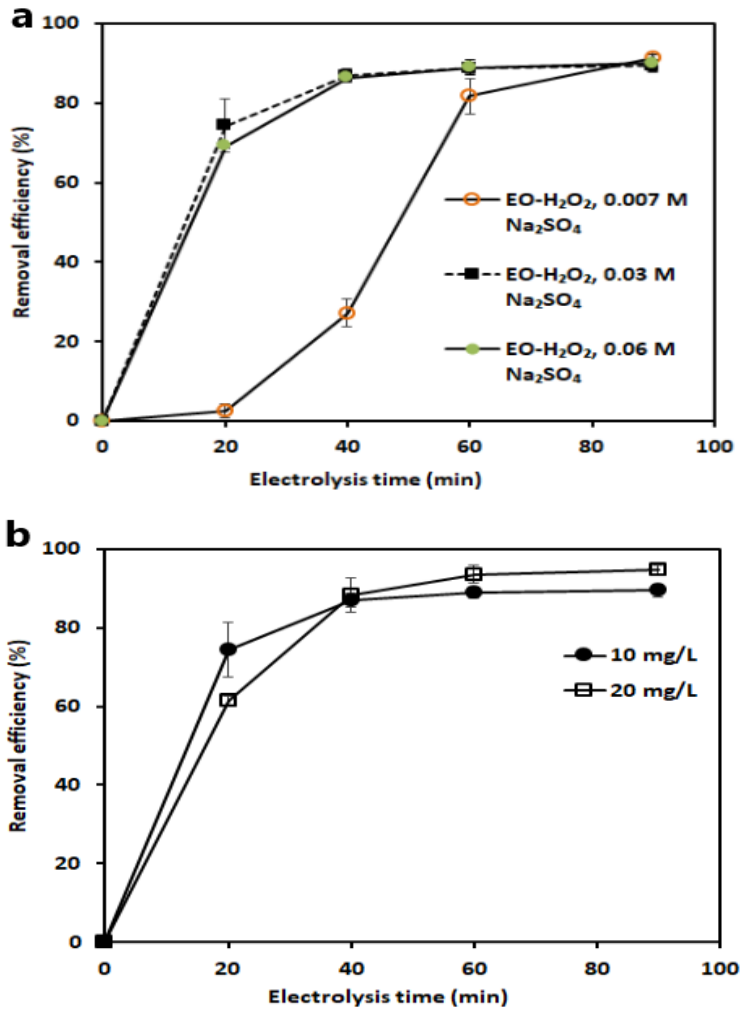

Figure 4. 7 : The effect of (a) Na_2SO_4 concentration, and (b) initial NPs concentration on the NPs removal efficiency of EO-H_2O_2 process, current density = 36 mA.cm^{-2}, [Na_2SO_4] = 0.03 M, air injection, volume = 800 mL.

4.3.7. Analysis of NPs degradation by 3D EEM

The evolution of the dissolved organic matter in our solution was followed using high-resolution mass spectrometry and spectral (UV-VIS and fluorescence) analysis. This method has been reported as a useful tool for the characterization of dissolved and colloidal organic matter in water (Jacquin *et al.*, 2017; Luo *et al.*, 2019; Ouarda *et al.*, 2020). In our study, the reactivity of nanoplastics organic matter (NPsOM) was monitored during electrolysis. The evolution of dissolved organic matter is shown in Fig. 4.7. 3D EEM analysis reveals the presence of three main peaks (a, b, and c) with high fluorophore intensity (FI). Peaks-a and b were located at the excitation/emission (Ex/Em) of 270-300/320 nm and 230/320 nm respectively. The peak-c was located at Ex/Em of 230/425 nm. Peaks a and b which are located at the same Em of 320 nm had been reported as aromatic-like peaks which may be associated with the benzene nucleus of PS in our study (Sheng & Yu, 2006; Yamashita & Tanoue, 2003). Peak-c is located in the region of Em > 380 nm represents humic acid-like substances which can be associated with surfactant alkoxyl substance in nanosphere standard (Chen *et al.*, 2003; Luo *et al.*, 2013; Wang *et al.*, 2009). After 20 min electrolysis time, all the peaks were disintegrated. Peak-a has been blue-shifted compared with the peak at t_0 (Fig. 4.7c). Blueshift is associated with the decrease in the number of aromatic rings and conjugated bonds in a chain structure (Coble, 1996; Swietlik *et al.*, 2004). After 40 min of electrolysis, FI of peak-b and c decreased significantly from 666 to 295, while peak-a decreased from approximately 295 to 146 (Fig. 4.7d). Peak-a got disappeared after 60 min of treatment (Fig. 4.7e). However, peak-b and c were further decayed. After 60 min, the synthetic NPs solution was weakly fluorescent (Fig. 4.7e). Thus, the decrease in the fluorescence signal could be attributed only to the elimination of NPs under the action of by $^{\bullet}OH$ and $SO_4^{\bullet-}$ radicals.

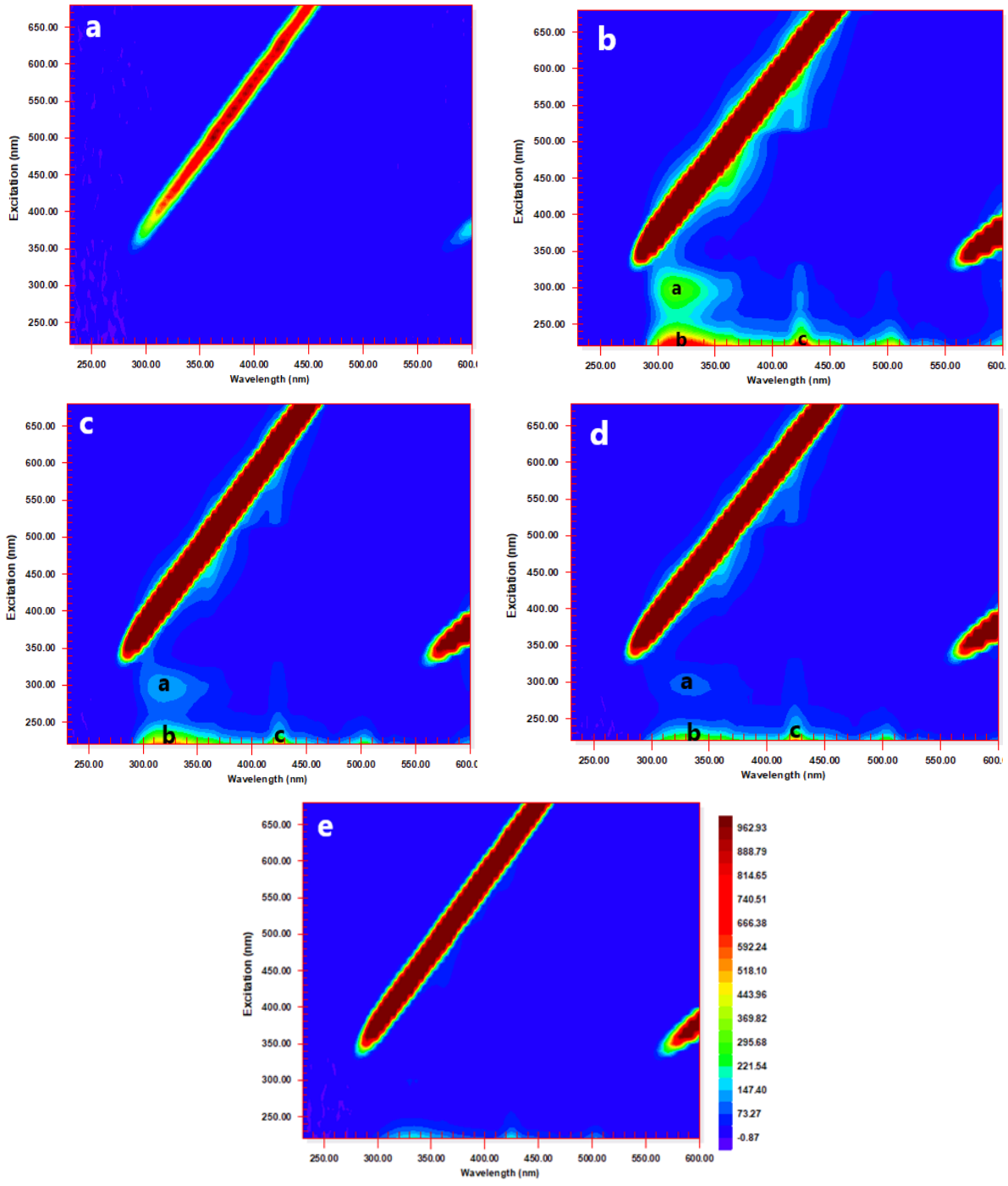

Figure 4. 8 : Evolution of 3D EEM fluorescence spectra while applying EO-H_2O_2 process for the treatment PS NP, 0.007 M Na_2SO_4 treatment : a) desionized water, b) NPs synthetic solution at t = 0 min, c) t = 20 min, d) t = 40 min, e) t = 60 min.

4.3.8. Analysis of energy and electrolyte cost

The economical aspect and especially the energy consumption expressed as $kWh.m^{-3}$ is an important concern in EAOPs. Therefore, the EO and EO-H_2O_2 treatment costs of PS NPs (including only chemical consumption and energy consumption) at the optimal conditions were estimated. the calculated costs analysis data are presented in Table 4.2. Energy consumption (in terms of $kWh.m^{-3}$) was calculated. A percentage of NPs degradation of 86.8 ± 1.8% was recorded after 0.67 h of electrolysis time in the presence of 0.03 M Na_2SO_4 using the EO-H_2O_2 process. By comparison, to reach approximately the same level of NPs degradation (80.4 ± 0.93%), a period of electrolysis of 6 h was required using the EO process. In addition, using two pieces of CF as cathodes in the EO-H_2O_2 process, an average 8.6 V potential difference between electrodes was recorded. By comparison, an average value of 16.2 V was recorded for the EO process (using one piece of Ti as the cathode). Accordingly, the energy consumption of 363.8 $kWh.m^{-3}$ was obtained for the EO process compared to only 21.6 $kWh.m^{-3}$ using the EO-H_2O_2 process. Thus, the operating cost could be reduced from 22.1 $US.m^{-3}$ (by using the EO process) to 2.6 $US.m^{-3}$ (by using the EO-H_2O_2 process).

Tableau 4. 2 : Cost analysis of NPs removal using EO, EO-H_2O_2 processes at 0.007 and 0.03 M Na_2SO_4.

	EO (0.007 M Na_2SO_4)	**EO-H_2O_2/$S_2O_8^{2-}$ (0.007 M Na_2SO_4)**	**EO-H_2O_2/$S_2O_8^{2-}$ (0.03 M Na_2SO_4)**
Time (h)	6	1	0.67
Optimal removal (%)	80.4 ± 0.93	83.2 ± 1.5	86.8 ± 1.8
T (V)	16.2	8.7	8.6
Energy consumption ($kWh.m^{-3}$)	363.8	32.8	21.6
Na_2SO_4 cost ($US.m^{-3}$)	0.3	0.3	1.3
Energy cost ($US.m^{-3}$)	21.8	1.9	1.6
Operating cost ($US.m^{-3}$)	22.1	2.3	2.8

4.4. Conclusion

The electrochemical process is a feasible technology for the treatment of water contaminated by NPs. The analysis of ROSs in EO-H_2O_2 process showed that H_2O_2 concentrations up to 24.2 × 10^{-3} M could be generated. The generated ROSs using EO-H_2O_2 process increased the NPs degradation around 2.6 times in comparison to EO process. 86.8 % ± 1.8 % NPs degradation efficiency was obtained by EO-H_2O_2 process at the optimized current density of 36 $mA.cm^{-2}$ in 40 min. 3D EEM fluorescence analysis also confirmed the degradation of NPs in EO-H_2O_2 process. TOC analysis revealed that the degraded NPs were mainly mineralized (TOC removal up to 76.5 ± 0.64%) and transformed into CO_2 and H_2O. Finally, an economic analysis of EO-H_2O_2 process showed that it has an operating cost of 2.3 $\$US.m^{-3}$, which is around 10 times less than the cost recorded for EO process. The current work showed the ROSs could have a great contribution in the degradation of NPs in water and significantly reduce the cost of process. However, further research is required to make the process faster and more economical. Prior treatment with nanofiltration followed by electrochemical degradation technique could form the basis process capable of effectively removing NPs from many waters (drinking water, municipal and industrial wastewaters).

Acknowledgments

The authors would like to acknowledge the financial support from the Fonds de recherche du Québec-Nature et technologies (FRQNT), the CREATE-TEDGIEER program, the National Sciences and Engineering Research Council of Canada (NSERC), and the Canadian Francophonie Scholarship Program.

A travers les résultats obtenus au chapitre 4 qui montrent que pour la dégradation des NPs, le procédé EO-H_2O_2 est plus performant que le procédé EO en termes de consommation énergétique, le procédé EO-H_2O_2 a donc été retenu pour traiter les NPs dans les eaux usées réelles de buanderie commerciale. La consommation énergétique était de 33 KWh.m^{-3} pour 1h d'EO-H_2O_2 avec une efficacité de dégradation de 83 % versus 364 KWh.m^{-3} pour 6h d'EO avec une efficacité de dégradation 80 %.

Vu que pour les eaux usées réelles, des interférences entre les oxydants produits *in situ* et les matières en suspension généralement présents dans ces eaux pourraient réduire l'efficacité de traitement, un traitement préalable (microfiltration) serait donc nécessaire afin de focaliser les efforts d'oxydation sur la partie dissoute. Ce qui permettrait à la quantité d'espèces radicalaires produits d'aller chercher (dégradation/minéralisation) aussi bien les NPs que la fraction dissoute des autres polluants de base présents (Cette hypothèse sera vérifié au chapitre 5). Cependant, dans l'optique de l'insertion de ce procédé dans une filière de traitement d'eau, il est nécessaire de connaitre l'influence des paramètres opératoires incluant les caractéristiques réelles des eaux et d'optimiser le procédé pour réduire davantage la consommation énergétique.

5. NANOPLASTICS REMOVAL FROM SPIKED LAUNDRY WASTEWATER USING ELECTRO-PEROXIDATION PROCESS

ÉLIMINATION DES NANOPLASTIQUES DES EAUX USÉES DE BUANDERIE DOPÉES PAR PROCÉDÉ D'ÉLECTRO-PEROXYDATION

Marthe Kiendrebeogo[a], Yassine Ouarda[a], M.R. Karimi Estahbanati[a], Patrick Drogui[a*], RD. Tyagi[b,a]

[a] Institut national de la recherche scientifique (INRS) - Centre Eau Terre Environnement (ETE), 490 rue de la Couronne, Québec (QC), CANADA, G1K 9A9

[b] Distinguished Prof Huzhou University, China, Chief Scientific Officer, BOSK Bioproducts, Québec, CANADA

Abstract.

Microplastics and nanoplastics (NPs) in laundry wastewater (LWW) are major sources of plastic particles in wastewater treatment plants. Unlike microplastics, almost no information exists in the literature on the degradation of NPs in LWW. In this work, the degradation of NPs in commercial LWW by the electro-peroxidation process is investigated. In this way, commercial LWW with a defined NP concentration was prepared and treated in an electrochemical reactor. The obtained results demonstrated that already existing ions in LWW such as Cl^- contribute to faster degradation of NPs and a complete removal could be obtained as fast as 40 min. To better understand the destruction mechanism of NPs and their interaction with other pollutions in LWW, three-dimensional excitation and emission matrix fluorescence analysis was performed, which revealed humic acid-like, aromatic proteins-like, and fulvic acid-like compounds could be oxidized after 20, 40, and 60 min of treatment respectively. Afterward, response surface methodology (RSM) models were developed to perform a parametric analysis of the process. A factorial experimental design was first used to determine the effects of the parameters on the responses. The initial TOC concentration was found to be the most important parameter influencing the percentage of NP degradation. The optimization of the process using a Central Composite methodology revealed that the energy consumption could be minimized at 31.2 $mA.cm^{-2}$ current density, 0.025 mol. L^{-1} [Na_2SO_4], and 52 min treatment time for 52.2 mg/L initial TOC. Under these conditions, 81±5% of NP and 43±3% of TOC could be simultaneously removed while imposing a relatively high level of initial TOC concentration (52.2 mg/L of TOC). Finally, analysis of treated LWW showed no toxicity on *Daphnia magna*, indicating mineralization of proteins-like NPs and nonylphenol and humic acids-like compounds or their degradation to non-toxic by-products. This study showed that the electro-peroxidation process can completely degrade NPs in industrial LWW without any remaining toxic compounds.

Keywords: Nanoplastic; industrial wastewater; electrooxidation; laundry; degradation, optimization.

5.1. Introduction

Over the last ten years, the micro-plastics (MPs) and nano-plastics (NPs) pollution sourced from plastics debris fragmentation, personal care products, and synthetic fabrics in the aquatic environment as well as their interaction with other contaminants like heavy metals, industrial dyes and organic pollutants has been an increasing concern. These emerging pollutants are introduced into the aquatic systems mainly via wastewater treatment plant effluents (Henry *et al.*, 2019; Iyare *et al.*, 2020) and MP fibers are the most common form of them (Sun *et al.*, 2019). Previous studies reported synthetic textile washing particles sourced from laundry wastewater (LWW) as an important source of MP fiber in municipal wastewater treatment plants (Acharya *et al.*, 2021; Tian *et al.*, 2021). MPs/NPs alone or combined with other pollutants showed some harmful effects on the reproduction, growth, feeding, and development of aquatic organism biological systems (Avio *et al.*, 2015; Trestrail *et al.*, 2020). Toxicological studies of MPs' effects on human health revealed MPs would be detected even in the human placenta and blood samples (Leslie *et al.*, 2022; Ragusa *et al.*, 2021). These pollutants are suspected to affect mainly the human intestinal microbiome and cause pulmonary cytotoxicity *in vitro* (Dong *et al.*, 2020; Smith *et al.*, 2018). With regard to their harmful effects and the inability of conventional water treatment processes to efficiently remove MPs/NPs as reported in previous studies (Carr *et al.*, 2016; Sun *et al.*, 2019; Zhang *et al.*, 2020b; Ziajahromi *et al.*, 2017b), an effective treatment technology is strongly desired to remove these pollutants from their main sources in the aquatic environment, particularly laundry and textile effluents.

Filtration (Simon *et al.*, 2018; Talvitie *et al.*, 2017a), flocculation-precipitation (Murray & Örmeci, 2020; Zhang *et al.*, 2021b), membrane filtration (Lares *et al.*, 2018; Pizzichetti *et al.*, 2021), and electrocoagulation (Perren *et al.*, 2018; Shen *et al.*, 2022) have been studied as alternative methods to remove MPs/NPs in aqueous matrix. These methods are based only on the transfer phase, and a second treatment is necessary to degrade or mineralize the transferred MPs/NPs in the solid phase. For the degradation of MPs/NPs, recent studies have focused on the investigation of advanced oxidation processes such as catalytic activation of peroxymonosulfate (Kang *et al.*, 2019), electro-Fenton-like (Miao *et al.*, 2020b), and electro-peroxidation (EO-H_2O_2) (Kiendrebeogo *et al.*, 2022). The electro-peroxidation process utilizes diverse ROSs to completely mineralize MPs/NPs in water. Sulfate radical ($SO_4^{\bullet-}$, E0 = 3.1 V vs NHE) and hydroxyl radical ($^{\bullet}OH$, E0 = 2.8 V vs NHE) represent powerful oxidants to decompose a large spectrum of

refractory organic contaminants in complex water matrices (Buxton *et al.*, 1988; Ren *et al.*, 2015). In this process, boron-doped diamond (BDD) can be used as an effective electrode to produce hydroxyl radicals from water discharge (Panizza & Cerisola, 2005) and also generate peroxymonosulfate in an electrolyte medium containing sodium sulfate (Davis *et al.*, 2014; Divyapriya & Nidheesh, 2021). Peroxymonosulfate has been widely applied in advanced oxidation processes to produce $SO_4^{\bullet-}$ and $^{\bullet}OH$ radicals (Dos Santos *et al.*, 2020; Hilles *et al.*, 2016a). Despite this, the electro-peroxidation process has some drawbacks including limitations in the treatment of industrial effluent as well as its high operating cost due to extensive electrical energy consumption. To the best knowledge of the authors, the application of electro-peroxidation in the degradation of NPs in industrial effluents has not been investigated.

The present work studies the degradation of NPs in commercial LWW using the electro-peroxidation process. In this regard, commercial LWW samples with a defined concentration of NPs were prepared and treated in an electrochemical reactor. The rates of NP removal and total organic carbon (TOC) removal were analyzed during the treatment process to evaluate the process efficacy as well as the interaction effect of NPs and organic compounds in LWW. In addition, three-dimensional excitation and emission matrix fluorescence (3D EEM) analysis was performed to explore NPs destruction mechanisms. Afterward, response surface methodology (RSM) models were developed to predict the rate of NPs removal, TOC removal, and energy consumption as a function of current density, electrolyte concentration, electrolysis time, and initial TOC concentration. In addition to the parametric study of the process, the developed model was used to optimize the value of operating parameters and minimize the operating cost. Finally, the toxicity of samples before and after treatment was analyzed by evaluating the Daphnia magna populations.

5.2. Materials and methods

5.2.1. Chemicals

Polystyrene NP suspension (CAS # FSSP9713546, EA BLU FL PS 0.15 µM 1% solid by weight) was purchased from Thermo Fisher Scientific. Reagent-grade anhydrous sodium sulfate (purity>98 %) was purchased from Sigma-Aldrich and used as an electrolyte.

5.2.2. Laundry water sampling and characteristics

LWW was sampled in March, April, and June from an automated commercial laundry facility in Québec City and coded as S1, S2, and S2, respectively. The samples were collected at the outlet of washing machines and stored in polypropylene bottles at 4 °C. The effluents were pre-filtrated with a glass microfiber filter (pore size 1.6 µm) to eliminate suspended solids. The composition of raw and filtered LWW is shown in Table 5.1. As it can be seen in this table 5.1, the filtration only changed turbidity, COD, and TSS.

Tableau 5. 1 : Characteristics of raw and pre-treated LWW samples.

Parameters	**S1**		**S2**		**S3**	
	Raw eff.	Filtrate	Raw eff.	Filtrate	Raw eff.	Filtrate
Turbidity (NTU)	25.7	3.51	23.6	3.26	24.7	3.30
COD (mg/L)	-	244±12	-	389.5 ±49	-	241 ±38
TSS (mg/L)	45 ±10	1.3 ±0.5	50.0 ±7.2	0.7 ±0.2	20 ±4.5	2.3 ±0.7
pH	9.97 ±0.30		10.50 ±0.38		9.10 ±0.50	
Conductivity (µs/cm)	849 ±39		336 ±31		289 ±20	
NPEOs (µg/L)	570 ±150		425 ±100		237 ±89	
SO_4^{2-} (mg/L)	18.50 ±0.14		15.00 ±1.55		16.80 ±0.21	
Cl^- (mg/L)	145.00 ±1.41		160.00 ±2.90		153.00 ±2.121	
Na (mg/L)	145.00 ±0.00		110.00 ±0.75		127.50 ±0.00	
Al (mg/L)	0.06 ±0.01		0.08 ±0.01		0.07 ±0.03	
Ca (mg/L)	17.15 ±0.21		19.10 ±1.27		18.20 ±0.25	
Mg (mg/L)	2.22 ±0.08		2.87 ±0.42		2.58 ±0.33	
K (mg/L)	1.66 ±0.03		3.51 ±1.29		2.6 ±0.01	
S (mg/L)	7.37 ±0.09		6.40 ±0.73		6.92 ±0.04	
Si (mg/L)	6.65 ±0.02		7.20 ±0.38		6.93 ±0.09	
B (mg/L)	0.01 ±0.00		0.01 ±00		0.01 ±0.01	
Ba (mg/L)	0.05 ±0.02		0.03 ±0.02		0.05 ±0.02	
Sr (mg/L)	0.08 ±0.00		0.1 ±0.01		0.09 ±0.00	
Zn (mg/L)	0.05 ±0.00		0.350 ±0.21		0.20 ±0.02	

Fe (mg/L)	0.07 ±0.01	0.05 ±0.03	0.02 ±0.02

5.2.3. LWW NP-spiking

In order to analyze the performance of the electro-peroxidation process in the degradation of NPs in laundry reals' effluents containing organic matter, filtered LWW samples were enriched with NPs to obtain 1 L of LWW sample with a final concentration of 10 mg/L. This has been performed by the addition of a supporting electrolyte as well as synthetic water to filtered LWW to obtain Na_2SO_4 concentrations as presented in Table 5.2. The LWW NP-spiked samples were codded as NP-S1, NP-S2, and NP-S3. For comparison purposes, synthetic water (NP-SW) was prepared by adding NPs to deionized water in the absence of LWW. Prior to electro-peroxidation treatment, the mixtures were mixed for 20 min to be completely homogenized.

5.2.4. Electrolytic reactor setup

Experiments were carried out in batch mode by recirculating the effluent in an undivided single parallelepipedic reactor made of Plexiglas with a dimension of 14.5 × 6.4 × 17.7 cm and a useful volume of 800 mL. A volume of 200 mL was recirculated in another tank (500 mL of capacity) made of Plexiglas. The electrode set consisted of one anode and two cathodes with a distance between the electrodes of 10 mm. One niobium-covered BDD circular-mesh electrode with a diameter of 12 cm, a thickness of 0.1 cm, and a surface area of 113.1 cm^2 was used as the anode. In addition, two carbon-felt electrodes with an 11 cm (length) × 9 cm (width) rectangular shape and a thickness of 1 cm were employed as the cathode. The agitation and homogenization of the solution were carried out using a PTFE-coated magnetic stirrer during electrolysis. The electro-peroxidation treatment of NP in the LWW was performed at room temperature. The solutions were continuously saturated with O_2 by bubbling compressed air at atmospheric pressure at a rate of about 0.9 L/min.

5.2.5. Experimental procedure

The first sets of electro-peroxidation experiments were conducted in three LWW NP-spiked samples containing different initial organic matter under the best conditions determined with synthetic water. Anodic current density and Na2SO4 concentration were 36 mA.cm-2 and 0.03

M, respectively. The recirculation flow rate and treatment time were respectively fixed at 400 mL/min and 1 h. During these tests, the concentration of NPs was analyzed using UV-Vis spectrophotometry at 225 nm wavelength, as discussed in section 5.2.7.1. In addition, TOC and 3D-EEM analyses were performed to evaluate the performance of the process. A central composite design (CCD) was applied to define the optimal conditions and analyze the parameters of the electro-peroxidation process in treating laundry effluents doped with NPs, as explained in section 5.2.6.

5.2.6. Experimental design and analysis

For statistical and ANOVA analysis, Design-Expert software version 13 (Stat-Ease Inc., USA) was used to design the experiments and develop an RSM model. RSM allows to evaluate and determine the optimum operating conditions. The experiments region investigated for LWW treatment and the code values are shown in Table 5.2. Experiments were defined using a factorial design and central composite design (CCD) method. Current density (X_1), Na_2SO_4 concentration (X_2), electrolysis time (X_3), and initial TOC concentration (X_4) were defined as independent variables. Initial TOC was defined based on FD in two levels while other independent variables were defined based on CCD in five levels. The range of independent variables was selected based on previous pre-experiments. On the other hand, NP removal efficiency (Y_{NP}), TOC removal efficiency (Y_{TOC}), and energy consumption (Y_{Energy}) were considered dependent variables (responses). Table 5.3 and 5.4 present the value of the independent variables along with the experimental values of responses. As seen, a total number of 32 experiments were defined which includes 16 factorial points (2^k, where k is the number of factors), 14 non-center points, and 2 replicated center points. Using the experimental values, a Response Surface Methodology (RSM) model was developed to model the responses as a function of independent parameters. In addition to parametric analysis, the developed RSM model was used to optimize the independent variables.

Tableau 5. 2 : Experiments levels and ranges for four independent variables

Coded variables (X_i)	Factor (U_i)	Experimental field		$U_{i,0}$	ΔU_i
		Min. value (-1)	Max. value (+1)		

X_1	U_A : Current density (mA.cm^{-2})	16.93	31.24	24.08	7.155
X_2	U_B : Na_2SO_4 (mo.L^{-1})	0.009	0.025	0.017	0.008
X_3	U_C : Electrolysis time (min)	28.1	51.9	40	11.9
X_4	U_D : Initial TOC	Low	High	-	-

5.2.7. Analytical methods

5.2.7.1. NP quantification

The UV-Vis absorbance of NPs was determined at different concentrations by UV-Vis spectrophotometric measurements (UV0811M136). The UV-Vis absorption spectroscopy results of NPs as a function of NP concentrations in the range of 0 to 12 mg/L are presented in Figure S1. The maximum absorption of NP was determined to be at 225 nm (Fig. AI.1a). Using the absorption values obtained at this wavelength, a calibration curve was plotted that shows the NP absorbance increases linearly by NP concentration with an R2 = 0.9964 (Fig. AI.1b). This calibration curve was used to calculate residual NP concentration and define the NP removal efficiency with Eq. (5.1).

Equation 5.1 : $NP\ removal\ (\%) = \frac{C_i - C_t}{C_i} \times 100$

where C_i and C_t represent the initial NP concentration and residual NP concentration after t minutes of electrolysis.

5.2.7.2. 3D EEM analysis

LWW samples were characterized using three dimensional fluorescence excitation-emission matrices (3D EEM) with Cary Eclipse Fluorescence Spectrophotometer from Varian Inc. (USA). The method used for the NP-doped LWW fluorescence spectra collection was referred to as domestic wastewater Effluents Organic Matter (EfOM) characterization in full-scale MBR (Jacquin *et al.*, 2017). Data were extracted in accordance with the division of the 3D fluorescence spectra representation into five different areas corresponding to different groups of fluorophores (Chen *et*

al., 2003). The spectra were collected from 230 to 450 nm at 10 nm increments by varying the excitation from 200 to 450 nm at 5 nm intervals.

5.2.7.3. Total organic carbon analysis

TOC analysis was performed using TOC-L Shimadzu 1.05.00 analyzer to verify the effectiveness of the electro-peroxidation process. TOC was considered as the difference between total carbon and inorganic carbon.

5.2.8. Economic analysis

Economic analysis of electrochemical water treatment processes is one of the major aspects to take into consideration because of its high amount of energy consumption. Energy consumption was calculated using Eq. (5.2).

Equation 5.2 *:* $EC\ (kWh.m^{-3}) = \frac{U \times I \times t}{V} \times 10^3$

where U, I, t, and V represent average cell voltage (V), applied current intensity (A), duration of electrolysis (h), and volume of treated solution (m^3), respectively.

5.2.9. Acute toxicity assessments

Toxicity tests were performed with Daphnia magna hatchling (< 24 h old) from Bureau Veritas laboratory culture at Saint-Laurent, Quebec. Their culture medium was reconstituted water with the following characteristics: 180 mg $CaCO_3$/L hardness, ≥ 80% dissolved oxygen, pH of 7- 8, 20.0 ± 2.0 °C temperature, and 16 h light – 8 h dark photoperiod). The organisms were fed once a day. In accordance with MA. 500-D.mag. analytical method, Daphnia magna (<24 h old) was exposed to 48 h, to non-doped LWW as well as NPs-doped LWW before and after treatment. For this analysis, 0.00%, 6.25%, 12.50%, 25.00%, 50.00%, 100.00% concentrations (v/v) were evaluated. Four replicates were performed for each concentration, with five hatchlings per test, placed in a bottle containing 10 mL of reconstituted water and LWW. Control tests were performed simultaneously to assure the accuracy of results. 37.5±12.5 mL/min/L air flow was applied for 30 min before starting the experiments to maintain the dissolved oxygen content close to 100%. Additive effects of chemical, biological, and physical parameters of effluents were evaluated through pH, hardness, dissolved oxygen, temperature, and conductivity measurements before

and after 48 h of exposure. The visual method was used to evaluate the criteria of toxicity consisting of immobility (antennae movement) and mortality (swimming).

5.3. Results and discussion

5.3.1. NPs degradation analysis

The performance of the electro-peroxidation process to degrade NPs in wastewater was assessed by analyzing the concentration of remaining NPs during the treatment process. To do so, the degradation of NPs was first analyzed using synthetic water (SW) samples containing NPs (NP-SW) and the results were compared with NP samples in LWW containing organic matter (NP-S1, NP-S2, and NP-S3). The samples of NP-S1, NP-S2 and NP-S3 initially contained 52.2±2.8 mg/L, 29.4±0.6 mg/L and 16.3±1.2 mg/L of TOC, respectively. The results of this comparison are demonstrated in Fig. 5.1. The tests were performed at a current density of 36 $mA.cm^{-2}$ and 0.03 M Na_2SO_4 was used as an electrolyte during 1 h of electrolysis. As shown in Fig. 5.1, for all the samples a high rate of NPs removal is observed up to around 30 min. In fact, almost complete removal of NPs was achieved after 40 and 50 min of treatment for NP-S2 and NP-S3, respectively. However, around 89.4 ±2.6% and 90.6 ±2.8% removal efficiencies were obtained after 60 min for NP-SW and NP-S1, respectively. In real LWW artificially contaminated by NP, the best performances of electro-peroxidation process were recorded (~100% of NP degradation) while treating samples having relatively low initial TOC concentrations (16 to 29 mg/L). However, when the initial concentration of TOC increased (52 mg/L of TOC), the percentages of NP degradation decreased to 90%. Indeed, competitive reactions took place between NP oxidation versus TOC oxidation when the initial TOC concentration was relatively high in LWW. The faster degradation of NPs in LWW could be attributed to the production of a higher amount of $^{\bullet}OH$, H_2O_2, $S_2O_8^{2-}$. These ROSs could be generated in the electrolysis environment due to the initial presence of ions such as SO_4^{2-} and Cl^- (Table 5.1) sourced from bleach and surfactants widely used for disinfecting clothes in laundries. The BDD anode could form additional oxidants such as HOCl and ClO^- mainly in the bulk solution by Cl^- oxidation following reactions (5.3-5.5) (Garcia-Segura *et al.*, 2015a).

Équation 5.3 : $Cl^- \rightarrow Cl_2(aq) + 2e^-$

Équation 5.4 : $Cl_2(aq) + H_2O \rightarrow HClO + Cl^- + H^+$

Équation 5.5 : $HClO \leftrightarrow ClO^- + H^+$

By comparison, the NP degradation in SW (NP-SW samples) was mainly attributed to $^{\bullet}OH$, H_2O_2, $S_2O_8^{2-}$ generated during electrolysis. Analysis of the initial pH of the solution showed that the pH of LWW was around 10 (Table 5. 1), while this was 5.70 ±0.10 for the NP-SW sample. After the electrolytic experiments, the pH dropped to 2.72 ±0.2 after 20 min of electrolysis. This significant decrease even for synthetic water can be explained mainly by the reaction between sulfate radicals and electro-generated H_2O_2 in the solution (Kiendrebeogo *et al.*, 2022).

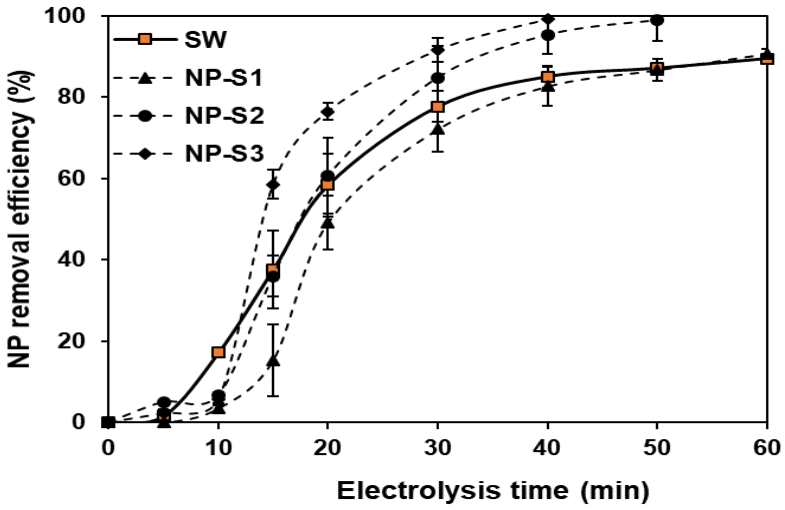

Figure 5. 1 : Degradation rate of NPs in synthetic water (NP-SW) and laundry wastewater samples (NP-S1, NP-S2, and NP-S3) using [Na_2SO_4] of 0.03 M and current density of 36 mA.cm^{-2}.

5.3.2. Total organic carbon analysis

TOC analysis was performed to evaluate the interaction effect of NP and organic matter initially present in the LWW. The initial TOC concentrations of NP-SW, NP-S1, NP-S2, and NP-S3 were 9.2 ±0.7, 52.2 ±2.8, 29.4 ±0.6, and 16.3 ±1.2 mg/L, respectively. The final residual TOC concentrations after 60 min of electrolysis were 2.8, 29.2, 15.0, and 7.6 mg/L on average for NP-SW, NP-S1, NP-S2, and NP-S3, respectively. The variation of TOC during the electrolytic experiments for these four samples is shown in Fig. 5.2. As seen, TOC removal efficiency for NP-SW reached a higher value in comparison to LWW samples. The TOC removal efficiencies was 69.6 ± 0.5% for NP-SW versus 51.1 ±3.3 %, 53.8 ±2.3%, and 56.6±3.7% for NP-S1, NP-S2, and NP-S3, respectively. The difference between the degradation kinetic of TOC removal efficiency of LWW samples is attributed to the difference in initial TOC. Around 87% of TOC removal was

reported in the previous works (Khosravanipour Mostafazadeh *et al.*, 2019) using electrolytic treatment of LWW concentrate containing 2 times more COD than the filtrate of LWW in the present study. This higher removal rate of TOC might be explained by the relatively high fraction of refractory compounds in the dissolved organic carbon part of LWW filtrate (Daghrir *et al.*, 2014; Sumisha *et al.*, 2015) than colloidal particles or suspended solids generated through electrocoagulation.

It can be seen from Fig. 5.2 that the TOC removal efficiency of NP-SW stabilized after 30 min despite the absence of additional organic matter which could interfere with NPs oxidation. This means before 30 min, longer aliphatic acid by-products formed from the gradual cleavage of benzene rings and accumulated in the medium. This would have finally allowed it to evolve to short-chain aliphatic acids and reach complete mineralization (Dos Santos *et al.*, 2020). After 30 min, short-chain carboxylic acids presented slower reaction kinetics (Dos Santos *et al.*, 2020; Ouarda *et al.*, 2020). It is important to notice that after 30 min, there was only less than about 30% of NPs remained in the NP-SW solution. This indicated the formation of acids and their mineralization rate became equal (Dos Santos *et al.*, 2020). However, for LWW samples, TOC removal efficiencies do not stabilize even after 60 min, especially for effluents with relatively high initial TOC. Consequently, the low TOC removal rate might be ascribed to a relatively low treatment time.

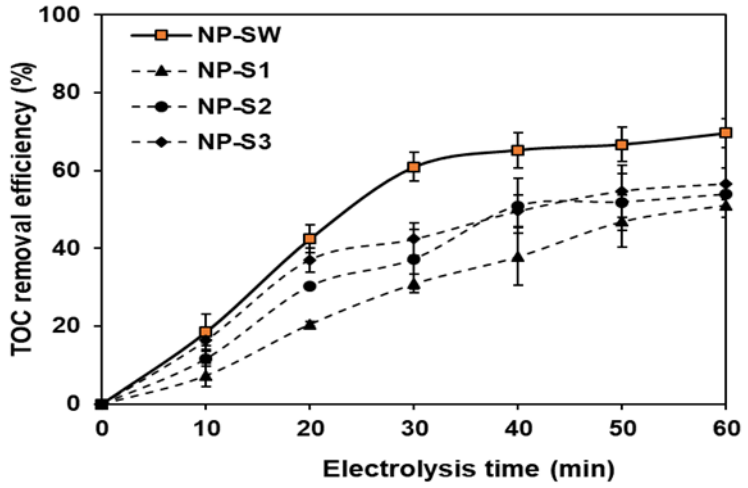

Figure 5. 2 : TOC removal efficiencies of NP-SW, NP-S1, NP-S2, and NP-S3 at [Na_2SO_4] of 0.03 M and current density of 36 $mA.cm^{-2}$.

5.3.3. EEM fluorescence spectra analysis

Fluorescence spectral characteristics of dissolved organic matter (DOM) during electrolysis were investigated using 3D EEM analysis to explore the destruction mechanisms of NPs in LWW. The EEM fluorescence spectra of synthetic water and LWW before and after spiking as well as during the electrolytic treatment are illustrated in Fig.5. 3. The reference peaks observed for spiked LWW were identified by comparing their fluorescence properties (excitation/emission (Ex/Em)) with those identified in standard dilutions of NPs (Figure no shown) and pure compounds, such as aromatic protein, tryptophan protein, humic and fulvic acid-like (Chen *et al.*, 2003). For NPs synthetic solution, the first main peak was located at the Ex range of 200-220 centered at Em 300 nm (Peak A), and the second was observed at the Ex/Em of 200-220/250 nm (Peak B) (Fig. 5.3a). The two peaks located had been reported as protein-like peaks, in which the fluorescence was associated with aromatic protein-like substances. A spot of fluorophores with high fluorescence intensity (FI) was presented in the region of Em > 380 nm. That represented fulvic acid-like substances for the region of ex 200-250 nm and 250-450 nm as humic acid-like substances (Chen *et al.*, 2003). It could represent the presence of surfactants in standard chemicals. The obtained fluorescence spectral map of NPs doped LWW clearly shows two maximum peaks A and B located at the same Ex/Em. (Fig. 5.3b (2), 5.3c (2)). It is important to notice that the initial fluorescence spectral map of LWW without NPs doping presented a peak (Ai) centered at 250/300 (Ex/Em) for both sampled wastewaters s1 and s2 (Fig. 5.3b (1), 5.3c (1). Consequently, initial peak A for doped effluents was the combination between LWW initial aromatic compounds and polystyrene benzene molecules. These features of the fluorescence spectrum have been attributed to the emission from molecules formed between pendant phenyl groups (Torkelson *et al.*, 1981). Thus, the correlation between NPs fluorophores intensity and concentration cannot be adequately established for LWW. By referring to the 3D EEM spectrum of non-fluorescent NPs obtained in our previous works, peak A seems the most suitable reference for polystyrene molecules.

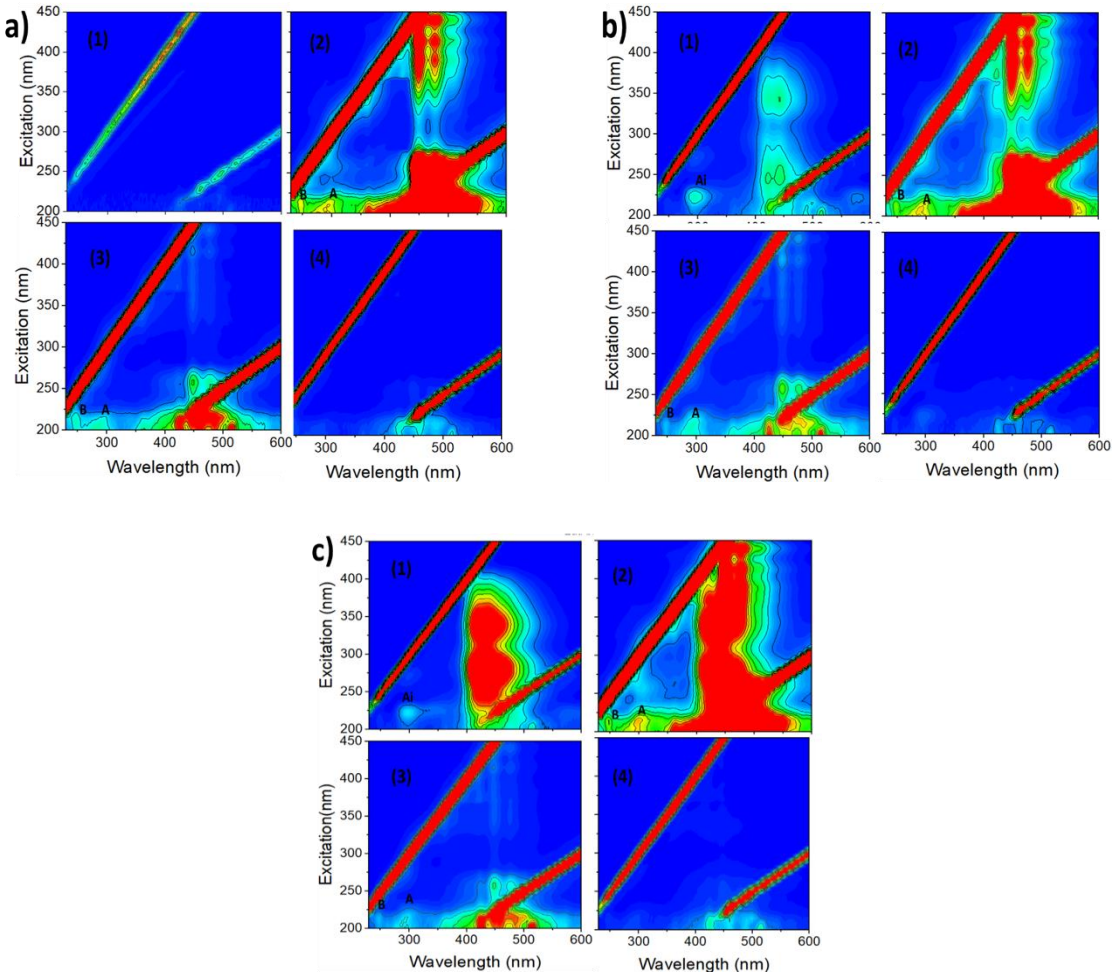

Figure 5. 3 : EEM fluorescence spectra of a) NP-SW, b) NP-S1, and c) NP-S2 samples. (1) Distilled water (a) or LWW (b and c), (2) Spiked sample a t = 0, (3) t = 20 min, and (4) t = 40 or 60 min.

EEM spectra of DOM from NP-spiked waters (NP-SW, NP-S1, and NP-S2) after electro-peroxidation treatment is illustrated in Fig. 5.3. It can be seen that even initial DOM from LWW, aromatic protein-like seem completely disappear from the waters after 40 min. From the EEM map, humic acid-like degraded after 20 min, aromatic proteins-like after 40 min and fulvic acid-like remained present for up to 60 min. The fast decrease of humic acid-like and aromatic proteins-like was observed because of the degradation and mineralization of these compounds where aromatic structure reacts quickly with $^{\bullet}OH$, active chlorine, and $SO_4^{\bullet-}$ (Garcia-Segura *et al.*, 2015a; Luo *et al.*, 2018). More precisely, the intensity of the peaks was followed during electrolysis at the excitation of 215 nm selected and peak intensity ratios are displayed in Table S1 which could be

used for semi-quantitative analysis. It can be seen in Table S1 that throughout the electro-peroxidation process, the FI (fluorophore intensity) of peaks A and B progressively decreased from 701 to 57 and from 674 to 49, respectively for NP-SW. In addition, Fluorophore initially located between emission 380 and 600 nm was narrowed to 410-500 nm and its intensity decreased. The ratio between average FI of spot and FI of peak A increased markedly throughout treatment from 0 to 40 min for synthetic water, i.e. FI of peak A decreased. The higher increase in ratio indicates the attack on aromatic protein-like substances (Peak A) was more rapidly in synthetic water than LWW. However, for LWW the ratio decreased after 20 min treatment time, corresponding to rapid decrease in average FI of spot compared to FI of peak A. the decrease in ratio suggests the degradation of fulvic acid-like is predominant after 20 min given humic acids-like were degraded during 0 to 20 min treatment time. Compared to residual TOC, there was no agreement between the efficiency of TOC removal and the fluorophore intensity remaining after 40 min treatment for effluents. That suggests less short-chain acid accumulated in the DOM has no fluorescence characteristics. Otherwise, that could also confirm fluorescence intensity being dependent on the molecular weight (Ishii *et al.*, 1978).

5.3.4. Analysis and optimization of operating parameters

During the treatment process, reactive oxygen species such as hydroxyl radicals (•OH), hydrogen peroxide (H_2O_2), and persulfates ($S_2O_8^{2-}$) were simultaneously electro-generated. NPs and initial organic compounds were mainly oxidized on the BDD surface by (i) •OH from water discharge and (ii) $SO_4^{\bullet-}$ via $S_2O_8^{2-}$ reaction with •OH. Organic compounds were additionally degraded by •OH formed from H_2O_2 direct decomposition as well as $SO_4^{\bullet-}$ generated from $S_2O_8^{2-}$ direct reaction with H_2O_2. H_2O_2 dissociation increased in the range of temperatures ranging from 30 to 40 ºC (Özcan *et al.*, 2008). In the present study, the experiments were performed with initial temperatures varying between 13 and14 ºC, whereas the temperatures ranging between 20 and 30 ºC were recorded at the end of the electrolysis, depending on the current intensity applied and the supporting electrolyte (Na_2SO_4) concentrations. Accordingly, in this work, in-situ electro-generated H_2O_2 plays a critical role by increasing hydroxyl radicals and sulfate radicals in the solution, via persulfate activation. It was reported that, $SO_4^{\bullet-}$ attacks organic compounds by electron transfer, however •OH oxidizes them mainly by H-abstraction after bringing unsaturated bonds (Cai *et al.*, 2018a; Lan *et al.*, 2017). Also, $SO_4^{\bullet-}$ has a longer lifetime (30-40 µs) than •OH

(20 ns) (Nidheesh & Rajan, 2016). The formation of mediated oxidation compounds is more effective than •OH. (Divyapriya & Nidheesh, 2021).

5.3.4.1. Effect of the experiment parameters on the NP degradation using the experimental factorial design methodology

Four parameters were studied by using a factorial design matrix (2^4): current density (X_1), Na_2SO_4 concentration (X_2), electrolysis time (X_3), and LWW initial TOC concentration (X_4). The influences of these parameters on the efficiencies of NP and TOC removal were investigated. The experimental design and results are summarized in Table 3. Y_{NP} represents the degradation efficiency of NP and Y_{TOC} represents the degradation efficiency of TOC. X_1, X_2, X_3 and X_4 represent the coded variables (-1 or +1) of the principal parameters. The estimations of the effects of the principal parameters are given by the coefficients associated to each parameter. X_1X_2, X_1X_3, X_1X_4, X_2X_3, X_2X_4 and X_3X_4 represent the interactions between the principal factors and their effects are estimated by the coefficients corresponding to these interactions. The experimental response is represented by a linear polynomial model with interactions (see equations 6 and 7). The coefficients of the polynomial model were calculated by means of Design-Expert Program Software (Design Expert 7, 2007, Sate-Ease Inc., Minneapolis):

Equation 5.6 : **NPs removal (%)**

$$Y_{NP} = 56.07 + 8.91X_1 + 10.07X_2 + 10.23X_3 - 27.09X_4 + 0.53X_1X_2 + 0.04X_1X_3 + 0.81X_1X_4 - 0.02X_2X_3 + 0.93X_2X_4 - 0.61X_3X_4$$

Equation 5.7 : **TOC removal (%)**

$$Y_{TOC} = 26.81 + 6.40X_1 + 6.32X_2 + 6.72X_3 - 1.29X_4 + 2.12X_1X_2 + 1.72X_1X_3 + 0.94X_1X_4 - 2.05X_2X - 0.91X_2X_4 - 0.87X_3X_4$$

From Equation 5.6, it can be seen that the degradation of NP is very influenced by the initial TOC concentration in LWW (X_4 coefficient = -27.09) having negative effect on the response. The percentage of NP degradation decreased on average of 54.2% (2 x 27.09) when the initial TOC concentration in LWW goes from Low (16 mg/L) to high (52 mg/L). The second most important parameter affecting NP degradation is the electrolysis time (X_3 coefficient = +10.23) having a positive effect. The increase of the electrolysis time (from 28 to 52 min) contributes to increase the percentage of NP degradation on average of 20.5% (2 x 10.23). The effects of the supporting

electrolyte (Na_2SO_4) concentration (X_2 coefficient = 10.07) and the current density (X_1 coefficient = 8.91) are quite similar to this recorded with electrolysis duration. Considering the interaction terms, X_2X_4 (Supporting electrolyte concentration and initial TOC concentration) and X_1X_4 (current density and initial TOC concentration) have the most important coefficients (+0.93 and + 0.81, respectively), the both interaction effects being positive.

From Equation 5.7, it can be seen that the current density (X_1 coefficient = +6.40), the supporting electrolyte (X_2 coefficient =+6.32) and the electrolysis time (X_3 coefficient = +6.72) are the most important parameters affecting positively the TOC removal and having approximatively equal levels of influence. For instance, the increase of the electrolysis time (from 28 to 52 min) contributes to increase the percentage of TOC removal by 13.4% (2 x 6.72). However, the effect of the initial TOC concentration (X_4 coefficient = -1.29) is relatively weak and its effect is negative. Considering the interaction terms, X_1X_2 (current density and supporting electrolyte concentration) and X_1X_3 (current density and electrolysis duration) have the most important coefficients (+2.12 and + 1.72, respectively), the both interaction effects being positive. The contribution of each factor can be calculated using the following equations based on Pareto analysis (Myers *et al.*, 2018) (Fig.AI. 3) :

Equation 5.8: $P_i = \left(\frac{b_i^2}{\Sigma b_i^2}\right) \times 100 \ \ (i \neq 0)$

b_i represents the coefficient associated to each factor i. It represents the estimation of the principal effect of the factor i. The contributions of the principal effects (X_1, X_2, X_3 and X_4) on the percentage of NP degradation are 7.38%, 9.43%, 9.72% and 68.23%, respectively. The contribution of the interaction effects (X_2X_4, and X_1X_4) on the percentage of NP degradation are 0.08% and 0.06%, respectively.

Tableau 5. 3 : Experimental factorial matrix in the 2^4 design for different levels of TOC concentrations (Low and high) and experimental results.

Experiment number	Experimental design				Experiment plan				Responses		
	X_1	X_2	X_3	X_4	A : ($mA.cm^{-2}$)	B : Na_2SO_4 ($mol.\ L^{-1}$)	C : time (min)	D : TOC effluent	Y_{NP} removal (%)	Y_{TOC} removal (%)	Y_{Energy} ($kWh.m^3$)
1	-1	-1	-1	-1	16.9	0.009	28.1	Low	42.77	5.70	6.51
2	-1	+1	-1	-1	16.9	0.025	28.1	Low	78.38	23.60	7.98
3	-1	-1	+1	-1	16.9	0.009	51.9	Low	79.74	27.39	11.89
4	-1	+1	+1	-1	16.9	0.025	51.9	Low	99.40	33.85	14.65
5	+1	-1	-1	-1	31.2	0.009	28.1	Low	76.73	14.67	23.38
6	+1	+1	-1	-1	31.2	0.025	28.1	Low	91.45	38.04	21.07
7	+1	-1	+1	-1	31.2	0.009	51.9	Low	96.86	35.71	41.02
8	+1	+1	+1	-1	31.2	0.025	51.9	Low	100	45.85	38.37
9	-1	-1	-1	+1	16.9	0.009	28.1	High	9.75	13.47	8.72
10	-1	+1	-1	+1	16.9	0.025	28.1	High	17.00	18.86	8.98
11	-1	-1	+1	+1	16.9	0.009	51.9	High	18.23	18.24	15.99
12	-1	+1	+1	+1	16.9	0.025	51.9	High	32.05	22.15	11.58
13	+1	-1	-1	+1	31.2	0.009	28.1	High	13.76	13.00	21.41
14	+1	+1	-1	+1	31.2	0.025	28.1	High	36.94	33.35	18.27
15	+1	-1	+1	+1	31.2	0.009	51.9	High	30.18	35.71	38.55
16	+1	+1	+1	+1	31.2	0.025	51.9	High	73.93	49.38	32.88

It can be interesting to analyze the interaction X_2X_4 having the most important contribution among the interaction terms (for NP degradation). The interpretation of the interactions X_2X_4 can be facilitated by analyzing the Figure 5.4. This figure represents a combination of the supporting electrolyte concentration and the initial TOC level. In this figure, the value of 92% is obtained by calculated the average of the experimental results from the experiments performed with a low level of TOC concentration (16 mg/L) and in the presence of 0.025 mol. L^{-1} of Na_2SO_4 (experiments 2, 4, 6 and 8). When the level of initial TOC concentration (variable X_4) is fixed at the lowest level (16 mg/L of TOC), the supporting electrolyte (X_2) had an influence on the response, the average percentage of NP degradation passed from 74 to 92%. However, if the initial TOC concentration is fixed at the highest level (52 mg/L), the supporting electrolyte concentration continue to have an influence on the response, but it more important than the first case while imposing low level of initial TOC concentration. The percentage of NP degradation passed from 18% to 40%. Consequently, it can be noticed that the effect of supporting electrolyte concentration is not constant; it depends on the type of the initial TOC concentration. The degradation rate of NP passed from 40% to 92 % (gaining 52% for NP degradation) when the supporting electrolyte concentration is fixed at the highest level (0.025 mol. L^{-1}). When Na_2SO_4 is fixed at the lowest concentration (0.009 mol. L^{-1}), the degradation rate of NP increased from 18% to 74% (gaining 56% for NP degradation). Consequently, level of initial TOC concentration is a major factor that influences the degradation rate of NPs but it directly depends of Na_2SO_4 concentration.

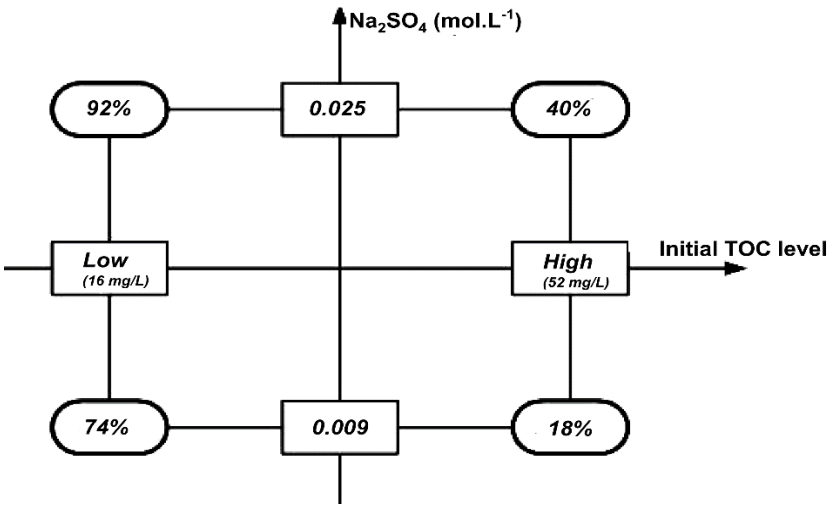

Figure 5. 4 : Interaction X_2X_4 between TOC initial level and Na_2SO_4 concentration.

5.3.4.2 Optimization conditions for NP degradation using central composite design methodology

Central composite matrix (Haaland, 1989) was used to optimize the degradation process in the all experimental region. Three quantitative factors (A, B and C) and one categorical factor (D) were used. The experimental matrix includes factorial matrix (described above) and sixteen additional experiments carried out at the center of experimental domain and around the central point of the experimental domain. In fact, a set of eight additional experiments were required for each categorical factor (low level of TOC and high level of TOC). A total of thirty-two experiments were carried out to describe the response surface modeling. According to results presented in Table 5.4, the response can be described by the polynominal model (quadratic model) from the following equations:

Equation 5.9: NPs removal (%)

$$= 53.35 + 11.05X_1 + 11.26X_2 + 11.29X_3 - 26.77X_4 + 1.05X_1^2 - 0.87X_2^2 + 1.63X_3^2 + 0.545X_1X_2 + 0.022X_1X_3 + 1.77X_1X_4 - 0.007X_2X_3 + 0.254X_2X_4 + 0.1083X_3X_4$$

Equation 5.10: TOC removal (%)

$$= 28.92 + 6.29X_1 + 6.55X_2 + 6.87X_3 - 0.53X_4 - 0.31X_1^2 - 0.90X_2^2 - 0.67X_3^2 + 2.12X_1X_2 + 1.72X_1X_3 + 0.85X_1X_4 - 2.05X_2X_3 - 0.32X_2X_4 - 0.90X_3X_4$$

According to equation 5.9, the initial TOC concentration is the most important parameter that influences NP degradation. It has a negative effect on NP degradation. An increase of initial TOC concentration decreases the electrochemical of degradation of NP. There are competitive reactions between NP degradation and TOC removal during electrolysis. When the initial TOC concentration increases, the fraction of current intensity used for TOC oxidation increases so that NP degradation decreases.

Tableau 5. 4: Central composite matrix and expérimental results.

	Experimental design			Experimental plan			Degradation % and Energy consumption		
	X1	X2	X3	**A** (mA.cm^{-2})	**B** (mol.L^{-1})	**C** (min)	NP removal (%)	TOC (%)	Energy (kWhm^{-3})
Low level TOC (**D**)									
17	-1.67	0	0	12.05	0.017	40	59.71	20.81	6.60
18	1.67	0	0	36.12	0.017	40	96.61	38.98	39.53
19	0	-1.67	0	24.09	0.004	40	46.67	12.90	30.07
20	0	1.67	0	24.09	0.030	40	92.56	34.30	19.23
21	0	0	-1.67	24.09	0.017	20	60.73	15.68	10.43
22	0	0	1.67	24.09	0.017	60	100	42.70	29.67
23	0	0	0	24.09	0.017	40	94.43	27.80	20.13
24	0	0	0	24.09	0.017	40	90.43	27.80	20.13
High level TOC (**D**)									
25	-1.67	0	0	12.05	0.017	40	3.04	15.34	5.08
26	1.67	0	0	36.12	0.017	40	60.77	38.45	31.0
27	0	-1.67	0	24.09	0.004	40	8.90	17.41	23.60
28	0	1.67	0	24.09	0.030	40	50.21	42.28	15.67
29	0	0	-1.67	24.09	0.017	20	9.63	15.27	8.83
30	0	0	1.67	24.09	0.017	60	56.28	35.87	21.40
31	0	0	0	24.09	0.017	40	18.77	29.93	15.17
32	0	0	0	24.09	0.017	40	10.63	29.93	15.33

Figure 5.5 compares the actual (measured from experiments) and predicted values of NP degradation and TOC removal. The actual and predicted values of NP degradation (and TOC removal) fitted very well. The data are in accordance with the statistical significance of the quadratic model presented in Table 5.5.

Table 5.5 presents the analysis of variance (ANOVA) of regression parameters of the predicted response models for NPs, TOC removal, and energy consumption. Considering the low probability values (P-values < 0.0001), all the models were significant at a 5% confidence level (Hilles *et al.*, 2016a). The coefficients of determination obtained in this study for the NPs, TOC removal, and energy consumption (R^2= 0.9814, 0.9921, and 0.9507, respectively) were all higher than 0.80 which represent a good agreement between the calculated and experimental results (García-Gómez *et al.*, 2014). In addition, ANOVA analysis showed the adjusted R^2 are close to 1 (R^2 = 0.9521, 0.9795, and 0.9150, respectively).

Tableau 5. 5: ANOVA results for the response surface quadratic model for NPs removal, TOC removal, and energy consumption.

Source	Sum of square	df	Mean of square	F-value	P-value	
NPs removal						
Model	34911.86	19	1837.47	33.41	< 0.0001	significant
Residual	659.90	12	54.99			
Lack of fit	618.72	10	61.87			
Pure error	41.17	2	20.59			
TOC removal						
Model	3980.86	19	209.52	79.01	< 0.0001	significant
Residual	31.82	12	2.65			
Lack of fit	31.82	10	3.18			
Pure error	0.0000	2	0.0000			
Energy consumption						
Model	4170.63	13	320.82	26.68	< 0.0001	significant
Residual	216.45	18	12.02			
Lack of fit	216.45	16	13.53			
Pure error	0.0000	2	0.0000			

R^2 = 0.98 (for NP removal) and R^2 = 0.99 (for TOC removal).

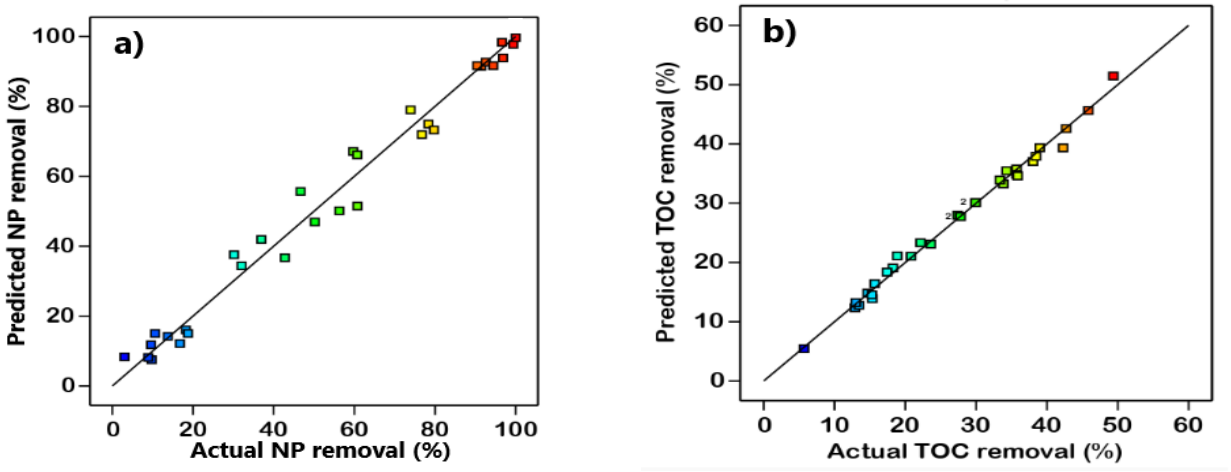

Figure 5. 5 : Comparison of actual and predicted values for (a) NPs removal and (b) TOC removal.

Tableau 5. 6: Optimal conditions determined by Design Expert Program software for NP degradation

Test number	Factors				Predicted responses			Experimental responses		
	U_A mA.cm^{-2}	U_B mol.L^{-1}	U_C min	U_D -	NP removal (%)	TOC removal (%)	Consumed energy (kWh m^{-3})	NP removal (%)	TOC (%)	Consumed energy (kWh m^{-3})
33	31.2	0.025	52	High TOC	79	48	38	81±5	43±3	34±0.5
34	31.2	0.025	52	Low TOC	99	46	37	-	-	-

In order to determine the optimal conditions for NP degradation and TOC removal in terms of cost and effectiveness, the energy consumption need to be considered. The criteria selected for the optimization conditions were following: (a) The removal efficiency of NP and TOC has to be maximized with the highest importance (with a minimum of 80 % of NP degradation is imposed) and (b) the energy consumption should be minimized with lesser importance in order to reduce the treatment cost related to the consumption of energy. Accordingly, the optimal conditions proposed by the Design Expert software were the following: 31.2 $mA.cm^{-2}$ current density, 0.025 mol. L^{-1} [Na_2SO_4], 52 min treatment time and 52 mg/L initial TOC. Under these conditions, the model predicts NPs and TOC removal efficiencies near 79% and 48% respectively and energy consumption of 38 $KWh.m^{-3}$ (Table 5.7). For a comparison, the predicted NPs and TOC removal efficiencies and energy consumption for 16 mg/L initial TOC, were near 100% and 46% respectively and 37 $KWh.m^{-3}$ under the same optimal conditions. In order to get closer to the reality of the initial TOC load of LWWs in general, 52 mg/L initial TOC was considered for experimental control. So, the prediction for 52 mg/L initial TOC was experimentally validated and the obtained results were 81 ±5% NP removal, 43 ±3% TOC removal and 33 ±0.5 $KWh.m^{-3}$ energy consumption which are close to the predicted values. The treatment cost (including energy and Na_2SO_4 consumption) was 3.05 US \$/m^3. To reduce energy consumption, the electrochemical treatments could be done at an initial temperature higher than 20 °C.

5.3.5. Toxicity analysis

To estimate the acute toxicity of the effluents before and after electrochemical treatment, three samples were subjected to analysis: i) Untreated LWW without NP addition; ii) Untreated LWW NP-spiked samples and; iii) Treated LWW NP-spiked samples. The optimal conditions (described above) were applied for the treated LWW NP-spiked samples (current density of 31.2 $mA.cm^{-2}$, concentration of supporting electrolyte of 0.025 mol. L^{-1} and treatment time of 52 min). Figure 5.6 presents the toxicity evaluation. The mortality percentage of Daphnia magma against the concentration of LWW was plotted (before and after treatment). The toxicity was no measured for the treated LWW NP-spiked samples (LC50>100%v/v). By comparison, LWW NP-spiked samples (without treatment) shows toxicity at relatively low concentrations (LC50<12% (v/v)), whereas a toxicity was measured at concentrations LC50<22.5% (v/v)) for untreated LWW samples without NP addition. This means that the addition of NP in LWW contributed to increase the toxicity in

untreated LWW. However, when LWW artificially contaminated by NP of polystyrene was subjected to electrochemical treatment, the toxicity disappeared owing to degradation/mineralization of toxic compounds. The compounds such as proteins-like (polystyrene NPs and nonylphenol) and humic acids-like compounds could be oxidized to non-toxic by-products. It has been reported by-previous studies (García-Gómez *et al.*, 2016; Yassine *et al.*, 2018), relating to electro-oxidation treatment of certain pollutants, an increase in *Daphnia magna* toxicity of treated water. That would due to the formation of toxic byproducts or attributed to the residual concentration of oxidants generated during the electrolytic treatment. While in our study a decrease in toxicity was obtained. Consequently, optimum operating conditions made it possible to obtain enviro-friendly treated water.

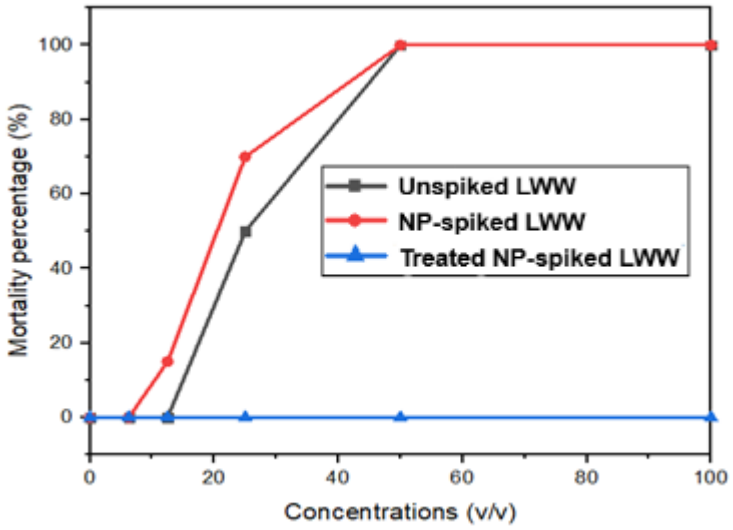

Figure 5. 6 : Toxicity assessment on Daphnia magna for untreated and treated NP-spiked s1 LWW

5.4. Conclusion

Since plastic particles in LWW are a major source of MPs and NPs in wastewater treatment plants, their removal at source is a promising approach to avoid further pollution of water resources. In this work, electro-peroxidation is studied as a process to degrade NPs in industrial LWW. Analysis of the rate of NPs removal revealed that naturally present ions in the LWW increased the rate of NPs degradation and a complete removal could be obtained after 40 min. However, the rate of TOC removal in industrial LWW was lower than that recorded in SW because of the higher initial

TOC concentration. 3D EEM analysis suggested that humic acid-like, aromatic proteins-like, and fulvic acid-like compounds could degrade after 20, 40, and 60 min of treatment, indicating the possibility of degrading intermediates by-products that would be generated from NPs. Analysis of the factorial design (FD) indicated that the level of initial TOC concentration was the most important parameter affecting NP degradation during the application of electro-peroxidation process. The percentage of NP degradation was reduced (on average) by 54% when the initial TOC concentration in LWW passed from the low level (16 mg/L) to the high level (52 mg/L). Using 2^4 factorial design, the best performance for NP degradation (100% of NP degradation) was recorded by imposing a current density of 31.2 $mA.cm^{-2}$ during 52 min of electrolysis time in the presence of 0.025 mol L^{-1} of Na_2SO_4. A central composite design was subsequently applied to determine the optimal conditions taking into account both responses NP degradation and TOC removal. A current density of 31.2 $mA.cm^{-2}$, 0.025 mol. L^{-1} of Na_2SO_4, and 52 min of treatment time were determined as optimal conditions in order to minimize the energy consumption. Under these conditions, 81$\pm$5% of NP and 43$\pm$3% of TOC could be simultaneously removed for a total cost of 3.05 US$.$m^{-3}$ of treated LWW. The total cost included energy and electrolyte consumption. Finally, toxicity analysis demonstrated that the electrochemically treated LWW samples containing NPs exhibited no toxicity, indicating mineralization of proteins-like (NPs and nonylphenol) and humic acids-like compounds or their degradation to non-toxic by-products. This study showed that the electro-peroxidation of NPs is a promising approach to degrade NPs in industrial LWW. However, the effluent is suggested to be concentrated before electro-peroxidation treatment to enhance the cost-effectiveness of the process.

Acknowledgments

The authors would like to acknowledge the financial support from the CREATE-TEDGIEER program and the Canadian Francophonie Scholarship Program.

6. DISCUSSION GENERALE ET CONCLUSION

Ces travaux ont permis d'évaluer l'efficacité d'un procédé d'oxydation électro-catalytique (OEC) utilisant des électrodes à fortes surtension d'oxygène pour le traitement d'effluents contaminés par des micro- et nano-plastiques tels que le polystyrène (PS). Cette section consiste en une discussion générale des différents résultats enregistrés.

6.1. Mise au point de méthodes qualitative et quantitative d'analyses des micro- et nano-plastiques dans l'eau

Les objectifs principaux de ce travail de thèse étaient de concevoir, tester et optimiser à l'échelle de banc d'essai en laboratoire, l'efficacité d'un procédé d'oxydation électro catalytique (OEC) pour la dégradation des micro-plastiques (MPs) et nano-plastiques (NPs) dans les eaux et effluents de buanderie. Pour répondre à ces objectifs, il a fallu dans un premier temps mettre au point une méthode analytique de quantification de micro-plastiques basée à la fois sur l'analyse granulométrique/massique et sur les propriétés morphologiques (analyse MEB) et physicochimiques de surface (analyse FTIR) des particules de micro-plastiques. Pour ce qui est de la quantification des nano-plastiques les méthodes traditionnelles de quantification telles que la mesure du carbone organique total, la méthode indirecte par spectrophotomètre UV-vis et la spectrophotométrie 3D de fluorescence d'acquisition de matrices d'émission-excitation (3D-EEM) ont été adaptées pour l'estimation des particules de nano-plastiques dans les eaux. Cette tâche d'ajustement de méthode analytique a été effectuée tout au long de cette thèse. Ces techniques analytiques ont été sélectionnées sur la base de la revue de littérature des techniques couramment utilisées pour l'analyse des MPs/NPs et leurs limites (Chapitre 2). Aujourd'hui, les méthodes de mesure des MPs/NPs résiduels au cours des procédés de traitement diffèrent d'une matrice aquatique à une autre (eau synthétique, eau usée réelle).

Pour l'eau synthétique plusieurs études ont utilisé la mesure de masse, le profil de taille des particules par diffusion dynamique de lumière laser et la turbidité pour suivre les performances d'élimination (séparation, dégradation) des MPs (tableau 2.1). Aucune limite liée à leurs résultats n'a été signalée pour le profil de taille et les pesées. Cependant il est noté que la turbidité n'était pas linéaire à la concentration des MPs pour des particules de 140 µm parce qu'elles avaient tendance à décanter plus rapidement (Lapointe *et al.*, 2020a). Dans le même temps il est connu que la pesée des MPs et le profil de taille des particules par DLS sont problématiques à cause

des faibles concentration et tailles des MPs. Il a donc été nécessaire de fixer les concentrations fiables de travail spécifiques aux particules de MPs de polystyrène de 25 µm utilisées au cours de ces travaux.

Pour commencer nos travaux, une dispersion de microbilles de polystyrène de 25 µm de diamètre nominale a été choisie comme source de micro-plastiques sur la base de la littérature. Le mode de la distribution des particules de micro-plastiques a été sélectionné pour suivre les modifications de la taille des particules au cours du traitement. Pour des résultats fiables de l'analyse granulométrique (c'est à dire baisse de transmittance de la lumière laser de 100% à 75-90% lorsque l'échantillon est introduit) une concentration de travail de 100 mg/L de MPs a donc été déterminée avec un volume utile de 50 mL pour chaque pas de prélèvement. Il faut noter que la baisse de la transmittance est reliée la quantité de matière présente dans l'échantillon d'eau. Par la suite, la masse de MPs dans les prélèvements de 50 mL de la solution de travail a été déterminée puis comparée à la masse théorique de MPs de 5 mg pour chaque échantillon. De plus petites concentrations avaient été aussi testées afin de prendre en compte la perte de masse au cours du traitement. Afin d'évaluer les résultats obtenus grâce à la mise au point de ces deux méthodes analytiques, les échantillons (50 mL) avant et après traitement ont été déshydratés et analysés au microscope à balayage électronique (MEB) et au spectroscopie IRTF. Ces analyses nous permettraient de voir respectivement la formation de plus petites particules et l'oxydation des MPs après traitement. Il est important de noter que le carbone organique total a aussi été mesuré dans les filtrats (0.22 µm) des échantillons prélevés au cours du traitement afin de vérifier la formation de sous-produits organiques. D'après l'analyse au MEB des échantillons prélevés après 1h de traitement, les particules avant et après traitement avaient presque la même taille et la morphologie était restée intacte. Cependant l'analyse granulométrique de ces mêmes échantillons montrait une diminution de la taille des particules lorsque qu'une réduction de masse de 55-60% (55-60 mg/L) avait été enregistrée. Dans le même temps l'analyse d'une concentration de 40% (40 mg/L) d'une eau non traitée a montré un profil de taille presque similaire à celle obtenue avec une concentration de 100 mg/L (concentration initiale) confirmant ainsi la réduction de taille des particules pendant le traitement. Une explication possible aux résultats obtenus par la microscopie à balayage électronique est que les prélèvements d'un volume de 50 mL/échantillon n'étaient pas suffisamment représentatifs pour voir les plus petites particules formées.

Des microbilles non fluorescentes de polystyrène de 100 nm de diamètre nominal et des microbilles fluorescents de polystyrène de 150 nm de diamètre nominal ont été choisis pour respectivement étudier les eaux synthétiques et les eaux usées réelles. Pour ces particules plus petites que les micro-plastiques, la méthode analytique par mesure d'absorbance au spectrophotomètre UV-vis a été examinée. Pour l'eau synthétique l'absorbance à 254 nm a été utilisée en se basant sur la caractérisation spécifique de cette longueur d'onde pour les substances aromatiques possédant plusieurs doubles liaisons comme le polystyrène. En plus l'eau synthétique ne contient que les nano-plastiques comme seule source de matière organique. Par contre pour les eaux usées contenant d'autre matière organique, l'intégration de la fluorescence dans les particules de nano-plastiques permettrait facilement leur traçabilité. Par la suite, les échantillons avant et après traitement ont été scanné au spectroscopie de fluorescence afin de caractériser et suivre l'évolution de la matière organique dissoute liée au nano-plastiques. Bien que les caractères complémentaires des différentes techniques analytiques utilisées nous ont permis de suivre approximativement les performances de dégradation par OEC des MPs/NPs il est nécessaire qu'une méthode analytique précise avec la GC-MS soit développée pour mieux quantifier les MPs/NPs et leurs sous-produits au cours des traitements de dégradation.

6.2. Oxydation anodique de micro-plastiques (MPs) de polystyrène (Chapitre 3)

Un réacteur électrolytique a premièrement été conçu en vue de faire la preuve du concept du processus d'oxydation anodique des MPs. Un réacteur parallélépipédique (14,5 cm (longueur) x 6,4 cm (largeur) x 17,7 (hauteur)) comprenant des électrodes circulaires (12 cm diamètre) a été utilisé. Des électrodes anodiques de diamant dopé au bore (DDB), de titane recouvert d'oxyde d'iridium (Ti/IrO_2) et d'oxyde de métal mixte (MMO) ont respectivement été utilisées, alors qu'une électrode de titane a été utilisée à la cathode. Le procédé OEC a été par la suite testé pour la dégradation des particules de micro-plastiques (MPs) de polystyrène de 25 µm de diamètre nominal dans un effluent synthétique. Le polystyrène appartient à la famille des polluants plastiques couramment rencontrés dans les eaux de surface et résiduaires. Lors de l'application du procédé OEC, plusieurs paramètres tels que, la densité de courant, le temps de traitement, le type d'électrode anodique et la surface des électrodes ont été étudiés. Les effluents synthétiques ont été contaminés par des microbilles de polystyrène de diamètre nominal de 25 µm et ayant une concentration initiale de 100 mg/L. Les résultats révèlent qu'un taux de dégradation de

58±21% (p/p) des micro-plastiques est enregistré après seulement 1h d'électrolyse. Cependant, lorsque l'électrolyse se poursuit pendant 6h, un taux d'abattement de 89±8% est enregistré en imposant une densité de courant de 108 $mA.cm^{-2}$. Des résultats similaires ont été rapportés par Miao et al., (2020) durant l'électrolyse de micro-plastiques de 100-200 µm de polychlorure de vinyle lorsqu'une technologie de type électro-fenton a été appliquée. Les taux de déchlorination et de minéralisation étaient de 75% et 56% après 6h d'électrolyse (Miao *et al.*, 2020b). De meilleurs résultats (99% de dégradation, 95% de minéralisation après 2h de traitement) ont été rapportés par VIRIDIS RESEARCH INC (2022) lors de l'électrolyse de microfibres de plastiques. La densité du courant était comprise entre 20-50 $mA.cm^{-2}$ en utilisant l'anode de BDD avec un réacteur amélioré en terme de transport de masse. Par conséquent, la configuration du réacteur est un élément essentiel sur lequel des efforts doivent être effectués pour un traitement efficace (performance, cout) des MPs/NPs. L'analyse au microscope électronique à balayage (MEB) de la suspension résiduelle de micro-plastique dans l'effluent traité indiquait une taille et une morphologie identiques à celles mesurées dans l'effluent initial, suggérant ainsi une minéralisation des micro-plastiques dégradés. Les analyses subséquentes par granulométrie laser (diffusion dynamique de la lumière), du carbone organique total et les analyses à infrarouge à transformée de Fourier (IRTF) indiquent que les micro-plastiques n'ont pas été simplement transformés en petites particules, mais qu'ils ont été complètement dégradés en CO_2 et H_2O. Les résultats de cette partie des travaux ont fait l'objet d'un article publié dans la revue de calibre international Environmental Pollution. L'hypothèse selon laquelle que la génération *in situ* d'espèces oxygénées réactives ($^{\bullet}OH$, $H_2S_2O_8$, etc) à la surface de l'anode ou dans l'électrolyte et l'utilisation d'électrodes volumiques sous forme de métal déployé seraient les deux éléments clés pour décontaminer les eaux des MPs/NPs a été partiellement confirmée. L'augmentation d'une surface d'anode de 41 à 83 cm^2 n'a pas eu un effet significatif sur le pourcentage d'élimination des MPs pour un même volume d'eau traité. Ce qui voudrait dire que les MPs ne sont pas dégradées seulement à la surface de l'anode mais aussi en solution par les oxydants qui y sont produits suggérant que les performances de dégradation seraient liées à la quantité totale et au type d'oxydant générés dans le réacteur et non à une plus grande surface des électrodes forcement. Par conséquent, la surface spécifique de l'électrode c'est-à-dire la surface utile de l'anode immergée (rapport surface/volume) et la présence des ions précurseurs des oxydants dans l'eau sont nécessaire au traitement des MPs par procédé OEC.

6.3. Dégradation électrochimique de nano-plastiques (NPs) de polystyrène : rôle des espèces oxygénées réactives (Chapitre 4)

Après avoir réussi à mettre au point le procédé d'OEC pour la dégradation de MPs de polystyrène, nous nous sommes attardés à élargir son spectre d'activités pour la dégradation des NPs. Il est important de souligner, ici, que la plupart des travaux antérieurs répertoriés dans la littérature portant sur le traitement de la pollution de l'eau par les plastiques se focalisent principalement sur les MPs. En revanche, un nombre limité de travaux portent sur le traitement de NPs. Dans la présente étude, nous nous sommes ainsi préoccupés à mettre en évidence le rôle des espèces oxygénées réactives (ex. :$^{\bullet}OH$, H_2O_2, $H_2S_2O_8$) dans le processus de dégradation NPs lors de l'électrolyse. Pour ce faire, deux approches de procédé d'oxydation électro-catalytique ont été testées : **i**) Le procédé d'électro-oxydation (EO) comprenant une anode de DDB et une cathode en titane (Ti); **ii**) Le procédé d'électro-peroxydation (EO-H_2O_2) comprenant une électrode anodique de DDB et une cathode de feutre de carbone (FC) permettant de générer *in situ* H_2O_2 par réduction cathodique de O_2 dissous. Il est important de rappeler, que les radicaux hydroxyles ($^{\bullet}OH$) sont générés exclusivement à la surface de DDB par décomposition homolytique de la molécule d'eau, alors que les persulfates ($H_2S_2O_8$) sont générés en solution suite à l'oxydation des ions sulfates sur l'électrode de DDB. La capacité du réacteur électrolytique à générer ces espèces oxygénées réactives a été évaluée en utilisant les deux approches de procédé d'oxydation électro-catalytique (EO et EO-H_2O_2) dans une eau synthétique sulfatée (0.03 et 0.07 M de Na_2SO_4) en l'absence de NPs. Différentes concentrations molaires de H_2O_2 (0.13 - 0.16 × 10^{-3} M), $^{\bullet}OH$ (0.39 - 1.11 × 10^{-5} M) et $H_2S_2O_8$ (0.4 - 0.65 × 10^{-3} M) ont été mesurées en fonction de la densité de courant se situant entre 36 et 108 mA.cm^{-2} et du temps d'électrolyse variant entre 20 et 60 min. Ainsi, au cours de l'application du procédé EO, les NPs sont principalement dégradés par $^{\bullet}OH$ et $SO_4^{\bullet-}$ (obtenu via l'oxydation de $S_2O_8^{2-}$ par $^{\bullet}OH$). En comparaison, dans le procédé EO-H_2O_2, en plus d'être dégradés par $^{\bullet}OH$ (obtenus par décomposition de H_2O_2), les NPs sont simultanément oxydés par $SO_4^{\bullet-}$ générés par la réaction directe et indirecte avec H_2O_2. L'hypothèse que l'EO-H_2O_2 permettrait de dégrader/minéraliser davantage les micro- et nano-plastiques par l'activation des persulfates en présence de H_2O_2 a été confirmé. L'analyse de la dégradation de NPs montre que le procédé EO-H_2O_2 est environ 2.6 fois plus efficace que le procédé EO. Ce résultat corrobore la revue de littérature. Le meilleur taux de dégradation de NPs (86,6 ± 1,8 %) a été obtenu en appliquant le procédé EO-H_2O_2 fonctionnant à une densité

de courant de 36 mA.cm^{-2} en présence de 0.03 Na_2SO_4, un pH initial et final d'environ de 6 et 2.5 respectivement et un temps d'électrolyse de 40 min. L'augmentation d'une concentration de 0.03 M à 0.06 M de Na_2SO_4 en appliquant l'EO-H_2O_2 n'a pas eu d'effet positif significatif sur la performance de dégradation des NPs. Cependant une baisse à 0.007 M a eu un impact négatif suggérant ainsi l'atteinte du meilleur ratio pour l'activation $S_2O_8^{2-}$/H_2O_2 avec une concentration de 0.03 M de Na_2SO_4. De plus l'effet seul des persulfates n'a présenté aucun effet sur l'efficacité de dégradation confirmant ainsi l'activation des persulfates en radicaux sulfates en présence de H_2O_2. L'analyse par spectrophotométrie 3D de fluorescence d'acquisition de matrices d'émission-excitation (3D-EEM) confirme la dégradation des NPs. Enfin, une évaluation économique incluant la consommation de l'énergie et de l'électrolyte a montré que le traitement des NPs par le procédé EO-H_2O_2 avait un coût d'opération de 2,3 $US.m^{-3}, soit environ 10 fois moins que le procédé EO. Cette étude a démontré que la génération in situ de ROS peut considérablement améliorer la dégradation des NP dans l'eau. Les résultats de cette partie des travaux ont fait l'objet d'un article publié dans la revue de calibre international Science of Total Environment.

6.4 Application au traitement des eaux réelles de buanderie contaminées par des nano-plastiques par un procédé d'électro-peroxydation (Chapitre 5)

Après avoir fait la preuve du concept de la dégradation électrolytique des MPs et NPs présents dans des effluents synthétiques (eaux polluées reconstituées), nous sommes attelés à tester la dégradation électro-catalytique des NPs dans les eaux usées réelles de buanderie. Rappelons, ici, que les eaux usées issues du lavage des vêtements dans les buanderies constituent l'une des sources potentielles de la pollution de l'environnement par les micro-plastiques. Il est à noter que plus de 80% de la pollution de l'environnement par les micro-plastiques provient des tissus synthétiques (35%), des pneux (28%) et des poussières urbaines (24%) (Statista, 2019). Les stations d'épuration des eaux (STEPs) ont des difficultés à les filtrer puisque 40% des micro- et nano-plastiques aboutissent dans les rivières, lacs et océans (Hou *et al.*, 2021; Talvitie *et al.*, 2015). Le traitement à la source des micro- et nano-plastiques, c'est-à-dire avant leur entrée dans l'environnement (ou avant leur rejet dans le réseau d'égout municipal), notamment à la sortie des buanderies, permettrait de limiter l'impact néfaste de ces rejets dans l'environnement.

Des essais ont donc été entrepris sur des échantillons d'eaux réelles issues de buanderie commerciale de la Ville de Québec. Ces eaux ont été initialement soumises à un prétraitement

par microfiltration en vue d'éliminer principalement les matières en suspension pour ainsi focaliser les forces d'oxydation sur les polluants plastiques principalement sous forme dissoute (< 0.001μm). Après prétraitement par microfiltration, ces eaux réelles ont été artificiellement contaminées par des microbilles fluorescentes de polystyrène de 150 nm de diamètre nominal (NPs) afin de simuler la présence des NPs. Le choix des caractéristiques fluorescentes des NPs permet de suivre et de quantifier les concentrations résiduelles de nano-plastiques en présence d'autres composés organiques et inorganiques dissous initialement décelés dans les réelles de buanderie (nonylphénol, métaux toxiques, chlorure, sulfate, COT, etc.).

Le procédé d'oxydation électro-catalytique a premièrement été appliqué en utilisant les meilleures conditions déterminées lors de la dégradation des NPs dans les effluents synthétiques. Un réacteur électrolytique de forme parallélépipédique (configuration EO-H_2O_2) composé d'une électrode anodique de DDB et de deux électrodes cathodiques de feutre de carbone a été utilisé. Le réacteur a pour dimension 14.5 cm de longueur, 6.4 cm de largueur et 17.7 cm de hauteur, pour un volume utile de 800 mL. Il est en plexiglas perforé à 2 cm dans sa partie inférieure et comporte une fenêtre dans sa partie supérieure. Il comportait un bac en plexiglas d'un volume de 500 mL afin de permettre la recirculation de l'eau d'un volume total de 1000 ml à traiter en mode continu à l'aide d'une pompe péristaltique fonctionnant à une vitesse constante de 400 $mL.min^{-1}$. Trois prélèvements d'eaux usées présentant une concentration de COT initial de 16.3, 29.4 et 52.2 mg/L ont été testés. L'hypothèse que le traitement des effluents avec préfiltration permettrait alors aux oxydants de dégrader et de minéraliser efficacement les nano-plastiques y comprise la fraction dissoute de polluants de base des eaux usées de buanderie a été confirmée. Les résultats ont montré une élimination complète des NPs après 50 min de traitement pour les eaux usées ayant une concentration de COT comprise entre 16 et 30 mg/L. Cependant, l'efficacité d'élimination était près de 87 % pour l'eau synthétique et l'eau usée contenant un COT initial relativement élevé de 52 mg/L indiquant que la présence des ions Cl^- (145-160 mg/L) initialement présents dans les effluents de buanderie ont pu s'oxyder à la surface de l'anode de DDB en acide hypochloreux contribuant ainsi à davantage oxyder les NPs. Par contre, une charge en matière organique dissoute relativement élevée (COT = 52.2 mg/L) est une limite à l'efficacité et à la robustesse du procédé d'OEC pour la dégradation des NPs. Une élimination relativement faible et variant entre 51,5 ± 3,31 % et 56,6 ± 3,7 de COT a été enregistrés pour les effluents réels après 1h de traitement. Les spectres 3D de fluorescence d'acquisition de matrices d'émission-excitation des échantillons avant et après traitement, ont indiqué un abattement presque total de

l'intensité des fluorophores associés aux composés aromatiques issus des polluants initiaux et des particules de polystyrène après 40 et 60 min de traitement. Les nano-plastiques ont bel et bien été totalement dégradés dans les eaux usées réelles de buanderie.

Subséquemment, un plan Plan Central Composite (PCC)) a été employé pour déterminer les conditions optimales de dégradation des NPs dans les eaux réelles. Quatre facteurs indépendants ont été testés : i) densité de courant (12.05 – 36.12 mA/cm^2) ; ii) concentration en électrolyte (0.004 – 0.030 M); iii) temps d'électrolyses (20 – 60 min) et; iv) charge de la matière organique (faiblement chargée (16 mg/L de COT) et relativement élevée (52 mg/L de COT). Les critères retenus pour les conditions d'optimisation du traitement électrochimique des eaux usées de buanderie sont les suivants : (a) L'efficacité d'élimination de NPs et du carbone organique total doit être maximisée avec la plus haute importance correspondant aux meilleurs taux de dégradation enregistrés au niveau des tests préliminaires (87 $\pm$ 3 % pour les NPs et 47 $\pm$ 7 % pour le COT après 50 min de traitement) et (b) la consommation d'énergie doit être minimisée avec une importance moindre (la consommation énergétique pour les tests préliminaires = 46 $\pm$ 1 KWh.m^{-3}) afin de réduire le coût de traitement lié à la consommation d'énergie. La température initiale des eaux était comprise entre 13 et 14 º C. Ainsi, la meilleure solution proposée par le logiciel (Design-Expert software version 13, Stat-Ease Inc., USA) satisfaisant aux critères imposés consistait à imposer une densité de courant de 31.24 mA cm^{-2}, pendant 52 min du temps de traitement à une concentration en électrolyte de 0.025 mol L^{-1} et en fixant une charge en COT relativement faible (52.2 mg/L de COT). Un taux d'abattement de dégradation de NPs allant jusqu'à 81 $\pm$ 5 % et un taux d'enlèvement du COT de 43 $\pm$3 % pour une consommation énergétique de 33 $\pm$ 0.5 kWh.m^{-3} ont été enregistrés dans ces conditions optimales. Aussi, l'application du traitement d'oxydation électro-catalytique a permis de réduire la toxicité (toxicité Aigüe, *D. magna*) de l'effluent brut artificiellement contaminés par des NPs. La toxicité est passée d'une valeur initiale de 5.1 UT (effluent brut) à une finale inférieure à 1UT (dans l'effluent électrolysé). Un article, portant sur la dégradation du NPs dans les eaux réelles de buanderie par le procédé d'OEC est en cours de préparation et est soumis dans la revue internationale Separation and Purification Technology.

6.5 Conclusion générale

Le plastique est utilisé au quotidien dans de nombreux secteurs tels que l'emballage alimentaire, le textile, la construction, la cosmétique etc. Cependant, la mauvaise gestion des déchets plastiques, l'abrasion des objets plastiques au cours de leur fabrication, utilisation et entretien induit la formation de débris de plastique de toute taille visible et invisible a l'œil nu dans les eaux. Il faut noter par ailleurs que des particules de plastique de taille micro et nanométrique sont volontairement ajoutées à des produits cosmétiques. Après utilisation de ces produits cosmétiques ces micro- et nano-plastiques se retrouvent également dans les eaux usées.

Plusieurs études ont permis de mettre en évidence la présence de ces débris de plastiques dans tous les milieux aquatiques : Eaux douces, marines, usées, potables, a des concentrations, tailles, type de polymère très variés. Il ressort également de ces études que la majeure partie des particules micro- et nanométriques de plastique dans les eaux proviennent du lavage de textiles synthétiques et de l'abrasion des pneus sur les routes.

Une analyse de la littérature a permis de montrer la difficulté de traiter un milieu aqueux contaminé par les micro- et nano-plastiques grâce aux traitements conventionnels (biologique, chimique et/ou physico-chimique). Les technologies avancées de traitement permettent leur séparation efficace des eaux mais présente une limite quant aux particules sub-micrométriques. Aussi la séparation des micro- et nano-plastiques des eaux ne fait que déplacer ce problème de pollution. Pour faire face à cette situation, une alternative de traitement des eaux et eaux usées de buanderie contaminée par des micro- et nana-plastiques à l'aide de procédés d'oxydation électro-catalytique peut être examiné.

Cette étude a permis de développer et d'évaluer les performances épuratoires d'un procédé d'oxydation électro-catalytique combinant simultanément les réactions anodiques et de réduction cathodique pour la dégradation des micro-et-nano-plastiques (MPs et NPs). Ce procédé a été conçu pour le traitement à la source des MPs et NPs (avant leur entrée dans l'environnement), par exemple à la sortie des buanderies (un vecteur potentiel de contamination des eaux par les micro-plastiques).

Deux types de configurations de réacteurs électrolytiques (réacteur pour le procédé EO et réacteur pour le procédé EO-H_2O_2) ont été conçus et caractérisés en terme de leur capacité à générer des espèces oxygénées réactives telles que $HO^{\bullet}$, H_2O_2, $H_2S_2O_8$. Les réacteurs

fonctionnaient en mode galvano-statique. Après avoir caractérisés les réacteurs électrolytiques et après avoir mis au point les méthodes qualitative et quantitatives d'analyses des MPs et NPs, Le procédé d'oxydation électro-catalytique a été testé pour la dégradation à la source de ces polluants plastiques.

La présente étude a permis de développer et d'évaluer les performances épuratoires des procédés d'électro-oxydation et d'électro-peroxydation pour la dégradation de micro- et nano-plastiques de polystyrène dans des effluents synthétiques et des eaux usées réelles d'une buanderie commerciale de la ville de Québec.

L'étude menée sur les eaux synthétiques artificiellement contaminées par MPs et NPs a fait ressortir les points pertinents suivants :

- Un réacteur composé d'une anode à forte surtension en oxygène telle que l'anode de niobum recouvert de diamant dopé au bore (DDB) assure une meilleure dégradation des micro-plastiques de 25 µm et des nano-plastiques de 100 nm de diamètre nominal.

- La densité du courant, le matériau de l'anode, le type d'électrolyte et la concentration d'électrolyte ont un impact positif sur la dégradation des MPs, tandis que la surface de l'anode a un effet négligeable sur l'efficacité du procédé EO.

- Le meilleur taux de dégradation (58 $\pm$ 21%) de micro-plastique (C0 = 100 mg/L) a été enregistré après 1 h de traitement en imposant une densité de courant de 108 $mA.cm^{-2}$, une concentration de 0.06 M de Na_2SO_4 et un pH = 6 pour le procédé d'EO. Par contre un taux de dégradation de 86.8% a été enregistré pour les nano-plastiques (C0 = 10 mg/L) pour l'EO-H_2O_2 en imposant une densité de courant de 36 $mA.cm^{-2}$, une concentration de 0.03 M de Na_2SO_4 après 40 min de traitement pour le procédé EO-H_2O_2. Le pH avait baissé de 6 à 2 après traitement.

- Les réactions anodiques sur l'électrode de DDB permettent la production de $^{\bullet}OH$ et de $S_2O_8^{2-}$ par oxydation respective de la molécule d'eau et des ions sulfates avec des concentrations de $^{\bullet}OH$ allant de 0.39 à 1.11 × 10^{-5} M et de $S_2O_8^{2-}$ (0.4 - 0.65 × 10^{-3} M).

- Les réactions cathodiques sur deux pièces électrodes en feutre de carbone permettent la production de H_2O_2 par réduction cathodique de l'oxygène dissous, avec des concentrations en H_2O_2 allant de 0.13 à 0.16 × 10^{-3} M. Sous irradiation UV, la scission hémolytique de H_2O_2 n'a pas eu d'impact positif sur l'efficacité de dégradation du procédé EO-H_2O_2 dans nos conditions opératoires.

- La présence de H_2O_2 permet l'activation des persulfates en radicaux sulfates qui a un impact positif sur l'efficacité de dégradation du procédé EO-H_2O_2. Cependant une augmentation de la concentration de persulfates électro-générés sans une augmentation du H_2O_2 n'a pas entrainé une augmentation de l'efficacité du procédé.

La partie de cette étude portant sur la dégradation de nano-plastiques de polystyrène par procédé électro-peroxydation dans les eaux usées réelles de buanderie a fait ressortir les points suivants :

- Un plan central composite a été employé dans l'optique de déterminer les conditions optimales de dégradation du NPs. L'imposition d'une densité de courant de 31.24 mA cm^{-2} pendant 52 min du temps de traitement à une concentration en électrolyte de 0.025 mol L^{-1} et en fixant une charge initiale en COT relativement faible (52.2 mg/L de COT) a été retenue comme conditions optimales en termes de coût et d'efficacité. Dans ces conditions, un taux dégradation allant jusqu'à 81 ± 5% NPs a été enregistré pour un coût total de 3.05 $ m^{-3} (incluant seulement les coûts d'énergie et d'électrolyte). Un taux de minéralisation de de la matière organique 43 $\pm$ 3 % d'élimination du COT a été enregistrée dans les conditions optimales. Une fraction non négligeable de la matière organique dans les eaux réelles a été transformé en des sous-produits durant l'application du procédé d'oxydation électro-catalytique

  - La rapidité de dégradation des fluorophores associés aux différents types de composés dans les eaux usées suit l'ordre suivant : les composés assimilés aux acides humiques suivis des composés assimilées aux protéines et enfin les composés assimilés aux acides fulviques.

- Par ailleurs, un taux d'abattement de 100% de la toxicité de l'effluent brut a été enregistré suite à l'application du procédé électro-catalytique.

L'effort déployé au cours de cette étude a permis de montrer que le procédé EO-H_2O_2 pourrait être utilisé efficacement comme traitement tertiaire pour l'élimination des NPs dans les eaux et effluents résiduaires des buanderies. Selon la charge initiale en polluant de base des effluents considérés, une filtration grossière ou une coagulation pourrait être appliquée au préalable afin d'éliminer les plus grosses particules et les matières colloïdales en suspension. Une consommation énergétique relativement élevée (33 ±0.3 $kWh.m^{-3}$) a été enregistrée pour une température initiale de traitement comprise entre 13 et 14 º C. Néanmoins, elle est comprise entre 16 et 100 $KWh.m^{-3}$ reportée dans la littérature comme ordre de grandeur de la consommation énergétique nécessaire pour un traitement efficace par oxydation électrochimique des effluents d'eau usées réelles (Garcia-Segura *et al.*, 2018). Le coût du procédé incluant la consommation énergétique et l'électrolyte est de 3.05 $\$.m^{-2}$. Le traitement préalable de microfiltration appliquée dans cette étude nécessiterait une consommation énergétique comprise entre 0.1 à 0.7 $KW\text{-}h.m^{-3}$. Une prise en compte de l'entretien (nettoyage, relargage) et de la durée de vie des électrodes est nécessaire pour une meilleure analyse des couts d'opération. Certes, un traitement des MPs/NPs au niveau des buanderies induirait des couts d'investissement et d'opération non négligeable. Mais au vu de l'ampleur du problème des MPs/NPs et du défi de leur élimination dans les stations de traitement d'eau usées nous recommandons de continuer les travaux de développement technologique. Il faudra diriger ces travaux vers une réduction encore plus de la consommation énergétique et augmentation du traitement globale en améliorant la configuration du réacteur (transport de masse), en testant l'électrode de Ti_4O_7 et en le combinant avec une cathode TiO_2/graphite, et développant d'autre type d'électrodes plus puissants en terme de production d'oxydants. Certes, les travaux de cette thèse ont démontré la faisabilité de la dégradation des MPs/NPs par oxydation électro-catalytique, mais certains aspects du développement de la technologie réduisent la portée de cette étude.

❖ Les limites de l'étude

L'étude réalisée comporte quelques limites évoquées ci-dessous :

- Des microbilles de polystyrène ont seulement été considérées comme source de MPs et NPs et ont été utilisées séparément dans cette étude. Vu que les MPs/NPs sont de différents types de polymère dans les eaux et que les microfibres de polyéthylène téréphtalate sont les plus abondants dans les eaux de lavage des habits. Et ce, dû à l'abrasion des fibres textiles, il aurait été souhaitable d'utiliser des microfibres de polyester pour mieux évaluer la faisabilité du procédé OEC.

- Les méthodologies d'analyse permettaient seulement la quantification des MPs et NPs de polystyrène, et ce d'une façon séparée. Donc, on méconnait si un mélange de MPs et NPs de différents formes et polymères influencerait la dégradation par procédé OEC.

- Les eaux ont été artificiellement contaminées par les MPs/NPs à des concentrations définies selon les limites analytiques. Compte tenu des faibles masses des MPs et NPs, il est requis une concentration préalable des particules par séparation avant l'application du traitement électrochimique. Ceci permettrait une augmentation de l'efficacité énergétique.

- L'identification et le suivi de la formation des sous-produits durant la dégradation par OEC du polystyrène dans l'eau synthétique ou dans effluent réel n'ont pas été réalisés.

- Une analyse technico-économique incluant les couts d'investissement et tous les couts opératoires n'a pas été réalisée. De ce fait, on ne connait pas le coût total de traitement en dollars canadiens par mètre cube ($\$.m^{-3}$) d'effluents de buanderie.

6.6 Recommandations

Ce travail a permis de montrer l'efficacité du procédé d'OEC pour le traitement à la source des MPs et NPs de polystyrène. Cependant, il serait important d'effectuer des travaux supplémentaires dans le but d'améliorer davantage ce procédé et développer son domaine d'application :

- Mettre au point la technique analytique de la microscopie a fluorescence pour suivre l'élimination des micro- et nano-plastiques en présence d'autres polluants organiques comme l'acide humique.
- Étudier la dégradation des MPs de diamètre nominale supérieure ou égale à 25 µm et d'autres polymères dans les effluents synthétiques.
- Tester l'efficacité du procédé d'oxydation électro-catalytique pour le traitement d'une eau usée contenant un mélange de micro- et nano-plastique à savoir le polystyrène, le polyéthylène, le polyéthylène téréphtalate, polypropylène et les additifs fréquemment ajoutés dans la fabrication des objets plastiques. Cette étude permettra de montrer si l'efficacité du procédé est liée à la structure des polymères et à la taille des particules.
- Identifier et étudier la toxicité des sous-produits de dégradation des MPs/NPs formés au cours du traitement électrochimique dans des matrices aqueuses par bio essais.
- Développer une approche de traitement combinant la concentration des MPs/NPs par un procédé de séparation et l'application de la technologie d'oxydation électro-catalytique pour le traitement des eaux usées issues d'autres buanderie avec une charge organique plus élevée (> 52 mg/L)
- Réaliser une étude économique incluant les couts et durée de vie des électrodes du procédé d'oxydation électro-catalytique.

APPENDIX I: SUPPLEMENTARY INFORMATION FOR CHAPTER 5

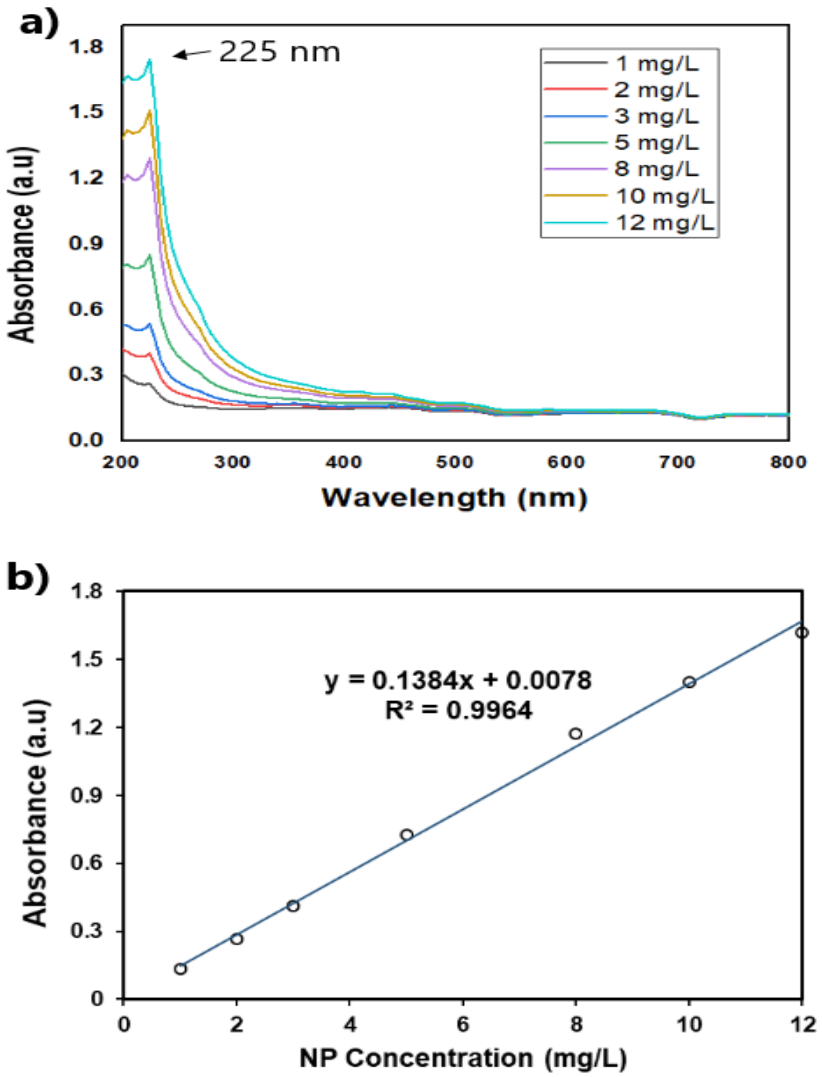

Figure AI. 1 : UV-Vis absorption spectra of NPs as a function of NP concentration. (a) absorption at different wavelengths, (b) calibration curve at 225 nm vs NP concentration.

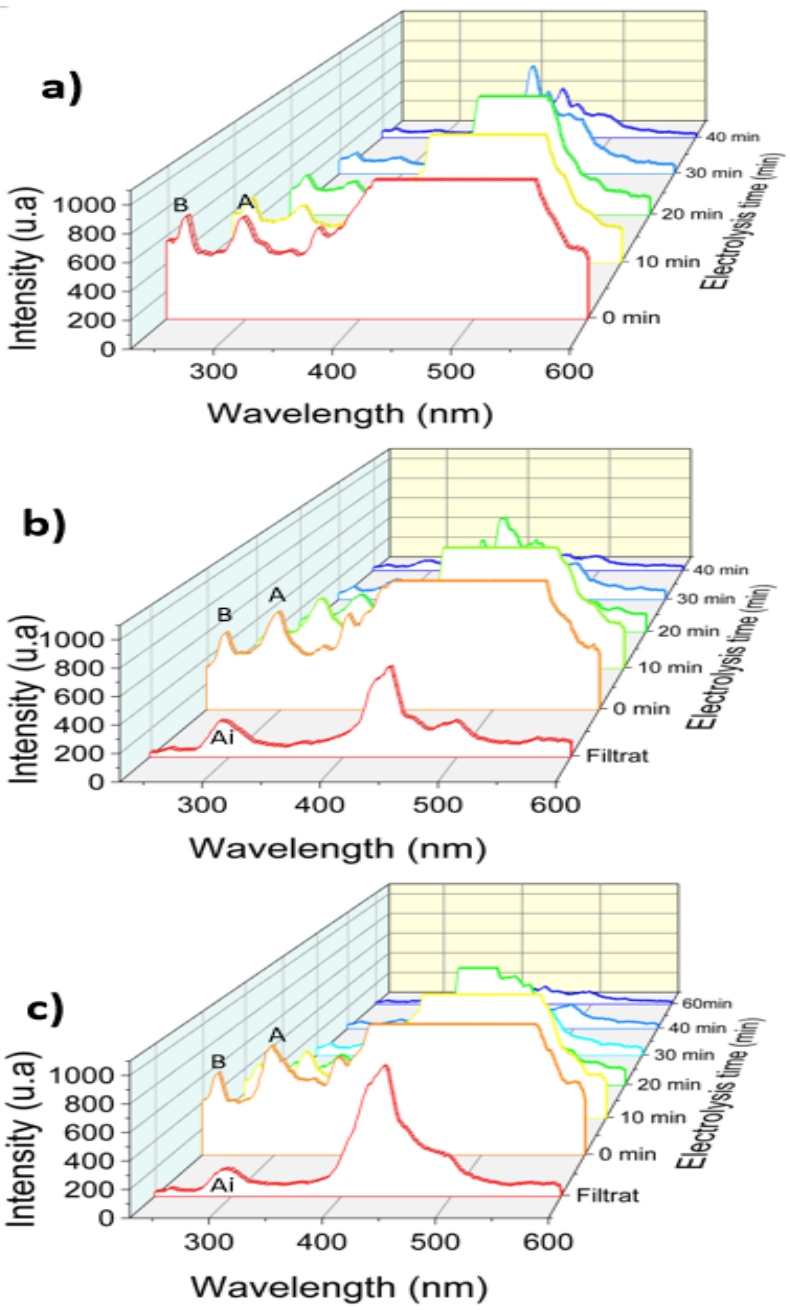

Figure AI. 2 : Peak intensity as a function of wavelength and electrolysis time at excitation of 215 nm. (a) NP-SW, (b) NP- S1, (c) NP- S2.

Tableau AI. 1 : Fluorescence spectra parameters of dissolved organic matter from NPs synthetic water and LWW NP spiked during the electro-peroxidation treatment at 215 nm excitation.

Samples	Fluorophores intensity (FI)			
Peaks	A (Em 300 nm)	B (Ex 250 nm)	Spot (Em 380-600 nm)	Spot/A
NP-SW				
t0	701	674	894	1.28
t20	243	300	581	2.39
t40	57	69	156	2.74
NP-S1 (10 mg/L)				
t0	730	575	900	1.23
t20	303	188	467	1.54
t40	92	47	91	0.99
NP-S2 (10 mg/L)				
t0	797	514	916	1.15
t20	229	169	555	2.42
t40	67	49	150	2.24

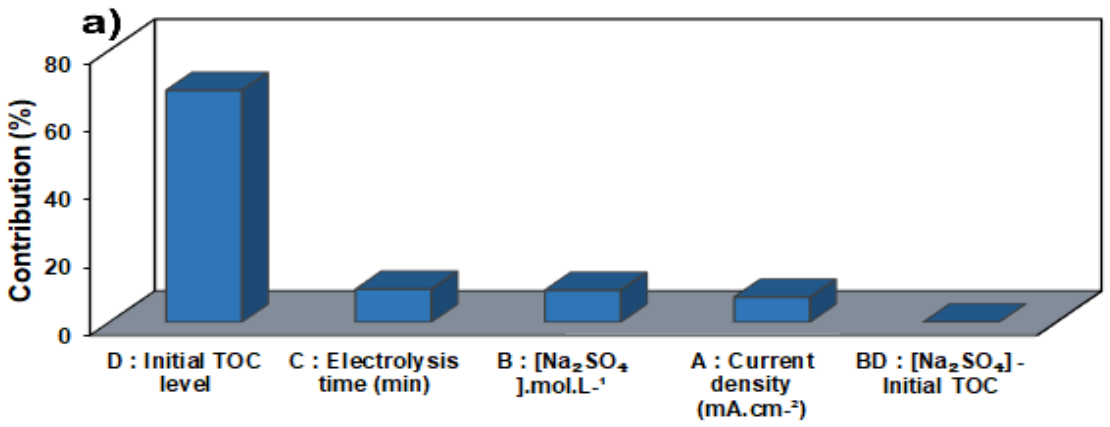

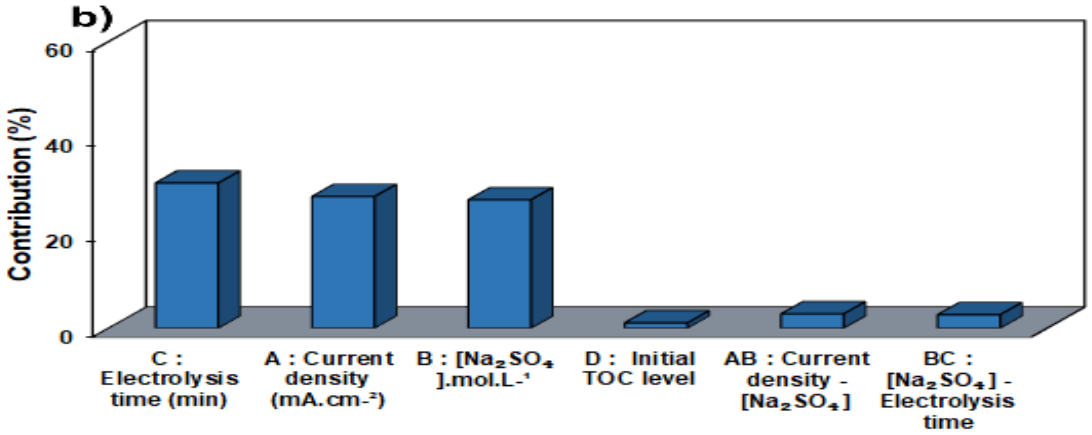

Figure AI. 3. Graphical Pareto analysis of the effect of current density, Na_2SO_4 concentration, electrolysis time, and initial TOC level on the removal of NP and TOC from LWW

REFERENCES

Acharya S, Rumi SS, Hu Y & Abidi N (2021) Microfibers from synthetic textiles as a major source of microplastics in the environment: A review. *Textile Research Journal* 91(17-18):2136-2156.

Ali MI, Ahmed S, Robson G, Javed I, Ali N, Atiq N & Hameed A (2014) Isolation and molecular characterization of polyvinyl chloride (PVC) plastic degrading fungal isolates. *J Basic Microbiol* 54(1):18-27.

Allé PH, Garcia-Muñoz P, Adouby K, Keller N & Robert D (2020) Efficient photocatalytic mineralization of polymethylmethacrylate and polystyrene nanoplastics by TiO_2/β-SiC alveolar foams. *Environmental Chemistry Letters* 10.1007/s10311-020-01099-2.

Almutairi MM, Gong C, Xu YG, Chang Y & Shi H (2016) Factors controlling permeability of the blood-brain barrier. *Cell Mol Life Sci* 73(1):57-77.

Alves SA, Ferreira TCR, Migliorini FL, Baldan MR, Ferreira NG & Lanza MRV (2013) Electrochemical degradation of the insecticide methyl parathion using a boron-doped diamond film anode. *J. Electroanal. Chem.* 702:1-7.

Amer Y (2019) "Electrochemical oxidation treatment of pesticide-laden agricultural releases,"thesis presented to Toulouse University 3 Paul Sabatier, for the degree of Doctor of Philosophy.

Andrady AL & Neal MA (2009) Applications and societal benefits of plastics. *Philos Trans R Soc Lond B Biol Sci* 364(1526):1977-1984.

Andrady AL & Rajapakse N (2017) Additives and Chemicals in Plastics. *Hazardous Chemicals Associated with Plastics in the Marine Environment*, Takada H & Karapanagioti HK (Édit.) Springer International Publishing, Cham10.1007/698_2016_124. p 1-17.

Anglada A, Urtiaga A & Ortiz I (2009) Contributions of electrochemical oxidation to waste-water treatment: fundamentals and review of applications. *Journal of Chemical Technology & Biotechnology* 84(12):1747-1755.

Araujo CF, Nolasco MM, Ribeiro AMP & Ribeiro-Claro PJA (2018) Identification of microplastics using Raman spectroscopy: Latest developments and future prospects. *Water Res* 142:426-440.

Ariza-Tarazona MC, Villarreal-Chiu JF, Barbieri V, Siligardi C & Cedillo-González EI (2019) New strategy for microplastic degradation: Green photocatalysis using a protein-based porous N-TiO_2 semiconductor. *Ceram. Int.* 45(7):9618-9624.

Avio CG, Gorbi S, Milan M, Benedetti M, Fattorini D, d'Errico G, Pauletto M, Bargelloni L & Regoli F (2015) Pollutants bioavailability and toxicological risk from microplastics to marine mussels. *Environ Pollut* 198:211-222.

Badellino C, Rodrigues CA & Bertazzoli R (2006) Oxidation of pesticides by in situ electrogenerated hydrogen peroxide: study for the degradation of 2,4-dichlorophenoxyacetic acid. *J. Hazard. Mater.* 137(2):856-864.

Bañuelos JA, García-Rodríguez O, El-Ghenymy A, Rodríguez-Valadez FJ, Godínez LA & Brillas E (2016) Advanced oxidation treatment of malachite green dye using a low cost carbon-felt air-diffusion cathode. *Journal of Environmental Chemical Engineering* 4(2):2066-2075.

Barreto JPdP, Araujo KCdF, de Araujo DM & Martinez-Huitle CA (2015) Effect of sp3/sp2 Ratio on Boron Doped Diamond Films for Producing Persulfate. *ECS Electrochemistry Letters* 4(12):E9-E11.

Batool A & Valiyaveettil S (2020) Coprecipitation—An Efficient Method for Removal of Polymer Nanoparticles from Water. *ACS Sustainable Chemistry & Engineering* 8(35):13481-13487.

Bayo J, Lopez-Castellanos J & Olmos S (2020) Membrane bioreactor and rapid sand filtration for the removal of microplastics in an urban wastewater treatment plant. *Mar Pollut Bull* 156:111211.

Bebelis S, Bouzek K, Cornell A, Ferreira MGS, Kelsall GH, Lapicque F, Ponce de León C, Rodrigo MA & Walsh FC (2013) Highlights during the development of electrochemical engineering. *Chem. Eng. Res. Des.* 91(10):1998-2020.

Beltran FJ, 2 GO & Acedo B (1993) Oxidation of atrazine in water by ultraviolet radiation combined with hydrogen peroxide. *War. Res. "Col. 27, No. 6, pp. 1013-1021, 1993* Col. 27, No. 6:1013-1021.

Bergami E, Bocci E, Vannuccini ML, Monopoli M, Salvati A, Dawson KA & Corsi I (2016) Nano-sized polystyrene affects feeding, behavior and physiology of brine shrimp Artemia franciscana larvae. *Ecotoxicol Environ Saf* 123:18-25.

Besseling E, Wang B, Lurling M & Koelmans AA (2014) Nanoplastic affects growth of S. obliquus and reproduction of D. magna. *Environ Sci Technol* 48(20):12336-12343.

Bhuta H (2014) Advanced treatment technology and strategy for water and wastewater management. *Industrial Wastewater Treatment, Recycling and Reuse, 1st ed.; Ranade, VV, Bhandari, VM, Eds* :193-213.

Bianco A, Sordello F, Ehn M, Vione D & Passananti M (2020) Degradation of nanoplastics in the environment: Reactivity and impact on atmospheric and surface waters. *Sci Total Environ* 742:140413.

Borràs N, Arias C, Oliver R & Brillas E (2013) Anodic oxidation, electro-Fenton and photoelectro-Fenton degradation of cyanazine using a boron-doped diamond anode and an oxygen-diffusion cathode. *J. Electroanal. Chem.* 689:158-167.

Boucher J & Friot D (2020) Microplastiques primaires dans les océans : évaluation mondiale des sources. *Gland, Suisse : UICN.* :44.

Brillas E, Banos MA, Skoumal M, Cabot PL, Garrido JA & Rodriguez RM (2007) Degradation of the herbicide 2,4-DP by anodic oxidation, electro-Fenton and photoelectro-Fenton using platinum and boron-doped diamond anodes. *Chemosphere* 68(2):199-209.

Brillas E, Boye B, Sirés I, Garrido JA, Rodríguez RMa, Arias C, Cabot P-Ls & Comninellis C (2004) Electrochemical destruction of chlorophenoxy herbicides by anodic oxidation and electro-Fenton using a boron-doped diamond electrode. *Electrochim. Acta* 49(25):4487-4496.

Brillas E, Sire´s I & Oturan MA (2009) Electro-Fenton Process and Related Electrochemical Technologies based on Fenton's Reaction Chemistry. *Chem. Rev.* 109:6570–6631.

Browne MA, Crump P, Niven SJ, Teuten E, Tonkin A, Galloway T & Thompson R (2011a) Accumulation of microplastic on shorelines woldwide: sources and sinks. *Environ Sci Technol* 45(21):9175-9179.

Browne MA, Crump P, Niven SJ, Teuten E, Tonkin A, Galloway T & Thompson R (2011b) Accumulation of microplastic on shorelines woldwide: sources and sinks. *Environ. Sci. Technol.* 45(21):9175-9179.

Buxton GV, Greenstock CL, Helman WP & Ross AB (1988) Critical Review of rate constants for reactions of hydrated electrons, hydrogen atoms and hydroxyl radicals (·OH/·O− in Aqueous Solution. *J. Phys. Chem. Ref. Data* 17(2):513-886.

Cai H, Xu EG, Du F, Li R, Liu J & Shi H (2021) Analysis of environmental nanoplastics: Progress and challenges. *Chem. Eng. J.* 410.

Cai J, Zhou M, Liu Y, Savall A & Groenen Serrano K (2018a) Indirect electrochemical oxidation of 2,4-dichlorophenoxyacetic acid using electrochemically-generated persulfate. *Chemosphere* 204:163-169.

Cai L, Wang J, Peng J, Wu Z & Tan X (2018b) Observation of the degradation of three types of plastic pellets exposed to UV irradiation in three different environments. *Sci Total Environ* 628-629:740-747.

Cai L, Wang J, Peng J, Wu Z & Tan X (2018c) Observation of the degradation of three types of plastic pellets exposed to UV irradiation in three different environments. *Sci Total Environ* 628-629:740-747.

Campanale C, Dierkes G, Massarelli C, Bagnuolo G & Uricchio VF (2020) A Relevant Screening of Organic Contaminants Present on Freshwater and Pre-Production Microplastics. *Toxics* 8(4).

Canizares P, A. Gadri JL, Lobato J, Lobato J, Nasr B, Paz R, Rodrigo MA & Sae C (2006) Electrochemical Oxidation of Azoic Dyes with Conductive-Diamond Anodes. *Ind. Eng. Chem. Res.* 45:3468-3473.

Canizares P, Lobato J, Paz R, Rodrigo MA & Saez C (2005) Electrochemical oxidation of phenolic wastes with boron-doped diamond anodes. *Water Res* 39(12):2687-2703.

Carr SA, Liu J & Tesoro AG (2016) Transport and fate of microplastic particles in wastewater treatment plants. *Water Res* 91:174-182.

Cedervall T, Hansson LA, Lard M, Frohm B & Linse S (2012) Food chain transport of nanoparticles affects behaviour and fat metabolism in fish. *PLoS ONE* 7(2):e32254.

Chae Y & An YJ (2017a) Effects of micro- and nanoplastics on aquatic ecosystems: Current research trends and perspectives. *Mar Pollut Bull* 124(2):624-632.

Chae Y & An YJ (2017b) Effects of micro- and nanoplastics on aquatic ecosystems: Current research trends and perspectives. *Mar Pollut Bull* 124(2):624-632.

Chen CS, Anaya JM, Zhang S, Spurgin J, Chuang CY, Xu C, Miao AJ, Chen EY, Schwehr KA, Jiang Y, Quigg A, Santschi PH & Chin WC (2011) Effects of engineered nanoparticles on the assembly of exopolymeric substances from phytoplankton. *PLoS ONE* 6(7):e21865.

Chen G (2004) Electrochemical technologies in wastewater treatment. *Sep. Purif. Technol.* 38(1):11-41.

Chen W, He C, Gu Z, Wang F & Li Q (2020a) Molecular-level insights into the transformation mechanism for refractory organics in landfill leachate when using a combined semi-

aerobic aged refuse biofilter and chemical oxidation process. *Sci Total Environ* 741:140502.

Chen W, Westerhoff P, LEenheer JA & Booksh K (2003) Fluorescence excitation-emission matrix regional integration to quantify spectra for dissolved organic Matter. *Environ. Sci. Technol.* 37:5701-5710.

Chen Y-J, Chen Y, Miao C, Wang Y-R, Gao G-K, Yang R-X, Zhu H-J, Wang J-H, Li S-L & Lan Y-Q (2020b) Metal–organic framework-based foams for efficient microplastics removal. *J Mater Chem A* 8(29):14644-14652.

Chen Z, Huang Z, Liu J, Wu E, Zheng Q & Cui L (2020c) Phase transition of Mg/Al-flocs to Mg/Al-layered double hydroxides during flocculation and polystyrene nanoplastics removal. *J Hazard Mater* https://doi.org/10.1016/j.jhazmat.2020.124697:124697.

Chen Z, Huang Z, Liu J, Wu E, Zheng Q & Cui L (2021) Phase transition of Mg/Al-flocs to Mg/Al-layered double hydroxides during flocculation and polystyrene nanoplastics removal. *J. Hazard. Mater.* 406:124697.

Chen Z, Liu J, Chen C & Huang Z (2020d) Sedimentation of nanoplastics from water with Ca/Al dual flocculants: Characterization, interface reaction, effects of pH and ion ratios. *Chemosphere* 252:126450.

Chu W, Wang YR & Leung HF (2011) Synergy of sulfate and hydroxyl radicals in UV/$S_2O_8^{2-}$/H_2O_2 oxidation of iodinated X-ray contrast medium iopromide. *Chem. Eng. J.* 178:154-160.

Ciríaco L, Anjo C, Correia J, Pacheco MJ & Lopes A (2009) Electrochemical degradation of Ibuprofen on Ti/Pt/PbO_2 and Si/BDD electrodes. *Electrochim. Acta* 54(5):1464-1472.

Claessens M, Van Cauwenberghe L, Vandegehuchte MB & Janssen CR (2013a) New techniques for the detection of microplastics in sediments and field collected organisms. *Mar Pollut Bull* 70(1-2):227-233.

Claessens M, Van Cauwenberghe L, Vandegehuchte MB & Janssen CR (2013b) New techniques for the detection of microplastics in sediments and field collected organisms. *Mar Pollut Bull* 70(1-2):227-233.

Coble PG (1996) Characterization of marine and terrestrial DOM in seawater using excitation-emission matrix spectroscopy. *Marine Chemistry 51* 51:325-346.

Cole M & Galloway TS (2015a) Ingestion of Nanoplastics and Microplastics by Pacific Oyster Larvae. *Environ Sci Technol* 49(24):14625-14632.

Cole M & Galloway TS (2015b) Ingestion of Nanoplastics and Microplastics by Pacific Oyster Larvae. *Environ Sci Technol* 49(24):14625-14632.

Cole M, Lindeque P, Halsband C & Galloway TS (2011) Microplastics as contaminants in the marine environment: a review. *Mar Pollut Bull* 62(12):2588-2597.

Cole M, Webb H, Lindeque PK, Fileman ES, Halsband C & Galloway TS (2014) Isolation of microplastics in biota-rich seawater samples and marine organisms. *Sci Rep* 4:4528.

Comninellis C (1994) Electrochemical Oxidation of Organic Pollutants for Wastewater Treatment. *Environmental Oriented Electrochemistry,* (Studies in Environmental Science: 10.1016/s0166-1116(08)70548-x. p 77-102.

Comninellis C & Chen G (2010) Electrochemistry for the Environment. *Springer New York Dordrecht Heidelberg London*.

Cook A, Devine B, Rodriguez C, Roser D, Khan S, McGuinness N, Ashbolt N & Weinstein P (2009) Assessing the public health impacts of recycled water use. Interim report 1. *Government of Western Australia Department of Water, Western Australia Premier's Water Foundation*.

Cooper DA & Corcoran PL (2010a) Effects of mechanical and chemical processes on the degradation of plastic beach debris on the island of Kauai, Hawaii. *Mar Pollut Bull* 60(5):650-654.

Cooper DA & Corcoran PL (2010b) Effects of mechanical and chemical processes on the degradation of plastic beach debris on the island of Kauai, Hawaii. *Mar Pollut Bull* 60(5):650-654.

Cotillas S, Llanos J, Rodrigo MA & Cañizares P (2015) Use of carbon felt cathodes for the electrochemical reclamation of urban treated wastewaters. *Applied Catalysis B: Environmental* 162:252-259.

Cozar A, Sanz-Martin M, Marti E, Gonzalez-Gordillo JI, Ubeda B, Galvez JA, Irigoien X & Duarte CM (2015) Plastic accumulation in the Mediterranean sea. *PLoS ONE* 10(4):e0121762.

D. Gandini, E. Mahe, P.A. Michaud, W. Haenni, A. Perret & Comninellis C (2000) Oxidation of carboxylic acids at boron-doped diamond electrodes for wastewater treatment. *J. Appl. Electrochem.* 30:1345-1350.

da Costa JP, Santos PSM, Duarte AC & Rocha-Santos T (2016) (Nano)plastics in the environment - Sources, fates and effects. *Sci Total Environ* 566-567:15-26.

Daghrir R, Drogui P & El Khakani MA (2013a) Photoelectrocatalytic oxidation of chlortetracycline using Ti/TiO2 photo-anode with simultaneous H2O2 production. *Electrochim. Acta* 87:18-31.

Daghrir R, Drogui P, Ka I, El Khakani MA & Robert D (2013b) Photoelectrocatalytic bleaching of p-nitrosodimethylaniline using Ti/TiO2 nanostructured electrodes deposited by means of a pulsed laser deposition process. *J. Appl. Electrochem.* 43(4):467-479.

Daghrir R, Drogui P, Tshibangu J, Delegan N & El Khakani MA (2014) Electrochemical treatment of domestic wastewater using boron-doped diamond and nanostructured amorphous carbon electrodes. *Environ Sci Pollut Res Int* 21(10):6578-6589.

Daghrir R[a, 1], Drogui P, Dimboukou-Mpira A & El Khakani MA (2013c) Photoelectrocatalytic degradation of carbamazepine using Ti/TiO_2 nanostructured electrodes deposited by means of a pulsed laser deposition process. *Chemosphere* 93(11):2756-2766.

Davis J, Baygents JC & Farrell J (2014) Understanding Persulfate Production at Boron Doped Diamond Film Anodes. *Electrochim. Acta* 150:68-74.

De Villiers S (2019) Short communication: Microfibre pollution hotspots in river sediments adjacent to South Africa's coastline. *Water SA* 45(1 January).

Debik E, Ulucan-Altuntas K & El Hadki A (2020) Bisphenol A Removal by Graphene Oxide Applied in Different Processes. *J. Eng. Technol. Sci* 52(3).

Dekiff JH, Remy D, Klasmeier J & Fries E (2014) Occurrence and spatial distribution of microplastics in sediments from Norderney. *Environ Pollut* 186:248-256.

Della Torre C, Bergami E, Salvati A, Faleri C, Cirino P, Dawson KA & Corsi I (2014) Accumulation and embryotoxicity of polystyrene nanoparticles at early stage of development of sea urchin embryos Paracentrotus lividus. *Environ Sci Technol* 48(20):12302-12311.

Deng H, Wei R, Luo W, Hu L, Li B & Shi H (2020) Microplastic pollution in water and sediment in a textile industrial area. *Environ Pollut* 258:113658.

Deng Y & Ezyske CM (2011) Sulfate radical-advanced oxidation process (SR-AOP) for simultaneous removal of refractory organic contaminants and ammonia in landfill leachate. *Water Res* 45(18):6189-6194.

Deng Y & Zhao R (2015) Advanced Oxidation Processes (AOPs) in Wastewater Treatment. *Current Pollution Reports* 1(3):167-176.

Di M & Wang J (2018a) Microplastics in surface waters and sediments of the Three Gorges Reservoir, China. *Sci Total Environ* 616-617:1620-1627.

Di M & Wang J (2018b) Microplastics in surface waters and sediments of the Three Gorges Reservoir, China. *Sci Total Environ* 616-617:1620-1627.

Dia O, Drogui P, Buelna G & Dubé R (2017) Strategical approach to prevent ammonia formation during electrocoagulation of landfill leachate obtained from a biofiltration process. *Separation and Purification Technology* 189:253-259.

Dia O, Drogui P, Dubé R & Buelna G (2016) Electrochemical processes using and their combinations with biological processes for the treatment of landfills leachate - a review. *Journal of Water Science* 29(1):63-89.

Divyapriya G & Nidheesh PV (2021) Electrochemically generated sulfate radicals by boron doped diamond and its environmental applications. *Curr. Opin. Solid State Mater. Sci.* 25(3).

Dominguez-Jaimes LP, Cedillo-Gonzalez EI, Luevano-Hipolito E, Acuna-Bedoya JD & Hernandez-Lopez JM (2021) Degradation of primary nanoplastics by photocatalysis using different anodized TiO_2 structures. *J. Hazard. Mater.* 413:125452.

Dong CD, Chen CW, Chen YC, Chen HH, Lee JS & Lin CH (2020) Polystyrene microplastic particles: In vitro pulmonary toxicity assessment. *J. Hazard. Mater.* 385:121575.

Dos Santos AJ, Brillas E, Cabot PL & Sires I (2020) Simultaneous persulfate activation by electrogenerated H_2O_2 and anodic oxidation at a boron-doped diamond anode for the treatment of dye solutions. *Sci Total Environ* 747:141541.

Dris R, Gasperi J, Rocher V, Saad M, Renault N & Tassin B (2015a) Microplastic contamination in an urban area: a case study in Greater Paris. *Environmental Chemistry* 12(5).

Dris R, Gasperi J, Rocher V, Saad M & Tassin B (2015b) Premières investigations sur la contamination en microplastiques d'une zone urbaine-Cas de l'agglomération parisienne. *Techniques Sciences Méthodes* (12):25-39.

Drogui P, Blais J-F & Mercier G (2007) Review of electrochemical technologies for environnement applications. *Recent patent of engineening* 1:257-272.

Dubaish F & Liebezeit G (2013) Suspended Microplastics and Black Carbon Particles in the Jade System, Southern North Sea. *Water, Air, & Soil Pollution* 224(2).

Duis K & Coors A (2016) Microplastics in the aquatic and terrestrial environment: sources (with a specific focus on personal care products), fate and effects. *Environ Sci Eur* 28(1):2.

Dumichen E, Eisentraut P, Bannick CG, Barthel AK, Senz R & Braun U (2017) Fast identification of microplastics in complex environmental samples by a thermal degradation method. *Chemosphere* 174:572-584.

Durán FE, de Araújo DM, do Nascimento Brito C, Santos EV, Ganiyu SO & Martínez-Huitle CA (2018) Electrochemical technology for the treatment of real washing machine effluent at pre-pilot plant scale by using active and non-active anodes. *J. Electroanal. Chem.* 818:216-222.

Dyachenko A, Mitchell J & Arsem N (2017) Extraction and identification of microplastic particles from secondary wastewater treatment plant (WWTP) effluent. *Analytical Methods* 9(9):1412-1418.

E. Weiss, K. Groenen-Serrano & Savall A (2006) Electrochemical Degradation of Sodium Dodecylbenzene Sulfonate on Boron Doped Diamond and Lead Dioxide Anode. *J. New Mater. Electrochem. Syst.* 9:249-256.

Eerkes-Medrano D, Leslie HA & Quinn B (2018) Microplastics in drinking water: A review and assessment. *Current Opinion in Environmental Science & Health* 7:69-75.

Ekvall MT, Lundqvist M, Kelpsiene E, Šileikis E, Gunnarsson SB & Cedervall T (2019) Nanoplastics formed during the mechanical breakdown of daily-use polystyrene products. *Nanoscale Advances* 1(3):1055-1061.

Elert AM, Becker R, Duemichen E, Eisentraut P, Falkenhagen J, Sturm H & Braun U (2017) Comparison of different methods for MP detection: What can we learn from them, and why asking the right question before measurements matters? *Environ Pollut* 231(Pt 2):1256-1264.

Elfgen R, Gehrke S & Hollóczki O (2020) Ionic Liquids as Extractants for Nanoplastics. *ChemSusChem* 13(20):5449-5459.

Elkhatib D & Oyanedel-Craver V (2020) A critical review of extraction and identification methods of microplastics in wastewater and drinking water. *Environ Sci Technol* 54(12):7037-7049.

Enfrin M, Dumee LF & Lee J (2019) Nano/microplastics in water and wastewater treatment processes - Origin, impact and potential solutions. *Water Res* 161:621-638.

Enfrin M, Lee J, Gibert Y, Basheer F, Kong L & Dumée LF (2020a) Release of hazardous nanoplastic contaminants due to microplastics fragmentation under shear stress forces. *Journal of hazardous materials* 384:121393.

Enfrin M, Lee J, Le-Clech P & Dumée LF (2020b) Kinetic and mechanistic aspects of ultrafiltration membrane fouling by nano-and microplastics. *J Membrane Sci* 601:117890.

Entezari MH & Kruus P (1994) Effect of frequency on sonochemical reactions. I: Oxidation of iodide. *Ultrason. Sonochem.* 1:75-79.

Eriksen M, Lebreton LC, Carson HS, Thiel M, Moore CJ, Borerro JC, Galgani F, Ryan PG & Reisser J (2014) Plastic Pollution in the World's Oceans: More than 5 Trillion Plastic Pieces Weighing over 250,000 Tons Afloat at Sea. *PLoS ONE* 9(12):e111913.

Eriksen M, Mason S, Wilson S, Box C, Zellers A, Edwards W, Farley H & Amato S (2013a) Microplastic pollution in the surface waters of the Laurentian Great Lakes. *Mar Pollut Bull* 77(1-2):177-182.

Eriksen M, Mason S, Wilson S, Box C, Zellers A, Edwards W, Farley H & Amato S (2013b) Microplastic pollution in the surface waters of the Laurentian Great Lakes. *Mar Pollut Bull* 77(1-2):177-182.

Eriksen M, Maximenko N, Thiel M, Cummins A, Lattin G, Wilson S, Hafner J, Zellers A & Rifman S (2013c) Plastic pollution in the South Pacific subtropical gyre. *Mar Pollut Bull* 68(1-2):71-76.

Erni-Cassola G, Gibson MI, Thompson RC & Christie-Oleza JA (2017) Lost, but Found with Nile Red: A Novel Method for Detecting and Quantifying Small Microplastics (1 mm to 20 μm) in Environmental Samples. *Environ. Sci. Technol.* 51(23):13641-13648.

Errami M, Salghi R, Zougagh M, Zarrouk A, Bazzi EH, Chakir A, Zarrok H, Hammouti B & Bazzi L (2012) Electrochemical degradation of buprofezin insecticide in aqueous solutions by anodic oxidation at boron-doped diamond electrode. *Res. Chem. Intermed.* 39(2):505-516.

Ersahin ME, Ozgun H, Tao Y & van Lier JB (2014) Applicability of dynamic membrane technology in anaerobic membrane bioreactors. *Water Res* 48:420-429.

Estahbanati MRK, Mahinpey N, Feilizadeh M, Attar F & Iliuta MC (2019) Kinetic study of the effects of pH on the photocatalytic hydrogen production from alcohols. *Int J Hydrogen Energ* 44(60):32030-32041.

Europe P (2021) An analysis of European plastics production, demand and waste data. *https://plasticseurope.org/*.

Fan G, Cang L, Fang G, Qin W, Ge L & Zhou D (2014) Electrokinetic delivery of persulfate to remediate PCBs polluted soils: effect of injection spot. *Chemosphere* 117:410-418.

Faure F, Saini C, Potter G, Galgani F, de Alencastro LF & Hagmann P (2015a) An evaluation of surface micro- and mesoplastic pollution in pelagic ecosystems of the Western Mediterranean Sea. *Environ Sci Pollut Res Int* 22(16):12190-12197.

Faure F, Saini C, Potter G, Galgani F, de Alencastro LF & Hagmann P (2015b) An evaluation of surface micro- and mesoplastic pollution in pelagic ecosystems of the Western Mediterranean Sea. *Environ Sci Pollut Res Int* 22(16):12190-12197.

Feilizadeh M, Attar F & Mahinpey N (2019) Hydrogen Peroxide-Assisted Photocatalysis under Solar Light Irradiation: Interpretation of Interaction Effects between an Active Photocatalyst and H_2O_2. *Can. J. Chem. Eng.* 97(7):2009-2014.

Feng L, van Hullebusch ED, Rodrigo MA, Esposito G & Oturan MA (2013) Removal of residual anti-inflammatory and analgesic pharmaceuticals from aqueous systems by electrochemical advanced oxidation processes. A review. *Chem. Eng. J.* 228:944-964.

Filipe V, Hawe A & Jiskoot W (2010) Critical evaluation of Nanoparticle Tracking Analysis (NTA) by NanoSight for the measurement of nanoparticles and protein aggregates. *Pharm. Res.* 27(5):796-810.

Flox C, Cabot PL, Centellas F, Garrido JA, Rodriguez RM, Arias C & Brillas E (2006) Electrochemical combustion of herbicide mecoprop in aqueous medium using a flow reactor with a boron-doped diamond anode. *Chemosphere* 64(6):892-902.

Fontanille M & Yves Gnanou ¡éP (2013) Chimie et physico-chimie des polymères.

Forte M, Iachetta G, Tussellino M, Carotenuto R, Prisco M, De Falco M, Laforgia V & Valiante S (2016) Polystyrene nanoparticles internalization in human gastric adenocarcinoma cells. *Toxicol In Vitro* 31:126-136.

Francisca CM, Sergi G-S, Vítor JPV, Rui ARB & Enric B (2013) Decolorization and mineralization of Sunset Yellow FCF azo dye by anodic oxidation, electro-Fenton, UVA photoelectro-Fenton and solar photoelectro-Fenton processes. *Appl. Catal. B: Environ.* 12553:14.

Free CM, Jensen OP, Mason SA, Eriksen M, Williamson NJ & Boldgiv B (2014) High-levels of microplastic pollution in a large, remote, mountain lake. *Mar Pollut Bull* 85(1):156-163.

Fries E, Dekiff JH, Willmeyer J, Nuelle MT, Ebert M & Remy D (2013) Identification of polymer types and additives in marine microplastic particles using pyrolysis-GC/MS and scanning electron microscopy. *Environ Sci Process Impacts* 15(10):1949-1956.

Frontistis Z, Antonopoulou M, Venieri D, Konstantinou I & Mantzavinos D (2017) Boron-doped diamond oxidation of amoxicillin pharmaceutical formulation: Statistical evaluation of operating parameters, reaction pathways and antibacterial activity. *J Environ Manage* 195(Pt 2):100-109.

Ganiyu SO & Martínez-Huitle CA (2019) Nature, Mechanisms and Reactivity of Electrogenerated Reactive Species at Thin-Film Boron-Doped Diamond (BDD) Electrodes During Electrochemical Wastewater Treatment. *ChemElectroChem* 6(9):2379-2392.

García-Gómez C, Drogui P, Seyhi B, Gortáres-Moroyoqui P, Buelna G, Estrada-Alvgarado MI & Álvarez LH (2016) Combined membrane bioreactor and electrochemical oxidation using Ti/PbO2 anode for the removal of carbamazepine. *Journal of the Taiwan Institute of Chemical Engineers* 64:211-219.

García-Gómez C, Drogui P, Zaviska F, Seyhi B, Gortáres-Moroyoqui P, Buelna G, Neira-Sáenz C, Estrada-alvarado M & Ulloa-Mercado RG (2014) Experimental design methodology applied to electrochemical oxidation of carbamazepine using Ti/PbO_2 and Ti/BDD electrodes. *J. Electroanal. Chem.* 732:1-10.

Garcia-Segura S, El-Ghenymy A, Centellas F, Rodríguez RM, Arias C, Garrido JA, Cabot PL & Brillas E (2012) Comparative degradation of the diazo dye Direct Yellow 4 by electro-Fenton, photoelectro-Fenton and photo-assisted electro-Fenton. *J. Electroanal. Chem.* 681:36-43.

Garcia-Segura S, Keller J, Brillas E & Radjenovic J (2015a) Removal of organic contaminants from secondary effluent by anodic oxidation with a boron-doped diamond anode as tertiary treatment. *J. Hazard. Mater.* 283:551-557.

Garcia-Segura S, Keller J, Brillas E & Radjenovic J (2015b) Removal of organic contaminants from secondary effluent by anodic oxidation with a boron-doped diamond anode as tertiary treatment. *J Hazard Mater* 283:551-557.

Garcia-Segura S, Ocon JD & Chong MN (2018) Electrochemical oxidation remediation of real wastewater effluents — A review. *Process Safety and Environmental Protection* 113:48-67.

Gewert B, Plassmann MM & MacLeod M (2015a) Pathways for degradation of plastic polymers floating in the marine environment. *Environ Sci Process Impacts* 17(9):1513-1521.

Gewert B, Plassmann MM & MacLeod M (2015b) Pathways for degradation of plastic polymers floating in the marine environment. *Environ Sci Process Impacts* 17(9):1513-1521.

Gies EA, LeNoble JL, Noel M, Etemadifar A, Bishay F, Hall ER & Ross PS (2018) Retention of microplastics in a major secondary wastewater treatment plant in Vancouver, Canada. *Mar. Pollut. Bull.* 133:553-561.

Gigault J, Halle AT, Baudrimont M, Pascal PY, Gauffre F, Phi TL, El Hadri H, Grassl B & Reynaud S (2018a) Current opinion: What is a nanoplastic? *Environ Pollut* 235:1030-1034.

Gigault J, Halle AT, Baudrimont M, Pascal PY, Gauffre F, Phi TL, El Hadri H, Grassl B & Reynaud S (2018b) Current opinion: What is a nanoplastic? *Environ Pollut* 235:1030-1034.

González-Pleiter M, Tamayo-Belda M, Pulido-Reyes G, Amariei G, Leganés F, Rosal R & Fernández-Piñas F (2019) Secondary nanoplastics released from a biodegradable microplastic severely impact freshwater environments. *Environmental Science: Nano* 6(5):1382-1392.

Grbic J, Nguyen B, Guo E, You JB, Sinton D & Rochman CM (2019) Magnetic Extraction of Microplastics from Environmental Samples. *Environ Sci Tech Let* 6(2):68-72.

Gregory MR (2010) Accumulation and distribution of virgin plastic granules on New Zealand beaches. *N Z J Mar Freshwater Res* 12(4):399-414.

Guinea E, Arias C, Cabot PL, Garrido JA, Rodriguez RM, Centellas F & Brillas E (2008) Mineralization of salicylic acid in acidic aqueous medium by electrochemical advanced oxidation processes using platinum and boron-doped diamond as anode and cathodically generated hydrogen peroxide. *Water Res* 42(1-2):499-511.

Guinea E, Garrido JA, Rodríguez RM, Cabot P-L, Arias C, Centellas F & Brillas E (2010) Degradation of the fluoroquinolone enrofloxacin by electrochemical advanced oxidation processes based on hydrogen peroxide electrogeneration. *Electrochim. Acta* 55(6):2101-2115.

Guitaya L, Drogui P & Blais JF (2015) In situ reactive oxygen species production for tertiary wastewater treatment. *Environ Sci Pollut Res Int* 22(9):7025-7036.

Guittonneau S, De Laat J, Dore M, Duguet JP & Honnel C (2005) Etude de la dégradation de quelques composés organochlorés volatils par photolyse du peroxyde d'hydrogène en milieux aqueux. *Rev Sci Eau* 1(1-2):35-54.

Gundogdu S, Cevik C, Guzel E & Kilercioglu S (2018a) Microplastics in municipal wastewater treatment plants in Turkey: a comparison of the influent and secondary effluent concentrations. *Environ Monit Assess* 190(11):626.

Gundogdu S, Cevik C, Guzel E & Kilercioglu S (2018b) Microplastics in municipal wastewater treatment plants in Turkey: a comparison of the influent and secondary effluent concentrations. *Environ Monit Assess* 190(11):626.

Haaland PD (1989) Experimental design in biotechnology Marcel Dekker. *Inc, United State of America*.

Hans Bouwmeester, Peter C.H. Hollman & Peters RJB (2015) Potential health impact of environmentally released micro- and nanoplastics in the human food production chain: experiences from nanotoxicology. *Environ Sci Technol*.

Hassen Trabelsi, Grah Patrick Atheba, Olfa Hentati, Yehe Dezirée Mariette, Didier Robert, Patrick Drogui & Ksibi1 M (2016) Solar Photocatalytic Decolorization and Degradation of Methyl Orange Using Supported TiO2. *J. Adv. Oxid. Technol. Vol. 19,* 19(1203-8407).

Henry B, Laitala K & Klepp IG (2019) Microfibres from apparel and home textiles: Prospects for including microplastics in environmental sustainability assessment. *Sci Total Environ* 652:483-494.

Herbort AF & Schuhen K (2017) A concept for the removal of microplastics from the marine environment with innovative host-guest relationships. *Environ Sci Pollut R* 24(12):11061-11065.

Herbort AF, Sturm MT, Fiedler S, Abkai G & Schuhen K (2018a) Alkoxy-silyl Induced Agglomeration: A New Approach for the Sustainable Removal of Microplastic from Aquatic Systems. *J Polym Environ* 26(11):4258-4270.

Herbort AF, Sturm MT & Schuhen K (2018b) A new approach for the agglomeration and subsequent removal of polyethylene, polypropylene, and mixtures of both from freshwater systems–a case study. *Environ Sci Pollut R* 25(15):15226-15234.

Hermabessiere L (2018) Les microplastiques et leurs additifs dans les produits de la pêche : développements méthodologiques et prévalence. Océan, Atmosphère. Université du Littoral Côte d'Opale. .

Hernandez LM, Yousefi N & Tufenkji N (2017) Are There Nanoplastics in Your Personal Care Products? *Environmental Science & Technology Letters* 4(7):280-285.

Hidalgo-Ruz V, Gutow L, Thompson RC & Thiel M (2012a) Microplastics in the marine environment: a review of the methods used for identification and quantification. *Environ Sci Technol* 46(6):3060-3075.

Hidalgo-Ruz V, Gutow L, Thompson RC & Thiel M (2012b) Microplastics in the marine environment: a review of the methods used for identification and quantification. *Environ. Sci. Technol.* 46(6):3060-3075.

Hidayaturrahman H & Lee TG (2019) A study on characteristics of microplastic in wastewater of South Korea: Identification, quantification, and fate of microplastics during treatment process. *Mar Pollut Bull* 146:696-702.

Hilles AH, Abu Amr SS, Hussein RA, Arafa AI & El-Sebaie OD (2015) Effect of persulfate and persulfate/H_2O_2 on biodegradability of an anaerobic stabilized landfill leachate. *Waste Manag* 44:172-177.

Hilles AH, Abu Amr SS, Hussein RA, Arafa AI & El-Sebaie OD (2016a) Optimization of leachate treatment using persulfate/H2O2 based advanced oxidation process: case study: Deir El-Balah Landfill Site, Gaza Strip, Palestine. *Water Sci Technol* 73(1):102-112.

Hilles AH, Abu Amr SS, Hussein RA, El-Sebaie OD & Arafa AI (2016b) Performance of combined sodium persulfate/H_2O_2 based advanced oxidation process in stabilized landfill leachate treatment. *J Environ Manage* 166:493-498.

Hintersteiner I, Himmelsbach M & Buchberger WW (2015) Characterization and quantitation of polyolefin microplastics in personal-care products using high-temperature gel-permeation chromatography. *Anal Bioanal Chem* 407(4):1253-1259.

Horikoshi S, Serpone N, Hisamatsu Y & Hidaka H (1998) Photocatalyzed degradation of polymers in aqueous semiconductor suspensions. 3. Photooxidation of a solid polymer: TiO2-blended poly (vinyl chloride) film. *Environ Sci Technol* 32(24):4010-4016.

Hou L, Kumar D, Yoo CG, Gitsov I & Majumder ELW (2021) Conversion and removal strategies for microplastics in wastewater treatment plants and landfills. *Chem. Eng. J.* 406.

Huerta Lwanga E, Gertsen H, Gooren H, Peters P, Salanki T, van der Ploeg M, Besseling E, Koelmans AA & Geissen V (2016) Microplastics in the Terrestrial Ecosystem: Implications for Lumbricus terrestris (Oligochaeta, Lumbricidae). *Environ Sci Technol* 50(5):2685-2691.

Hurley RR, Lusher AL, Olsen M & Nizzetto L (2018) Validation of a Method for Extracting Microplastics from Complex, Organic-Rich, Environmental Matrices. *Environ Sci Technol* 52(13):7409-7417.

Ignasi S, Enric B, Giacomo C & Marco P (2008) Comparative depollution of mecoprop aqueous solutions by electrochemical incineration using BDD and PbO_2 as high oxidation power anodes. *J. Electroanal. Chem.* 613:151–159.

IndustrievereinigungChemiefaser (2018/2019) Die Chemiefaserindustrie in der Bundesrepublik Deutschland. . *Disponible sur: https://www.ivc-ev.de/*

Ishibashi K-i, Fujishima A, Watanabe T & Hashimotoa K (2000) Quantum yields of active oxidative species formed on TiO_2 photocatalyst. *Journal of Photochemistry and Photobiology A: Chemistry* 134:139–142.

Ishii T, Handa T & Matsunaga S (1978) Effect of Molecular Weight On Excimer Formation of Polystyrenes in Solution. *Macromolecules* 11:40-46.

Ivleva NP, Wiesheu AC & Niessner R (2017) Microplastic in Aquatic Ecosystems. *Angew. Chem. Int. Ed. Engl.* 56(7):1720-1739.

Iyare PU, Ouki SK & Bond T (2020) Microplastics removal in wastewater treatment plants: a critical review. *Environmental Science: Water Research & Technology* 6(10):2664-2675.

Jacquin C, Lesage G, Traber J, Pronk W & Heran M (2017) Three-dimensional excitation and emission matrix fluorescence (3DEEM) for quick and pseudo-quantitative determination of protein- and humic-like substances in full-scale membrane bioreactor (MBR). *Water Res* 118:82-92.

Jean-Luc Gardette, Mohamed Baba, Bénédicte Mailhot, Sandrine Morlat-Thérias & Rivaton A (2008) Polymer photodegradation [Photodégradation des matériaux polymères]. *https://www.researchgate.net/publication/235339600*.

Jeong CB, Won EJ, Kang HM, Lee MC, Hwang DS, Hwang UK, Zhou B, Souissi S, Lee SJ & Lee JS (2016a) Microplastic Size-Dependent Toxicity, Oxidative Stress Induction, and p-JNK and p-p38 Activation in the Monogonont Rotifer (Brachionus koreanus). *Environ. Sci. Technol.* 50(16):8849-8857.

Jeong CB, Won EJ, Kang HM, Lee MC, Hwang DS, Hwang UK, Zhou B, Souissi S, Lee SJ & Lee JS (2016b) Microplastic Size-Dependent Toxicity, Oxidative Stress Induction, and p-JNK and p-p38 Activation in the Monogonont Rotifer (Brachionus koreanus). *Environ Sci Technol* 50(16):8849-8857.

Jiang R, Lu G, Yan Z, Liu J, Wu D & Wang Y (2020) Microplastic degradation by hydroxy-rich bismuth oxychloride. *J Hazard Mater* https://doi.org/10.1016/j.jhazmat.2020.124247:124247.

Julie Masura, Joel Baker, Gregory Foster & Courtney Arthur3 (2015) Laboratory methods for the analysis of microplastics in the marine environment: recommendations for quantifying synthetic particles in waters and sediments. NOAA Technical Memorandum NOS-OR&R-48.

Kang J, Zhou L, Duan X, Sun H, Ao Z & Wang S (2019) Degradation of Cosmetic Microplastics via Functionalized Carbon Nanosprings. *Matter* 1(3):745-758.

Kaposi KL, Mos B, Kelaher BP & Dworjanyn SA (2014) Ingestion of microplastic has limited impact on a marine larva. *Environ Sci Technol* 48(3):1638-1645.

Karami A, Golieskardi A, Keong Choo C, Larat V, Galloway TS & Salamatinia B (2017) The presence of microplastics in commercial salts from different countries. *Sci Rep* 7:46173.

Karami A, Romano N, Galloway T & Hamzah H (2016) Virgin microplastics cause toxicity and modulate the impacts of phenanthrene on biomarker responses in African catfish (Clarias gariepinus). *Environ Res* 151:58-70.

Karbalaei S, Hanachi P, Walker TR & Cole M (2018) Occurrence, sources, human health impacts and mitigation of microplastic pollution. *Environ Sci Pollut Res Int* 25(36):36046-36063.

Karimi Estahbanati MR, Feilizadeh M, Babin A, Mei B, Mul G & Iliuta MC (2020) Selective photocatalytic oxidation of cyclohexanol to cyclohexanone: a spectroscopic and kinetic study. *Chem. Eng. J.* 382:DOI: https://doi.org/10.1016/j.cej.2019.122732.

Karimi Estahbanati MR, Feilizadeh M & Iliuta MC (2017) Photocatalytic valorization of glycerol to hydrogen: Optimization of operating parameters by artificial neural network. *Appl Catal B: Environ* 209:483-492.

Karimi Estahbanati MR, Feilizadeh M & Iliuta MC (2019a) An intrinsic kinetic model for liquid phase photocatalytic hydrogen production. *AlChE J.* DOI: https://doi.org/10.1002/aic.16724.

Karimi Estahbanati MR, Feilizadeh M, Shokrollahi Yancheshmeh M & Iliuta MC (2019b) Effects of carbon nanotube and carbon sphere templates in TiO_2 composites for photocatalytic hydrogen production. *Ind Eng Chem Res* 58:2770−2783.

Karimi Estahbanati MR, Kiendrebeogo M, Khosravanipour Mostafazadeh A, Drogui P & Tyagi RD (2021a) Treatment processes for microplastics and nanoplastics in waters: State-of-the-art review. *Mar Pollut Bull* 168:112374.

Karimi Estahbanati MR, Kong XY, Eslami A & Soo HS (2021b) Current Developments in the Chemical Upcycling of Waste Plastics Using Alternative Energy Sources. *ChemSusChem* 14(19):4152-4166.

Karimi Estahbanati MR, Kumar S, Khajvand M, Drogui P & Tyagi RD (2021c) Environmental Impacts of Recovery of Resources From Industrial Wastewater. *Biomass, Biofuels, Biochemicals,* Elsevier. p 121-162.

Karlsson TM, Vethaak AD, Almroth BC, Ariese F, van Velzen M, Hassellov M & Leslie HA (2017a) Screening for microplastics in sediment, water, marine invertebrates and fish: Method development and microplastic accumulation. *Mar Pollut Bull* 122(1-2):403-408.

Karlsson TM, Vethaak AD, Almroth BC, Ariese F, van Velzen M, Hassellov M & Leslie HA (2017b) Screening for microplastics in sediment, water, marine invertebrates and fish: Method development and microplastic accumulation. *Mar. Pollut. Bull.* 122(1-2):403-408.

Kashiwada S (2006) Distribution of nanoparticles in the see-through medaka (Oryzias latipes). *Environ Health Perspect* 114(11):1697-1702.

Kelly MR, Lant NJ, Kurr M & Burgess JG (2019) Importance of Water-Volume on the Release of Microplastic Fibers from Laundry. *Environ Sci Technol* 53(20):11735-11744.

Khandegar V & Saroha AK (2013) Electrocoagulation for the treatment of textile industry effluent--a review. *J Environ Manage* 128:949-963.

Khataee AR, Safarpour M, Zarei M & Aber S (2011) Electrochemical generation of H_2O_2 using immobilized carbon nanotubes on graphite electrode fed with air: Investigation of operational parameters. *J. Electroanal. Chem.* 659(1):63-68.

Khosravanipour Mostafazadeh A, Benguit AT, Carabin A, Drogui P & Brien E (2019) Development of combined membrane filtration, electrochemical technologies, and adsorption processes for treatment and reuse of laundry wastewater and removal of nonylphenol ethoxylates as surfactants. *Journal of Water Process Engineering* 28:277-292.

Kiendrebeogo M, Karimi Estahbanati MR, Khosravanipour Mostafazadeh A, Drogui P & Tyagi RD (2021a) Treatment of microplastics in water by anodic oxidation: A case study for polystyrene. *Environ Pollut* 269:116168.

Kiendrebeogo M, Karimi Estahbanati MR, Khosravanipour Mostafazadeh A, Drogui P & Tyagi RD (2021b) Treatment of microplastics in water by anodic oxidation: A case study for polystyrene. *Environ Pollut* 269:116168.

Kiendrebeogo M, Karimi Estahbanati MR, Ouarda Y, Drogui P & Tyagi RD (2022) Electrochemical degradation of nanoplastics in water: Analysis of the role of reactive oxygen species. *Sci Total Environ* 808:151897.

Koda S, Kimura T, Kondo T & Mitome H (2003) A standard method to calibrate sonochemical efficiency of an individual reaction system. *Ultrason. Sonochem.* 10(3):149-156.

Komtchou S, Dirany A, Drogui P & Bermond A (2015) Removal of carbamazepine from spiked municipal wastewater using electro-Fenton process. *Environ Sci Pollut Res Int* 22(15):11513-11525.

Kosuth M, Mason SA & Wattenberg EV (2018) Anthropogenic contamination of tap water, beer, and sea salt. *PLoS ONE* 13(4):e0194970.

Koziara JM, Lockman PR, Allen DD & Mumper RJ (2003) In Situ Blood–Brain Barrier Transport of Nanoparticles. *Pharm. Res.* Vol. 20, No. 11.

Lambert S & Wagner M (2016) Characterisation of nanoplastics during the degradation of polystyrene. *Chemosphere* 145:265-268.

Lan Y, Coetsier C, Causserand C & Groenen Serrano K (2017) On the role of salts for the treatment of wastewaters containing pharmaceuticals by electrochemical oxidation using a boron doped diamond anode. *Electrochim. Acta* 231:309-318.

Lapointe M, Farner JM, Hernandez LM & Tufenkji N (2020a) Understanding and Improving Microplastic Removal during Water Treatment: Impact of Coagulation and Flocculation. *Environ Sci Technol* 54(14):8719-8727.

Lapointe M, Farner JM, Hernandez LM & Tufenkji N (2020b) Understanding and Improving Microplastic Removal during Water Treatment: Impact of Coagulation and Flocculation. *Environ Sci Tech* 54(14):8719-8727.

Lares M, Ncibi MC, Sillanpaa M & Sillanpaa M (2018) Occurrence, identification and removal of microplastic particles and fibers in conventional activated sludge process and advanced MBR technology. *Water Res* 133:236-246.

Law KL, Morét-Ferguson S, Maximenko NA, Proskurowski G, Peacock EE, Hafner J & Reddy CM (2010) Plastic Accumulation in the North Atlantic Subtropical Gyre. *SCIENCE* 329 (5996):1185-1188.

Lechner A, Keckeis H, Lumesberger-Loisl F, Zens B, Krusch R, Tritthart M, Glas M & Schludermann E (2014) The Danube so colourful: a potpourri of plastic litter outnumbers fish larvae in Europe's second largest river. *Environ Pollut* 188:177-181.

Lee KW, Shim WJ, Kwon OY & Kang JH (2013) Size-dependent effects of micro polystyrene particles in the marine copepod Tigriopus japonicus. *Environ Sci Technol* 47(19):11278-11283.

Leslie HA, Brandsma SH, van Velzen MJ & Vethaak AD (2017a) Microplastics en route: Field measurements in the Dutch river delta and Amsterdam canals, wastewater treatment plants, North Sea sediments and biota. *Environ Int* 101:133-142.

Leslie HA, Brandsma SH, van Velzen MJ & Vethaak AD (2017b) Microplastics en route: Field measurements in the Dutch river delta and Amsterdam canals, wastewater treatment plants, North Sea sediments and biota. *Environ Int* 101:133-142.

Leslie HA, van Velzen MJM, Brandsma SH, Vethaak AD, Garcia-Vallejo JJ & Lamoree MH (2022) Discovery and quantification of plastic particle pollution in human blood. *Environ Int* 163:107199.

Li J, Liu H & Paul Chen J (2018a) Microplastics in freshwater systems: A review on occurrence, environmental effects, and methods for microplastics detection. *Water Res* 137:362-374.

Li L, Xu G, Yu H & Xing J (2018b) Dynamic membrane for micro-particle removal in wastewater treatment: Performance and influencing factors. *Sci Total Environ* 627:332-340.

Li L, Xu G, Yu H & Xing J (2018c) Dynamic membrane for micro-particle removal in wastewater treatment: Performance and influencing factors. *Sci Total Environ* 627:332-340.

Li M, Feng C, Zhang Z, Lei X, Chen R, Yang Y & Sugiura N (2009) Simultaneous reduction of nitrate and oxidation of by-products using electrochemical method. *J. Hazard. Mater.* 171(1-3):724-730.

Li Y, Zhang Y, Xia G, Zhan J, Yu G & Wang Y (2020) Evaluation of the technoeconomic feasibility of electrochemical hydrogen peroxide production for decentralized water treatment. *Frontiers of Environmental Science & Engineering* 15(1).

Liao C-H & Gurol MD (1995) Chemical oxidation by photolytic decomposition of hydrogen peroxide. *Environ. Sci. Techno* 29:3007-3014.

Lin CK, Bashir MJ, Abu Amr SS & Sim LC (2016) Post-treatment of palm oil mill effluent (POME) using combined persulphate with hydrogen peroxide ($S_2O_8^{2-}/H_2O_2$) oxidation. *Water Sci Technol* 74(11):2675-2682.

Lithner D, Larsson A & Dave G (2011) Environmental and health hazard ranking and assessment of plastic polymers based on chemical composition. *Sci Total Environ* 409(18):3309-3324.

Liu L, Fokkink R & Koelmans AA (2016) Sorption of polycyclic aromatic hydrocarbons to polystyrene nanoplastic. *Environ Toxicol Chem* 35(7):1650-1655.

Liu W, Zhang J, Liu H, Guo X, Zhang X, Yao X, Cao Z & Zhang T (2020) A review of the removal of microplastics in global wastewater treatment plants: Characteristics and mechanisms. *Environment International* 146:106277.

Liu W, Zhang J, Liu H, Guo X, Zhang X, Yao X, Cao Z & Zhang T (2021) A review of the removal of microplastics in global wastewater treatment plants: Characteristics and mechanisms. *Environ Int* 146:106277.

Llorente-García BE, Hernández-López JM, Zaldívar-Cadena AA, Siligardi C & Cedillo-González EI (2020) First Insights into Photocatalytic Degradation of HDPE and LDPE Microplastics by a Mesoporous N–TiO_2 Coating: Effect of Size and Shape of Microplastics. *Coatings* 10(7):658.

Löder MGJ, Kuczera M, Mintenig S, Lorenz C & Gerdts G (2015) Focal plane array detector-based micro-Fourier-transform infrared imaging for the analysis of microplastics in environmental samples. *Environmental Chemistry* 12(5).

Lu D, Cheng W, Zhang T, Lu X, Liu Q, Jiang J & Ma J (2016) Hydrophilic Fe2O3 dynamic membrane mitigating fouling of support ceramic membrane in ultrafiltration of oil/water emulsion. *Sep. Purif. Technol.* 165:1-9.

Luo H, Liu C, He D, Xu J, Sun J, Li J & Pan X (2021) Environmental behaviors of microplastics in aquatic systems: A systematic review on degradation, adsorption, toxicity and biofilm under aging conditions. *J. Hazard. Mater.* 423:126915.

Luo H, Xiang Y, He D, Li Y, Zhao Y, Wang S & Pan X (2019) Leaching behavior of fluorescent additives from microplastics and the toxicity of leachate to Chlorella vulgaris. *Sci Total Environ* 678:1-9.

Luo K, Yang Q, Li XM, Chen HB, Liu X, Yang GJ & Zeng GM (2013) Novel insights into enzymatic-enhanced anaerobic digestion of waste activated sludge by three-dimensional excitation and emission matrix fluorescence spectroscopy. *Chemosphere* 91(5):579-585.

Luo S, Wei Z, Spinney R, Villamena FA, Dionysiou DD, Chen D, Tang CJ, Chai L & Xiao R (2018) Quantitative structure-activity relationships for reactivities of sulfate and hydroxyl radicals with aromatic contaminants through single-electron transfer pathway. *J. Hazard. Mater.* 344:1165-1173.

Lusher A, Hollman P & Mendoza-Hill J (2017) Microplastics in fisheries and aquaculture : status of knowledge on their occurrence and implications for aquatic organisms and food safety. in: 615, F.a.A.T.P.N. (Ed.). FAO, Rome, Italy.

Lusher AL, Tirelli V, O'Connor I & Officer R (2015) Microplastics in Arctic polar waters: the first reported values of particles in surface and sub-surface samples. *Sci Rep* 5:14947.

Lv X, Dong Q, Zuo Z, Liu Y, Huang X & Wu W-M (2019) Microplastics in a municipal wastewater treatment plant: Fate, dynamic distribution, removal efficiencies, and control strategies. *J. Clean. Prod.* 225:579-586.

M. Panizza , P.A. Michaud , G. Cerisola & Ch. Comninellis b (2001) Anodic oxidation of 2-naphthol at boron-doped diamond electrodes. *Journal of Electroanalytical Chemistry 507* :206–214.

Ma B, Xue W, Ding Y, Hu C, Liu H & Qu J (2019a) Removal characteristics of microplastics by Fe-based coagulants during drinking water treatment. *J Environ Sci (China)* 78:267-275.

Ma B, Xue W, Hu C, Liu H, Qu J & Li L (2019b) Characteristics of microplastic removal via coagulation and ultrafiltration during drinking water treatment. *Chem. Eng. J.* 359:159-167.

Ma Y, Huang A, Cao S, Sun F, Wang L, Guo H & Ji R (2016) Effects of nanoplastics and microplastics on toxicity, bioaccumulation, and environmental fate of phenanthrene in fresh water. *Environ Pollut* 219:166-173.

Magalhães S, Alves L, Medronho B, Romano A & Rasteiro MdG (2020) Microplastics in Ecosystems: From Current Trends to Bio-Based Removal Strategies. *Molecules* 25(17):3954.

Magnusson K & Norén F (2014) Screening of microplastic particles in and down-stream a wastewater treatment plant

Mahon AM, O'Connell B, Healy MG, O'Connor I, Officer R, Nash R & Morrison L (2017) Microplastics in sewage sludge: effects of treatment. *Environ Sci Technol* 51(2):810-818.

Maliwan T, Pungrasmi W & Lohwacharin J (2020) Effects of microplastic accumulation on floc characteristics and fouling behavior in a membrane bioreactor. *J Hazard Mater* 411:124991.

Marselli B, Garcia-Gomez J, Michaud PA, Rodrigo MA & Comninellis C (2003) Electrogeneration of Hydroxyl Radicals on Boron-Doped Diamond Electrodes. *J. Electrochem. Soc.* 150(3).

Martínez-Huitle CA & Brillas E (2009) Decontamination of wastewaters containing synthetic organic dyes by electrochemical methods: A general review. *Applied Catalysis B: Environmental* 87(3-4):105-145.

Martínez-Huitle CA & Panizza M (2018) Electrochemical oxidation of organic pollutants for wastewater treatment. *Current Opinion in Electrochemistry* 11:62-71.

Martínez-Huitle CA, Quiroz MA, Comninellis C, Ferro S & Battisti AD (2004) Electrochemical incineration of chloranilic acid using Ti/IrO_2, Pb/PbO_2 and Si/BDD electrodes. *Electrochim. Acta* 50(4):949-956.

Martinez-Huitle CA, Rodrigo MA, Sires I & Scialdone O (2015) Single and coupled electrochemical processes and reactors for the abatement of organic water pollutants: A critical review. *Chem. Rev.* 115(24):13362-13407.

Mason SA, Garneau D, Sutton R, Chu Y, Ehmann K, Barnes J, Fink P, Papazissimos D & Rogers DL (2016a) Microplastic pollution is widely detected in US municipal wastewater treatment plant effluent. *Environ Pollut* 218:1045-1054.

Mason SA, Garneau D, Sutton R, Chu Y, Ehmann K, Barnes J, Fink P, Papazissimos D & Rogers DL (2016b) Microplastic pollution is widely detected in US municipal wastewater treatment plant effluent. *Environ Pollut* 218:1045-1054.

Matta R, Tlili S, Chiron S & Barbati S (2010) Removal of carbamazepine from urban wastewater by sulfate radical oxidation. *Environmental Chemistry Letters* 9(3):347-353.

Mattsson K, Ekvall MT, Hansson LA, Linse S, Malmendal A & Cedervall T (2015) Altered behavior, physiology, and metabolism in fish exposed to polystyrene nanoparticles. *Environ Sci Technol* 49(1):553-561.

McCormick A, Hoellein TJ, Mason SA, Schluep J & Kelly JJ (2014a) Microplastic is an abundant and distinct microbial habitat in an urban river. *Environ Sci Technol* 48(20):11863-11871.

McCormick A, Hoellein TJ, Mason SA, Schluep J & Kelly JJ (2014b) Microplastic is an abundant and distinct microbial habitat in an urban river. *Environ Sci Technol* 48(20):11863-11871.

Melián EP, López CR, Santiago DE, Quesada-Cabrera R, Méndez JAO, Rodríguez JMD & Díaz OG (2016) Study of the photocatalytic activity of Pt-modified commercial TiO_2 for hydrogen production in the presence of common organic sacrificial agents. *Appl. Catal. A- Gen* 518:189-197.

Miao F, Liu Y, Gao M, Yu X, Xiao P, Wang M, Wang S & Wang X (2020a) Degradation of polyvinyl chloride microplastics via an electro-Fenton-like system with a TiO_2/graphite cathode. *J Hazard Mater* 399:123023.

Miao F, Liu Y, Gao M, Yu X, Xiao P, Wang M, Wang S & Wang X (2020b) Degradation of polyvinyl chloride microplastics via an electro-Fenton-like system with a TiO2/graphite cathode. *J. Hazard. Mater.* 399:123023.

Michaud P-A, E. Mahé, W. Haenni, A. Perret & Ch. Comninellisa (2000) Preparation of Peroxodisulfuric Acid Using Boron-Doped Diamond Thin Film Electrodes. *Electrochem. Solid-State Lett.* 3 (2):77-79.

Michielssen MR, Michielssen ER, Ni J & Duhaime MB (2016) Fate of microplastics and other small anthropogenic litter (SAL) in wastewater treatment plants depends on unit processes employed. *Environmental Science: Water Research & Technology* 2(6):1064-1073.

Mintenig SM, Bäuerlein PS, Koelmans AA, Dekker SC & van Wezel AP (2018) Closing the gap between small and smaller: towards a framework to analyse nano- and microplastics in aqueous environmental samples. *Environmental Science: Nano* 5(7):1640-1649.

Mintenig SM, Int-Veen I, Loder MGJ, Primpke S & Gerdts G (2017) Identification of microplastic in effluents of waste water treatment plants using focal plane array-based micro-Fourier-transform infrared imaging. *Water Res* 108:365-372.

Mintenig SM, Loder MGJ, Primpke S & Gerdts G (2019) Low numbers of microplastics detected in drinking water from ground water sources. *Sci Total Environ* 648:631-635.

Misra A, Zambrzycki C, Kloker G, Kotyrba A, Anjass MH, Franco Castillo I, Mitchell SG, Güttel R & Streb C (2020) Water Purification and Microplastics Removal Using Magnetic Polyoxometalate-Supported Ionic Liquid Phases (magPOM-SILPs). *Angew Chem Int Edit* 59(4):1601-1605.

Miyake Y, Tokumura M, Wang Q, Amagai T & Horii Y (2017) Rate of hexabromocyclododecane decomposition and production of brominated polycyclic aromatic hydrocarbons during combustion in a pilot-scale incinerator. *J Environ Sci (China)* 61:91-96.

Moore CJ (2008) Synthetic polymers in the marine environment: a rapidly increasing, long-term threat. *Environ Res* 108(2):131-139.

Muff J, Bennedsen LR & Søgaard EG (2011) Study of electrochemical bleaching of p-nitrosodimethylaniline and its role as hydroxyl radical probe compound. *J. Appl. Electrochem.* 41(5):599-607.

Mughini-Gras L, van der Plaats RQJ, van der Wielen PWJJ, Bauerlein PS & de Roda Husman AM (2021) Riverine microplastic and microbial community compositions: A field study in the Netherlands. *Water Research* 192:116852.

Murphy F, Ewins C, Carbonnier F & Quinn B (2016a) Wastewater Treatment Works (WwTW) as a Source of Microplastics in the Aquatic Environment. *Environ Sci Technol* 50(11):5800-5808.

Murphy F, Ewins C, Carbonnier F & Quinn B (2016b) Wastewater Treatment Works (WwTW) as a Source of Microplastics in the Aquatic Environment. *Environ. Sci. Technol.* 50(11):5800-5808.

Murray A & Örmeci B (2020) Removal effectiveness of Nanoplastics (<400 nm) with separation processes used for water and wastewater treatment. *Water* 12(3).

Murugananthan M, Latha SS, Bhaskar Raju G & Yoshihara S (2011) Role of electrolyte on anodic mineralization of atenolol at boron doped diamond and Pt electrodes. *Sep. Purif. Technol.* 79(1):56-62.

Murugananthan M, Yoshihara S, Rakuma T & Shirakashi T (2008) Mineralization of bisphenol A (BPA) by anodic oxidation with boron-doped diamond (BDD) electrode. *J. Hazard. Mater.* 154(1-3):213-220.

Myers RH, Montgomery DC, Vining GG, Borror CM & Kowalski SM (2018) Response Surface Methodology: A Retrospective and Literature Survey. *Journal of Quality Technology* 36(1):53-77.

Nabi I, Bacha A-U-R, Li K, Cheng H, Wang T, Liu Y, Ajmal S, Yang Y, Feng Y & Zhang L (2020) Complete Photocatalytic Mineralization of Microplastic on TiO_2 Nanoparticle Film. *iScience* 23(7):101326.

Napper IE, Bakir A, Rowland SJ & Thompson RC (2015a) Characterisation, quantity and sorptive properties of microplastics extracted from cosmetics. *Mar Pollut Bull* 99(1-2):178-185.

Napper IE, Bakir A, Rowland SJ & Thompson RC (2015b) Characterisation, quantity and sorptive properties of microplastics extracted from cosmetics. *Mar Pollut Bull* 99(1-2):178-185.

Napper IE & Thompson RC (2016a) Release of synthetic microplastic plastic fibres from domestic washing machines: Effects of fabric type and washing conditions. *Mar Pollut Bull* 112(1-2):39-45.

Napper IE & Thompson RC (2016b) Release of synthetic microplastic plastic fibres from domestic washing machines: Effects of fabric type and washing conditions. *Mar Pollut Bull* 112(1-2):39-45.

Ngo PL, Pramanik BK, Shah K & Roychand R (2019) Pathway, classification and removal efficiency of microplastics in wastewater treatment plants. *Environ Pollut* 255(Pt 2):113326.

Nidheesh PV & Rajan R (2016) Removal of rhodamine B from a water medium using hydroxyl and sulphate radicals generated by iron loaded activated carbon. *RSC Advances* 6(7):5330-5340.

Niu T, Cai J, Shi P & Zhao G (2020) Unique electrochemical system for in situ SO4− generation and pollutants degradation. *Chem. Eng. J.* 386.

Nizzetto L, Futter M & Langaas S (2016) Are Agricultural Soils Dumps for Microplastics of Urban Origin? *Environ Sci Technol* 50(20):10777-10779.

Nuelle MT, Dekiff JH, Remy D & Fries E (2014) A new analytical approach for monitoring microplastics in marine sediments. *Environ Pollut* 184:161-169.

OCDE (2022) Perspectives mondiales des plastiques, Scénarios d'action a l'horizon 2060, l'essentiel.

OECD (2009) Emission scenario document on plastic additives. Series on emission scenario documents, no. 3. Paris: Environmental directorate, OECD Environmental Health and Safety Publications.

Ossmann BE, Sarau G, Holtmannspotter H, Pischetsrieder M, Christiansen SH & Dicke W (2018) Small-sized microplastics and pigmented particles in bottled mineral water. *Water Res* 141:307-316.

Ouarda Y, Trellu C, Lesage G, Rivallin M, Drogui P & Cretin M (2020) Electro-oxidation of secondary effluents from various wastewater plants for the removal of acetaminophen and dissolved organic matter. *Sci Total Environ* 738:140352.

Ozcan A, Sahin Y, Koparal AS & Oturan MA (2008) Propham mineralization in aqueous medium by anodic oxidation using boron-doped diamond anode: influence of experimental parameters on degradation kinetics and mineralization efficiency. *Water Res* 42(12):2889-2898.

Özcan A, Şahin Y, Savaş Koparal A & Oturan MA (2008) Carbon sponge as a new cathode material for the electro-Fenton process: Comparison with carbon felt cathode and application to degradation of synthetic dye basic blue 3 in aqueous medium. *J. Electroanal. Chem.* 616(1-2):71-78.

Paco A, Duarte K, da Costa JP, Santos PSM, Pereira R, Pereira ME, Freitas AC, Duarte AC & Rocha-Santos TAP (2017) Biodegradation of polyethylene microplastics by the marine fungus Zalerion maritimum. *Sci Total Environ* 586:10-15.

Padervand M, Lichtfouse E, Robert D & Wang C (2020) Removal of microplastics from the environment. A review. *Environ. Chem. Lett.* 18(3):807-828.

Panizza M & Cerisola G (2005) Application of diamond electrodes to electrochemical processes. *Electrochim. Acta* 51(2):191-199.

Panizza M & Cerisola G (2009) Direct And Mediated Anodic Oxidation of Organic Pollutants. *Chem. Rev* 109:6541–6569.

Panizza M, Michaud PA, Cerisola G & Comninellis C (2001) Electrochemical treatment of wastewaters containing organic pollutants on boron-doped diamond electrodes: Prediction of specific energy consumption and required electrode area. *Electrochem. Commun.* 3:336±339.

Pecora R (2000) Dynamic light scattering measurement of nanometer particles in *Journal of Nanoparticle Research 2: 123–131,* .

Perren W, Wojtasik A & Cai Q (2018) Removal of Microbeads from Wastewater Using Electrocoagulation. *ACS Omega* 3(3):3357-3364.

Phonsy PD, Anju SG, Jyothi KP, Suguna Y & Yesodharan EP (2015a) Semiconductor mediated photocatalytic degradation of plastics and recalcitrant organic pollutants in water: effect of additives and fate of Insitu formed H_2O_2. *J. Adv. Oxid. Technol.* 18:85-97.

Phonsy PD, Anju SG, Jyothi KP, Yesodharan S & Yesodharan EP (2015b) Semiconductor mediated photocatalytic degradation of plastics and recalcitrant organic pollutants in water: effect of additives and fate of insitu formed H2O2. *J Adv Oxid Technol* 18(1):85-97.

Pittura L, Foglia A, Akyol C, Cipolletta G, Benedetti M, Regoli F, Eusebi AL, Sabbatini S, Tseng LY, Katsou E, Gorbi S & Fatone F (2021) Microplastics in real wastewater treatment schemes: Comparative assessment and relevant inhibition effects on anaerobic processes. *Chemosphere* 262:128415.

Pivokonsky M, Cermakova L, Novotna K, Peer P, Cajthaml T & Janda V (2018) Occurrence of microplastics in raw and treated drinking water. *Sci Total Environ* 643:1644-1651.

Pizzichetti ARP, Pablos C, Álvarez-Fernández C, Reynolds K, Stanley S & Marugán J (2021) Evaluation of membranes performance for microplastic removal in a simple and low-cost filtration system. *Case Studies in Chemical and Environmental Engineering* 3.

Plastics (2019) Plastics – the Facts 2019 : An analysis of European Plastics production, demand and waste data, 2019. Plastics Europe Brussels Belgium. . https://www.plasticseurope.org/download_file/force/3183/181.

PlasticsEurope (2018) An analysis of European plastics production, demand and waste data.

PlasticsEurope (2022) Plastics-the facts 2022. https://plasticseurope.org/knowledge-hub/plastics-the-facts-2022/.

Poerio T, Piacentini E & Mazzei R (2019) Membrane Processes for Microplastic Removal. *Molecules* 24(22).

Pozza Ad, Ferrantelli P, Merli C & Petrucci E (2005) Oxidation efficiency in the electro-Fenton process. *J. Appl. Electrochem.* 35(4):391-398.

Ragusa A, Svelato A, Santacroce C, Catalano P, Notarstefano V, Carnevali O, Papa F, Rongioletti MCA, Baiocco F, Draghi S, D'Amore E, Rinaldo D, Matta M & Giorgini E (2021) Plasticenta: First evidence of microplastics in human placenta. *Environ Int* 146:106274.

Rajala K, Gronfors O, Hesampour M & Mikola A (2020a) Removal of microplastics from secondary wastewater treatment plant effluent by coagulation/flocculation with iron, aluminum and polyamine-based chemicals. *Water research* 183:116045.

Rajala K, Grönfors O, Hesampour M & Mikola A (2020b) Removal of microplastics from secondary wastewater treatment plant effluent by coagulation/flocculation with iron, aluminum and polyamine-based chemicals. *Water Research* 183:116045.

Rajkumar D, Song BJ & Kim JG (2007) Electrochemical degradation of Reactive Blue 19 in chloride medium for the treatment of textile dyeing wastewater with identification of intermediate compounds. *Dyes and Pigments* 72(1):1-7.

Razali NA, Abdullah WRW & Mohd N (2020) EFFECT OF THERMO-PHOTOCATALYTIC PROCESS USING ZINC OXIDE ON DEGRADATION OF MACRO/MICRO-PLASTIC IN AQUEOUS ENVIRONMENT. *J Sustain Sci Manag* 15(6):1-14.

Reisser J, Shaw J, Wilcox C, Hardesty BD, Proietti M, Thums M & Pattiaratchi C (2013) Marine plastic pollution in waters around Australia: characteristics, concentrations, and pathways. *PLoS ONE* 8(11):e80466.

Ren W, Zhou Z, Zhu Y, Jiang L-M, Wei H, Niu T, Fu P & Qiu Z (2015) Effect of sulfate radical oxidation on disintegration of waste activated sludge. *Int Biodeterior Biodegrad* 104:384-390.

Renata BAdS & Luís AMR (2013) Phenol Electrooxidation in Different Supporting Electrolytes Using Boron-Doped Diamond Anodes. *Int. J. Electrochem. Sci* 8:643 - 657.

Rios Mendoza LM, Karapanagioti H & Álvarez NR (2018) Micro(nanoplastics) in the marine environment: Current knowledge and gaps. *Current Opinion in Environmental Science & Health* 1:47-51.

Rius-Ayra O, Bouhnouf-Riahi O & Llorca-Isern N (2020) Superhydrophobic and Sustainable Nanostructured Powdered Iron for the Efficient Separation of Oil-in-Water Emulsions and the Capture of Microplastics. *ACS Appl. Mater. Inter.* 12(40):45629-45640.

Robert D, Lichtfouse E & Wang C (2022) Eliminer les microplastiques. *Le CNRS en chine* 36:47-50.

Rochman CM, Kross SM, Armstrong JB, Bogan MT, Darling ES, Green SJ, Smyth AR & Verissimo D (2015) Scientific Evidence Supports a Ban on Microbeads. *Environ Sci Technol* 49(18):10759-10761.

Rodrigo MA, Cañizares P, Sánchez-Carretero A & Sáez C (2010) Use of conductive-diamond electrochemical oxidation for wastewater treatment. *Catal. Today* 151(1-2):173-177.

Rodriguez-Seijo A, Lourenco J, Rocha-Santos TAP, da Costa J, Duarte AC, Vala H & Pereira R (2017) Histopathological and molecular effects of microplastics in Eisenia andrei Bouche. *Environ Pollut* 220(Pt A):495-503.

Rossi G, Barnoud J & Monticelli L (2014a) Polystyrene Nanoparticles Perturb Lipid Membranes. *J Phys Chem Lett* 5(1):241-246.

Rossi G, Barnoud J & Monticelli L (2014b) Polystyrene nanoparticles perturb lipid membranes. *J. Phys. Chem. Let* 5(1):241-246.

Sadri SS & Thompson RC (2014) On the quantity and composition of floating plastic debris entering and leaving the Tamar Estuary, Southwest England. *Mar Pollut Bull* 81(1):55-60.

Salerno C, Vergine P, Berardi G & Pollice A (2017) Influence of air scouring on the performance of a Self Forming Dynamic Membrane BioReactor (SFD MBR) for municipal wastewater treatment. *Bioresour Technol* 223:301-306.

Salmerón I, Plakas KV, Sirés I, Oller I, Maldonado MI, Karabelas AJ & Malato S (2019) Optimization of electrocatalytic H2O2 production at pilot plant scale for solar-assisted water treatment. *Applied Catalysis B: Environmental* 242:327-336.

Sangkham S, Faikhaw O, Munkong N, Sakunkoo P, Arunlertaree C, Chavali M, Mousazadeh M & Tiwari A (2022) A review on microplastics and nanoplastics in the environment: Their occurrence, exposure routes, toxic studies, and potential effects on human health. *Mar Pollut Bull* 181:113832.

Sanni I, Karimi Estahbanati MR, Carabin A & Drogui P (2021) Coupling electrocoagulation with electro-oxidation for COD and phosphorus removal from industrial container wash water. *Sep. Purif. Technol.* :119992.

Schwaferts C, Niessner R, Elsner M & Ivleva NP (2019) Methods for the analysis of submicrometer- and nanoplastic particles in the environment. *TrAC, Trends Anal. Chem.* 112:52-65.

Schymanski D, Goldbeck C, Humpf HU & Furst P (2018) Analysis of microplastics in water by micro-Raman spectroscopy: Release of plastic particles from different packaging into mineral water. *Water Res* 129:154-162.

Serrano K, Michaud PA, Comninellis & Savall A (2002) Electrochemical preparation of peroxodisulfuric acid using boron doped diamond thin film electrodes. *Electrochim. Acta* 48:431- 436.

Shahi NK, Maeng M, Kim D & Dockko S (2020) Removal behavior of microplastics using alum coagulant and its enhancement using polyamine-coated sand. *Process Saf. Environ. Prot.* 141:9-17.

Sharma S, Basu S, Shetti NP, Nadagouda MN & Aminabhavi TM (2020) Microplastics in the environment: Occurrence, perils, and eradication. *Chem. Eng. J.* https://doi.org/10.1016/j.cej.2020.127317:127317.

Shen M, Song B, Zhu Y, Zeng G, Zhang Y, Yang Y, Wen X, Chen M & Yi H (2020) Removal of microplastics via drinking water treatment: Current knowledge and future directions. *Chemosphere* 251:126612.

Shen M, Zhang Y, Almatrafi E, Hu T, Zhou C, Song B, Zeng Z & Zeng G (2022) Efficient removal of microplastics from wastewater by an electrocoagulation process. *Chem. Eng. J.* 428.

Sheng GP & Yu HQ (2006) Characterization of extracellular polymeric substances of aerobic and anaerobic sludge using three-dimensional excitation and emission matrix fluorescence spectroscopy. *Water Res* 40(6):1233-1239.

Shim WJ, Hong SH & Eo SE (2017) Identification methods in microplastic analysis: a review. *Analytical Methods* 9(9):1384-1391.

Shosuke Yoshida, Kazumi Hiraga, Toshihiko Takehana, Ikuo Taniguchi, Hironao Yamaji, Yasuhito Maeda, Kiyotsuna Toyohara, Kenji Miyamoto, Yoshiharu Kimura & Oda K (2016) A bacterium that degrades and assimilates poly(ethylene terephthalate). *Science China Chemistry* 351 (6278):1196-1199.

Sigler PB & MAster BJ (1957) Hydrogen peroxide-induced ce*(III)-ce(IV) exchange syste. *J Am Chem Soc* 79:6353-6357.

Silva AB, Bastos AS, Justino CIL, da Costa JP, Duarte AC & Rocha-Santos TAP (2018) Microplastics in the environment: Challenges in analytical chemistry - A review. *Anal Chim Acta* 1017:1-19.

Simon M, van Alst N & Vollertsen J (2018) Quantification of microplastic mass and removal rates at wastewater treatment plants applying Focal Plane Array (FPA)-based Fourier Transform Infrared (FT-IR) imaging. *Water Res* 142:1-9.

Simon M, Vianello A & Vollertsen J (2019) Removal of >10 µm Microplastic Particles from Treated Wastewater by a Disc Filter. *Water* 11(9).

Simonsen ME, Muff J, Bennedsen LR, Kowalski KP & Søgaard EG (2010) Photocatalytic bleaching of p-nitrosodimethylaniline and a comparison to the performance of other AOP technologies. *Journal of Photochemistry and Photobiology A: Chemistry* 216(2-3):244-249.

Sires I, Brillas E, Oturan MA, Rodrigo MA & Panizza M (2014) Electrochemical advanced oxidation processes: today and tomorrow. A review. *Environ Sci Pollut Res Int* 21(14):8336-8367.

Sirés I, Cabot PL, Centellas F, Garrido JA, Rodríguez RM, Arias C & Brillas E (2006) Electrochemical degradation of clofibric acid in water by anodic oxidation. *Electrochim. Acta* 52(1):75-85.

Sirés I, Garrido JA, Rodríguez RM, Brillas E, Oturan N & Oturan MA (2007) Catalytic behavior of the Fe3+/Fe2+ system in the electro-Fenton degradation of the antimicrobial chlorophene. *Applied Catalysis B: Environmental* 72(3-4):382-394.

Sirés I, Garrido JA, Rodríguez RMa, Cabot Plls, Centellas F, Arias C & Brillas E (2006) Electrochemical Degradation of Paracetamol from Water by Catalytic Action of Fe[sup 2+], Cu[sup 2+], and UVA Light on Electrogenerated Hydrogen Peroxide. *J. Electrochem. Soc.* 153(1).

Skaf DW, Punzi VL, Rolle JT & Kleinberg KA (2020) Removal of micron-sized microplastic particles from simulated drinking water via alum coagulation. *Chem. Eng. J.* 386:123807.

Smit W & Hoogland JG (1971a) The mechanism of the anodic formation the of the peroxodisulphate ion on platinum-I. Establishment of participing anion. *Electrochim. Acta* 16:1-18.

Smit W & Hoogland JG (1971b) The mechanism of the anodic formationthe of the peroxodisulphate ion on platinum-II. Time dependence of the anode potential. *Eectrochimica Acta* 16: 821 to 831.

Smith M, Love DC, Rochman CM & Neff RA (2018) Microplastics in Seafood and the Implications for Human Health. *Curr Environ Health Rep* 5(3):375-386.

Sol D, Laca A, Laca A & Diaz M (2020) Approaching the environmental problem of microplastics: Importance of WWTP treatments. *Sci Total Environ* 740:140016.

Statista (2019) D'où viennent les microplastiques qui polluent nos océans ?

Stichnothe H, Kellera A, Thöming J, Lohmann N & Calmano W (2002) Reduction of tributyltin (TBT) and other organic pollutants of concern in contaminated sediments by means of an electrochemical oxidation. *Acta Hydrochim Hydrobiol* 30:87-93.

Strungaru S-A, Jijie R, Nicoara M, Plavan G & Faggio C (2019) Micro- (nano) plastics in freshwater ecosystems: Abundance, toxicological impact and quantification methodology. *TrAC, Trends Anal. Chem.* 110:116-128.

Sturm MT, Herbort AF, Horn H & Schuhen K (2020) Comparative study of the influence of linear and branched alkyltrichlorosilanes on the removal efficiency of polyethylene and polypropylene-based microplastic particles from water. *Environ Sci Pollut R* 27(10):10888-10898.

Sumisha A, Arthanareeswaran G, Lukka Thuyavan Y, Ismail AF & Chakraborty S (2015) Treatment of laundry wastewater using polyethersulfone/polyvinylpyrollidone ultrafiltration membranes. *Ecotoxicol Environ Saf* 121:174-179.

Sun J, Dai X, Wang Q, van Loosdrecht MCM & Ni BJ (2019) Microplastics in wastewater treatment plants: Detection, occurrence and removal. *Water Res* 152:21-37.

Sun M, Chen W, Fan X, Tian C, Sun L & Xie H (2020) Cooperative recyclable magnetic microsubmarines for oil and microplastics removal from water. *Appl. Mater. Today* 20:100682.

Sun Y & Plgnatello JJ (1993) Photochemical Reactions Involved in the Total Mineralization of 2,4-D by Fe^{3+}/H_20_2/UV. *Environ. Sci. Technol.* 27:304-310.

Sutton R, Mason SA, Stanek SK, Willis-Norton E, Wren IF & Box C (2016) Microplastic contamination in the San Francisco Bay, California, USA. *Mar. Pollut. Bull.* 109(1):230-235.

Swietlik J, Dabrowska A, Raczyk-Stanislawiak U & Nawrocki J (2004) Reactivity of natural organic matter fractions with chlorine dioxide and ozone. *Water Res* 38(3):547-558.

Tagg AS, Harrison JP, Ju-Nam Y, Sapp M, Bradley EL, Sinclair CJ & Ojeda JJ (2016) Fenton's reagent for the rapid and efficient isolation of microplastics from wastewater. *Chem Commun (Camb)* 53(2):372-375.

Tagg AS, Sapp M, Harrison JP & Ojeda JJ (2015) Identification and Quantification of Microplastics in Wastewater Using Focal Plane Array-Based Reflectance Micro-FT-IR Imaging. *Anal. Chem.* 87(12):6032-6040.

Talvitie J, Heinonen M, Paakkonen JP, Vahtera E, Mikola A, Setala O & Vahala R (2015) Do wastewater treatment plants act as a potential point source of microplastics? Preliminary study in the coastal Gulf of Finland, Baltic Sea. *Water Sci Technol* 72(9):1495-1504.

Talvitie J, Mikola A, Koistinen A & Setala O (2017a) Solutions to microplastic pollution - Removal of microplastics from wastewater effluent with advanced wastewater treatment technologies. *Water Res* 123:401-407.

Talvitie J, Mikola A, Setala O, Heinonen M & Koistinen A (2017b) How well is microlitter purified from wastewater? - A detailed study on the stepwise removal of microlitter in a tertiary level wastewater treatment plant. *Water Res* 109:164-172.

Tan C, Gao N, Deng Y, Zhang Y, Sui M, Deng J & Zhou S (2013) Degradation of antipyrine by UV, UV/H(2)O(2) and UV/PS. *J. Hazard. Mater.* 260:1008-1016.

Tang WZ & Huang CP (1996) 2,4-Dichlorophenol Oxidation Kinetics by Fenton's Reagent. *Environ. Technol.* 17(12):1371-1378.

Tang Y, Zhang S, Su Y, Wu D, Zhao Y & Xie B (2021) Removal of microplastics from aqueous solutions by magnetic carbon nanotubes. *Chem. Eng. J.* 406:126804.

Ter Halle A, Jeanneau L, Martignac M, Jarde E, Pedrono B, Brach L & Gigault J (2017) Nanoplastic in the North Atlantic Subtropical Gyre. *Environ Sci Technol* 51(23):13689-13697.

Thompson RC, Olsen Y, Mitchell RP, Davis A, Rowland SJ, John AWG, McGonigle D & Russell3 AE (2004) Lost at sea: where is all the plastic? *Sci Justice* 304:838-838.

Tian Xia, Michael Kovochich, Monty Liong, Jeffrey I. Zink & Nel aAE (2008) Cationic Polystyrene Nanosphere Toxicity Depends on Cell-Specific Endocytic and Mitochondrial Injury Pathways. *ACS Nano* 2 No. 1:85–96.

Tian Y, Chen Z, Zhang J, Wang Z, Zhu Y, Wang P, Zhang T, Pu J, Sun H & Wang L (2021) An innovative evaluation method based on polymer mass detection to evaluate the contribution of microfibers from laundry process to municipal wastewater. *J Hazard Mater* 407:124861.

Tiwari E, Singh N, Khandelwal N, Monikh FA & Darbha GK (2020) Application of Zn/Al layered double hydroxides for the removal of nano-scale plastic debris from aqueous systems. *J Hazard Mater* 397:122769.

Tofa TS, Kunjali KL, Paul S & Dutta J (2019a) Visible light photocatalytic degradation of microplastic residues with zinc oxide nanorods. *Environmental Chemistry Letters* 17(3):1341-1346.

Tofa TS, Ye F, Kunjali KL & Dutta J (2019b) Enhanced Visible Light Photodegradation of Microplastic Fragments with Plasmonic Platinum/Zinc Oxide Nanorod Photocatalysts. *Catalysts* 9(10):819.

Torkelson JM, Lipsky S & Tirrell M (1981) Polystyrene fluorescence: effects of molecular weight in various solvents. *Macromolecules 14* :1601–1603.

Tran LH (2009) "Destruction par voie électrochimique d'hydrocarbures aromatiques polycycliques contenus dans des matrices fortement contaminées," thesis presented to University of Quebec, national Institute of Scientific Research Center Water, Earth and Environment for the degree of Ph.D. philosophiae in water science.

Trestrail C, Nugegoda D & Shimeta J (2020) Invertebrate responses to microplastic ingestion: Reviewing the role of the antioxidant system. *Sci Total Environ* 734:138559.

Tsitonaki A, Petri B, Crimi M, MosbÆK H, Siegrist RL & Bjerg PL (2010) In situ chemical oxidation of contaminated soil and groundwater using persulfate: A review. *Critical Reviews in Environmental Science and Technology* 40(1):55-91.

Uheida A, Mejia HG, Abdel-Rehim M, Hamd W & Dutta J (2021) Visible light photocatalytic degradation of polypropylene microplastics in a continuous water flow system. *J. Hazard. Mater.* 406:124299.

Uheida A, Mejía HG, Abdel-Rehim M, Hamd W & Dutta J (2020) Visible light photocatalytic degradation of polypropylene microplastics in a continuous water flow system. *J Hazard Mater* https://doi.org/10.1016/j.jhazmat.2020.124299:124299.

Urtiaga A, Fernandez-Castro P, Gómez P & Ortiz I (2014) Remediation of wastewaters containing tetrahydrofuran. Study of the electrochemical mineralization on BDD electrodes. *Chem. Eng. J.* 239:341-350.

USEPA (2002) Methods for measuring the acute toxicity of effluents and receiving waters to freshwater and marine organisms, fifth edition.

Vermaire JC, Pomeroy C, Herczegh SM, Haggart O, Murphy M & Schindler DE (2017) Microplastic abundance and distribution in the open water and sediment of the Ottawa River, Canada, and its tributaries. *Facets* 2(1):301-314.

Wacławek S, Lutze HV, Grübel K, Padil VVT, Černík M & Dionysiou DD (2017) Chemistry of persulfates in water and wastewater treatment: A review. *Chem. Eng. J.* 330:44-62.

Wang JG & Li XM (2011) Electrochemical Treatment of Wastewater Containing Chlorophenols Using Boron-Doped Diamond Film Electrodes. *Advanced Materials Research* 356-360:1418-1422.

Wang L, Kaeppler A, Fischer D & Simmchen J (2019) Photocatalytic TiO_2 Micromotors for Removal of Microplastics and Suspended Matter. *ACS Appl. Mater. Inter.* 11(36):32937-32944.

Wang R, Zhang L, Chen B & Zhu X (2020a) Low-pressure driven electrospun membrane with tuned surface charge for efficient removal of polystyrene nanoplastics from water. *J Membrane Sci* 614:118470.

Wang S, Liu M, Wang J, Huang J & Wang J (2020b) Polystyrene nanoplastics cause growth inhibition, morphological damage and physiological disturbance in the marine microalga Platymonas helgolandica. *Mar Pollut Bull* 158:111403.

Wang Y, Li Yn, Tian L, Ju L & Liu Y (2020c) The removal efficiency and mechanism of microplastics enhancement by positive modification dissolved air flotation. *Water Environ. Res*.

Wang Z, Lin T & Chen W (2020d) Occurrence and removal of microplastics in an advanced drinking water treatment plant (ADWTP). *Sci Total Environ* 700:134520.

Wang Z, Sedighi M & Lea-Langton A (2020e) Filtration of microplastic spheres by biochar: removal efficiency and immobilisation mechanisms. *Water. Res.* 184:116165.

Wang Z, Wu Z & Tang S (2009) Characterization of dissolved organic matter in a submerged membrane bioreactor by using three-dimensional excitation and emission matrix fluorescence spectroscopy. *Water Res* 43(6):1533-1540.

Ward JE & Kach DJ (2009) Marine aggregates facilitate ingestion of nanoparticles by suspension-feeding bivalves. *Mar Environ Res* 68(3):137-142.

WEF (2016) The New Plastics Economy Rethinking the future of plastics. *(disponible sur www3.weforum.org/docs/WEF_The_New_Plastics_Economy).pdf*.

Wegner A, Besseling E, Foekema EM, Kamermans P & Koelmans AA (2012) Effects of nanopolystyrene on the feeding behavior of the blue mussel (Mytilus edulis L.). *Environ Toxicol Chem* 31(11):2490-2497.

White KL (1986) An overview of immunotoxicology and carcinogenic polycyclic aromatic hydrocarbons. *Environmental Carcinogenesis Reviews* 4(2):163-202.

Williams T, Walsh C, Murray K & Subir M (2020) Interactions of emerging contaminants with model colloidal microplastics, C(60) fullerene, and natural organic matter - effect of surface functional group and adsorbate properties. *Environ Sci Process Impacts* 22(5):1190-1200.

Wojnarovits L & Takacs E (2019) Rate constants of sulfate radical anion reactions with organic molecules: A review. *Chemosphere* 220:1014-1032.

Woodall LC, Sanchez-Vidal A, Canals M, Paterson GL, Coppock R, Sleight V, Calafat A, Rogers AD, Narayanaswamy BE & Thompson RC (2014a) The deep sea is a major sink for microplastic debris. *R Soc Open Sci* 1(4):140317.

Woodall LC, Sanchez-Vidal A, Canals M, Paterson GL, Coppock R, Sleight V, Calafat A, Rogers AD, Narayanaswamy BE & Thompson RC (2014b) The deep sea is a major sink for microplastic debris. *R Soc Open Sci* 1(4):140317.

Xiang Q, Yu J & Wong PK (2011) Quantitative characterization of hydroxyl radicals produced by various photocatalysts. *J. Colloid Interface Sci.* 357(1):163-167.

Xiong Y, Zhao J, Li L, Wang Y, Dai X, Yu F & Ma J (2020) Interfacial interaction between micro/nanoplastics and typical PPCPs and nanoplastics removal via electrosorption from an aqueous solution. *Water. Res.* 184:116100.

Xu B, Gao NY, Cheng H, Xia SJ, Rui M & Zhao DD (2009) Oxidative degradation of dimethyl phthalate (DMP) by UV/H_2O_2 process. *J. Hazard. Mater.* 162(2-3):954-959.

Yakimenko O, Khundzhua D, Izosimov A, Yuzhakov V & Patsaeva S (2016) Source indicator of commercial humic products: UV-Vis and fluorescence proxies. *J Soils Sediments* 18(4):1279-1291.

Yamashita R & Tanimura A (2007) Floating plastic in the Kuroshio Current area, western North Pacific Ocean. *Mar Pollut Bull* 54(4):485-488.

Yamashita Y & Tanoue E (2003) Chemical characterization of protein-like fluorophores in DOM in relation to aromatic amino acids. *Mar. Chem.* 82(3-4):255-271.

Yang S, Wang P, Yang X, Shan L, Zhang W, Shao X & Niu R (2010) Degradation efficiencies of azo dye Acid Orange 7 by the interaction of heat, UV and anions with common oxidants: persulfate, peroxymonosulfate and hydrogen peroxide. *J. Hazard. Mater.* 179(1-3):552-558.

Yaranal NA, Subbiah S & Mohanty K (2020) Identification, extraction of microplastics from edible salts and its removal from contaminated seawater. *Environ. Technol. Innov.* https://doi.org/10.1016/j.eti.2020.101253:101253.

Yassine O, Bhagyashree T, Antonin A, Marc-Antoine V, Sokhna D, Ndiaye,, Patrick D, Rajeshwhar D, Tyagi, , Sebastien S, Melanie D, Gerardo B & Rino D (2018) Synthetic hospital wastewater treatment by coupling submerged membrane bioreactor and electrochemical advanced oxidation process: Kinetic study and toxicity assessment. *Chemosphere* 193:160-169.

Yassine Ouarda, Bhagyashree Tiwari, Antonin Azaïs, Marc-Antoine Vaudreuil, Sokhna Dieng Ndiaye, Patrick Drogui, Rajeshwhar Dayal Tyagi, Sebastien Sauve, Melanie Desrosiers, Gerardo Buelna d & Dube R (2018) Synthetic hospital wastewater treatment by coupling submerged membrane bioreactor and electrochemical advanced oxidation process: Kinetic study and toxicity assessment. *Chemosphere 193* 10.1016/j.chemosphere.2017.11.010:160-169.

Yin K, Wang Y, Zhao H, Wang D, Guo M, Mu M, Liu Y, Nie X, Li B, Li J & Xing M (2021) A comparative review of microplastics and nanoplastics: Toxicity hazards on digestive, reproductive and nervous system. *Sci. Total Environ.* 774.

Yu X, Zhou M, Hu Y, Groenen Serrano K & Yu F (2014) Recent updates on electrochemical degradation of bio-refractory organic pollutants using BDD anode: a mini review. *Environ Sci Pollut Res Int* 21(14):8417-8431.

Yue J, Epstein AJ & MacDiarmid AG (1990) Sulfonic acid ring-substituted polyaniline, a self-doped conducting polymer. *Molecular Crystals and Liquid Crystals* 189(1):255-261.

Zanin H, Teófilo RF, Peterlevitz AC, Oliveira U, de Paiva JC, Ceragioli HJ, Reis EL & Baranauskas V (2012) Diamond cylindrical anodes for electrochemical treatment of persistent compounds in aqueous solution. *J. Appl. Electrochem.* 43(3):323-330.

Zaouri N, Cheng H, Khairunnisa F, Alahmed A, Blilou I & Hong PY (2021) A type dependent effect of treated wastewater matrix on seed germination and food production. *Sci Total Environ* 769:144573.

Zarfl C & Matthies M (2010) Are marine plastic particles transport vectors for organic pollutants to the Arctic? *Mar Pollut Bull* 60(10):1810-1814.

Zepp RG (1992) Hydroxyl Radical Formation in Aqueous Reactions (pH 3-8) of Iron(I1) with Hydrogen Peroxide: The Photo-Fenton Reaction. *Envlron. Sci. Technol.* 26:313-319.

Zhang C, Jiang Y, Li Y, Hu Z, Zhou L & Zhou M (2013) Three-dimensional electrochemical process for wastewater treatment: A general review. *Chem. Eng. J.* 228:455-467.

Zhang H, Fei C, Zhang D & Tang F (2007) Degradation of 4-nitrophenol in aqueous medium by electro-Fenton method. *J. Hazard. Mater.* 145(1-2):227-232.

Zhang M, Yang J, Kang Z, Wu X, Tang L, Qiang Z, Zhang D & Pan X (2021a) Removal of micron-scale microplastic particles from different waters with efficient tool of surface-functionalized microbubbles. *J Hazard Mater* 404:124095.

Zhang S, Wang J, Liu X, Qu F, Wang X, Wang X, Li Y & Sun Y (2019) Microplastics in the environment: A review of analytical methods, distribution, and biological effects. *TrAC Trends in Analytical Chemistry* 111:62-72.

Zhang X, Chen J & Li J (2020a) The removal of microplastics in the wastewater treatment process and their potential impact on anaerobic digestion due to pollutants association. *Chemosphere* 251:126360.

Zhang Y, Diehl A, Lewandowski A, Gopalakrishnan K & Baker T (2020b) Removal efficiency of micro- and nanoplastics (180 nm-125 mum) during drinking water treatment. *Sci Total Environ* 720:137383.

Zhang Y, Diehl A, Lewandowski A, Gopalakrishnan K & Baker T (2020c) Removal efficiency of micro- and nanoplastics (180 nm–125 μm) during drinking water treatment. *Sci Total Environ* 720:137383.

Zhang Y, Zhao J, Liu Z, Tian S, Lu J, Mu R & Yuan H (2021b) Coagulation removal of microplastics from wastewater by magnetic magnesium hydroxide and PAM. *Journal of Water Process Engineering* 43.

Zhang Z & Chen Y (2020) Effects of microplastics on wastewater and sewage sludge treatment and their removal: A review. *Chem. Eng. J.* 382:122955.

Zhao X, Hou Y, Liu H, Qiang Z & Qu J (2009) Electro-oxidation of diclofenac at boron doped diamond: Kinetics and mechanism. *Electrochim. Acta* 54(17):4172-4179.

Zheng L, Song Z, Meng P & Fang Z (2016) Seasonal characterization and identification of dissolved organic matter (DOM) in the Pearl River, China. *Environ Sci Pollut Res Int* 23(8):7462-7469.

Zhou G, Wang Q, Li J, Li Q, Xu H, Ye Q, Wang Y, Shu S & Zhang J (2021) Removal of polystyrene and polyethylene microplastics using PAC and $FeCl_3$ coagulation: Performance and mechanism. *The Science of the total environment* 752:141837.

Zhou W, Gao J, Kou K, Meng X, Wang Y, Ding Y, Xu Y, Zhao H, Wu S & Qin Y (2018) Highly efficient H_2O_2 electrogeneration from O2 reduction by pulsed current: Facilitated release of H_2O_2 from porous cathode to bulk. *Journal of the Taiwan Institute of Chemical Engineers* 83:59-63.

Zhou W, Meng X, Gao J & Alshawabkeh AN (2019) Hydrogen peroxide generation from O_2 electroreduction for environmental remediation: A state-of-the-art review. *Chemosphere* 225:588-607.

Ziajahromi S, Neale PA, Rintoul L & Leusch FD (2017a) Wastewater treatment plants as a pathway for microplastics: development of a new approach to sample wastewater-based microplastics. *Water. Res.* 112:93-99.

Ziajahromi S, Neale PA, Rintoul L & Leusch FD (2017b) Wastewater treatment plants as a pathway for microplastics: Development of a new approach to sample wastewater-based microplastics. *Water Res* 112:93-99.